Low Temperature Environmentally Friendly Self–Assembled Nano–Materials

Nicole Kirsten Whitelaw

Doctor of Philosophy

University of York

Chemistry

December 2016

Dedicated to my beloved Mum and Gran

Abstract

Low molecular weight gelators are highly versatile molecular building blocks which have proven uses in many applications, however none have been proven useful at sub-zero temperatures. Using a library of known hydro and organogelators we discovered the use of 1,3:2,4-Dibenzylidene-D-sorbitol (DBS) to have the ability to enhance the effects of anti-freeze fluids used on aircrafts in winter conditions.

Although DBS showed greatly improved attributes when in glycol solvent systems its ability to form gels in dilute aqueous systems was limited. Through derivatisation of the aromatic rings of DBS a library of DBS derivatives were created which imparted hydrophilic and hydrophobic components to the molecule. From the DBS derivatives synthesised oxyether, DBS-OCH_3, and thioether, DBS-SCH_3, derivatives had the ability to form gels in more aqueous environments at lower concentrations than the original unmodified DBS. Full gelation ability and thermal stability profiles were obtained as well as how each molecule aggregates and self assembles to form the fibrous nanostructured 3D sample spanning network as viewed by SEM.

The ability of DBS, DBS-OCH_3 and DBS-SCH_3 to form gels with complex fluids was determined through the use of industrially relevant de-icing products. With the incorporation of DBS and its derivatives to a de-icing fluid we created a thickened anti-icing product where the gels were stiff with high G' values, strong, could be used in dilute systems and at low concentrations. The thickened gels formed were counter intuitive to normal anti-icing fluids with the protection provided to aircrafts (holdover time) in winter actually increasing with increasing water content, potentially lowering the costly and environmentally damaging glycol loading.

Finally we demonstrated the potential of hybrid gel systems in the de/anti-icing industry by forming hybrid gels with DBS and its derivatives in complex anti-icing fluids containing polymeric thickeners. Incorporating a gelator into a complex fluid such as an anti-icing fluid reduces the required concentration of gelator, increases the thermal stability and forms strong resistant stiff gels. Using hybrid gels allows for the holdover time to be increased by >50% even in dilute systems whilst having minimal effects on the aerodynamics.

Table of Contents

Table of Figures

Table of Tables

Table of Schemes

Acknowledgements

I would like to sincerely thank my academic supervisor, Professor David Smith, for his invaluable help and expertise, and for his patience and guidance throughout my studies whilst at the university. I would also like to thank him for sharing his vast knowledge of everything that is gel and for his assistance in writing my thesis.

Thanks also goes to my industrial supervisors Dr Lee Stokes and Dr Jerry Lewis, whose expert knowledge of the aviation industry helped me achieve a greater understanding of how to link industry with academia. I would also like to say a special thanks to Dr Lee Stokes for teaching me the difficult subject of rheology.

I especially thank and acknowledge my sponsor Kilfrost Limited, without this support and funding this endeavor would not have been possible.

Thanks also goes to the support and technical staff at the university who helped me with various techniques, they are Meg Stark (FEG-SEM/TEM), Dr Andrew Leech (CD), Dr Karl Heaton (MS) and Heather Fish (NMR).

All the people I have worked with past and present in the Smith group and made very good friends with, particularly Dr Dan Cornwell and Dr Tunde Okesola for helping me in the early days with the organic synthesis, Vania Veira, Buthania Albanyan, Lizzie Wheeldon, Dr Ana Campo-Rodrigo, Jorge Ruiz, Dr Rex Chang, Dr Stephen Bromfield and Phil Chivers for all the laughs, keeping me entertained in the lab and the new cultural experiences. I would also like to thank my many colleagues at Kilfrost especially the technical team for keeping me entertained and motivated throughout my research.

I am also very grateful for the support, motivation and encouragement I have received from my family especially from my Dad, step mum, sisters and brothers and I am especially grateful to John, without whom I would not have been able to do this. With your love, support, encouragement and understanding, you showed me that anything is possible.

Declaration

I declare that the work presented within this thesis is entirely my own, except where otherwise acknowledged.

B. O. Okesola, V. M. P. Vieira, D. J. Cornwell, N. K. Whitelaw and D. K. Smith, *Soft Matter*, 2015, **11**, 4768-4787.

This work has not previously been presented for an award at this, or any other University. All sources are acknowledged as references.

Chapter 1

Introduction

Chapter 1 Introduction

1.1 Transportation in Winter

In winter the formation of ice, frost and snow can cause hazardous conditions leading to potential disruption, delays and accidents when trying to travel. Unlike smaller vehicles, where ice and snow can be physically removed through the use of mechanical techniques and de-icing sprays, aeroplanes require a more comprehensive de-icing protocol ensuring the safe take-off of the aircraft and the safety of its passengers.

For an aeroplane to take off safely in winter conditions the aeroplane's critical surfaces and sensors must be free of any frozen contamination and follow the "clean aircraft concept" (see Section 1.2).[1-3] The critical surfaces of an aircraft include the wings, flaps, ailerons, horizontal and vertical stabilisers and propellers, in addition to other areas of the aircraft which must remain free of frozen contamination (see Figure 1.1).[4-7] The presence of frozen contamination on the critical surfaces of an aircraft is detrimental, as it adds weight, reduces lift, impedes the movement of the flaps and rudders, and disrupts the smooth airflow across the critical aerodynamic surfaces of the aircraft.

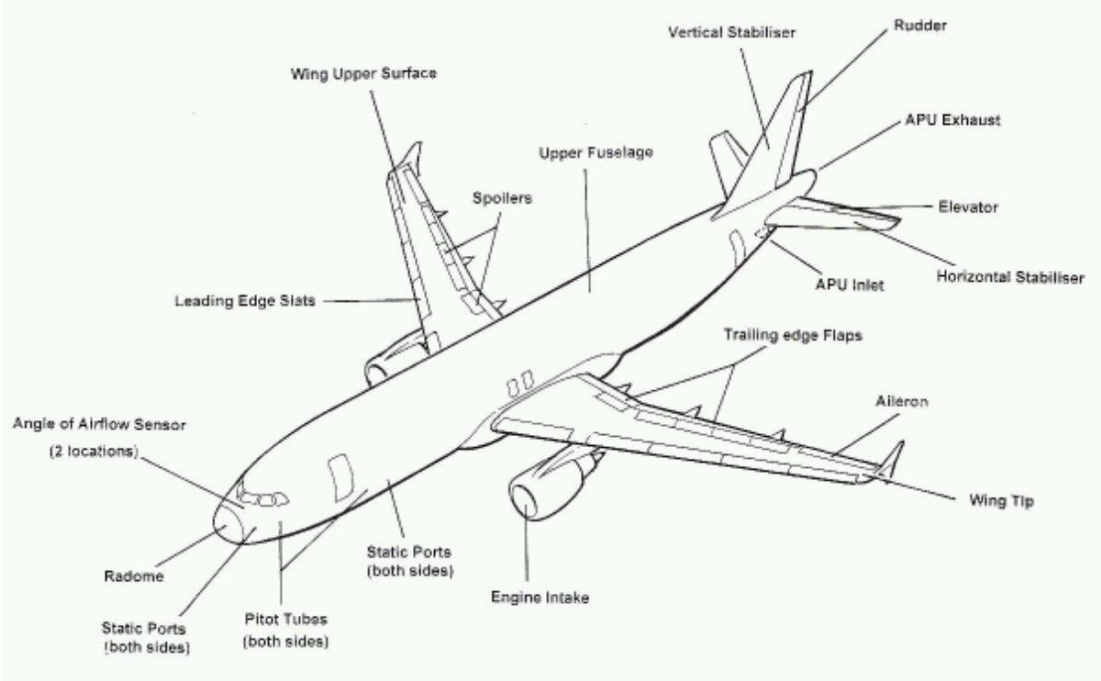

Figure 1.1 Critical surfaces and sensors on an Aeroplane

An aircraft flies by making use of four different forces, lift, thrust, drag and gravity (weight) (see Figure 1.2).[8,9]

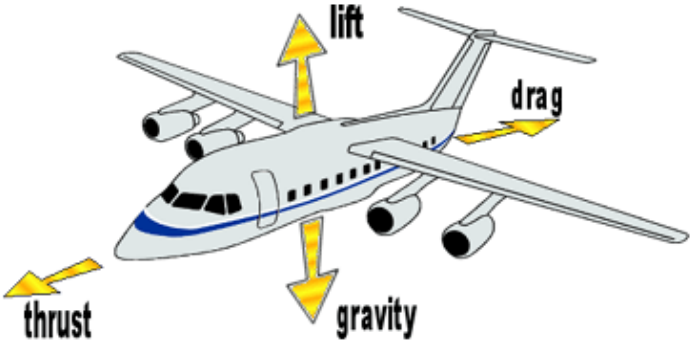

Figure 1.2 Forces of Flight

To understand how an aircraft can fly using these four forces we must consider the aerodynamics of an aircraft[10] which can be explained through the use of Bernoulli's Theorem and Newton's Third Law of Motion. An aircraft is designed using the predictable effects of airflow over clean, smooth wings also known as an airfoil.[11] An airfoil is designed so that the upper surface has more curvature than the lower surface. Based on this structure, an airfoil can generate lift by two processes, pressure differential and ram air.[12,13]

Lift generated by pressure differentials is based upon the theory of Daniel Bernoulli (Bernoulli's Theorem)[14] which states "The faster a fluid flows, (air is considered as a fluid) the lower the pressure will be surrounding it given the differences in curvature between the upper and lower surfaces". Therefore, the air above an airfoil has a greater distance to travel and hence travels faster than the air travelling beneath the airfoil. This creates a lower air pressure above the airfoil, displacing the airfoil upwards towards the lower pressure above the wing. This accounts for approximately 50% of the lift generated whilst the remainder is generated by ram air. Ram air, effectively rams air under the airfoil creating high pressure beneath the airfoil and a resultant upward movement. Ram air is based upon Isaac Newton's Third Law of Motion[15] which states "For every action, there is an equal and opposite reaction" or the application of a force causes an equal and opposite force to be generated.

Generating lift based on the above requires thrust to be applied from the engine of the aircraft.[16] When considering how lift is generated we must also consider the angle at which the airfoil is tilted in relation to the airflow, known as the angle of attack.[17] Lift can vary with the angle of attack, but generally the greater the angle of attack the

greater the lift. An angle greater than 16° is referred to as the critical angle of attack[18]. Above this critical angle, the smooth laminar airflow above the airfoil is displaced by turbulent airflow (see Figure 1.3) during which the differential pressure collapses, drag exceeds the lift, resulting in insufficient lift to counteract the weight giving rise to the aircraft stalling, known as the "Stall Angle".

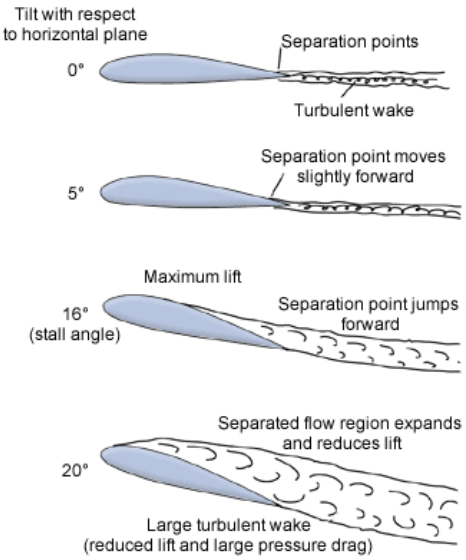

Figure 1.3 Formation of turbulent airflow with increasing angle of attack

Aircraft can also stall due to low speed; this generally happens when the aircraft has no angle of attack indicators and the angle of attack is estimated by the airspeed. An aircraft stalling due to low speed is known as "Stall speed".[11,17,18] Therefore to operate an aircraft safely, the correct amount of thrust and required angle of attack is critically important in creating the necessary lift to counteract drag and gravity forces.

Ice, frost and snow all have negative effects on the forces required by an aircraft to take-off.[9] Any form of frozen contamination on the critical surfaces of the aircraft, particularly the wings (airfoil), not only creates additional weight but will also changes the shape and texture of the airfoil, changing the airflow over it, both of which can seriously affect the lift that an airfoil can generate.

Throughout aviation history there have been a number of examples where the degradation in an aircraft's performance has been a result of ice, frost or snow on the critical surfaces of the aircraft. On 13th January 1982, Air Florida Flight 90 scheduled to Florida took off from Washington D.C.'s National Airport.[19] During take-off the flight failed to gain enough altitude, stalled, hit a bridge and crashed into the Potomac River. The National Transportation Safety Board reported[20] the official cause of the

incident as pilot error. Before the take-off of Flight 90 there had been heavy snow fall, resulting in the scheduled flight being delayed by 1 hour 45 minutes. During this time snow had accumulated on the airfoil of the aircraft. As the flight was manoeuvring away from the gate the pilot noticed the engines were not producing as much power as indicated on their instruments, but failed to abort the take-off. The pilot's limited knowledge of de-icing practices and decision to take-off with snow adhering to the airfoil, the anomalous reading on the engines instruments and the failure to turn on the engine's internal anti-icing system all contributed to the disaster of Flight 90 which killed 77 people.

Figure 1.4 Wreckage of Air Florida Flight 90

On 10th March 1989, Air Ontario Flight 1363, a scheduled passenger plane, took off from Dryden Regional Airport. Fifteen seconds after take-off flight 1363 crashed into the trees just beyond the edge of the runway. Flight 1363 similar to Flight 90 was unable to attain sufficient altitude to clear the trees at the end of the runway due to snow and ice on the wings. The investigation[21] revealed that an auxiliary power unit (APU) was unserviceable which resulted in questionable decision making. Flight 1363 was unable to shut down the engines at the airport due to this unserviceable APU, as if shutdown the engines could not be restarted. To prevent further delay the aircraft was refuelled with passengers on board and the engines running, during which time snow was accumulating on the wings. Due to the type of aircraft, it was not de-iced before take-off due to the risk of toxic fumes entering the passenger cabin, however, the airline instructions were unclear on this point. The investigation[22] revealed that due to inadequate practices and procedures in the industry, the pilot was placed in a difficult position when making his decisions. This accident consequently resulted in significant changes being made to the Air Regulations, including new procedures

regarding re-fuelling and de-icing as well as a number of general safety regulations which remain in place today.

Figure 1.5 Wreckage of Air Ontario Flight 1363

1.2 Air Regulations

For aircraft to operate safely in winter conditions they must follow and adhere to set regulations and recommendations provided by aviation regulatory bodies. In the US, de-icing procedures are regulated by the Federal Aviation Administration (FAA), in Canada, by Transport Canada Civil Aviation (TCCA) and in Europe, regulated by the European Aviation Safety Agency (EASA). One of the most important regulations that is followed globally is described as the "Clean Aircraft Concept". The FAA describes this in its Code of Federal Regulations (CFR) Sec. 121.629[23]:

"No person may takeoff an aircraft when frost, ice, or snow is adhering to the wings, control surfaces, propellers, engine inlets, or other critical surfaces of the aircraft or when the takeoff would not be in compliance with paragraph (c) of this section. Takeoffs with frost under the wing in the area of the fuel tanks may be authorized by the Administrator".

Paragraph (c) mentioned above states that no person can dispatch or takeoff unless they are a certificate holder of an approved de-icing / anti-icing program. The TCCA[24] and EASA[25] describe this in a similar manner.

The clean aircraft concept effectively describes an aircraft that is aerodynamically clean[10,16-18] and free from frozen contaminants. This concept is important as mentioned in **Section 1.1**. An aircraft's takeoff performance is designed around the predictable effects of airflow over clean wings, which allow for the generation of the four required forces needed for an aircraft to takeoff.

The clean aircraft concept can be achieved through following a de-icing and anti-icing program.

The regulatory bodies also provide regulations regarding what is required for obtaining approval of de-icing programs[26], de-icing training requirements[27] for personnel, de-icing procedures[28], and aircraft de-icing facilities[29] as well as general airworthiness and safety regulations.[30]

From the regulations set by the regulatory bodies, recommendations are available from the Association of European Airlines (AEA)[31] and the Civil Aviation Administration of China (CAAC), these are recommendations only. These recommendations act to promote and develop a set of commonly agreed recommended safe practices and ground procedures for de-icing an aircraft which best reflects the current industry practices.

For a de-icing or anti-icing fluid to be used on an aircraft it first needs to meet the criteria set by the Society of Automotive Engineers (SAE). The SAE produce standards for the aviation industry. SAE AMS (Aerospace Materials Specification) 1424 (de-icing fluids)[32] and SAE AMS 1428 (anti-icing fluids)[33] are the two most important standards produced by the SAE for the qualification of de-icing and anti-icing fluids. These standards detail the necessary test criteria a fluid must pass to be certified as a listed product for use on aircrafts. The regulatory bodies make use of the SAE's standards[34] to set regulations in relation to de-icing and anti-icing fluids and their correct application procedures.

The standards set by the SAE are then used by independent test houses to qualify each fluid for use to either de-ice or anti-ice an aircraft. These test houses are based in North America. APS Aviation Inc located in Montreal, Quebec, with their role being to conduct testing related to the effectiveness of product methodologies and operations under icing conditions in locations exposed to the appropriate weather conditions in the field. The Anti-icing Materials International Laboratory (AMIL) associated with the University of Quebec, undertake performance evaluation of de/anti-icing fluids through the use of climatic chambers and wind tunnels in a laboratory setting. These test houses importantly generate holdover time (HOT) and aerodynamic data. Holdover time (HOT) refers to the amount of time an aircraft is protected from further accumulation of frost, ice or snow on its critical surfaces through the use of an anti-icing fluid, before reapplication would be required. From the holdover data collated by AMIL and APS, the regulatory bodies publish holdover tables[35] annually

for each product on how they can be used and the holdover protection that can be expected when being used on aircraft for anti-icing purposes.

The third test house, Scientific Materials International (SMI) based in Miami, Florida, unlike the other two test houses, conducts aircraft material compatibility testing. Each fluid submitted for testing must pass all the required test criteria set by each of the three independent test houses. The results from the test houses are available to the regulatory bodies and reported to the fluid manufacturers. Producing products in this way ensures all manufacturers use the same standards and specifications' ensuring each product is fit for purpose. Once a product has been listed as a certified product by the regulatory bodies it can be sold to end users. Fluid manufacturers sell their products to airports which then make each of the different fluids available to airlines. Airlines will then request from the airport to be de-iced or anti-iced prior to takeoff. To ensure that the airports are maintaining the fluids on site appropriately, the De-icing/Anti-icing Quality Control Pool (DAQCP)[36] audits the airports at particular stages throughout the year whereby they send samples of each fluid back to the manufacturers for testing to ensure the fluids still meet the required specification set by the regulatory bodies and the SAE. De-icing or anti-icing of an aircraft is heavily regulated as described above and shown in **Figure 1.6** to ensure the optimum performance and safety of the aircraft and of its passengers at all times.

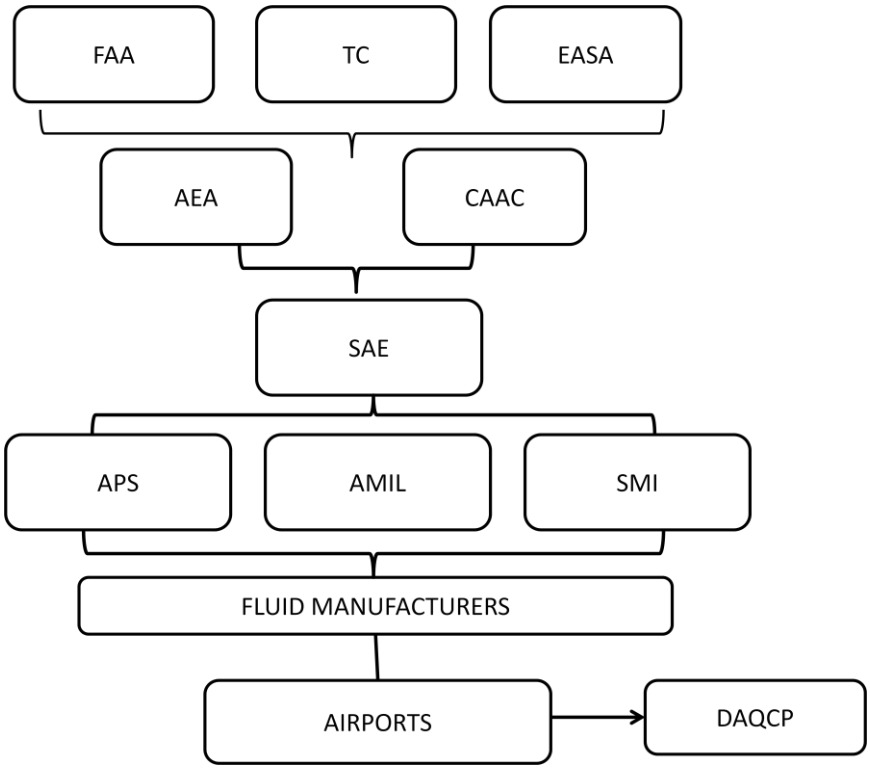

Figure 1.6 Organisation of regulation, recommendation and testing in Aviation.

1.3 De-icing and Anti-icing

The process of de-icing removes accumulated ice, frost and snow from an aircraft.[37,38] It is achieved through a combination of thermal energy and mechanical force which act to melt and remove any frozen contamination from the critical surfaces of an aircraft. Hot water and or heated mixtures of water and a de-icing fluid are sprayed onto the surfaces of an aircraft at high pressure to accomplish this. Although there are other approved methods for de-icing such as the use of hot air, the primary method used worldwide is the use of chemical de-icing fluids.

Anti-icing is the means of protecting from further adherence of ice, frost or snow to the surfaces of an aircraft for a given time known as the holdover time (HOT).[37,38] Anti-icing fluids are thickened fluids. They are most effective when applied unheated and undiluted to clean airplane surfaces. As soon as an anti-icing fluid is applied the holdover protection begins.[35] When applied to a clean surface, the fluid forms a protective layer, see **Figure 1.7.**[39] This layer has a lower freezing point than the frozen precipitation, which melts on contact with the fluid. As the layer becomes diluted by the melting precipitation, it becomes less effective and frozen precipitation can begin to accumulate. When the holdover time is exceeded for the particular fluid applied, the plane must return to the start of the de/anti-icing operation. A secondary application of an anti-icing fluid must never be carried out due to the possibility of gel residues forming which can collect in aerodynamic quiet cavities.[16,24,37]

There are a number of listed products available to perform ground de-icing and anti-icing operations on an aircraft.

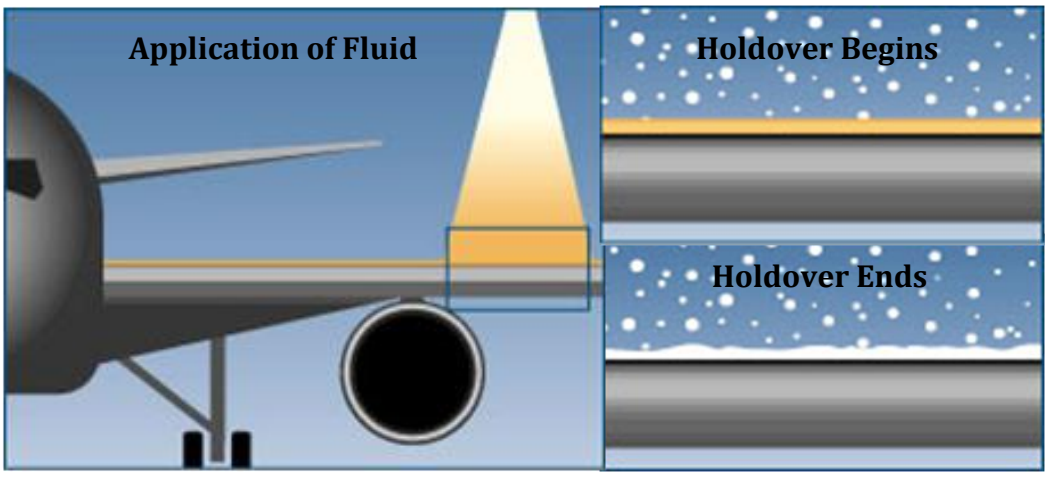

Figure 1.7 Application of an Anti-icing Fluid and Holdover Time

1.4 Fluids and their Properties

De-icing and anti-icing fluids are freezing point depressants. They commonly consist of a freeze point depressant, propylene glycol or ethylene glycol, as well as additives such as surfactants, corrosion inhibitors and dyes.[39-41] Anti-icing fluids also contain a thickening agent. Technical standards and specifications set by the SAE for de-icing and anti-icing fluids categorise them into four different classifications based on their properties, known as Type I, Type II, Type III and Type IV.[32,33]

Type I products are manufactured and qualified to SAE AMS1424[32] specification. Type I products are predominantly used as de-icing fluids based on 1,2-propylene glycol and aqueous mixtures of this. They typically have high glycol content (80%) with low viscosity (described as "unthickened") in their concentrated form. They are predominantly used for removal of frozen deposits from the surfaces of aircraft.[41-43] Due to the low viscosity, they create thin films that do not offer any significant anti-icing holdover protection, especially in freezing precipitation. With this type of fluid no additional protection is provided to an aircraft by increasing the concentration of the fluid in the fluid/water mix.[35] These products are coloured orange to aid with identification and application.

Type II products are manufactured and qualified to SAE AMS1428[33] specification. They can be used for de-icing purposes but are more commonly used for anti-icing. They are freezing point depressants based on 1,2–propylene glycol aqueous mixtures and contain a minimum glycol content of 50% as well as a pseudoplastic thickening polymer.[41-43] The polymer enables the product to create a thick film on the external surfaces of an aircraft (fluids are referred to as "thickened" as a result of this) and can provide holdover protection against subsequent frozen contamination for a limited period of time. The pseudoplastic nature of the product makes it shear thinning which allows the fluid to reduce in viscosity and flow off the critical surfaces under shear stress at the point of takeoff without affecting the aerodynamics[44]. With this type of fluid the holdover time can be extended by increasing the concentration of the fluid in the fluid water mix, with the maximum holdover time achieved through using the undiluted fluid.[35] These products are normally straw or yellow in colour.

Type III products are manufactured and qualified to SAE AMS 1428[33] specification. They have similar properties to Type II fluids but provide slightly lower holdover times.[35,41] Type III fluids were designed for use on aircrafts with low rotation takeoff

speeds of less than 100 knots, typically commuter planes.[43] These are coloured bright yellow.

Type IV products are manufactured and qualified to SAE AMS 1428[33] like Type II and III products. These products can be used as a de-icing fluid but are commonly used as an anti-icing fluid. Type IV fluids provide the maximum holdover protection of all four fluid classifications.[35] They are very similar to Type II fluids in both composition and operation. However, they use a different thickening system to provide longer holdover times than Type II fluids when used in concentrated form. Type IV products are coloured green.

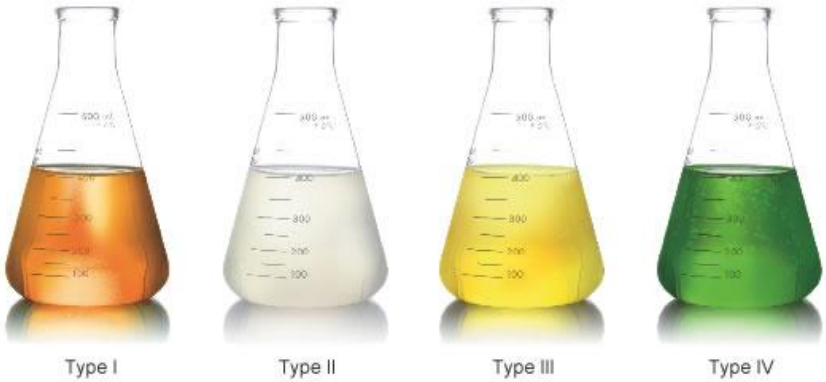

Figure 1.8 The Four different classifications of fluids.[42]

All of the above classifications of fluids contain ≤80% propylene or ethylene glycol. This is primarily due to the effects pure propylene or ethylene glycols have at low temperatures. Pure propylene or ethylene glycol have much higher freezing points than each of the glycols diluted with water. At low temperatures they can become viscous which has been found to contribute to reduced lift upon takeoff.[24,38] All of the above types of fluids are not intended to be used in the undiluted state unless recommended by the aircraft manufacturer.

1.5 De-icing Pads and the Environment

De-icing and anti-icing of an aircraft most commonly is carried out in designated areas within an airport. These areas include terminal gates, apron areas as well as de-icing pads also known as centralised de-icing facilities. In the UK, de-icing is commonly carried out at terminal gates or on the apron due to airport size and land constraints of installing de-icing pads. De-icing pads are currently being introduced into the UK especially for larger airports such as Heathrow where the installation of two de-icing pads, “North Vader” and “South Vader” is currently underway.[45,46] De-

icing pads and centralised de-icing facilities are more common in Canada and the US.[4,5,24,38,47]

A de-icing pad is a designated area close to the start of the runway. They allow for the confinement of de-icing activity to one area, and for the containment of spent de-icing fluids which can be collected, contained and recycled.[48-51] Each aircraft is de-iced in this area using trucks fitted with heated spray guns. Any excess fluid after application that runs off the aircraft to the ground is collected via storm drains. Instead of the fluid being discharged into the waterways through these storm drains, the fluid is redirected into collection tanks and reservoirs underneath the ground. This fluid is then contained in these tanks for processing and or recycling to make new de-icing fluid. The largest centralised de-icing facility to date can be found at Toronto's Lester B. Pearson International Airport where up to 12 aircraft can be de-iced at any one time.[52]

The introduction of de-icing pads and centralised de-icing facilities allows for aircraft to be de-iced faster and more efficiently. It also means fluids with shorter holdover times can be used more often, as there are shorter taxi distances to the runway before takeoff. They have increased safety by isolating the de-icing practise to one area which can cause slipperiness to ground surfaces affecting personnel and they have also helped to reduce the environmental impact de-icing fluids have on the environment.

De-icing fluids have been shown to have a negative impact on the environment, primarily from the glycols contained within the products.[53,54] If these glycols find their way into waterways they have been shown to deplete oxygen levels, this is because the biochemical oxygen demand (BOD) required during their degradation increases, having major impacts for aquatic life and mammals. As such glycols are now considered toxic to wildlife and aquatic organisms. Most airports around the world however were built long before there were any environmental regulations in place for de-icing fluids. As such most airports do not have the facilities to contain and or collect spent de-icing fluids. Due to the limited environmental regulations in this area, airports have been freely discharging the spent fluids into the waterways. However, over the last few years the Environmental Protection Agency (EPA)[55,56] in the US have been taking a more active role. In the UK the environmental regulation and advice for each airport is provided by each county's environmental body,[57] but as of yet there is not one environmental standard used across all airports. Therefore the

need to create more environmentally friendly de-icing fluids is becoming greater. The SAE are currently working on setting an aviation de-icing fluid (ADF) standard to encourage manufacturers to use environmentally benign[58,59] chemicals to reduce toxicity and reduce the environmental impact.

1.6 Selection and Application

Before an aircraft is de-iced or anti-iced the pilot in command (PIC) of the aircraft must consider the lowest operational use temperature (LOUT) of the fluid they wish to use, the outside air temperature (OAT) and the holdover time that is required.[4,31,37,38,54,60] This is primarily due to de-icing fluids having specific operational temperatures.

The LOUT is concentration dependent and is normally determined from the glycol concentration which can be determined through the use of a refractometer. The LOUT is the lowest temperature at which the fluid meets the aerodynamic acceptance test, as tested by the test houses, or it is the actual freezing point of the fluid plus a freezing point buffer. Buffers have been put in place to act as a safety net. Type I fluids have a 10°C buffer and Type II, III and IV, 7°C buffer.[32,33,37,61] These values are stated by the manufacturers. A fluid must not be used when the outside air temperature is below the LOUT of the fluid. Once the OAT and LOUT of the chosen fluid is determined the correct concentration of fluid can be applied to give the required holdover as published in the regulations.[2,35]

Fluids can be applied in two ways, either by using a one step procedure or a two step procedure. A one step procedure is normally selected for use when there is visible frozen contamination on the critical surfaces of the aircraft but there is no further precipitation.[26,37,54,60] This is performed by using heated diluted Type I de-icing fluids and is sprayed at temperatures of 80–95°C through a high pressure nozzle directly onto the surfaces of the aircraft to remove any ice, frost or snow. A one step procedure can also be performed when a heated Type II/IV anti-icing fluid is used as a de-icing and an anti-icing fluid in one. It can be used in this way when it is applied hot (60–70°C) and undiluted. Holdover time (HOT) starts as soon as the fluid is applied to the surfaces.[35]

De-icing and anti-icing products can also be applied in a two step process.[34,47,50,52,54,61] This involves using two different products. Firstly a de-icing fluid diluted accordingly is applied heated to the surfaces of the aircraft through a high pressure nozzle to

remove any frozen contamination. De-icing fluids have very low HOT of 3 minutes[35] therefore the second step must be started straight after the application of the de-icing fluid. The second step makes use of an anti-icing fluid.[33] But unlike the one step process the anti-icing fluids are applied cold and diluted. Type II/IV fluids can also be applied heated and diluted as the first step and then unheated and undiluted as the second step. In a two step process the holdover protection starts as soon as the second step is started and the anti-icing fluid is applied.

Each airport has their preferred method of choice based on the type of fluids they purchase, equipment available and the number of aircrafts to be de-iced.

1.7 New Technology introductions

De-icing and anti-icing fluids remain the most popular method for removing frost, ice and snow from aircrafts, however, there are other methods in use including the use of mechanical techniques and storage solutions. As well as the current methods being used, research and development into new advanced ways to remove ice, frost and snow from an aircraft are being developed. Infrared technology and the use of ice-phobic coatings are some of the new ways in which aircrafts can be de-iced.

1.7.1 Brooms

Although the de-icing of an aircraft is very well developed, in heavy snow conditions the method of choice to remove snow is through the use of brooms, scrapers and ropes.[2,4,31,37,38] These are used in the same way as you would with a car. This is because large amounts of snow would require large volumes of de-icing and anti-icing fluids therefore to minimise the use of these fluids the snow is first of all removed taking care to not damage any of the critical surfaces or sensors using the brooms. Ropes are generally only used on wings and stabilisers, and used by creating a seesaw motion across the contaminated surface to remove the ice, frost and snow. Although these techniques are thought of as being dated they are still relied upon today. These techniques still require the aircraft to be de-iced using a de-icing fluid afterwards.

Figure 1.9 Removal of snow using brooms and brushes

1.7.2 Hangars

One of the simplest techniques to prevent the build up of ice, frost and snow on an aircraft is to store the aircraft in a hangar.[47,62] Storing aircrafts in heated hangars prevents any accumulation of frozen contamination on the critical surfaces of the aircraft and hence does not require the use of ADF's to de-ice the critical surfaces. However, to ensure the aircraft can taxi safely from the hangar to the runway, anti-icing fluids may be applied if there is falling precipitation. Hangars can be an effective way of cutting the cost and use of de-icing fluids but the effectiveness of a hangar depends on the size of the aircraft, space available, departures times and amount of traffic. Therefore this technique is commonly employed in smaller airports due to the cost and space that would be required for larger aircraft.

1.7.3 Forced air

Forced air is a technique used when there is dry powder snow on the critical surfaces of an aircraft. Air is heated by a burner system which is then blown at high pressure across the surfaces of an aircraft removing the dry snow.[4,38] If there is wet snow on the surfaces this system can also make use of anti-icing fluids to create a hybrid system, whereby the anti-icing fluid is added to the air stream as it is applied to the surfaces of the aircraft.[62] Some airports have adopted this technique as part of their de-icing program and most commonly use it to blow dry snow from aircrafts that are parked overnight. Although this technique can reduce the amount of de-icing fluids to be used it does not eliminate them, especially when there are icy and wet snow conditions.

1.7.4 Hot water

As well as de-icing fluids, hot water can be used to de-ice aircrafts. As long as the ambient air temperature is above -2°C (27°F) hot water can be used as a de-icer. The

water being used must be at least 60°C (140°F) and can be applied by spraying over the critical surfaces of the aircraft. This technique is only permitted if an anti-icing fluid is then applied on top. This technique can cut the expense of using de-icing fluids and is successful during relatively mild winters.

1.7.5 Infrared

Infrared technology is one of the newest means of de-icing aircrafts without the use of de-icing fluids.[56,63] Aircrafts are de-iced using infrared energy that is generated from energy processing units (EPUs) that are placed in an open ended hangar structure. The EPUs are fuelled by natural gas or propane fired emitters which emit IR beams on to the surfaces of the aircraft contaminated with ice, frost or snow. The IR acts by melting the frozen contamination which can then evaporate off of the surfaces, the IR beams do not heat up the surrounding air and if the surfaces are dry the IR beams are reflected off the surface.[62] The IR energy generated from this system can be adjusted to suit different types of aircraft and severity of frozen contamination. This technique is very successful when used to de-ice aircraft and has similar de-icing times to that of conventional de-icing fluids. There are currently three IR de-icing facilities in the US in operation with the largest based at JFK International Airport as well as one in Norway, Oslo. Whilst this type of system is very successful at de-icing aircrafts it cannot provide anti-icing protection, therefore until this technology is improved to provide such properties, the use of anti-icing fluids after de-icing using IR is still required.

Figure 1.10 Infrared hangar structure for de-icing

1.7.6 Ice-phobic coatings

One of the newest areas that is gaining interest very rapidly is ice-phobic coatings.[64,65] These coatings are typically used on power lines, turbines and buildings to prevent the formation of ice. The use of ice-phobic coatings in the aviation industry could potentially isolate the use and need for de-icing fluids. Unlike de-icing fluids which are applied every time an aircraft needs de-iced an icephobic coating would be

applied once to the surfaces of the aircraft, removing the need for it to be applied every time the weather changes. These types of coatings have included the development of super hydrophobic surfaces[66,67] created through the use of polymers such as Teflon (PTFE)[68] or silicon[69] based matrices. Some of the early examples were created around the idea of lotus leaves, with its high water repellency and self cleaning properties being applied to ice-phobic coatings.

Figure 1.11 Water repellent Lotus leaves

Creating coatings with polymers or nanoparticles can result in textured surfaces. One design makes use of textured surfaces to trap air,[70] which prevents the water from freezing when in contact with the surface; however these encounter problems if the grooves on the surfaces become blocked with frost. Another type of coating makes use of the latent heat[71] released from the water droplets as they freeze to deflect them away from the surface, but this only works well below atmospheric pressure. Biomimetic ideas from nature and biology, such as penguin feathers[71,72] are currently being developed with the properties of water repellency and ice prevention being key. The most successful icephobic coating created to date was published in March 2016, from the University of Michigan.[73,74] They created an icephobic coating using knowledge based on the ice adhesion strength relative to different surface materials. A polydimethylsiloxane (PDMS) elastomer impregnated with oil with low degrees of cross linking was created that had ice adhesion strength of 6 kPa. A coating with ice adhesion strength below 100 kPa is classified as icephobic. Surfaces with low ice adhesion strengths prevent ice from sticking to them and instead the ice slides off. However, although these type of coatings are great in principle, they are not permanent and would need reapplication after a set amount of time, the durability of the coatings during de-icing cycles has been shown to decrease with use, and the

process of applying these coatings is expensive. Research into this area continues to grow with emphasis on using ideas from nature.

1.7.7 SLIPS and SLUGS

Slippery liquid-infused porous surfaces (SLIPS) and self lubricating organogels (SLUGS) are alternative types of icephobic coatings[64,65] which are being developed to provide anti-icing protection to aircrafts. SLIPS are porous textured monolayer solids with lubricating films. One example from Wyss Institute,[75,76] showed the creation of a monolayer of polypyrrole (PPy). A highly textured layer of PPy was applied by electrodeposition on to an aluminium surface which was then fluorinated with a low viscosity lubricant that infiltrates the porous monolayer structure creating a lubricating film.

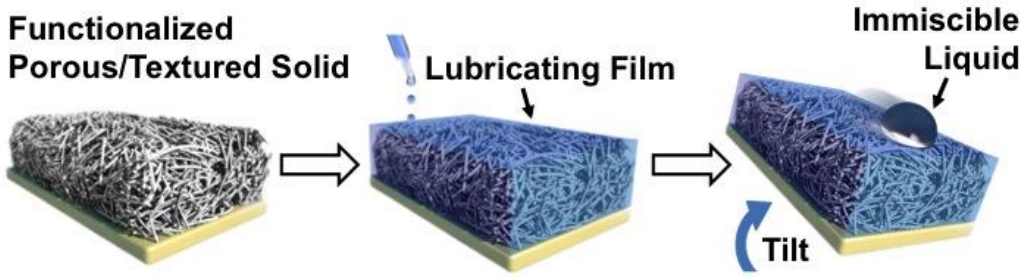

Figure 1.12 Creation of SLIPS and their water and ice repellent properties.[76]

These structures are water and ice repellent. However, environmentally, fluorinated solvents are an issue and alternatives need to be sought to act as lubricating films. The endurance and durability of these coatings are still questionable at high shear rates but they do have attractive repellent properties more suited to other industries.[77,78]

Similarly, SLUGS, (derived from the mollusc which secretes a mucus film for protection), makes use of polymers in a range of organic solvents which can spontaneously release liquids from an inner matrix to the outer surfaces to act as a protective barrier, known as the phenomenon syneresis.[79] Using the concept of syneresis these gels can be tuned by impregnating the PDMS network with organic liquids and the behaviour can be activated through the use of temperature. An advantage that SLUGs possess compared to SLIPS is that they are temperature dependent. At low temperatures these organogels leach solvent to act as a protective barrier and as they warm up again re-absorb the solvent back into the PDMS matrix.

In theory these types of gels would work well on aircrafts in winter conditions. However, although this is a nice concept when the solvent leaches from the gel it creates a thick layer on top of the coating which could potentially grow as the temperature drops and the aircrafts altitude increases. This could potentially affect the aerodynamics of an aircraft and cause mechanical failure of flaps and ailerons, similar to the effects experienced by frost, ice and snow.

Overall advancements are being seen within this area of self-de-icing and anti-icing aircrafts which may require less usage of de-icing fluids. However, all the icephobic, SLIPS and SLUG coatings that have been created so far all show difficulties when applying this to an aircraft, the lifespan of such a coating is uncertain, the endurance and durability is limited and they are currently expensive.

Research into new advanced coatings is underway as described above but research into alternative gel materials is an area that has not been thoroughly investigated or published in the literature. Developing new types of materials that can act as gels within de-icing or anti-icing fluids and hence form protective coatings at low temperatures could potentially allow for materials to be programmed with specific properties. Low molecular weight gels are one type of material which could potentially be used in this way.

1.8 Introduction to Low Molecular Weight Gelators

1.8.1 Soft Materials-Gels

Colloidal soft materials such as gels are commonly found in everyday applications.[80-84] They are generally easily recognised from their visual appearance as soft solids. However, being able to scientifically define a gel has shown to be notoriously difficult. The first attempt to define a gel was by Thomas Graham in 1861.[85] However the most famous and prophetic definition came almost sixty years later in 1926 by Dorothy Jordan Lloyd.[86,87] She noted that “the colloidal condition, the “gel”, is one which it is easier to recognize than to define”[86] however these empirical definitions of a gel relied upon the qualitative macroscopic observations that were available at the time. The first attempt to try and link the macroscopic properties with the microscopic properties were from Hermans in 1949.[88] Hermans suggested the following criteria:

(a) Gels are coherent colloidal dispersed systems consisting of at least two components

(b) They exhibit mechanical properties characteristic of the solid state

(c) Both the dispersed component and the dispersion medium are extended continuously throughout the system.

Flory[89-93] then went on to further define a gel using this as a basis. He stated that a gel has a continuous structure with macroscopic dimensions that is permanent on the time scale of an analytical experiment and is solid-like in its rheological behaviour. Due to the number of different materials that could potentially be classified as a gel Flory[89] went on to classify gels into four categories:

(i) Well-ordered lamellar structures

(ii) Covalent polymeric networks; completely disordered

(iii) Polymer networks formed through physical aggregation

(iv) Particulate disordered structures.

Although the definitions have advanced somewhat throughout the years it is still hard to find a simple definition for a gel, as a result many researchers revert to the definition provided by Dorothy Jordan Lloyd.[86]

1.8.2 Classification of Gels

Gels generally consist of two different phases which co-exist. These phases include a solid-like phase (also known as gelator molecules) and a liquid-like phase (solvent). A gel is formed when the solid-like phase is dispersed throughout the liquid-like phase, which then commonly forms a fibrous 3D network where the liquid-like phase is entrapped within the network.[87,91,94-97] The solvent is immobilised within the network due to capillary forces and surface tension preventing the bulk flow of solvent on the macroscopic level.[93,98] Technically a gel is neither solid nor liquid but instead may be thought of as an intermediate state. The coexistence of the two phases in a gel distinguishes it from a solid or a liquid, but also gives rise to the unique visco-elastic properties.

There are many different types of substances which could be classified as gels however the most common way of categorising a gel is based upon how the solid-like 3D network is formed and how reversible the bonds that stabilise the network are. Using this basis gels can be classified as chemical gels or physical gels.

Undoubtedly the most common gel we encounter in our daily lives are chemical gels. Chemical gels are usually derived from polymeric compounds.[99,100] A chemical gel is formed from covalent bonding and cross-linking between polymer chains. This gives

rise to an entangled polymeric chain network which extends throughout the liquid phase. The formation of these gels through strong chemical bonds such as covalent bonds means that these types of gels cannot be re-dissolved and are thermally irreversible.[101] The widespread exploitation of chemical gels is generally because they are chemically inert, stable, safe and reliable even after years of use. However, focus has increasingly shifted from chemical gels to physical gels, which allows the use of small molecules that can be programmed for use in responsive high-tech smart applications.

Physical gels also known as supramolecular gels are derived from low molecular weight molecules (gelator molecules) which self assemble and aggregate to form an entangled self-assembled fibrillar network (SAFIN).[90,94] The aggregation of the molecules is driven through complementary non-covalent interactions such as hydrogen bonding, π-π stacking, dipole-dipole interactions, van der Waals forces as well as hydrophobic and solvophobic interactions which immobilise the solvent and induce gelation in one dimension.[82,101-103] Due to the dynamic and weak nature of non-covalent interactions that stabilise the aggregates, supramolecular gels generally exhibit thermal reversibility.[101] These gels tend to be more responsive due to the non-covalent interactions and as a result are highly versatile systems.[104]

Low molecular weight gels (LMWGs) are a type of supramolecular gel. They are typically made up of small organic molecules with molecular weights below 2000 Da and can induce gelation in organic solvents and water. When they induce gelation in organic solvents they are classified as organogels, in oil, oleogels, in ionic liquids, ionogels and in water, hydrogels.[93,94] LMWGs often only require a few weight percent (or less) of the gelator to fully immobilise a solvent.[83] The small molecules used to create LMWGs are readily synthesisable and the ease of synthesis and the small nature of the molecules allows us to probe the molecular structure and characterise these gels easily to understand what controls the gelation event. Being able to synthesise these molecules easily and the formation of gels through non-covalent interactions makes it easier to incorporate functionality into the molecule, leading to more tuneable responsive materials.[102,104-106]

1.8.3 Formation of Gels

The formation of gels and hence the mechanism of gel formation can be broken down into its respectable primary, secondary and tertiary structures similar to proteins.[95]

This way, the gelation mechanism can be categorised from the molecular scale all the way to the macromolecular scale.

A typical gel is usually formed by adding a small quantity of a solid gelator which is insoluble or partially soluble at room temperature, to a solvent. Heat is then applied to the solvent which dissolves the gelator molecules creating a saturated isotropic solution, however other stimuli can be used to solubilise the gelator molecules.[80,83,93,107] In the isotropic solution the gelator molecules have a low degree of aggregation. Upon cooling the solution the intermolecular complementary non-covalent interactions provide the driving force for the molecules to self assemble to form the primary structure. Due to the anisotropy of the interactions this promotes the hierarchical self assembly of the molecules with one dimensional order.[98,108,109] This typically leads to the formation of fibrils, which self assemble and interact with one another to form fibres and/or fibre bundles which can give rise to tape, ribbon, fibre, sheet, vesicle or micelle morphologies which is directly influenced by the molecular structure (secondary structure).[81,95] The secondary structures then interact and aggregate further to form the tertiary structure. However, the transition from the secondary to the tertiary structure is determined by the type of interactions that can occur between the fibres. To form the continuous gel network cross-links between the fibres must be present. These can arise from the entanglement and/or branching of the fibres which can therefore entrap and immobilise the solvent.[108,110] Due to the nature of the cross-links being non-covalent they are therefore reversible. The subsequent interactions and cross-linking of the fibres with one another ultimately leads to the formation of a 3D sample spanning self assembled fibrillar network (SAFIN) corresponding to a gel on the macroscopic level (see **Figure1.13**).[93,94,96] These types of gels can assemble across multiple length scales and as such modifications on the molecular level can be expressed on the macroscopic level.

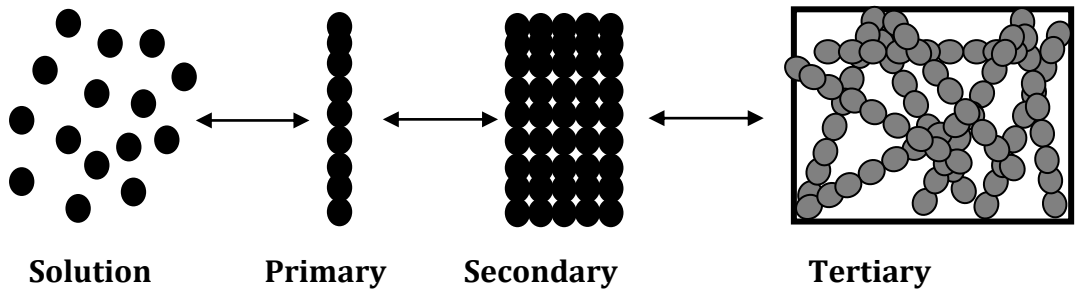

Figure 1.13 Formation of a gel from the isotropic solution to the tertiary structure that forms the macroscopic gel.

1.8.4 Gelation and Crystallisation

The formation of a LMWG through self assembly is closely related to crystallisation. It has often been noted that gelation and crystallisation are in fact competing processes.[111-113] By preparing a sample through the formation of a supersaturated solution and then allowing it to cool, it has been noted that instead of only gelation occurring there are in fact three possible outcomes. These include the highly ordered aggregation of the molecules giving rise to crystals, a random aggregation which results in an amorphous precipitate and/or an aggregation process between these two which gives rise to a gel (see **Figure 1.14**).[80,98,101] Therefore through this means of preparation there are obvious competing interactions occurring where ordered assembly of gelator molecules in one dimension leads to gel fibres whilst ordered assembly in three dimensions leads to crystallisation. With this in mind gelation is sometimes colloquially referred to as crystallisation gone wrong.[111]

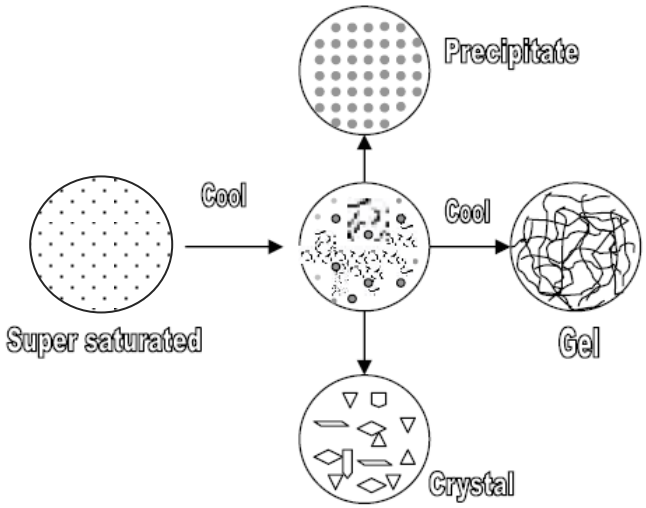

Figure 1.14 Three possible outcomes from the aggregation of molecules from a saturated solution.[80]

Crystal formation from a gel is based upon the fact that the gel state is a metastable kinetically trapped state where the gelator molecules are contained in both the gel and solution phases.[111,114,115] Over time, the free gelator molecules in the solution phase can aggregate and nucleate which instigates crystal growth and formation, which effectively decreases the concentration of gelator molecules such that more gelator is released into the solution phase. This promotes dissociation of the gel fibres and hence more of the gelator molecules are incorporated into the formation of the resulting crystals,[116] see **Figure 1.15**.

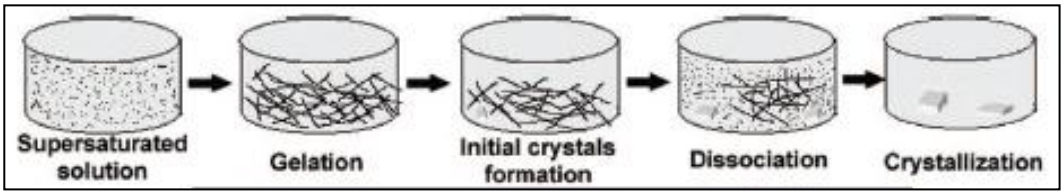

Figure 1.15 Conversion of a saturated solution to a gel and crystals with time.[116]

Therefore the ability of a LMWG to crystallise over time is a major drawback of these materials, and ultimately results in the collapse of the gel which limits its lifetime stability.[117] Therefore this is, and will be an area of great interest to develop in the future to identify accurately how to prevent crystallisation in gels.

Some authors researching this area have stated that slight changes in the molecular structure of the gelator molecules can cause one pathway to be favoured over another[112,113,117-121] however, this is still unpredictable. Others have tried to link the crystal's molecular packing structure to the molecular packing within a gel or xerogel,[116,120,122] although they show similarities, they often have different arrangements depending whether they are in the crystal or gel form. Most commonly the packing within a gel and a crystal cannot be correlated[114] however, being able to understand or even observe the packing of gelators in the gel phase is problematic and in many cases unattainable. It is clear that a simple method to predict the packing of potential gelators and their ability to form a gel or crystallise would revolutionise this field.

It remains a difficult and challenging task to design a gelator molecule from first principles and identify whether it will form a gel or crystallise, however there is sufficient literature available now that allows for broad assumptions to be made into the capability of a molecule to form a gel or not.[97,123-125] These assumptions include the solubility profile of a molecule, which has to be partially soluble but not too soluble such that it would dissolve, as well as partially insoluble, but not too insoluble such that it would precipitate or crystallise in a chosen solvent. The molecules must also be able to form strong self complementary non-covalent interactions which should have a tendency to form in a one dimensional direction to encourage fibril assembly rather than three dimensional crystal formation.[81-83,126] Despite these broad assumptions for the design of gelator molecules it still remains a trial and error process and gelators are often discovered through serendipity.[124] It is somewhat easier to modify a known gelator in order to modify its gelation profile and/or introduce new aspects of functional behaviour.

1.8.5 Stimuli used for the formation and destruction of gels

LMWGs are commonly formed through the use of an external stimulus. External stimuli may be physical or chemical.[80,93,101,110,127-129] Being formed in this way opens the possibility for these types of gels to be responsive to many varying stimuli potentially enabling many different applications.[101,128] The most common way of forming a gel is by heating a small amount of solid gelator in a chosen solvent until a homogeneous solution is formed. This solution is then allowed to cool and over time a gel forms. Using heat-cool cycles in this way allows for the gelator molecules to be dissolved and the interactions to be formed between the gelator molecules to aggregate and form a gel. However applying high temperatures to a formed gel can also disassemble the gel into its solution state. This transition from a gel to solution is a property that is commonly measured and is referred to as the temperature of the gel-sol transition known as the T_{gel}. As the formation of a LMWG is usually enthalpy driven an increase in temperature shifts the equilibrium to the solution state, where the entropy gain of having the gelator molecules free in solution rather than in organised aggregates becomes more favoured. As the temperature increases it will eventually reach a temperature where the entropy will outweigh the enthalpic benefit of the intermolecular interactions that form the aggregates within the gel and the gel network will disassemble.[95,96,123,127,130] Whilst heat-cool cycles are the most common type of stimulus used to form gels there are a number of other external and chemical stimuli that may be better suited to particular applications to create responsive gel systems.

Gels have been shown to form through the use of ultrasound/sonication.[131-134] A nice example where a gel was induced by sonication/ultrasound was by Naoto and Koori.[135] They demonstrated that a dinuclear palladium complex could instantly gelate a number of organic solvents when irradiated with ultrasound for a few seconds, turning the homogeneous solutions into opaque gels (**Figure 1.16**). The stable gels were also thermoreversible when heated above their T_{gel} values. They noted that the sol-gel transition could be repeated indefinitely with no degradation of the gelator molecules. They rationalised that gelation is not induced in the solution phase due to the "clothespin-like" bent conformation of the complex, only when sonication/ultrasound is applied the polymerisation is initiated which causes a selflock-interlock conversion where the complex is stabilised by intramolecular π stacking interactions.

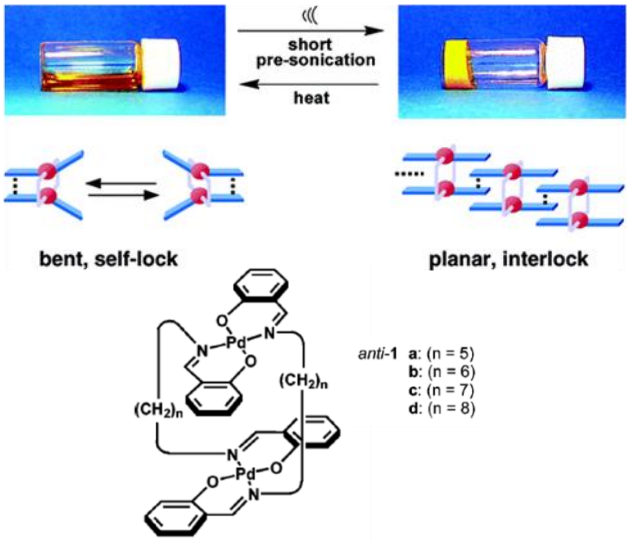

Figure 1.16 Ultrasound induced gelation of a dinuclear palladium complex[135]

Photoresponsive gels can also be formed using light to trigger a reversible gel-sol transition.[94,136,137] By incorporating responsive groups into the molecular building blocks of a LMWG, such as azobenzene moieties which are known for their photoresponsive properties,[138,139] photoresponsive gels can be formed. Shinkai and co workers[140] used this concept to design a LMWG with an azobenzene group on a cholesterol based gelator (**Figure 1.17**). They demonstrated that gelation could be induced by the *trans-cis* photoisomerisation of the azobenzene moiety. By irradiating a formed gel in butanol with UV light (330-380nm) they could convert the gel to the solution state where the gelator isomerised to the *cis* form.[140] If the solution was then irradiated with visible light (>460nm) the solution could be converted to the gel form by isomerising the *cis* form to the *trans* form of the gelator which gives rise to the gel.

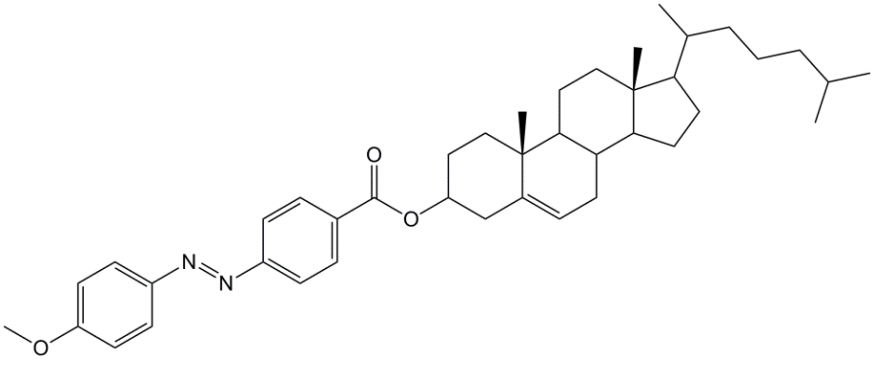

Figure 1.17 Photoresponsive azobenzene cholesterol based gelator[140]

As well as physical stimuli such as temperature, sonication and light, as described above, gels can also be formed through the use of chemical stimuli such as a change in pH,[114,141-145] the use of anions and/or cations, redox reagents[92,146-150] as well as enzymes.[151-153] Adams *et al*[141] have created a protocol to induce gelation through the

means of pH by using glucono-δ-lactone (GdL) instead of dilute aqueous acids. Using dilute acids to change the pH of a system does work well however it has been noted that the gels formed are inhomogeneous. GdL allows for a more controlled pH change, due to the slow hydrolysis of GdL into gluconic acid. Using this principle they designed Fmoc-dipeptide gelators (**Figure 1.18**) which allowed for the formation of controlled, reproducible and uniform transparent gels. The Smith group[143] have designed some novel LMWGs which make use of the GdL principle reported by the Adams group. They showed that basic solutions of dibenzylidene-D-sorbitol appended with carboxylic acid groups could also be formed in this way. Using this simple pH changing method allows for the formation of LMWG that have the potential to extract dyes from water and hence be used in water purification[154] and environmental remediation applications.[155]

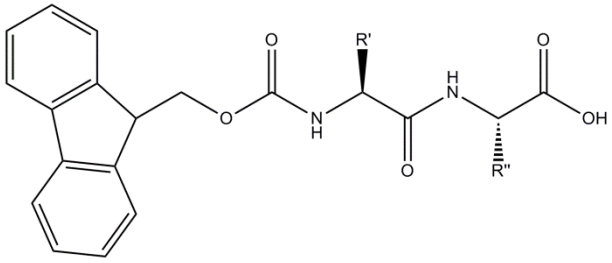

Figure 1.18 Generic structure of Fmoc-dipeptide gelator. R' and R'' = alkyl chains.

Some applications however, require instant gelation. This has been commonly reported for reducing the environmental impact of oil spills.[127,156,157] The first report of this type of gelation was by Bhattacharya and Krishnan-Ghosh.[156] They reported the phase selective gelation of oil from oil/water mixtures. Using a simple amino acid derivative, *N*-lauroyl-L-alanine, they demonstrated that oil could be selectively gelled from an oil/water mixture. However due to the LMWG requiring heat to be solubilised they reasoned this significantly limited their use for the containment of oil spills. John and co workers[157] went on to develop this idea further using open chain dialkanoate derivatives of the sugar alcohols mannitol and sorbitol. They demonstrated that gels based upon mannitol could immobilise food and fuel oils in the presence of an aqueous phase at room temperature through the use of a carrier solvent (ethanol). Using the carrier solvent to solubilise the gelator this then could be added to the biphasic mixture of oil and water. Forming gels in this way sees the ethanol partition into the aqueous phase whilst the gelator partitions into the organic phase which induces gelation. The authors also showed that the gelled oil could be recovered by removing the water and distilling the oil above the T_{gel} of the gel

(**Figure 1.19**). Therefore not only could they recover the oil but the LMWG could also be recovered which could be reused again. Therefore this type of LMWG has the ability to gel potential crude oil in sea water by limiting the spread of the pollutant and aiding the recovery of the oil. Raghavan and co workers[158] have developed a similar system which makes use of co solvents that can induce gelation in underwater pipes for the self repair of oil leaks.

Gels do not of course just have to be responsive to one type of stimuli, they can be multi-responsive.[96,128,159,160] By incorporating several stimuli responsive moieties into LMWGs, multi-responsive gels can be formed. A number of examples of responsive gelators which respond to multiple stimuli have been published. Each of the examples that have been demonstrated above shows the diversity in which gels can be responsive.

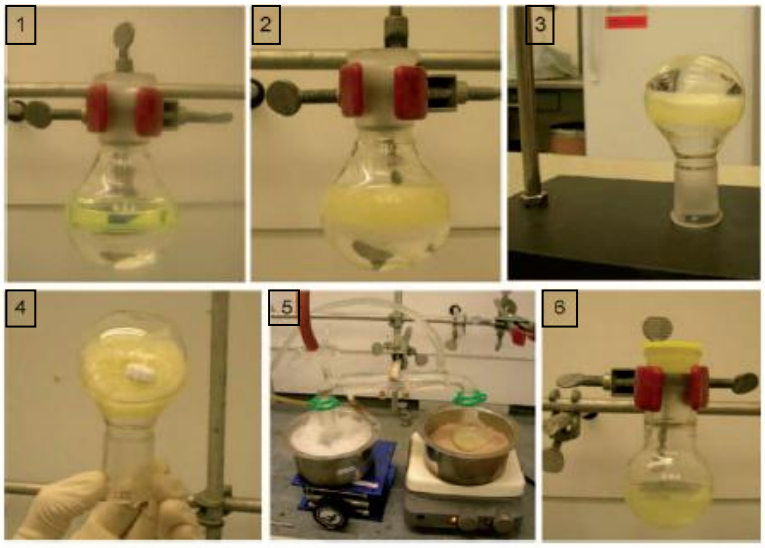

Figure 1.19 Sugar alcohol derived LMWG capable of gelling an organic phase in the presence of water. The gelled oil shown in **2**, **3** and **4** can be recovered by distillation (**5** and **6**) and the gelator reused.[157]

1.8.6 Influence of Solvent

When considering the formation of a supramolecular gel, it is tempting to focus on the structure of the gelator molecule that forms the self assembled 3D gel network. However, the vast majority of a gel is solvent. Most commonly a gel will be comprised of 99% solvent, or in some cases more.[80,93,96,127,161-163] Therefore because the solvent/liquid-like phase is the major component of a gel it is vitally important that we understand the role played by the solvent in controlling the materials performance and properties.

For gelation to occur it is necessary to have the correct balance of solubility and insolubility. Given the similarities to crystallisation it is not surprising that the solubility of a given molecule is important. Therefore if a molecule exhibits high solubility in a chosen solvent the solvent-gelator interactions will be favoured preventing gelator-gelator interactions from occurring to form a gel producing a solution. However, if the molecules are too insoluble it will form a precipitate. Gelation can therefore be thought of as an intermediate state somewhere between solubility and crystallisation, where the correct solubility balance is achieved.

LMWGs are known to have the capability to gel a number of solvents including organic solvents,[81,90,110,164-167] aqueous media,[95] ionic liquids[168-170] and liquid crystals.[171-173] In some cases more than one type of solvent can be gelled by a particular molecule but being able to predict which solvent will gel and which won't is a difficult task. An example where a gelator molecule was able to gel more than one type of solvent was demonstrated by Maruyama and co workers.[168] They showed that a family of peptide based amphiphiles had the ability to form gels in aqueous solutions, organic solvents, edible oil, biodiesel and ionic liquids requiring only low concentrations of gelator, 0.1-2 wt %, see **Figure 1.20**.

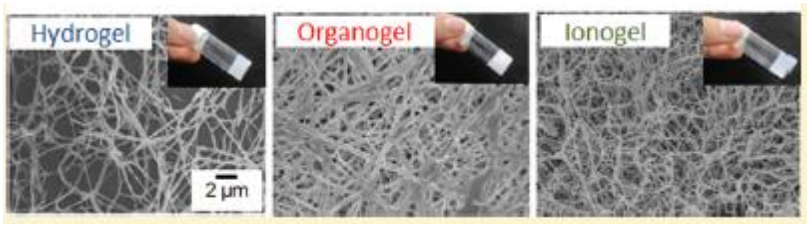

Figure 1.20 Gels formed in aqueous media, organic solvents and an ionic liquid by peptide based amphiphiles. SEM images shows the fibrous nature of the gel networks formed in each solvent.[168]

To find a versatile gelator molecule is difficult, as most gelators are only capable of forming gels in a particular type of solvent depending on the types of interactions it can form. From **Figure 1.20** we can also see from the SEM images of the fibrillar networks that the solvent creates morphological effects which are dependent on the solvent. Solvent effects, on the morphology and chirality of gels have been reported by a number of groups.[124,161,168,174-182]

As versatile gelators are difficult to discover, most researchers are now focussed on understanding and obtaining the correct balance between solubility and insolubility in order to achieve gelation. Most commonly, researchers have tried to deduce the correct balance through the use of solubility and dissolution parameters.[174,183,184] An

incisive review by Rogers and co workers[185] demonstrates the vast amount of research that has been undertaken in understanding the effects solvents have on gelation through solvent parameters. As such researchers have tried to correlate the macroscopic properties of a gel with different solvent parameters including dielectric constant (ε_r),[186-188] refractive index (RI),[185] Reichardt's $E_T(30)$[186,188-190] and Hildebrand solubility parameters,[189,191] however each of these on their own lack the specificity to achieve a global perspective for a range of gelators. Other authors have also looked into the solvent properties through the use of multi-term solvent parameters such as Kamlet-Taft,[163,188,192,193] Catalan's,[194-197] Swain,[198] solvatochromic, Flory Huggins[199,200] and Hansen solubility parameters.[187,188,201-203] Although these solubility parameters can help improve upon the knowledge of solvent effects, how a solvent may interact, gel stability and how they assemble hierarchically they are more successful when determining the solvent effects for a particular molecule. However, at the moment there seems to be no known universal approach to determine the gelation ability of a particular molecule with a type of solvent. In order to develop a universal gelator *a priori*,[185,202] a greater understanding of the relationships between the different properties associated with each of the solubility parameters of a solvent with the varying molecular structure of the gelator molecule may make this possible.

Within de/anti-icing the major component within any of the products is glycol. However, within the literature it is apparent that monomeric glycols and aqueous mixtures of them with low molecular weight gelators have not been the focus of significant study. The focus remains primarily with polymeric glycols and how their performance and attributes with low molecular weight gels can be used within industries such as cosmetics and plastics.[204-208] Therefore this study will enlighten on the use and gelation capabilities of such solvents for future potential use in de/anti-icing applications.

1.8.7 Types of Gelator Molecules

New types of low molecular weight gelators are often described as being discovered serendipitously rather than through design.[97,123,124,126,129,167,209] Many have attempted to try and determine a way of designing LMWGs but to no avail. The difficulty of designing a LMWG primarily lies within the molecular structure. The diversity of the molecular building blocks which are capable of forming gels are so unpredictable that it is a challenging and daunting task to identify what has the potential to form a gel and what has not. However, what is known is that the molecular building blocks must

have the capability to form strong intermolecular non-covalent interactions in one direction which encourages the growth of the molecular building blocks into fibrils, then fibres which creates the 3D self-supporting gel network.[80,93,97,101,110,129,162,185,210,211] As well as this, on the molecular level the molecular building blocks must have a solubility profile which exists between complete solubilisation and insolubility for gelation to be induced.

The simplest LMWGs based upon their structure are n-alkanes, see **Figure 1.21(1)**. Abdallah and Weiss[110,166,212] have reported how long alkanes with between 24 to 36 carbons can immobilise a number of organic solvents, including shorter chain alkanes. It was surprising to these authors that these molecules could in fact form gels due to the molecule not having functional groups which could donate H-bonds. Therefore these types of gelators solely rely on van der Waals forces to provide solid gel networks. These very simple gelators were shown to be highly effective despite being formed only through van der Waals forces. Alkanes can also often be found as being a functional group within other gelator molecules. The incorporation of alkyl chains allows for the introduction of van der Waals interactions as well as tuning the solubility of a molecule in a chosen solvent.

The lack of hydrophilic groups within alkane gelators results in poor water solubility, making them unsuitable for hydrogelation. Therefore, incorporating an oxygen or nitrogen functional group within the molecule can potentially increase the molecules solubility in polar or water-based solvents by increasing the different types of interactions that can occur. Further additions to alkanes such as a carboxylic acid group on a C18 alkane chain leads to one of the most famous and widely studied molecular gelators, *R*-12-hydroxystearic acid (HSA),[213,214] see **Figure 1.21(2**) which has been successfully used within the lubrication industry.[215-217]

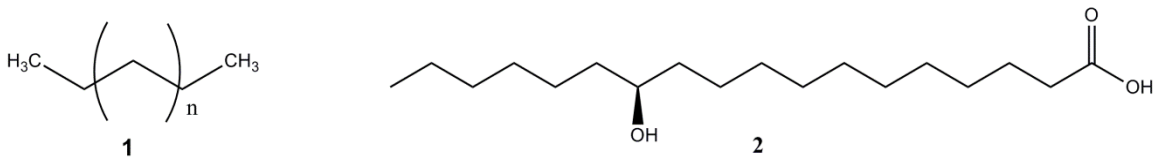

Figure 1.21 Molecular structures of n-alkane gelators (**1**) and *R*-12-hydroxystearic acid (**2**).

By adding functional groups to what starts as simple molecular structures we can make even more complex and diverse LMWGs. The various different amino acids that are available, allow for the creation of peptide and urea based molecules which have shown to act as effective LMWGs, see **Figure 1.22**. With the addition of these

functional groups Hanabusa[218-221] and van Esch[222] have shown that LMWGs assemble through the formation of intermolecular hydrogen bonds of the amide or urea groups, and if they are appended to alkyl chains, van der Waals forces also contribute to the formation of a gel. Bisamides and bisureas have also shown potential as LMWGs.[81,138,223-225] Peptide based gelators have been extensively studied[113,132,133,137,142,152,164,226-229] and many LMWGs have peptides conjugated to aromatic groups,[230-235] including Fmoc dipeptides,[141,236-243] pyrene dipeptides[244] and naphthalene peptides.[245-247] These types of gels are commonly formed as a result of hydrogen bonding between peptides and π-π interactions between the aromatic groups.

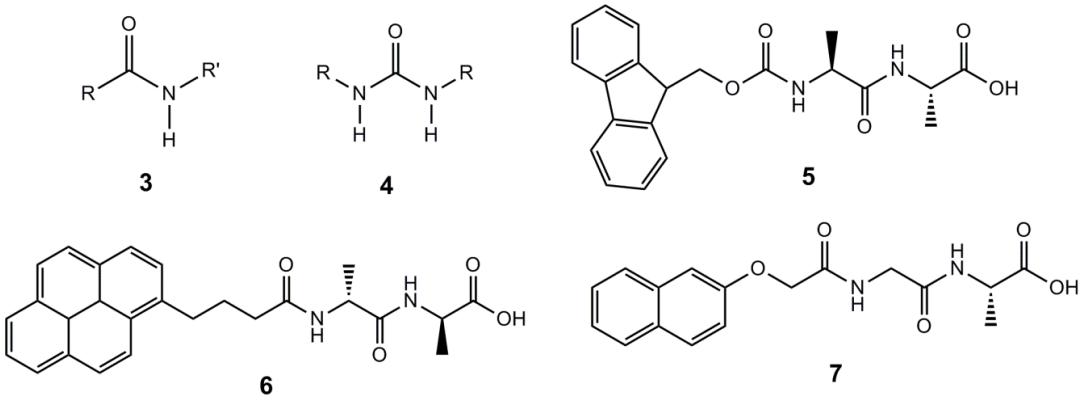

Figure 1.22 Peptide (**3**) urea (**4**), Fmoc-dipeptide (**5**), pyrene dipeptide (**6**) and naphthalene dipeptide LMWG (**7**).[127,142] R=Alkyl chain R'=Aromatic/Alkyl chain.

There are also other gelator molecules which are based upon biological molecules including a range of steroids,[93,95,97,101] sugars[105,157,248,249] and nucleobases[250] which have all proven effective at forming gels, see **Figure 1.23**. Even more complex systems somewhat similar to polymers such as oligomers and dendrimers[251,252] have also proven they have the ability to form LMWGs. The dependence of a molecule to be able to form a gel is based upon whether it can form multiple self complementary non-covalent interactions between the building blocks. Molecular structures containing more functional and varied groups will therefore be able to make numerous different types of interactions to aid directional self assembly, although they may find it more challenging to organise them effectively.

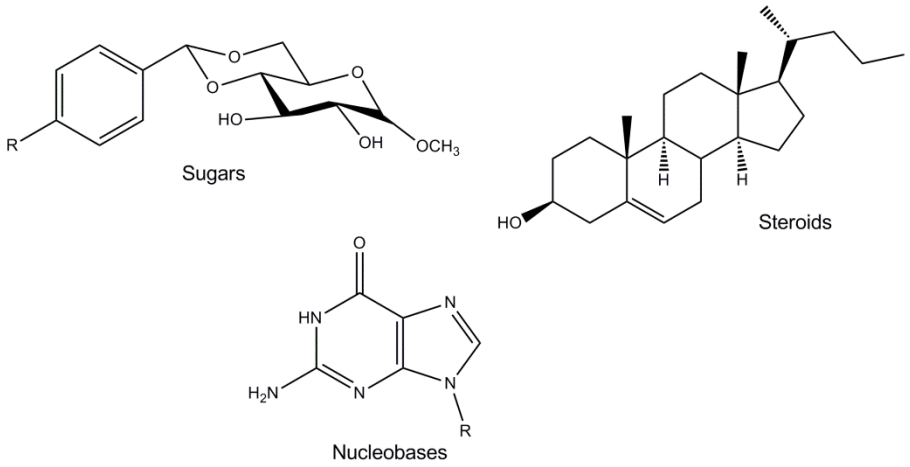

Figure 1.23 Complex LMWG based upon sugars, steroids and nucleobases.[93-95,121] R=Alkyl chain.

LMWGs are most commonly found building on the success of one molecule. From a single molecule the structure can be manipulated and amended in such a way to create possible libraries of LMWGs. Hanabusa and Feringa are some of many researchers that have extensively exploited this concept with urea-urea hydrogen bonding, showing that one dimensional self assembled gels can form organogelators that can comprise of acyclic,[253,254] cyclic,[255] geminal[256] and tripodal[257] urea groups (**Figure 1.24**). However, although LMWG structures seem to show endless possibilities there is not one universal gelator that has the capability of gelling all types of solvent.

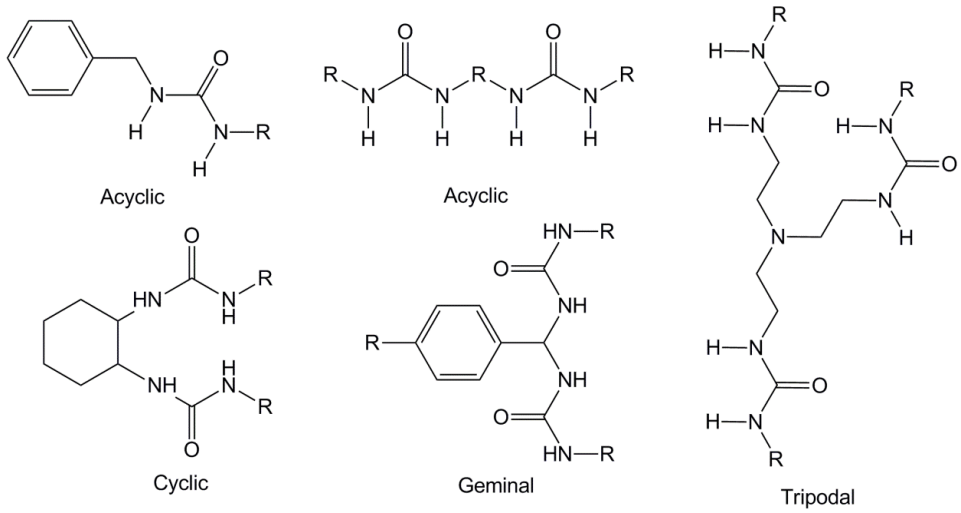

Figure 1.24 Extensive exploitation of urea hydrogen bonding motifs that can create larger families of LMWG's. R=Alkyl chain.

LMWGs have shown to be versatile, diverse, multifunctional materials and as such have seen widespread use in a number of applications ranging from tissue engineering,[109,258] drug delivery,[101,109,259,260] food,[229,259,261,262] cosmetics,[263-265] electronics, bio and chemical sensors[102] as well as environmental remediation[155,266]

and pollutant removal.[267,268] The diverse range of molecular architectures that act as LMWGs, and their ability to form gels in a range of differing solvents, means they can be specifically tuned to a particular application. This research will therefore focus on their properties and performance capability to act as a potential de/anti-icing fluid additive for use on aircrafts in winter conditions.

1.9 Aims

This project will investigate the use of simple, easily synthesisable, cheap and environmentally friendly low molecular weight gelators to act as alternative thickeners for use as de/anti-icing fluids on aircraft in winter conditions. Initially, we aim to identify potential hydrogelators and organogelators from the literature to create a family of molecules varying in molecular structure. Using this family of LMWGs, their ability to gel industrially relevant solvents such as 1,2-monopropylene glycol, 1,3-monopropylene glycol, monoethylene glycol as well as aqueous mixtures of glycols used within the de/anti-icing industry will be investigated. We will then identify the lowest possible useable concentrations as well as their response to temperature before analysing the different types of supramolecular nano-structures formed from the varying LWMGs.

We will identify an optimum molecular framework for this application. Using this molecule as a template we will synthesise a library of derivatives to optimise the ability to form gels in aqueous environments, for example by introducing hydrophilic and hydrophobic substituents. Investigating this library of LMWGs potential to form gels in glycol and aqueous glycol mixtures will give us a greater insight into the minimum concentrations required for gels to form, their response to temperature and how solvent mixtures effects the nano-structures formed from these types of molecules.

Specific optimised derivatives will then be investigated further to identify how they self assemble and how their assembly changes with solvent, before looking at their rheological profiles. Rheology will determine the strength, stability, nature of the samples and how these types of molecules respond to changes in temperature. Morphological analysis of gels formed in industrially relevant solvents will be investigated to identify if changes in the way how gels are formed changes the molecular architecture of a gel network, simulating real-life application.

With the potential of LMWGs to act as alternative thickeners, we will then investigate the potential of using these optimised molecules in complex de-icing fluids, to identify any changes in the gelation capability with the inclusion of other additives. To understand fully how this type of system could be used within the de/anti-icing industry we will analyse the effects through rheology to determine how strong the gels are, their stability, response to temperature as well as how long a gel would take to form if applied to an aircraft. To determine whether these types of systems could potentially be used in industry we will employ industrial testing to determine the holdover ability (how long an aircraft could be protected for) and how this type of gel system could potentially affect the aerodynamics of an aircraft.

Finally we will analyse the effects of adding LMWGs to even more complex fluids known as anti-icing fluids, which unlike de-icing fluids contains an additional polymeric thickener which under normal circumstances aids extended holdover times. By adding LMWGs to this type of system which already contains a gel network we will investigate the potential of creating hybrid gel systems. With the potential of increasing holdover times further we will investigate the ability of gels to be formed, their rheological profiles and morphology before subjecting them to industrial test methods to understand the effects to holdover and aerodynamics of an aircraft.

Overall this research will investigate the properties and potential performance of LMWGs in industrial solvents which could be used in the de/anti-icing industry to protect aircraft in winter conditions.

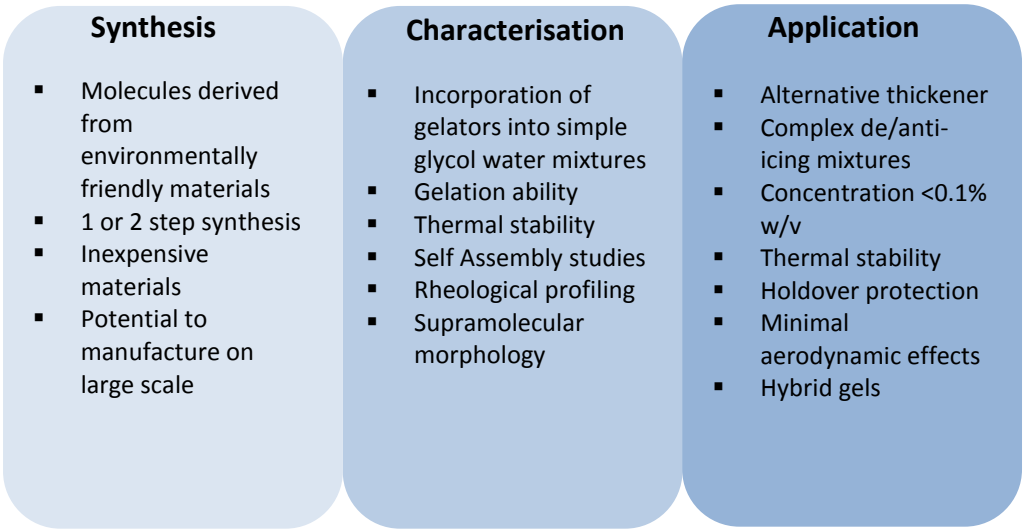

Figure 1.25 Summary of thesis aims.

Chapter 2

Low Molecular Weight Gelators

Chapter 2 Low Molecular Weight Gelators

2.1 Introduction to Low Molecular Weight Gelators

Low molecular weight gelators, as described in the introduction, are molecules which are capable of self organising into molecular gel networks. They can form gels in organic solvents, monomers, or polymeric melts (organogels), water (hydrogels) and ionic liquids (ionogels). They can be formed through the use of stimuli such as temperature, a change in pH or UV light to mention a few.[80,93,110,167] Upon the application of the stimulus the gelator molecules spontaneously form a 3D gel network which is held together through non covalent interactions such as hydrogen bonding, van der Waals interactions, solvophobic effects and π-π stacking. Low molecular weight gelators exist in a wide range of molecular structures including peptides, ureas, sugars, bile acids and alkanes amongst others.[81,90,93,95,115,129,166] These molecules have the ability to be used in various applications. They have been shown to possess the ability to be used in drug delivery, as biological and chemical sensors, electronics, lubricants, and within foods. The emphasis now lies on exploring these molecules in more depth to determine how they can be used in more advanced high tech applications.[101,102,109,155,267-269]

Many examples of low molecular weight gelators can be found within the literature, with wide structural variation. The large variety of these molecules allows for their potential introduction into and use in commercial applications. Some types of low molecular weight gelators have been shown to be successful in biomaterials where they can create scaffolds for tissue engineering[109] and nerve growth.[102,270] For example in a key study conducted by Ellis-Behnke et al,[270] hamsters were surgically blinded in one eye by severing the optic nerve. A peptide hydrogelator known to form a gel network of nanofibres, see **Figure 2.1**, through hydrogen bonding and hydrophobic interactions was injected into the severed optic nerve of a number of the test hamsters.

Figure 2.1 Self Assembly of peptide hydrogelator for use as biological scaffolds[270]

The hamsters which were treated with the hydrogelator showed 80% regeneration of sight in the damaged eye as demonstrated by the hamster's response to stimuli, see **Figure 2.2**, whilst the untreated hamsters remained blind.

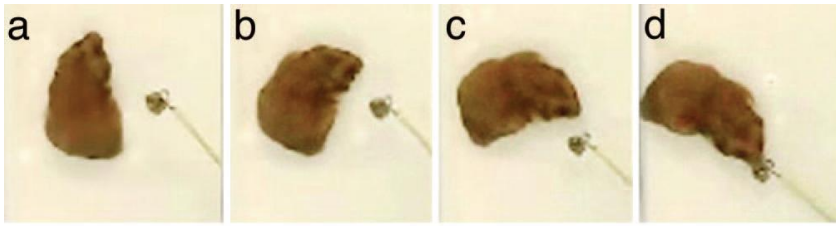

Figure 2.2 Hamsters response to stimuli demonstrating the restoration of sight.[270]

This remarkable regeneration of sight through the use of low molecular weight gelators demonstrates the successful ability of these types of gels to act as scaffolds for nerve re-growth as well as good compatibility within biological systems.

Low molecular weight gelators are also gaining momentum in drug delivery systems.[101,109] Van Bommel et al[153] have demonstrated the use of a cyclohexane trisamide-based hydrogelator to release drugs in a two step system. By using a previously reported cyclohexane trisamide[222,271] gelator as a scaffold they demonstrated through its modification by addition of an L-phenylalanyl-amidoquinoline (L-Phe-AQ)[272,273] moiety and ethylene glycol chains, a gel could be created which was responsive to both temperature and enzymes.

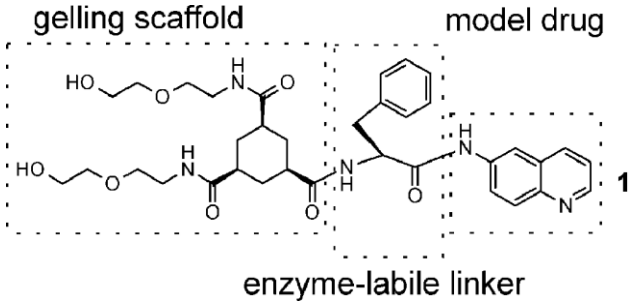

Figure 2.3 Cyclohexane tris-amide based hydrogelator used for two-stage enzyme mediated drug release.[153]

This gelator was able to contain the enzyme required for enzymatic cleavage of the model drug without losing any functionality. They showed through the use of temperature the gel nanofibres can be disassembled in the first step with the enzyme becoming activated thereafter, and hence cleaving the drug and releasing it to the specific target site. These drug delivery systems have the potential to reduce the toxicity attributed to drugs by delivering them to specific target sites and thus increasing their efficiency and efficacy.

Low molecular weight gelators are also starting to be used in foods to substitute trans and saturated fats which are detrimental to health. Rogers and co workers have demonstrated the use of phytosterols and γ-oryzanol[262] to form molecular gels to gel sunflower oil, see **Figure 2.4**. Using molecular gelators to structure oils has shown to have the additional benefits of reducing saturated fat content and in some cases also introduce health benefits associated with the molecules.[165]

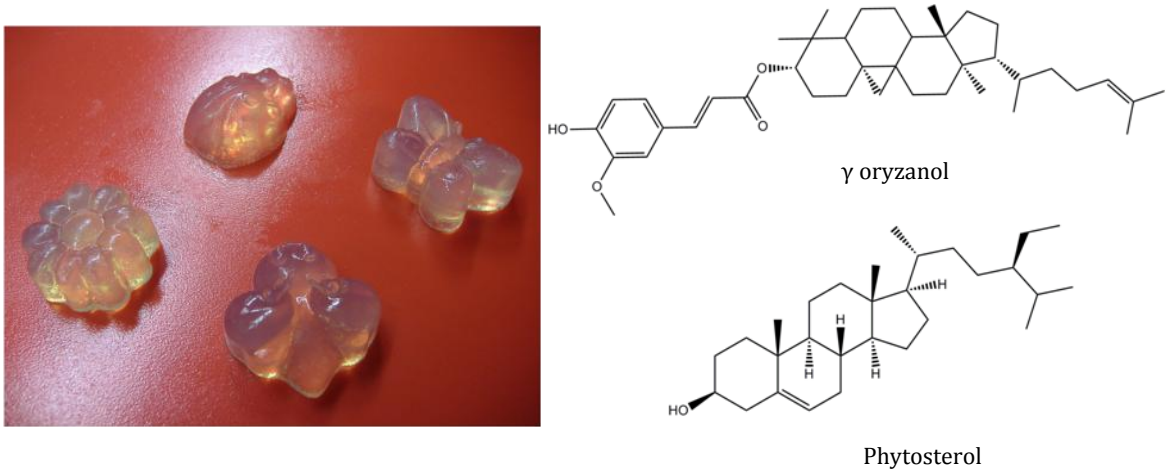

Figure 2.4 Left: Oleogels formed in sunflower oil for use in foods. **Right:** Structures of γ oryzanol and phytosterol.

Rogers and Wang have also shown through using a combination of phytosterols, fatty acids and ceramides, that oleogels[274] of sunflower oil can be made which can potentially be used in sauces and margarines. Using low molecular weight gelators as structuring agents in oils not only potentially helps to eliminate trans fat and reduce saturated fats it may open up a new area of advancement where foods can be used as a form of medication to reduce health complications (so called 'nutraceuticals'),[229,259,261,275] and provide new culinary experiences to our palates in the future.

Another field where low molecular weight gelators have proved to be viable is in the remediation of oil spills.[156,157,276-279] A recent study conducted by Raghavan and co workers[158] introduced a new paradigm for responsive gelation through the use of a sugar-based low molecular weight gelator to prevent oil spills before they happen. Unlike other gel systems which use external stimuli to induce gelation they demonstrated the use of co-solvents to act as a stimulus for gelation. Through the incorporation of a gelator in the oil phase and a co-solvent, the gelator effectively acts

as a safe guard to any leaks when oil is being pumped or transferred through pipes underwater, as gelation is activated if the system comes into contact with water.

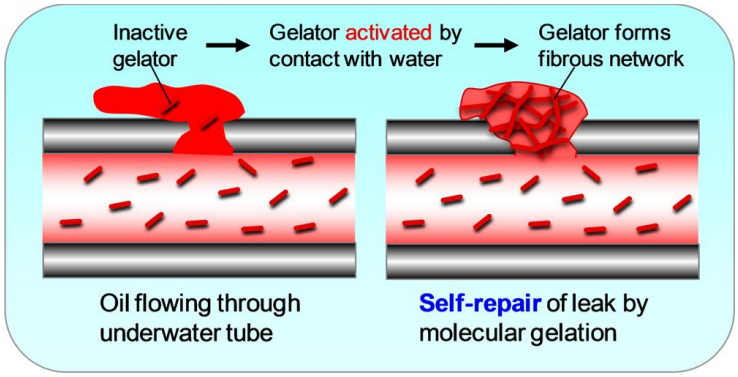

Figure 2.5 Responsive gelation of gelators in underwater pipes.[158]

They simulated an experiment to show the use of such systems in underwater pipes which may be used on oil rigs. Creating an artificial leak in a pipe they showed when the oil mixture with gelator comes into contact with water the co-solvent can immediately diffuse out into the surroundings of the leak point and induce gelation creating a seal to prevent further loss of oil, see **Figure 2.5**. This type of technology has the potential to be used in other areas highlighted by Raghavan and co workers such as the repair of biological tissue around wounds or other underwater and underground applications such as heating systems.

In most of the applications described in this section low molecular weight gelators are being used as potential alternatives to polymers which are used in everyday applications. Polymers are very large molecules which can prove difficult to control and are often not recyclable or environmentally compatible like low molecular weight gelators which form gels reversibly. The de/anti-icing aviation industry is an area where polymers are currently being used. Within de/anti-icing products the most common solvent systems encountered include glycols and aqueous glycol mixtures with added polymers. The polymers within these products act as thickening agents to create thick films. These films provide a specific amount of protection to an aircraft in winter conditions to allow it to take off safely. These products are sprayed at high temperatures which then set and create thick films when they cool down. One of the biggest problems with these products is that they are often stored at elevated temperatures for long periods of time, which can result in the degradation of the polymer and loss of its effectiveness to create thick films. Environmentally, polymers are difficult to collect and recycle into new products, and regulations are becoming more prevalent in this industry to prevent environmental contamination. Therefore

low molecular weight gelators could potentially eliminate the polymer degradation problem as they are reversible materials at elevated temperatures, whereby they remain as solutions of small molecules at high temperatures without degrading but can still form effective films for protection in winter conditions. Being able to tune and modify the structures of these molecules also allows for the adaptation and creation of environmentally-friendly gelator systems which could gel glycol and aqueous glycol mixtures which will be the focus in the future for this industry.

In this chapter we wanted to synthesise or source commercially, low molecular weight gelators which were easily synthesised, inexpensive and environmentally friendly. It is then intended that each of the molecules ability to act as a hydrogelator or organogelator in solvent systems relevant to the de/anti-icing aviation industry will be screened and their potential compatibility in this application identified. Their behaviour to temperature will be probed, to identify if they could be used in the required application, before finally gaining an insight into the internal structure and assembly of such gel systems.

2.2 Results and Discussion

2.2.1 Synthesis

The molecules illustrated in **Figure 2.6** were selected from reviews[95,102,211] published in the literature and had been described as hydrogelators or organogelators. The molecules were selected based on their ease of synthesis, one or two steps, (such that they could be manufactured and scaled up easily if required) and/or their commercial availability, the cost of starting materials and their associated environmental impact. The selected molecules were primarily based upon simple sugars or amino acids, as these motifs are known to have good environmental and biological compatibility. Nine molecules were selected with two being commercially available, ascorbic acid–6–palmitate and ditoluidene sorbitol.

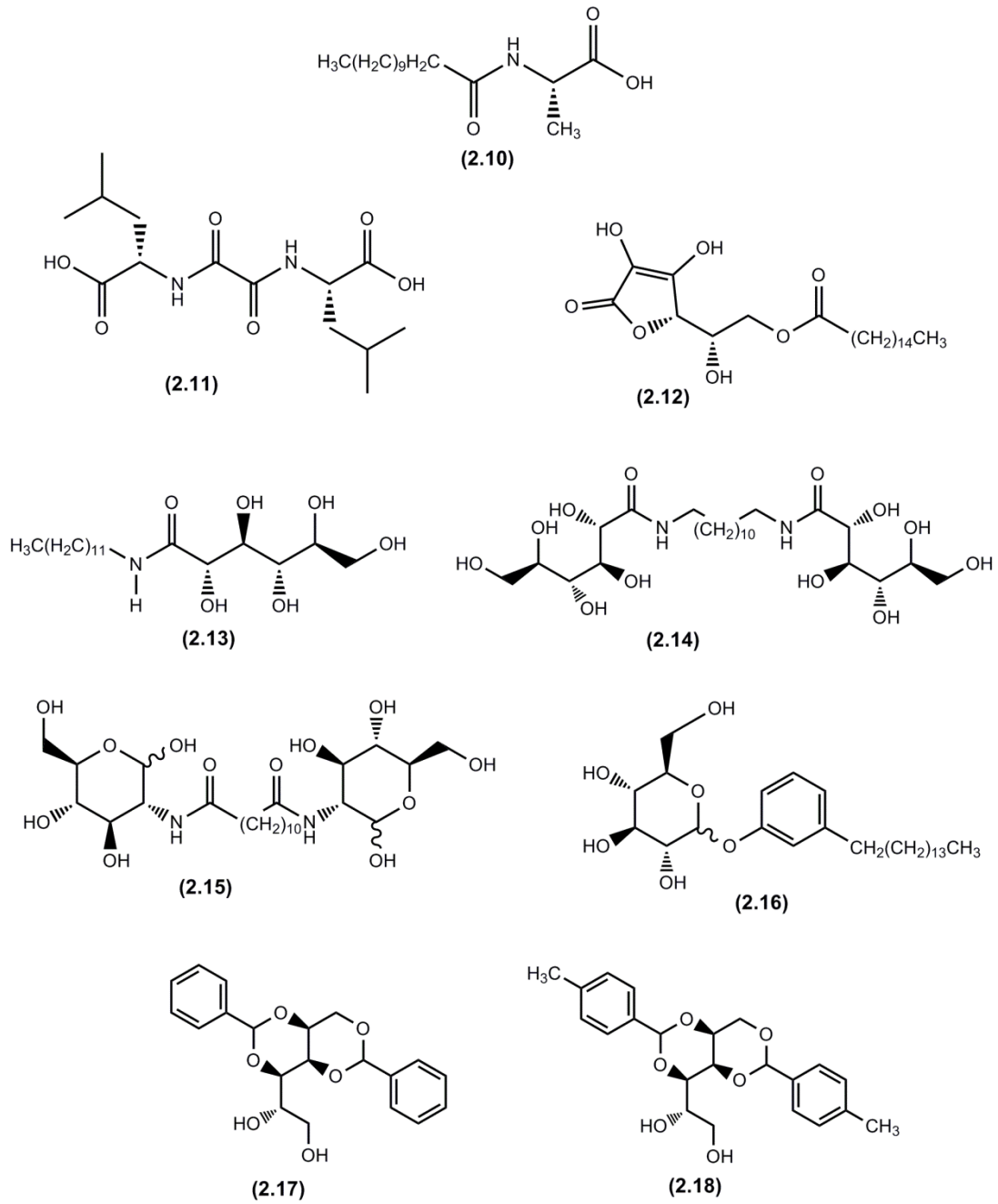

Figure 2.6 Structures of the nine molecules selected for testing.

N–dodecanoyl–L–alanine **(2.10)** was synthesised using a known synthetic procedure from the literature.[280] This molecule was formed through the addition of sodium hydroxide to L–alanine to form the salt which is more soluble in aqueous media. To this, dodecanoyl chloride was added in order to form the amide linkage. Finally acidification with hydrochloric acid reprotonates the molecule to form the carboxylic acid (**Scheme 2.1**). This was a very simple one pot reaction which gave the product as a white powder in very high yield (93%). NMR and MS characterisation demonstrated the success of this process.

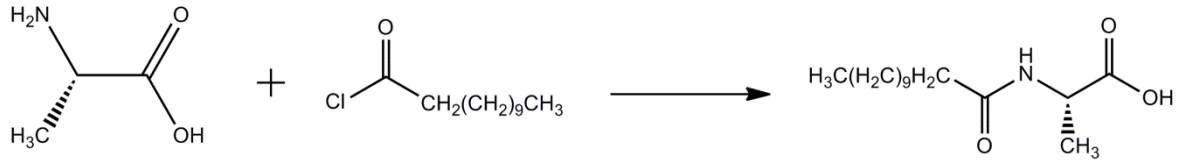

Scheme 2.1 Reaction scheme for *N*-dodecanoyl-L-alanine **(2.10)**.

Bis-(Leucine)-oxalyl amide **(2.11)** was also synthesised using a previously published method as shown in **Scheme 2.2**.[224] L–leucine was added to an aqueous solution of potassium hydroxide to form the leucine salt. Oxalyl chloride in dichloromethane and a solution of 4M potassium hydroxide was then added to create the amide linkages on either end of the molecule, with the potassium hydroxide solution acting to keep the molecule in the salt form. This exothermic reaction was performed at 0°C. The molecule was finally acidified to restore the carboxylic acid groups on either end of the molecule before being purified and dried. This produced a yellow powder with moderate to poor yield (30%). Once again all characterisation techniques supported the formation of the desired product.

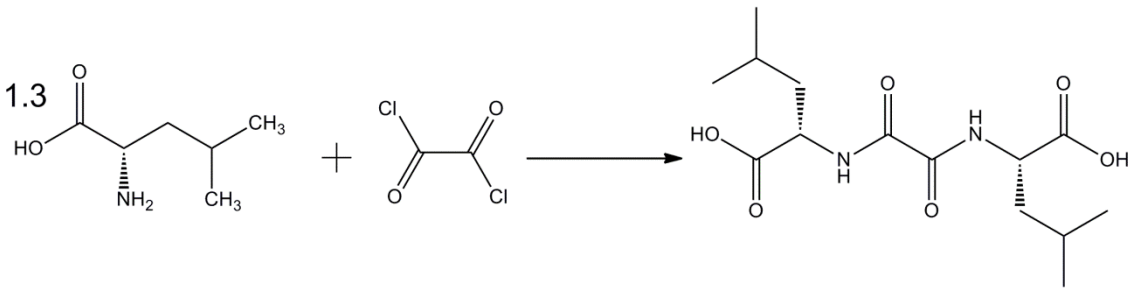

Scheme 2.2 Reaction scheme for Bis-(Leucine)-oxalyl amide **(2.11)**.

Ascorbic acid–6–palmitate **(2.12)** (**Figure 2.7**) was not synthesised for this study and was commercially available from Alfa Aesar. The molecule was tested using mass spectroscopy and NMR to confirm the correct structure and compared to the technical data provided by the manufacturer.

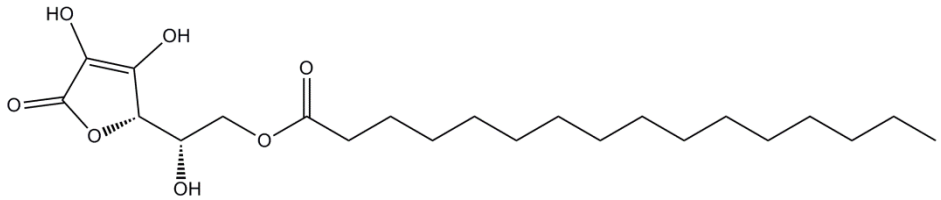

Figure 2.7 Structure of ascorbic acid-6-palmitate **(2.12)** used within this study.

N–dodecyl–D–gluconamide[281] **(2.13)** was synthesised extremely simply using a published method from the literature. Gluconolactone was reacted with dodecylamine in a methanol solution. This allows the nucleophilic addition of the amine attacking the carbonyl group in the gluconolactone ring. This then leads to ring

opening of the ester functional group to give rise to linear *N*–dodecyl–D–gluconamide **(2.13)** as a white crystalline solid in very good yield (92%), see **Scheme 2.3**. This reaction is stated within the literature to take approximately 30 minutes, however during the synthesis when the combined solution of gluconolactone and dodecylamine was refluxed for 10 minutes, the product appeared to have fully precipitated. After purification and drying, the identity of the product was confirmed through MS and NMR.

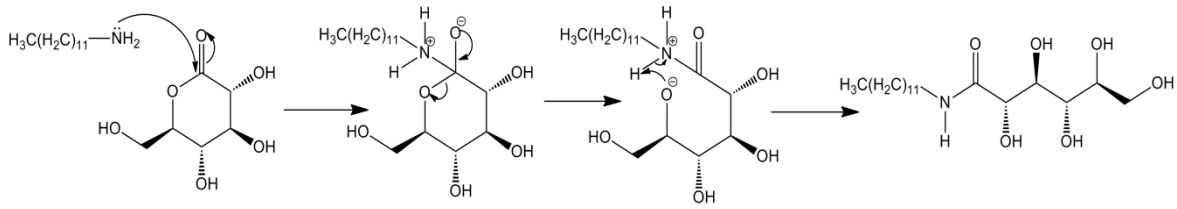

Scheme 2.3 Reaction mechanism for *N*-dodecyl-D-gluconamide

Two molecules with very similar structures were also synthesised to try and determine if open or closed rings affected the potential of a molecule to act as a gelator. These molecules were 1,12–digluconaminododecane **(2.14)** and Diglucosaminododecane **(2.15)**.

1,12–digluconaminododecane **(2.14)** was synthesised using a previously published synthesis [225] This was a one step reaction between 1,12–diaminododecane with gluconolactone in methanol which was stirred for 24 hours at room temperature (**Scheme 2.4**). Each end of the amine acts to open one equivalent of the ester group in gluconolactone to yield the product. This was purified and dried giving a white solid in very good yield (99%).

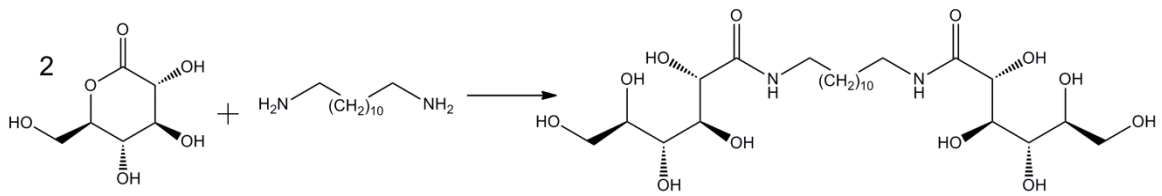

Scheme 2.4 Reaction scheme for synthesis of 1,12-digluconaminododecane **(2.14)**

However, to form the bolaamphiphile with closed sugar rings proved more difficult. This required a two step synthesis.[248] Firstly mercaptothiozoline and triethylamine were added to dichloromethane to deprotonate the ring nitrogen, then 1,12–dodecane dioyl chloride was dissolved in dichloromethane and added to the mixture and stirred for 3 hours to create the activated ester type intermediate in step 1, see **Scheme 2.5**. A mixture of glucosamine, triethylamine and the intermediate made in step 1 was then added to dimethylformamide (DMF) and reacted at 70°C for 6.5

hours then at room temperature for 20.5 hours (step 2), with nucleophilic addition of the glucosamine and substitution of the mercaptothiozoline unit creating the final desired product, which was a white powder with moderate yield (47%).

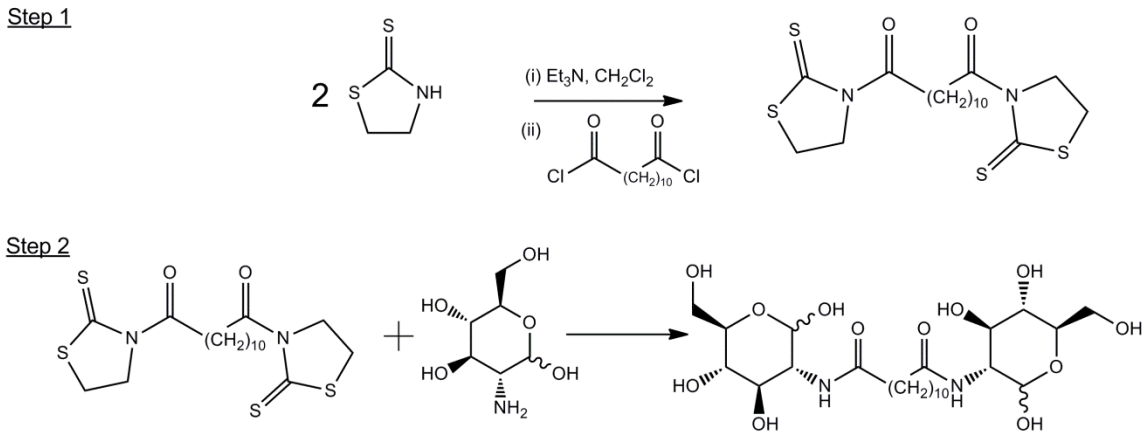

Scheme 2.5 Two step reaction scheme for the synthesis of Diglucosaminododecane **(2.15)**

Pentadecylphenylglucopyranoside **(2.16)** a cardinal glycoside[211] was synthesised to determine if this type of molecule, which makes use of by-product waste from cashew nut shells, formed using renewable raw materials was an effective gelator. This molecule was synthesised in two steps. Firstly 3–pentadecylphenol in dry dichloromethane was reacted with glucose pentaacetate and $BF_3.OEt_2$ in an inert atmosphere for 24 hours.[282] This was then purified to give a cream-coloured intermediate of the intended molecule protected with acetate groups. The protected molecule was then deprotected[283] by adding K_2CO_3 and methanol giving a white solid in good yield (54%), see **Scheme 2.6**.

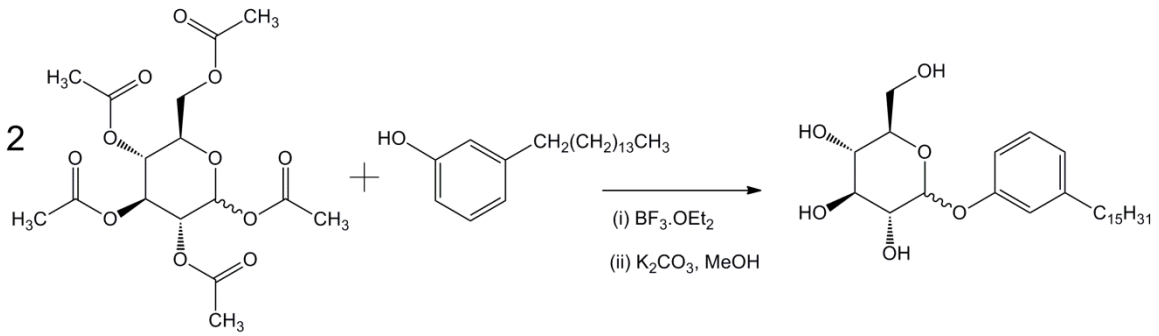

Scheme 2.6 Synthesis of Pentadecylphenylglucopyranoside **(2.16)**

1,3:2,4–Dibenzylidene–D–sorbitol (DBS) **(2.17**) was synthesised using an acid catalysed condensation/dehydration reaction published in the literature.[284] One mole of D–sorbitol was reacted with two moles of benzaldehyde in methanol with para-toluenesulfonic acid monohydrate (p-TSA) as a catalyst. In this preliminary synthesis, this produced a very hard waxy like filter cake which had to be broken down.

Methanol was added to the broken filter cake and mixed until absorbed, before leaving to air dry for 24 hours. This gave a fine white powder with very poor yield (8%), see **Scheme 2.7**. It is thought that by washing with methanol many times the intermediate by-products / unreacted materials that possibly formed during the synthesis were more soluble in this solvent and resulted in the low yield obtained. This synthesis could be optimised through the use of elevated temperatures to encourage better yields of the final desired product.

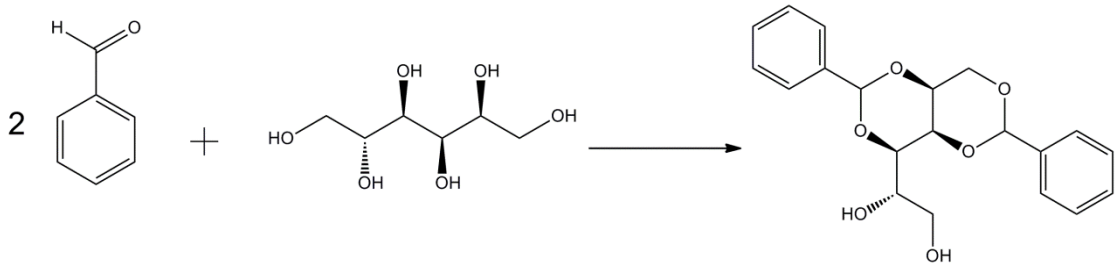

Scheme 2.7 Synthesis of 1,3:2,4-Dibenzylidene-D-sorbitol **(2.17)**

1,3:2,4–Methyldibenzylidene–D–sorbitol (DBS-CH_3) **(2.18)** was commercially available from Milliken & Co. However, due to the short supply of this material a synthesis was also found within the literature[285] to increase stock for use in testing. Similarly to DBS described above, the reaction was an acid-catalysed condensation reaction but made use of acetonitrile as the reaction solvent instead of methanol. This too formed a hard filter cake which needed to be broken down before being purified with hot water and cyclohexane. This gave a white solid but with much better yields (75%), see **Scheme 2.8**.

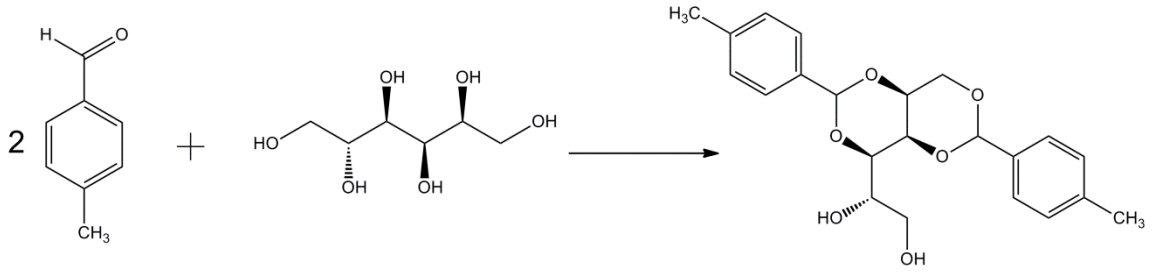

Scheme 2.8 Synthesis of 1,3:2,4-methyldibenzylidene-D-sorbitol **(2.18)**

Each of these molecules, whether they be commercially available or synthesised through 1 or 2 simple steps, was then analysed and tested for the potential gelation ability with de-icing and anti-icing solvent compositions to identify whether they could potentially act to enhance the performance of such fluids or indeed create a new fluid with better properties.

2.3 Gelation Ability

Each of the synthesised gelators was screened for their gelation ability in industrially relevant solvents for the de-icing industry. These solvents included monoethylene glycol (MEG), 1,2–monopropylene glycol (MPG), 1,3–propanediol (PDO) and aqueous mixtures of these (**Figure 2.8)**. In the de-icing industry, the dilutions are commonly described as percentages. The percentage dilutions that were used were 100% (undiluted glycol), 75% meaning 75 % glycol with 25% water and 50%, 50% glycol with 50% water. These dilutions are described in the regulations and are usable concentrations for customers. Dilutions of 100% and 50% are measured as the worst case scenario. De-icing fluids are never used below 50% glycol in order to achieve the correct freeze point.

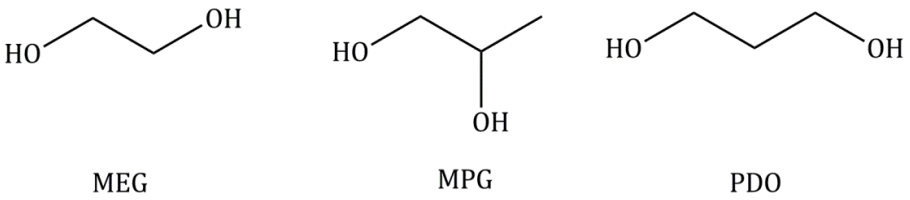

Figure 2.8 Different types of glycols used for screening and in the de-icing industry.

Each of the gelator molecules were screened in each of the above described glycols and dilutions to determine their gelation ability. The samples used for screening were made by weighing out a known amount of gelator into a glass vial. Each gelator was screened at high (1 % w/v, 10 mg/ml), medium (0.5 % w/v, 5 mg/ml) and low (0.1 % w/v, 1 mg/ml) concentrations. To the glass vial, 1 ml of solvent was added. Each sample was sonicated for 1 hour before being heated to just below the boiling point of the solvent to create a clear homogenous solution. Temperature was used as the trigger as this would be the stimulus used within the de-icing industry to achieve gelation. Duplicate samples were made for all compounds in each of the different solvent systems. One set of samples were left overnight to cool at room temperature on the bench whilst the remaining set was placed into a freezer set to -20°C and results recorded the next day.

The tube inversion method[286] was used to determine whether a gel had formed. Samples were deemed to be a gel if when each of the vials was inverted, there was no flow of the contents under gravity for a period of several minutes.

Table 2.1 demonstrates the results for each of the gelator molecules tested at 1 % w/v. It shows that of the nine molecules tested only, *N*–dodecanoyl–L–alanine and

ascorbic acid–6–palmitate, act as efficient organogelators in 100% glycols at low temperatures. The ability of *N*–dodecanoyl–L–alanine and ascorbic acid–6-palmitate to form fibres in glycols may be attributed to their structure. Their surfactant like structure[95,211] containing a hydrophilic head group with a very hydrophobic long alkyl chain provides them with a greater ability to form intermolecular interactions with one another and hence assemble into fibres creating an entangled 3D network.

The majority of compounds, including bis(Leucine)-oxalyl amide, *N*-dodecyl-D-gluconamide, 1,12-digluconaminododecane, diglucosaminododecane and pentadecylphenylglucopyranoside all remained fully soluble and could not gel the three different glycols at 100%. This may be due to the polarity of the glycols solvating these molecules efficiently and hence preventing the gelator molecules from interacting with one another through van der waals and hydrogen bonding interactions to create gel fibres. The molecules which could not gel 100% glycols were tested in aqueous mixtures of glycols. These compounds showed to switch from being too hydrophilic where they were fully dissolved in the solvent to being insoluble, with the exception of 1,12-digluconaminododecane and diglucosaminododecane which remained soluble throughout the different solvent mixtures. The ability of these two molecules to exist in the soluble state within the aqueous glycol mixtures may be attributed to their structure. Their bolaamphiphile-like structures could potentially make them more hydrophilic than the other molecules which have alkyl chains, hence they can dissolve better unlike the hydrophobic characteristic of the alkyl chains within the other compounds which prevents the molecules from dissolving and remains insoluble. These molecules were tested across different concentration ranges but still showed the inability to form a gel in the required solvents with the exception of *N*-dodecanoyl-L-alanine and ascorbic acid-6-palmitate. Due to the inability of these molecules to form gels in any of the solvents they have been ruled out for further examination at this time.

From **Table 2.1** it is also clear that none of the molecules could form a pure hydrogelator in water and remained insoluble. As such, they are all too hydrophobic to dissolve in these conditions and are hence unable to assemble into gel fibres. When these molecules were incorporated into aqueous mixtures of glycol their ability to gel significantly reduced with increasing water.

Table 2.1 Gelation ability of synthesised gelators at 1% w/v. G = Gel, PG = Partial Gel, S = Soluble, I = Insoluble, ***I*** = Insoluble but gels below 1% w/v, **S**= Soluble but gels above 1% w/v.

		Solvents									
Molecules	**Temp / °C**	**100% MPG**	**100% MEG**	**100% PDO**	**75% MPG**	**75% MEG**	**75% PDO**	**50% MPG**	**50% MEG**	**50% PDO**	**100% H_2O**
N–Dodecanoyl–L–alanine	20	**S**	**S**	***S***	I	I	I	I	I	I	I
	-20	**G**	**G**	***G***	I	I	I	I	I	I	I
Bis (Leucine) Oxalyl Amide	20	S	S	S	I	I	I	I	I	I	I
	-20	S	S	S	I	I	I	I	I	I	I
Ascorbic acid–6–Palmitate	20	**S**	**G**	**S**	I	I	I	PG	I	I	I
	-20	**G**	**G**	**G**	I	I	I	PG	I	I	I
N–dodecyl–D–gluconamide	20	S	S	S	I	I	I	I	I	I	I
	-20	S	S	S	I	I	I	I	I	I	I
1,12–digluconaminododecane	20	S	S	S	S	I	S	I	I	S	I
	-20	S	S	S	S	I	S	I	I	S	I
Diglucosamidodecane	20	S	S	S	S	S	S	S	S	S	I
	-20	S	S	S	S	S	S	S	S	S	I
Pentadecylphenylglucopyranoside	20	S	S	S	I	I	I	I	I	I	I
	-20	S	S	S	I	I	I	I	I	I	I
1,3:2,4–Dibenzylidene–D–Sorbitol	20	**S**	**S**	**S**	**G**	S	S	***I***	I	***I***	I
	-20	**S**	**S**	**S**	**G**	S	S	***I***	I	***I***	I
Ditoluidene Sorbitol	20	S	S	S	I	S	PG	I	I	I	I
	-20	S	S	S	I	S	PG	I	I	I	I

Imae and co workers[287,288] have extensively studied amino acid surfactants in water and showed that *N*–dodecanoyl–L–alanine can form a hydrogel when the pH is between 4 and 5. Therefore in this instance *N*–dodecanoyl–L–alanine was tested at low pH (pH 3) in water but a gel was not formed.

They also conducted a study on a similar molecule *N*–acyl–L-aspartic acid[287] and showed by increasing the alkyl chain length increases the molecules ability to form gels at higher pH values creating more thermally stable gels. It is well-known that controlling pH to change from soluble carboxylate form to insoluble carboxylic acid can induce gelation – but such an approach is not practical in the desired application. Modified versions of this molecule with longer alkyl chains could potentially work in water if pH was also used as a trigger. Bhattacharya and co workers[156] have demonstrated the selective gel formation of *N*–dodecanoyl–L–alanine in mixed organic aqueous mixtures. Although Imae has shown this molecule gels water, when in a mixed system the molecule selectively gels only the organic solvent and not the water. They have been able to deduce from FTIR studies that solvents capable of hydrogen bonding suppress gelation by disallowing self assembly and when in water the presence of the hydrophobic alkyl chain exerts a hydrophobic effect which excludes the water with the aggregates being stabilised through the van der Waals interactions between the alkyl chains.[289] As such being able to determine the correct balance of solubility and insolubility that can be attained from solvents has shown to be key in the ability of a molecule to form a gel.

Research conducted by Vemula and co workers[173,211] has shown that ascorbic acid–6–palmitate should act as a hydrogelator. They have studied a number of different analogues of ascorbic acid based amphiphiles with increasing alkyl chain lengths. Therefore, their research would suggest that ascorbic acid–6–palmitate could in fact form hydrogels if used at higher concentrations (2% w/v) than what was tested within this study. However, within the de-icing industry it would be strongly preferred to use concentrations below 1 % w/v to reduce costs, as such this was not probed further.

The results highlighted in bold in **Table 2.1**, were investigated further across a range of concentrations. The gelation ability of *N*–dodecanoyl–L–alanine increased with increasing concentration above 1% w/v up to and including 3% w/v before any insolubility of the molecule could be identified in 100% glycols. Gels recorded in MEG were only possible at 1% w/v (**Table 2.2**).

Table 2.2 Concentration range in which *N*-dodecanoyl-L-alanine in 100% glycols can form gels.

Molecule	Concentration range in each solvent		
	100% MPG	**100% MEG**	**100% PDO**
N-dodecanoyl-L-alanine	1-3 % w/v	1 % w/v ***ONLY***	1-3 % w/v

Luo and co workers[289] have demonstrated this molecule's ability to form organogels in a range of non–polar solvents. They have shown and proven that this molecule self assembles through hydrogen bonding of the carboxylic acid and amide functional groups with a neighbouring molecule and van der Waals interactions from the long alkyl chain, to create bilayer aggregates, see **Figure 2.9**.

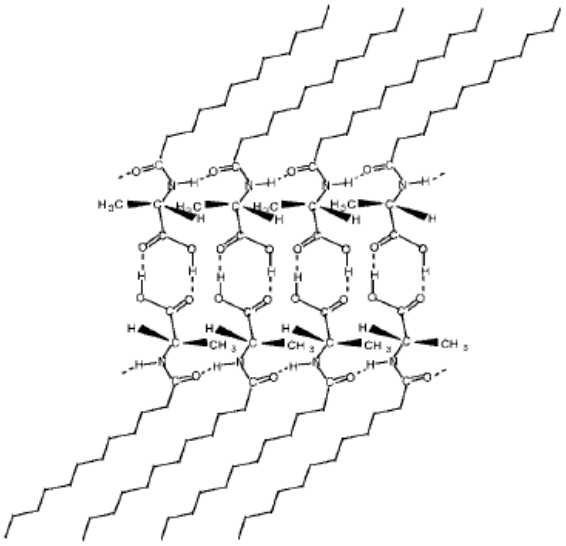

Figure 2.9 Self assembly mechanism of *N*-dodecanoyl-L-alanine[289]

Although the glycols used within this study are polar they may act similarly to water where it competes for the hydrogen bonding sites in the gelator molecule, which can in turn disrupt the self association of the gelator molecules, preventing gelation. This may explain why such high concentrations of gelator are required to form gels in these solvents. Therefore using high concentrations of the gelator allows more molecules to be present to overcome the competing effects from the solvent, enabling the formation of hydrogen bonding between each of the molecules when in 100% glycols.

Ascorbic acid–6–palmitate when tested further increased its gelation ability at both higher and lower concentrations than 1 % w/v, and showed to form gels between 0.5–3 % w/v in 100 % glycols. This molecule is known to be ambidextrous,[290] with the ability to gel water and non polar organic solvents. Vemula and co workers[173]

have proposed a gelation mechanism for ascorbic acid esters when in water and organic solvents. Due to the nature of the molecule's structure it has been shown that when in water the molecules will choose to have the hydrophilic head groups in the water whilst keeping the hydrophobic tails within its nanostructure motif, where it creates layers of molecules making fibres. However, when in organic solvents the opposite is true, whereby the interactions still occur through the same regions i.e. hydrogen bonding between the head groups and van der Waals between the alkyl chains, however the molecule will exist with their heads together stacked one on top of the other with their tails out horizontally or with the tails diagonally, see **Figure 2.10**, therefore two forms could potentially exist within ascorbic acid organogels. Therefore at low concentrations in 100% glycols this molecule is able to interact with its respective counterpart of the other molecule to form fibres which interact through hydrogen bonding and van der Waals interactions synergistically and not compete with the solvent like *N*–dodecanoyl–L-alanine.

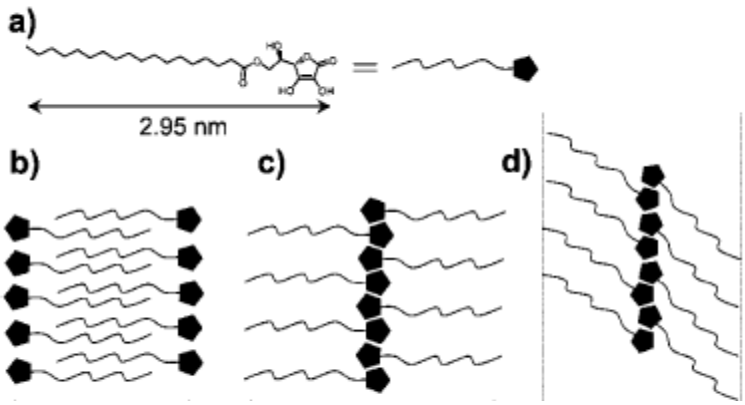

Figure 2.10 Self assembly mechanism of ascorbic acid esters shown in (**a**) in water (**b**) and organic solvents (**c** and **d**).[173]

Although both of these molecules are known hydrogelators within the literature, both molecules still only showed gelation behaviour when in 100% glycols and no other dilution with water. The only other compound which showed gelation potential in the initial screening were the DBS derivatives.

The gelation ability of one particular molecule, 1,3:2,4–Dibenzylidene–D–sorbitol (DBS) was notably increased especially with increasing water content at very low concentrations. This molecule had the ability to form gels at very low concentrations of <0.1% w/v in 50% MPG and 50% PDO. Indeed the ability of this molecule to form gels increased when the concentration reduced and the water content increased, indicating the need for effective solubilisation followed by hydrophobic interactions

for gelation to be achieved. Gelation was possible in all dilutions of MPG with this molecule. Similarly with 100% PDO and 50% PDO, gels could be formed at low concentrations below 1% w/v. Unlike the samples tested in MPG, where gels formed in 100% MPG required DBS concentrations above 1% w/v, DBS in 100% PDO could form gels below 1% w/v, at a very similar concentration range to the gels formed in 50% PDO. No gels could be formed in 75% PDO. It is important to note that as water content increases the gelator becomes less soluble and favours the more solid like network until the correct balance is achieved. Therefore we see that although water can enhance the molecule's ability to form a gel and enhance the hydrophobic effect, too much water can lead to insolubility and precipitation hindering the molecules ability to form a gel. This is in agreement with Rogers and Raghavans studies on the impact of solvent modification on gelator activity. This molecule has been extensively researched for the use in industry[109,158,167,260,263,264,291-303]. Roll-on deodorant sticks demonstrate their usefulness in similar types of alcohol-based solvent to those used within this study. Numerous patents[265,292,295,304-306] have been filed on this subject and all have noted that it is possible to make gels with glycols and alcohols, but not in water. The glycols commonly reported are butylene glycol and hexylene glycol, slightly longer carbon chains than the propylene and ethylene glycols used within this study. However, this does not affect the ability to form gels. Many researchers have attempted to understand the gelation mechanism of DBS through both experimental[307-310] and *in silico* approaches[311]. It is thought that the butterfly–like structure of DBS self assembles through hydrogen bonding of the pendant hydroxyl groups and the cyclic acetals within the body of the molecule and π-π stacking of the aromatic rings or solvophobic interactions between them. Therefore in the glycol water solvent system it shows as the water increases the solvophobic interactions with the aromatic rings most likely increase, which allows for the formation of gels at low concentrations which are more thermally stable.

Due to the success of DBS-forming gels in the desired glycol water solvent systems a derivative of DBS was also tested which was commercially available, ditoluidene sorbitol (DBS-CH_3). However, this molecule showed poor gelation ability, remaining completely insoluble when in water and aqueous glycol mixtures, and being soluble when in 100% glycols. Therefore this slight modification in this molecules structure has shown to affect its ability to form gels within these solvent systems. This is somewhat surprising as this compound is a known gelator for organic polymer

systems but it is likely that the methyl group modification makes the system just too hydrophobic to dissolve in mixed aqueous media.

The three molecules, *N*–dodecanoyl–L–alanine, ascorbic acid–6–palmitate and DBS, that showed potential to act as low molecular weight gelators (LMWG) in these solvent mixtures were tested further to identify their minimum gelation concentration and their thermal stabilities.

2.3.1 Minimum Gelation Concentration (MGC)

Each of the molecules which successfully gelled the required solvents was tested for their minimum gelation concentration (MGC) in the chosen solvents. Samples were made as described in **Section 2.3** with decreasing concentrations, until a sample was formed which did not act as a gel when inverted in its vial.

Table 2.3 Minimum gelation concentration of the three molecules that could act as low molecular weight gelators (I = Insoluble).

Solvents	**Molecules**		
	***N*–dodecanoyl–L–alanine**	**Ascorbic acid–6–palmitate**	**1,3:2,4–Dibenzylidene–D-sorbitol**
100% MPG	1%	0.70%	1.30%
100% MEG	1%	0.50%	I
100% PDO	1%	0.80%	0.30%
75% MPG:H_2O	I	I	0.10%
50% MPG:H_2O	I	I	0.07%
50% PDO:H_2O	I	I	0.07%

Table 2.3 shows that each of the molecules are capable of forming organogelators at high concentrations in 100% glycols with *N*–dodecanoyl–L–alanine and ascorbic acid–6–palmitate having very similar concentration ranges. DBS however has the ability to form gels at low concentrations across the range of solvent systems with the exception of 100% MPG, where high concentrations are required similar to the other two molecules. DBS, when in aqueous glycol mixtures acts as a super gelator, forming gels below 0.1% w/v. This demonstrates the ability of solvent ratio to tune the gelation ability of a molecule in dramatic and remarkable ways.

2.4 Thermal Stability

The thermal stability of each gel formed for each of the different gelator molecules was measured by finding the T_{gel} of the sample. The T_{gel} is the temperature of the gel – sol transition. This is measured using a tube inversion test. The samples are heated at

1.0°C min^{-1}, as the temperature increased the sample vial was inverted after each increment and eventually the gel collapsed. The temperature at which this occurs was recorded as the $T_{gel.}$

All of the gelator molecules that were tested showed the same general behaviour, as concentration increased the T_{gel} increased, as would be expected and is typical for many gelators due to the gel network becoming more extensive on increasing the concentration of the gelator.

N–dodecanoyl–L–alanine and ascorbic acid–6–palmitate show similar behaviour in each of the different glycols. These gelator molecules create more thermally stable gels as the glycol changes from MEG>PDO>MPG respectively, see **Figure 2.11** and **Figure 2.12**. The increasing number of carbons within the solvent from MEG>PDO>MPG and the lower polarity shows to have a contributory negative impact on the ability of the molecules to interact with one another to create more thermally stable gels presumably because as polarity decreases the gelator becomes more soluble. These gelators also form gels at low temperatures below 20°C, which has never been reported in the literature before. This is in agreement with the gelation ability results obtained above where we could see the samples remained as solutions at 20°C and only formed gels when at freezing temperatures. This indicates that for these molecules to form gels they require thermal energy at lower temperatures for the intermolecular interactions to occur between the molecules to create fibres to form a gel. Such low-temperature nanomaterials could find some interesting and unique applications.

Ascorbic acid-6-palmitate however forms more thermally stable gels than *N*–dodecanoyl-L-alanine even at lower concentrations than 1 % w/v, with some gels forming and remaining stable above 20°C at high concentrations.

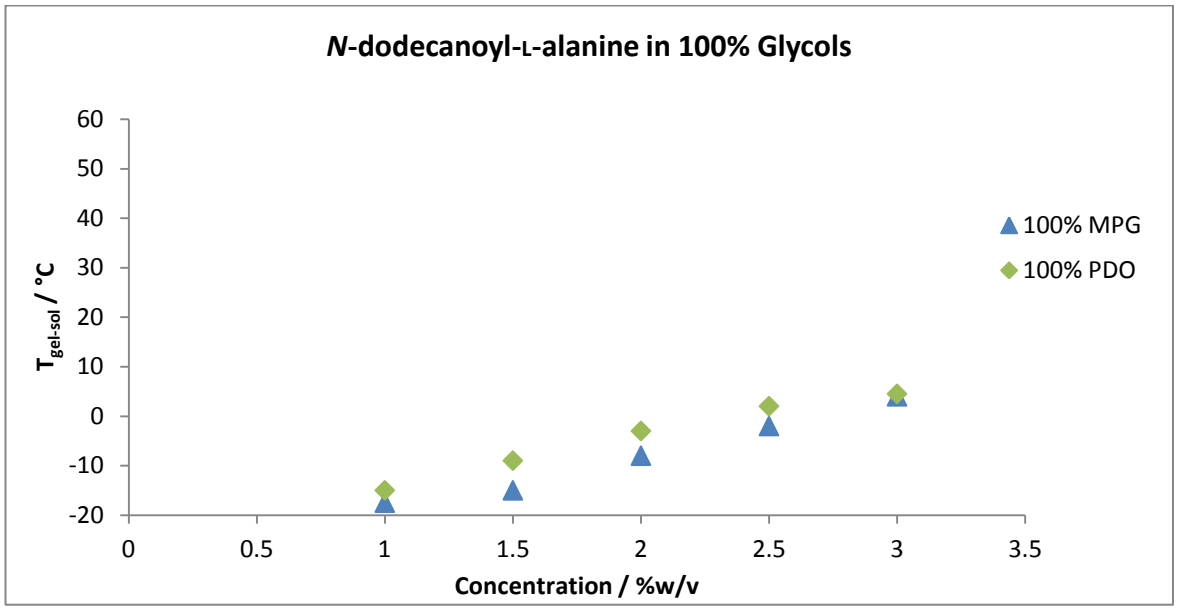

Figure 2.11 Thermal stability of *N*-dodecanoyl-L-alanine in 100% glycols.

The thermal stability profiles of these two gelator molecules would be perfect for use as a de-icing fluid on aircrafts. Ideally the sample would remain as a solution at 20°C and above and form gels once applied to a cold surface to provide freeze protection from frost, ice and snow. However, their inability to form gels in aqueous glycol mixtures significantly limits their use, and if used in 100% glycol would significantly increase the operational costs and the environmental burden of de/anti-icing fluids.

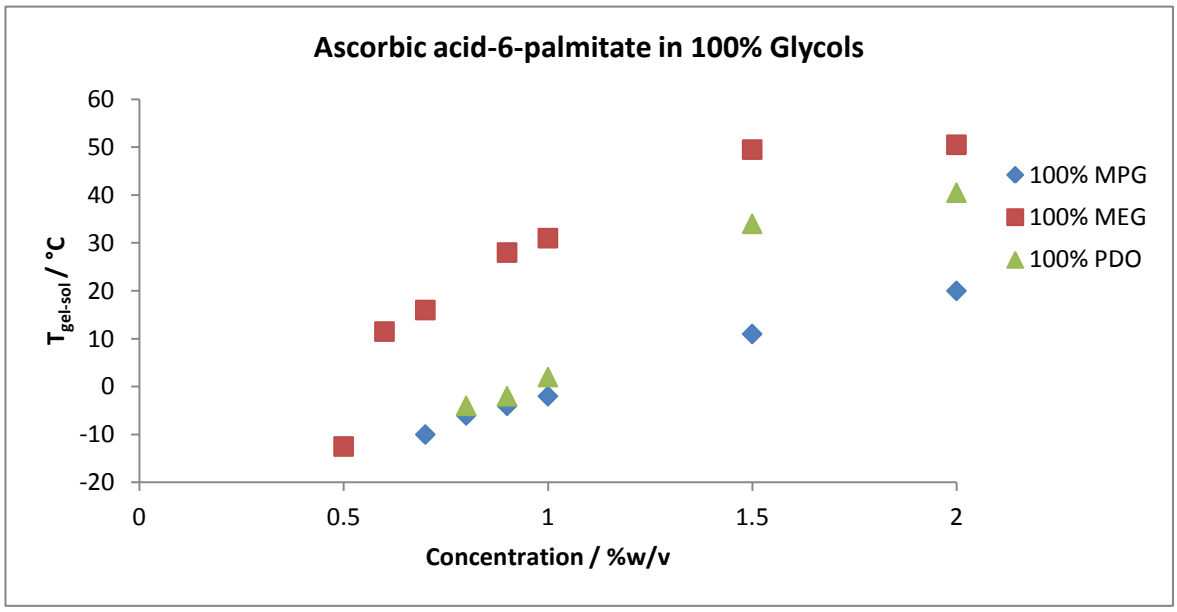

Figure 2.12 Thermal stability of ascorbic acid-6-palmitate in 100% glycols.

1,3:2,4–Dibenzylidene–D–sorbitol unlike the other two gelators shows the ability to gelate aqueous glycol mixtures. What is apparent from the thermal stability profiles of this molecule is as the water ratio increases from 0% (100%) to 25% (75%) to

50% (50%) the thermal stability of the gel increases, with gels formed in 50% water: glycol being the most thermally stable, see **Figures 2.13** and **2.14**.

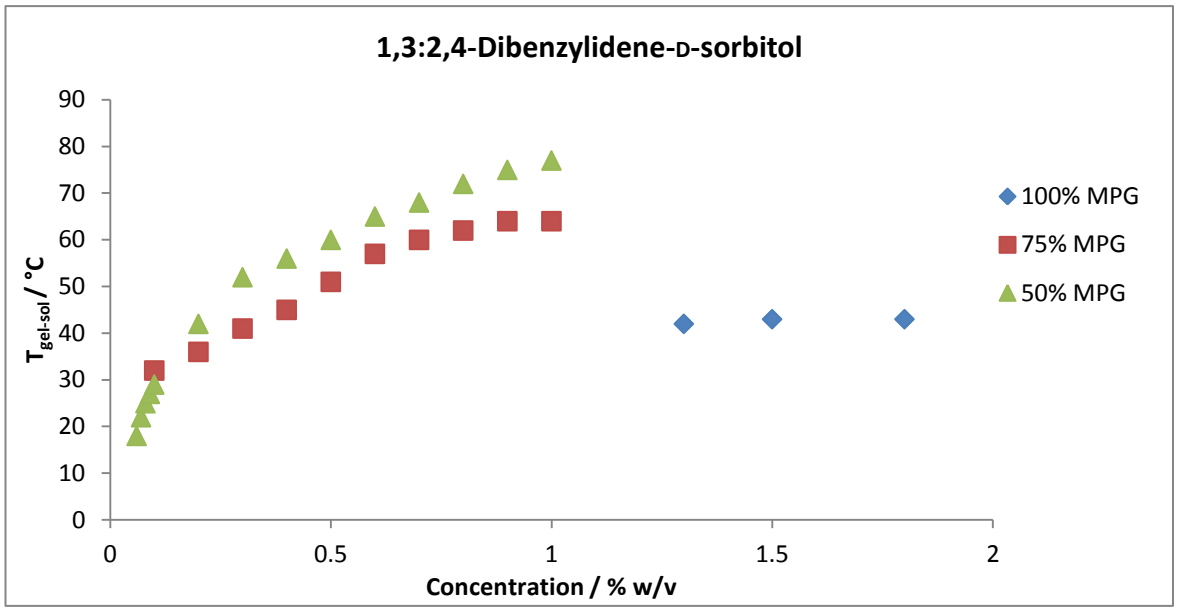

Figure 2.13 Thermal stability of 1,3:2,4-Dibenzylidene-D-sorbitol in MPG and aqueous mixtures of MPG.

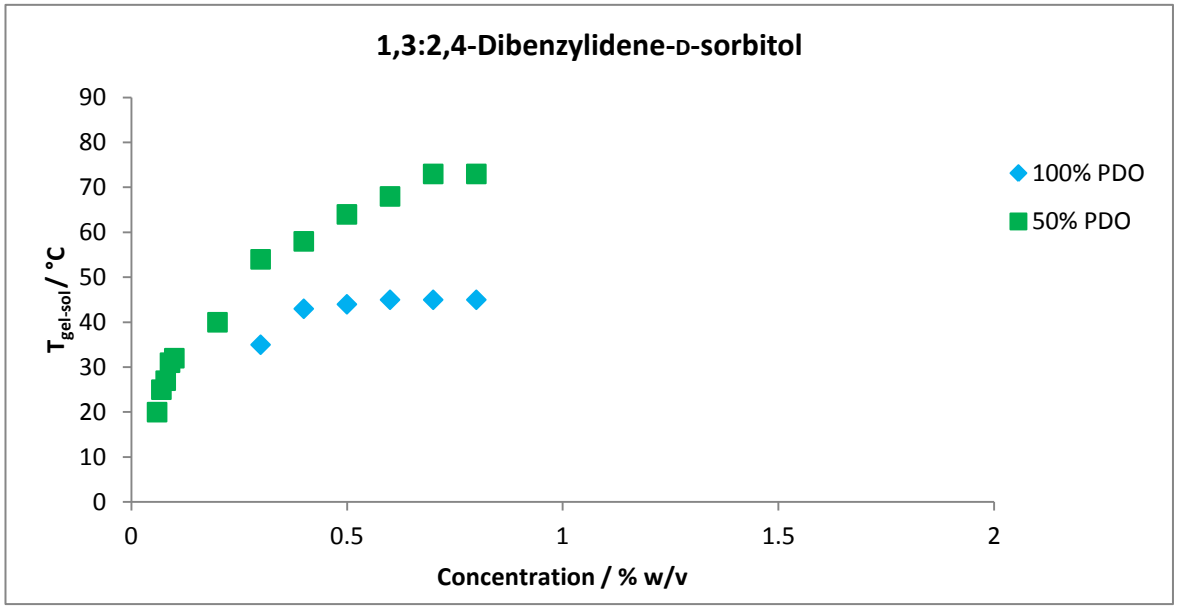

Figure 2.14 Thermal stability of 1,3:2,4-Dibenzylidene-D-sorbitol in PDO and aqueous mixtures of PDO.

This can be accounted for by the hydrophobic effect. The hydrophobic effect for this molecule becomes more dominant as the water ratio increases, which encourages the gelator molecules to interact and aggregate more effectively, hence producing more thermally stable gel networks.

From **Figure 2.13** it also evident that when gels are formed in more aqueous environments (75% and 50% MPG) the self assembly processes are different. The self assembly for 75% and 50% MPG gels suggests that they may form through isodesmic polymerisation, where the self assembly is comparable to a step growth polymerisation where the association constant of every step of chain growth is equivalent. Whereas gels formed in 100% MPG is more suggestive of cooperative polymerisation, gels are formed at higher concentrations where the polymer starts to grow and it is more likely that the monomers will form interactions with the polymer than another monomer.

Although this gelator creates gel networks which require higher temperatures to break the gel down, it could still work very well in the de-icing industry. This is primarily down to the mode of application. De-icing fluids can be applied from 80 – 95°C and anti-icing fluids from 60 – 80°C. Therefore having higher temperatures would allow these samples to still be applied in the same way without damaging their structure, but with the potential of using much lower concentrations of gelator compared to concentrations of polymer currently used (0.2-0.4 % w/v) with greater dilutions of glycol. This molecule could potentially allow for the application temperature of a de/anti –icing fluid to be tuned more effectively based on its concentration and freeze point required.

2.5 Scanning Electron Microscopy (SEM)

2.5.1 Visualisation of gel networks

Each of the three potential gelator molecules were imaged using scanning electron microscopy (SEM) to try and identify the supramolecular structures formed in the gel state and understand what may be happening on the microscopic scale. SEM allows for nanoscale objects to be observed. It works somewhat similarly to an optical microscope but instead of using light, uses an electron beam. The electron beam is made up of primary electrons which act to knock secondary electrons out of the sample being imaged when focused on a small area of the sample. The electrons are then collected by a detector which is at an angle to the surface of the sample. The signal generated is converted into a black and white image which shows the topography of the surface.

Samples of *N*–dodecanoyl–L–alanine were prepared by spreading a small amount of a gel sample over a flat aluminium stub, because these samples only form gels at

temperatures below 20°C they were then freeze dried. The other gelator samples were prepared in the same way but not freeze dried. These samples were left to dry in a dessicator until the solvent was removed and a dried film was present on the stub. Drying samples in this way causes the gel network to collapse forming a xerogel. To ensure the samples are conductive, they were then coated with a thin layer of Au/Pd using a sputter coater. Therefore the sample being viewed is a dried, collapsed, coated form of the gel network within each of the samples. It is therefore important to recognise that the images obtained for each of the sample here is not how the gel network would exist in the solvated state. However, this approach can give an indication of the type and size of the supramolecular structures that are formed and can be useful when comparing to other molecules.

N–dodecanoyl–L–alanine in 100% glycols proved extremely difficult to image. As gels only form at low temperatures with this molecule it was firstly difficult to remove the solvent at low temperatures as below -49°C the glycols begin to boil off from the sample under vacuum. Therefore from the images obtained in **Figure 2.15** at low magnification (x 2000) no fibre like structure can be observed instead what is seen are most likely drying artefacts from the freeze drying technique. The sample appears to have dried and cracked on the surface however, there are dense areas which indicate that fibres are possibly present which have snapped and collected in one area but it could also suggest that this molecule does not form a homogeneous gel structure and is more solid like. It is very difficult to determine any supramolecular structures from these images and the results shown are most likely artefacts from the solvent removal and the sample preparation.

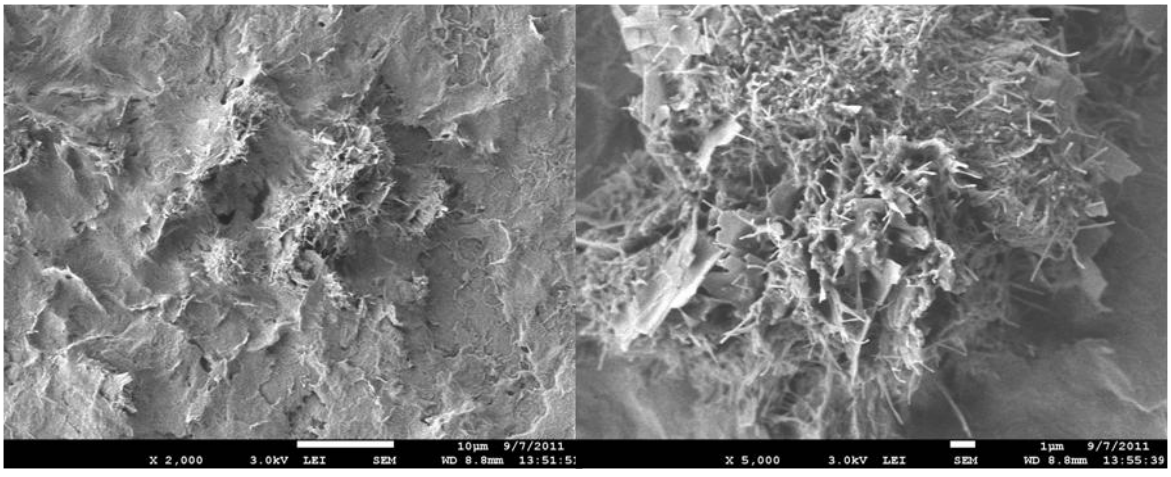

Figure 2.15 SEM of *N*-dodecanoyl-L-alanine at 2 % w/v in 100% MPG

Like *N*–dodecanoyl–L–alanine the preparation of ascorbic acid–6–palmitate imaging samples proved to be difficult in 100% glycols. Although gels formed in all of these

solvents only images of ascorbic acid–6–palmitate in 100% MPG could be obtained. From **Figure 2.16** it is clear to see the images that have been obtained are still heavily solvated with glycol due to the difficulty of removing the high boiling solvent. However, fibres can be seen which make up the gel network. When imaged using a different detector, it appears that the fibres formed from this molecule are flat and quite large tape-like objects ca. 1 μm and are connected to one another forming bundles of fibres with diameters of 3 – 4 μm. It is not clear where one fibre starts and the other ends as they intertwine with one another forming the entangled network. Therefore the sizes of the fibres which have been indicated may not be accurate due to the sample being heavily solvated. The fibres could potentially be smaller but cannot be seen due to the overlapping and the presence of the solvent. This could suggest that the morphology evolves depending on how effectively the solvent has been removed.

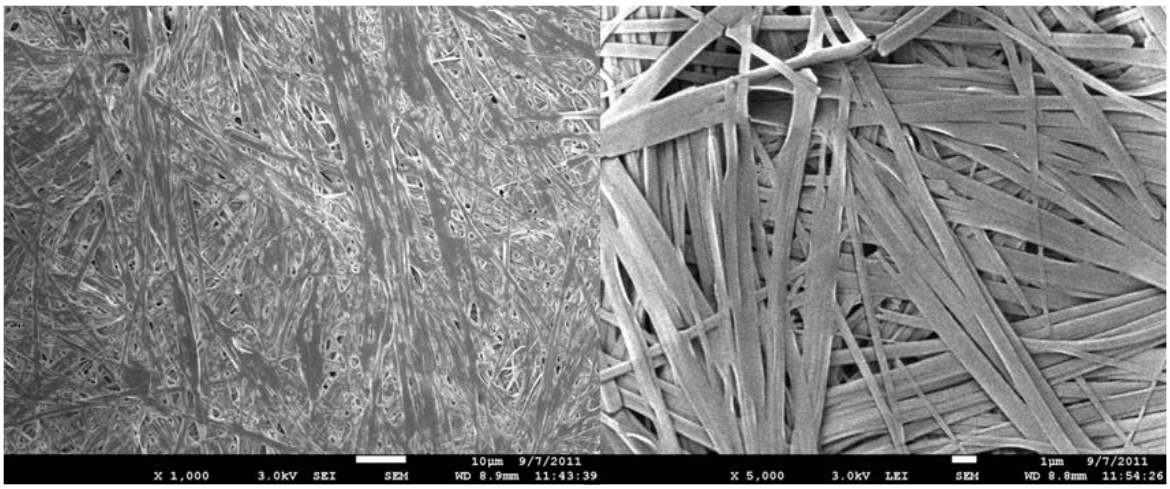

Figure 2.16 SEM of ascorbic acid-6-palmitate at 2 % w/v in 100% MPG.

SEM images for DBS in 100% glycols also proved difficult to prepare. Although samples were prepared through freeze drying and through the use of a dessicator it proved impossible to fully remove the solvent, and as a result when imaged, no supramolecular nanostructures could be observed. However, with the incorporation of water in 75% and 50% glycol dilutions, images could be obtained.

Interestingly in 75% MPG:water DBS gels, we observed long thin twisted nanofibres having diameters of ca. 5 nm. These twisted fibres were seen to create many fibre bundles having diameters ranging from 10–100 nm. The twisted shape of these fibres could potentially be accounted for by the chirality of the molecule hence, giving rise to helical twists which we see in the images, see **Figure 2.17**.

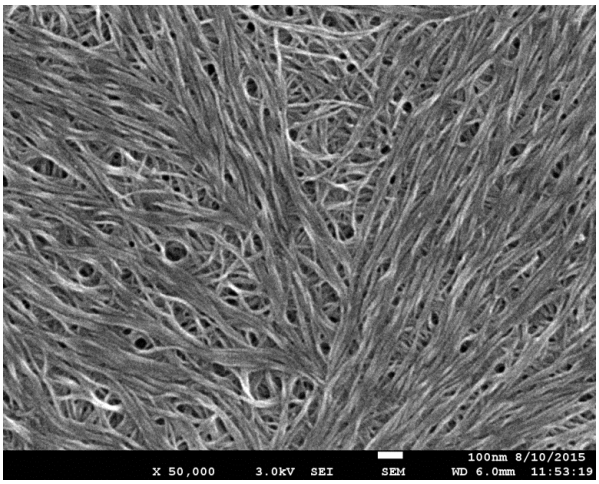

Figure 2.17 SEM of DBS at 0.5 % w/v in 75 % MPG:water.

When DBS was imaged at 50% MPG:water dilution, it showed similar fibre types being created throughout its supramolecular structure. The fibres, as above, appear very thin and long with a twisted effect see **Figure 2.18**. They appear to be a similar size (ca. 5 nm). However, it is very difficult to determine fibre bundle sizes as it appears the fibres are so convoluted and spread throughout the sample that no distinction between the different fibre bundles can be made.

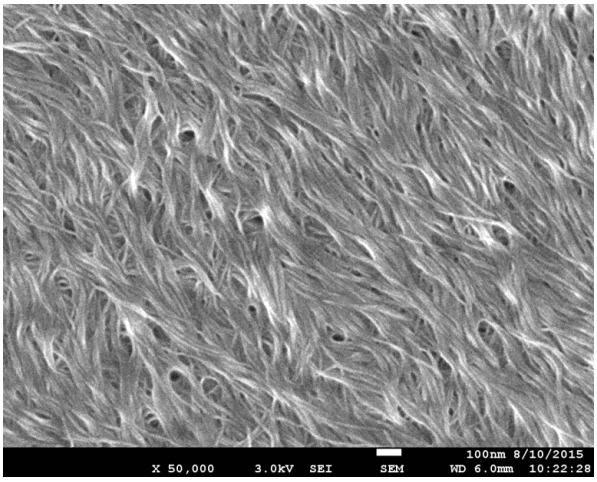

Figure 2.18 SEM of DBS at 0.5 % w/v in 50 % MPG:water.

By increasing water content from 25% to 50% within the solvent system, this molecule shows an even more expansive entangled fibre network than when only 25% water is present. This would agree with the proposed self assembly process where the incorporation of more water is providing a more hydrophobic environment where interactions between the gelator molecules are greater, which in turn creates more effective network self-assembly and a more thermally stable gel.

2.6 Conclusions

A library of low molecular weight gelators from the literature, based upon amino acids or sugars with different structural motifs and functional groups were synthesised. Each of the molecules was synthesised either through a one or two step method or was commercially available.

The gelation ability of each of the molecules was determined by using glycol:water solvent systems which are important for the de-icing and anti-icing industry. Of all of the molecules tested only three, *N*–dodecanoyl–L–alanine, ascorbic acid–6–palmitate and 1,3:2,4–Dibenzylidene–D–sorbitol, had potential industrial relevance. Each of these molecules had the ability to form gels in one or more of the desired solvent systems. None of the molecules synthesised showed the ability to act as a pure hydrogelator, at least using simple heat-cool cycles for gel formation.

Ascorbic acid–6–palmitate and *N*–dodecanoyl–L–alanine when in aqueous glycol mixtures showed no capability to form a gel, and instead existed as a precipitate. This clearly demonstrated the importance of the solvent composition to aid with solubility and the formation of intermolecular and intramolecular interactions between gelator molecules to form 3D sample spanning networks. Not having the capacity to form gels in aqueous mixtures of glycols greatly reduces the use of these molecules for de/anti-icing purposes. Although these systems have the correct thermal behaviour for this application, to be able to use these gelators at low temperatures very high concentrations are required.

1,3:2,4–Dibenzylidene–D–sorbitol (DBS) was the most successful gelator tested in this study. This molecule was capable of forming gels across the various glycol:water dilutions, at very low concentrations to produce thermally stable gel networks. This molecule however could not form a pure hydrogel but demonstrated the importance of hydrophobic effects from partial water dilutions to aid in self assembly. DBS is already in industrial use as a bulk chemical and therefore has commercial relevance.

SEM analysis of the three successful molecules demonstrated the difficulty of producing images in solvents with high boiling points and at low temperatures. As a result no clear images could be obtained to understand how *N*–dodecanoyl–L–alanine gel network is formed. However, ascorbic acid–6–palmitate and DBS showed examples of the different types of fibres that are possible from different molecular

building blocks. More importantly the aggregation of the fibres within DBS gels was denser and more compact when more water was present.

Of the low molecular weight gelators that were selected and screened from the literature for use within a de/anti-icing application, DBS, had the most desirable properties. It possesses the ability to form gels at low concentrations, helping to reduce costs, its starting materials are based upon sugars, hence reducing environmental impact, it is easily synthesised in a one step reaction and it can form gels in glycols and aqueous glycol mixtures that is required within the de/anti-icing industry.

DBS however, cannot form gels in pure water. Having identified this lead molecule, the next steps are therefore to further investigate this low molecular weight gelator for de/anti-icing application by modifying the molecules structure to increase its solubility in water. Derivatising DBS with hydrophilic substituents, to create a library of DBS molecules, would potentially allow for increased solubility in the desired solvent systems and the use of even lower concentrations. In this way we hope to develop a structure-activity relationship understanding of the performance of DBS gels.

Chapter 3

Dibenzylidene–D–Sorbitol (DBS) and its Derivatives as Gelators

Chapter 3 Dibenzylidene–D–Sorbitol (DBS) and its Derivatives as Gelators

The majority of this chapter's introduction has been adapted from a review we published in Soft Matter, 2015, 11, 4768 – 4787.

3.1 Introduction

3.1.1 1,3:2,4–Dibenzylidene-D-sorbitol (DBS)

DBS is a chiral low molecular weight amphiphile having a butterfly-shape conformation (**Figure 3.1**)‑it can be considered that the sorbitol backbone is the 'body' and the phenyl rings are the 'wings'. It is a white, crystalline substance derived from the naturally occurring hexose sugar, D-sorbitol, and can be synthesized by a condensation reaction between D-sorbitol and benzaldehyde. The earliest report of DBS was by Meunier[312] who reported that DBS could be synthesised through the acid-catalysed condensation of D-sorbitol and two equivalents of benzaldehyde to yield a mixture of two isomeric diacetals, each having a unique solubility in boiling water and different melting points, one of which formed a gel while the other did not.

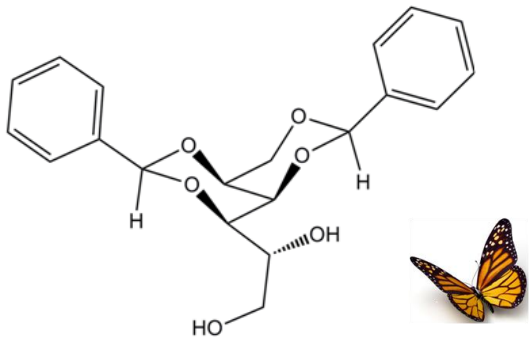

Figure 3.1 DBS - Butterfly-like structure.

It wasn't until 1926 that DBS was further investigated by Thomas and Sibi. They demonstrated the ability of DBS to form organogels and hydrogels in a number of different organic solvents and water.[313,314] Interest in LMWGs was re-ignited in the 1940s, primarily as a result of the Second World War. This led to the development of LMWG applications relevant to the military such as engine lubricants and greases (based on lithium 12-hydroxystearate in oils),[315] and napalm.[316,317] In those days, long before the availability of NMR for structural determination, a number of studies also explored the reactivity, and hence chemical structure of DBS.

Wolfe and co-workers[318] then went on to discover that DBS actually existed as a single species rather than being a mixture of isomers as reported earlier. However, it was noted that both the mono- and the tri-substituted benzylidene derivatives of the protected D-sorbitol could be present as by-products (MBS and TBS respectively **Figure 3.2**).

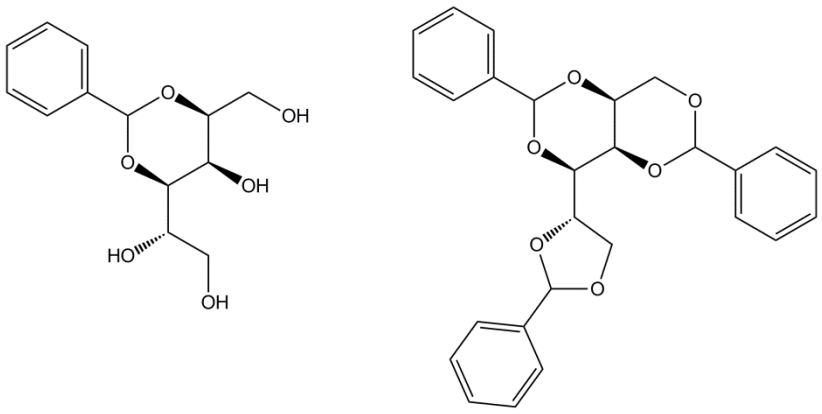

Figure 3.2 Structure of 2,4-monobenzylidene-D-sorbitol (MBS) (left) and 1,3:2,4:5,6-tribenzylidene-D-sorbitol (TBS) (right).

The structure of DBS was confirmed by Angyal and Lawler as having a 1,3:2,4 connection pattern. They achieved this through the hydrolysis of DBS to yield 2,4-monobenzylidene-D-sorbitol.[319] This compound had been previously reported and structurally characterised by Vargha,[320] and has since been shown to form via the rearrangement of an intermediate, less stable, 2,3-monobenzylidene-D-sorbitol with a five-membered ring.[321] The acetal carbon atoms within the ring structure of DBS are themselves new chiral centres. Knowing that their formation is thermodynamically controlled; it is a safe assumption that the bulky phenyl groups occupy the equatorial positions. It wasn't until the 1970's however, that Brecknell and co-workers assigned the correct name to DBS. The structure of DBS can therefore be described more fully as 1,3(R):2,4(S)-Dibenzylidene-D-sorbitol.[322]

3.1.2 DBS Derivatives

The synthesis of DBS is well established, and because the compound is of industrial importance,[284,285,323-335] there have been a number of attempts to enhance and optimise the methodology. Furthermore there has been growing interest in creating derivatives of DBS. Derivatives of DBS can be achieved by either:

(i) modification of the aromatic 'wings'

(ii) modification of the free alcohol groups on the sorbitol 'body'

In addition to the number of patents that have been published with regard to the various different syntheses of DBS, the synthesis of simple DBS derivatives with modified aromatic groups using substituted benzaldehydes during acetal formation are also detailed. In 2007, Feng et al. reported the synthesis of DBS and a number of new derivatives, see **Figure 3.3**.[336] Similar to the method of Gardlik and Burkes,[284] they used a dual solvent reaction medium and catalyst, with the incorporation of a Dean-Stark apparatus, which allowed for the recycling of solvents. Through the use of this synthesis they were able to obtain products (**Figure 3.3**) in very good yields (69-99%).

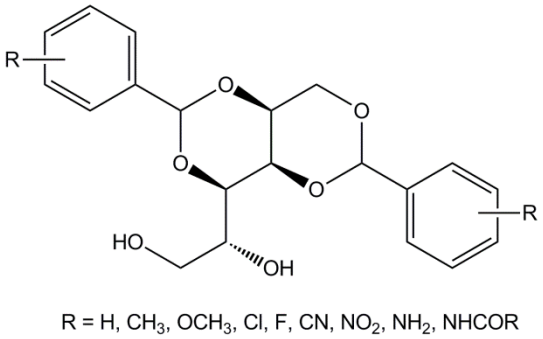

Figure 3.3 DBS derivatives achieved through the modification of the aromatic wings by Feng et al[336]

From simple modification of the aromatic wings on the DBS structure, Feng et al[336] were able to produce a number of DBS derivatives. They also showed that further derivatisation of these molecules was possible by converting nitro groups to amines by catalytic hydrogenation ,with further derivatisation of the amines being possible via amide coupling with carboxylic acids to yield amides. The reduction of nitro groups to form amines has also been reported by Stan and co-workers.[337]

The Smith group has generated some novel derivatives of DBS with modified aromatic 'wings'. Using their modified synthetic approach similar to Gardlik and Burkes as well as that of Feng described above, they were able to purify their products utilising dichloromethane and boiling water to remove the TBS and MBS by-products respectively. Using this synthesis they reported the syntheses of DBS derivatives functionalised with ester,[143] carboxylic acid[143] and acyl hydrazide[155] groups. The latter two systems acted as hydrogels – the first reported based on DBS.

In addition to modifying the aromatic wings of DBS, derivatives can be created through the modification of the free alcohol groups on the DBS body. The earliest reports of this being implemented is from the 1940s in which such derivatisation helped determine the structure of DBS.[318] In general, the primary alcohol (6-OH) is

more reactive than the secondary (5-OH), and hence more easily modified using standard methods such as tosylation, esterification etc. Feng et al.[336] used this principle to demonstrate how acid chlorides could convert DBS and its derivatives, into mono- or bis-esters, depending on the molar ratio of base and acid chloride used, **Figure 3.4**.

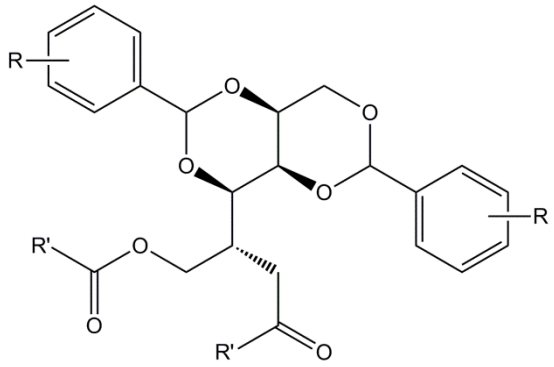

Figure 3.4 Esterification of the free alcohol groups on DBS. R = H, R' = C(O)Y where Y = C_2-C_{25} radical / aryl radical

A similar approach has recently been demonstrated in a patent by Malle and Luukas,[263] who reported esters of DBS in which the modification lies on the primary alcohol, or on both primary and secondary alcohols. This approach was also used to tether together the primary alcohol units of two DBS molecules in order to form bola-amphiphiles with DBS head groups, see **Figure 3.5**.

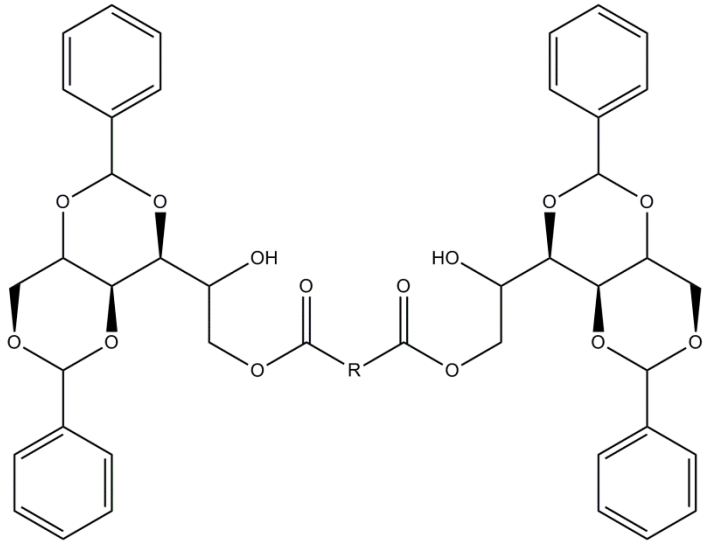

Figure 3.5 The tethering of primary alcohol units of two DBS molecules to create bola-amphiphiles. R = C_1-C_{52} / substituted arylene / silicone radical.

From some of the examples shown above we can start to see how DBS can be considered as a versatile building block for further modification. The aromatic 'wings' of DBS offer considerable scope for variation, and the free hydroxyl groups of the sorbitol backbone can be readily functionalised. It is also possible to generate more

complex derivatives using more extended synthetic procedures. Obviously such derivatisation can impact, either positively or negatively, on gelation. In order to understand the ways in which this can occur, it is vital to fully understand the gelation mechanism of native DBS.

3.1.3 Self - Assembly

There has been a number of studies conducted into the molecular self assembly of DBS, in an attempt to understand the gelation mechanism. Authors have employed both experimental and *in silico* approaches. The butterfly-like structure of DBS has two potential molecular recognition motifs:

(i) hydrogen bonding involving the 'body' of the structure between 5-OH/6-OH groups of one molecule as hydrogen bond donor and the 5-OH/6-OH or the cyclic acetals of another as hydrogen bond acceptor, and

(ii) π-π stacking or solvophobic interactions between the aromatic 'wings' of the gelator group of one molecule and those of another.

The structure and mechanism of DBS has triggered some controversy. Early studies conducted by Yamasaki and co-workers, explored the impact of different solvents with differing polarities on the self-assembly of DBS. [307] In low polarity solvents, intra- and intermolecular H-bonding of DBS was favoured, whilst in high polarity solvents, H-bonding between DBS and the solvent, which does not underpin gel assembly, became favoured. They then explored the roles that each of the free hydroxyl groups have in the self-assembly of the molecule by selectively converting each of the 5-OH and 6-OH groups into methoxy groups.[308] By doing so they observed that no gelation occurred when the terminal (6-OH group) was protected, while gelation still occurred with the 5-OH group protected. Therefore this suggests that the 6-OH is more important for the self assembly of DBS most likely because it can form an intermolecular hydrogen bond with the acetal groups of another DBS. Through further analysis they found that the 5-OH group can either intramolecularly hydrogen bond to an acetal oxygen, or intermolecularly to the surrounding solvent which is not involved in underpinning gelation. The 6-OH group is intermolecularly hydrogen bonded to an acetal oxygen and supports self assembly and finally that the phenyl groups are ordered side by side. From their analysis they were then able to propose a qualitative self-assembly model of DBS shown in **Figure 3.6** where hydrogen bonding primarily contributes to the self assembly of DBS.

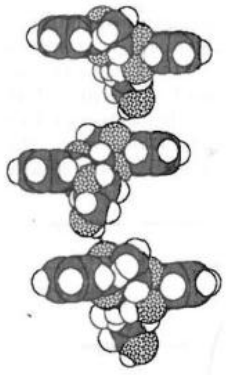

Figure 3.6 Qualitative model proposed by Yamasaki and co workers.[308]

Other researchers went on to demonstrate that modification of the 6-OH group, with hydrogen bond donor moieties, does not prevent gelation. This therefore supported the importance of intermolecular hydrogen bond donation from the 6-OH position of DBS in low polarity solvents.[294]

Watase et al[309] investigated the ground state dimerization of DBS molecules in relatively polar alcoholic solvents. This study demonstrated that the self-assembly of DBS was mediated by π-π stacking of the molecules on top of one another to form a molecular fibre. To form these fibres it was suggested that the 1,3-phenyl ring overlapped that of another molecule, while the 2,4-phenyl ring overlapped that of another molecule which showed to be different to the Yamasaki model.

In 2003, Wilder and co-workers for the first time used a computational approach ‑ to determine the configuration of DBS and the intermolecular interactions which underpin its self-assembly.[310] Molecular mechanic analysis of a single DBS molecule produced an energy minimized structure with equatorial, approximately co-planar aromatic rings, see **Figure 3.7**.

Figure 3.7 Lowest energy minimized structure of a single DBS molecule from two different angles.[310]

Conformational searches exploring the structural variation showed four other energy minimized structures of DBS, suggesting that the molecular configuration of DBS can potentially switch between several low energy structures.

Wilder et al also investigated dimerisation of DBS using the same computational methodology. With respect to intermolecular interactions, they found that for the initial energy-minimized configuration of DBS, the only interaction in the dimer was the formation of a hydrogen bond between the 6-OH group of one DBS molecule and an acetal oxygen of the other, see **Figure 3.8**, which is in agreement with Yamasaki's proposed model.[307]

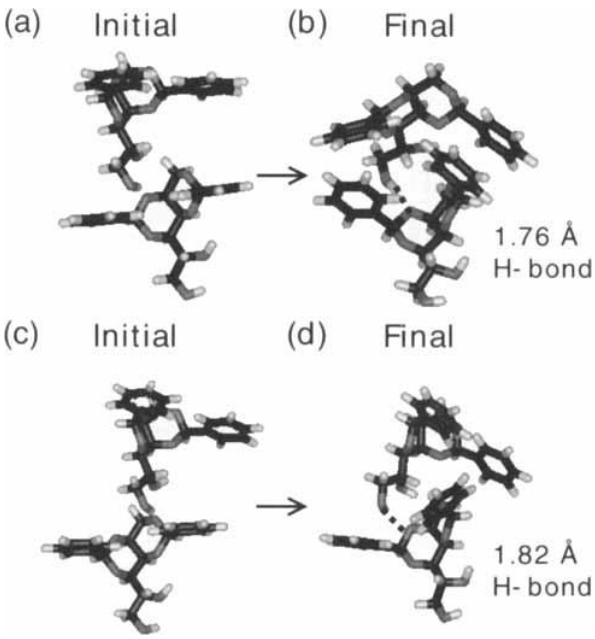

Figure 3.8 Two examples of DBS dimers before (**a**,**c**) and after (**b**,**d**) energy minimization. The formation of intermolecular hydrogen bonds in (**b**) and (**d**) are indicated by the dashed line.[310]

The alternative energy-minimized conformations of DBS, showed that π-π interactions were also present, in some agreement with the results of Watase.[309] They therefore demonstrated that H-bonding and π-π interactions must be considered in the mechanism of DBS self-assembly, as well as the degree of fluxionality.

Ten years after Wilder et al had published their results, Alperstein and Knani[311] used quantum mechanics to determine the molecular configuration of a single molecule and a dimer of DBS. Their study showed similar results of Wilder[310] where the phenyl rings are in an almost equatorial position, but they also showed that the 5-OH group pointed towards the 6-OH group where an intramolecular hydrogen bond forms between them. Using molecular mechanics and dynamic simulations they investigated DBS as a gelator for polypropylene. Through this they found that the major intermolecular interaction was hydrogen bonding between the O6 and H-O6 groups, with O5/H-O6 and O5/H-O5 interactions also contributing. Their finding therefore agreed with the work from Yamasaki[307] and Wilder[310] and demonstrated

the importance of the 6-OH group, but they also proposed the destination of the intermolecular hydrogen bond to be different. No significant π-π interactions were observed in their simulations, and they argued that the main contribution from phenyl groups was to stiffen the molecular structure. They also noted that the hydrogen bonding interactions were much stronger in the hydrophobic environment of polypropylene, suggesting that the nature of the solvent does indeed affect the intermolecular interactions in DBS fibre formation – this may also be the reason that the π-π interactions were less significant.

Song and co-workers was another group of authors that used SEM to demonstrate that the nanofibres of the xerogels of a derivative of DBS; 1,3:2,4-di(3,4-dichlorobenzylidene)-D-sorbitol (DCDBS) exhibited different structures in polar solvents (non-helical fibre aggregates) and non-polar solvents (rope-like helical fibres) (**Figure 3.9**).[338]

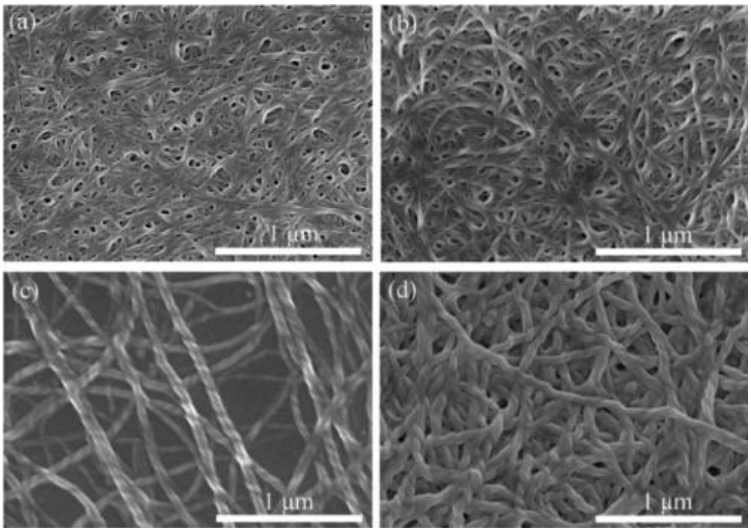

Figure 3.9 SEM of DCDBS xerogels made by Song and co-workers demonstrating the solvent control over nanoscale morphology. (**a**) DMSO-H_2O (7:3 v/v) (**b**) ethylene glycol (**c**) n-octanol (**d**) o-dichlorobenzene.[338]

They used molecular mechanics like Alperstein and Knani, to suggest that the gelator molecules adopt a planar-type conformation in polar solvents. This causes the molecules to stack on top of each other, with π-π interactions being primarily responsible for self-assembly. They suggested that the π-π interactions prevent individual molecules bending, leading to the observed non-helical fibres. However, in non-polar solvents, H-bonding between the 6-OH and an acetal oxygen was found to be the driving force responsible for the self-assembly; with the intermolecular interactions having different effects on each side of the molecule, creating the helical twisted fibres. Song and co-workers also suggested that the positioning of

substituents on the aromatic wings when creating derivatives of DBS determines whether a gel will form or not. They demonstrated this nicely through the use of 1,3:2,4-di(2,4,6-trimethylbenzylidene)-D-sorbitol (2,4,6- TMDBS) and 1,3:2,4-di(2,4,5-trimethylbenzylidene)-D-sorbitol (2,4,5-TMDBS) (**Figure 3.10**).[339]

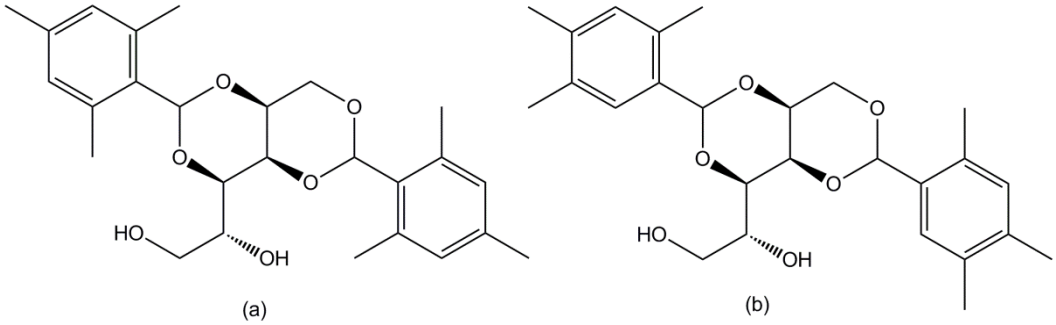

Figure 3.10 Structures of (**a**) 2,4,6-TMDBS (**b**) 2,4,5-TMDBS

The former is an efficient organogelator but the latter does not form gels in the solvents tested. This inability of 2,4,5-TMDBS could be attributed to steric effects of the meta substituents disrupting the interactions between one molecule of DBS and another during gelation-or alternatively could be due to the substitution inducing conformational changes or slight differences in the overall solubility. This example demonstrates that DBS gelation is held in a subtle balance by various different factors.

Considering the results obtained from each of the authors that studied the self-assembly of DBS we can see there is a combination of factors that lead to the self-assembly of DBS. These include the fluxionality of DBS and its ability to exist in a number of low energy conformations as well as the differing effects observed in different solvents. Where in non polar solvents intermolecular hydrogen bonding, from the 6-OH group, predominantly underpins self-assembly, whilst in polar solvents the hydrogen bonding of the 6-OH is less significant owing to the competition for these interactions from the solvent, and π-π stacking and/or solvophobic interactions between the aromatic wings of the gelator.

Clearly, DBS is a versatile and responsive gelator which can, to some extent, adapt to the environment in which it finds itself. This means that as a gelation system it has a relatively broad scope, and clearly synthetic derivatisation as described in **Section 3.1.2**, can extend this yet further.

3.1.4 Industrial Application

DBS has a long history of industrial use, and as such, has attracted a very large number of patents, which have seen it employed in a wide range of different

industrial sectors. Furthermore, as gel chemists increasingly consider high-tech applications for these responsive self-assembled materials,[87,101,102,175] DBS and its derivatives are well-placed for potential future use, given the long history of precedent - studies to expand the scope of DBS applications are underway.[87,263]

DBS has a long history of being used in the formulation of personal care products. It possesses the ability to gel the desired ingredients within the cosmetics industry, which enables products to be produced that has the desired thickness, adhesion, strength, and consistency-the use of DBS in this industry is widespread. Since the late 1970's, DBS has been explored as a gellant to create clear antiperspirant sticks (**Figure 3.11**). Roehl[305,306] patented the DBS-mediated gelation of glycols and alcohols with acidic aluminium antiperspirant salts which gave rise to clear solid antiperspirant sticks, with suitable stick hardness and adhesion. However, it was noticed that these formulations were not stable over time, did not have adequate shelf life, and deteriorated at elevated temperatures. These drawbacks could be attributed to the instability of the 10-membered acetal ring of DBS in acidic media.

Figure 3.11 Example of a solid DBS based antiperspirant deodorant stick.

Therefore, several patents were developed in which less reactive solvents were used and stabilizing agents were added into the DBS gel to try and remedy this problem. Schamper et al.[265] described the use of alcohols which would be less reactive in the presence of acidic antiperspirant salts and the addition of a gel stabilizer such as zinc acetate. This formulation was an improvement over the earlier versions as it reduced the degradation of the gel sticks and enhanced stability at elevated temperatures.[291] Agents such as guanidines,[304] polypropylene glycol ethers of fatty alcohols, zinc and magnesium acetate,[340] silicone elastomers,[292] and amino acid salts,[295] have also been used to stabilize deodorants containing DBS gels in the past decades.

Given the ability of DBS to form gels in solvents such as alcohols and glycols when used in deodorants, it is clear that they may also have potential to be used in other industries such as de/anti-icing of aircrafts which use similar solvent systems. The ability of DBS to form gels in glycols and alcohols suggests that gels could be formed where the stiffness and strength could be adapted for de/anti-icing in aviation where the removal of the gel from the surfaces before takeoff is imperative, but that it can also create films which could potentially protect an aircraft from winter conditions. The successful use of DBS within deodorants, demonstrates that the cost of using such molecules would be similar to the cost of polymers which are presently used within de/anti-icing formulations. Therefore no additional cost should be accumulated but additional properties could be gained from using such molecules. The use of DBS in such items as deodorants also demonstrates that the environmental and toxicity profile of such molecules are low, and as a result this compound is available in every supermarket today. Using a molecule such as DBS or a derivative of it, it potentially allows for the polymers to be reduced or potentially phased out, as well as using a molecule which is cost effective, as it is already used industrially, is safe, as it is used in applications for human use and has low toxicity, hence low environmental impact.

Within this chapter we wanted to demonstrate the derivatisation of DBS. By derivatising the aromatic wings of this molecule we wanted create a library of DBS derivatives which incorporated hydrophilic and hydrophobic substituents on the para position of the aromatic wings. This would allow us to gain greater insight into the significance of modifying the structure of this molecule and what effects this would have on the solubility and gelation ability in industrially relevant solvents for the de/anti-icing industry. Each of the derivatives will be tested for their gelation efficacy, to identify whether modification allows for these molecules to be used at lower concentrations or in different solvent mixtures. The thermal stability profiles will be obtained for each of the successful derivatives and compared to unmodified DBS to understand whether structural modification has a negative or positive impact when applied in de/anti-icing solvents.

3.2 Results and Discussion

3.2.1 Synthesis

The gelator molecules were synthesised using a previously published method,[284,339] which was adapted by the Smith group.[143] The method involves a condensation/dehydration reaction between a substituted benzaldehyde, (in this study we only look at para-substituted benzaldehydes) with D–sorbitol in a 2:1 ratio, in the presence of an organic catalyst (p-toluenesulfonic acid monohydrate), see **Scheme 3.1**.

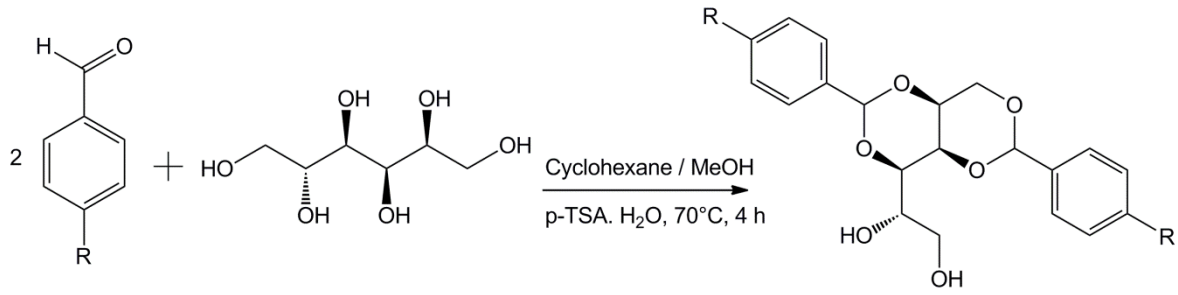

Scheme 3.1 Reaction scheme for the synthesis of DBS and its derivatives, see Figure 3.12 on for R groups.

D–Sorbitol was added to a three neck round bottom flask containing the cyclohexane/methanol solvent mixture. To this flask an overhead mixer was attached with a nitrogen inlet and a Dean-Stark apparatus. This solvent system was used as it forms an azeotropic mix with the water from the condensation/dehydration reaction, this therefore helps to remove the water whilst at the same time the cyclohexane helps to precipitate the product. This mixture was then stirred and heated at 50°C for 20 minutes in a nitrogen atmosphere. In a separate flask, para-substituted benzaldehyde, p-TSA.H_2O and methanol were stirred at room temperature until the starting materials became soluble. This mixture was then transferred to a dropping funnel and added to the D–sorbitol mixture dropwise, over a period of 2–4 h at 70°C until a white solid or paste was formed. The reaction was left to cool before being purified see **Experimental Section 9.3.2**.

Each of these reactions produced two by-products, mono–benzylidene sorbitol (MBS) and tri–benzylidene sorbitol (TBS). Due to their differing solubilities, MBS being more hydrophilic and TBS being more hydrophobic, we found the best way to purify the reaction was through washing with boiling water, to remove MBS and dichloromethane (DCM) to remove TBS. The reaction was also washed with cold ethanol which acts to remove any unreacted starting materials and catalyst without

losing any of the desired di-acetal products. The various DBS derivatives obtained **see Figure 3.12** had fair to excellent yields (18–88%) but could all be obtained in sufficient quantity and purity for testing.

Where:

R = H	**75%**	**R = SCH_3**	**88%**	**R = $CONHNH_2$**	**83%**
(3.10 & 3.11)		**(3.16)**		**(3.21)**	
R = CO_2CH_3	**64%**	**R = SO_2CH_3**	**65%**		
(3.12)		**(3.17)**			
R = OCH_3	**52%**	**R = CF_3**	**50%**		
(3.13)		**(3.18)**			
R = OCH_2CH_3	**58%**	**R = NO_2**	**18%**		
(3.14)		**(3.19)**			
R = $O(CH_2)_2CH_3$	**29%**	**R = COOH**	**78%**		
(3.15)		**(3.20)**			

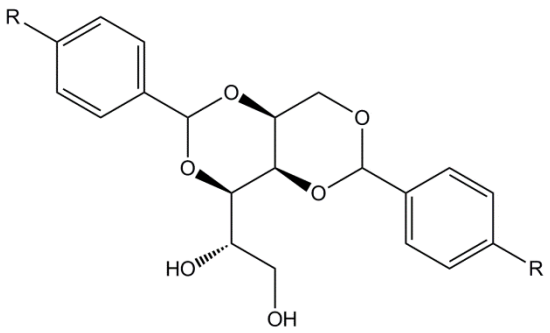

Figure 3.12 General structure of gelator molecules studied.

Each of the products identity and purity were characterised using TLC, mass spectrometry, ^{1}H NMR, ^{13}C NMR and IR. The ^{1}H NMR spectrum for a newly formed DBS derivative molecule would typically appear as in **Figure 3.13**, with additional peaks for their specific functional groups added by the para-substituted benzaldehydes. Typically the protons associated with the aromatic rings in the structure would be seen between 7.3–7.8 ppm, integrating for 8–10 protons depending on whether the para position of the aromatic ring has an additional functional group attached, the benzylic protons could be seen as a distinct singlet at 5.7± 0.1 ppm, integrating for 2 protons, and the body of the structure based upon the

sugar could be observed between 3.2–4.5 ppm, integrating for 10 protons representative of the CH, CH_2 and OH protons within the structure.

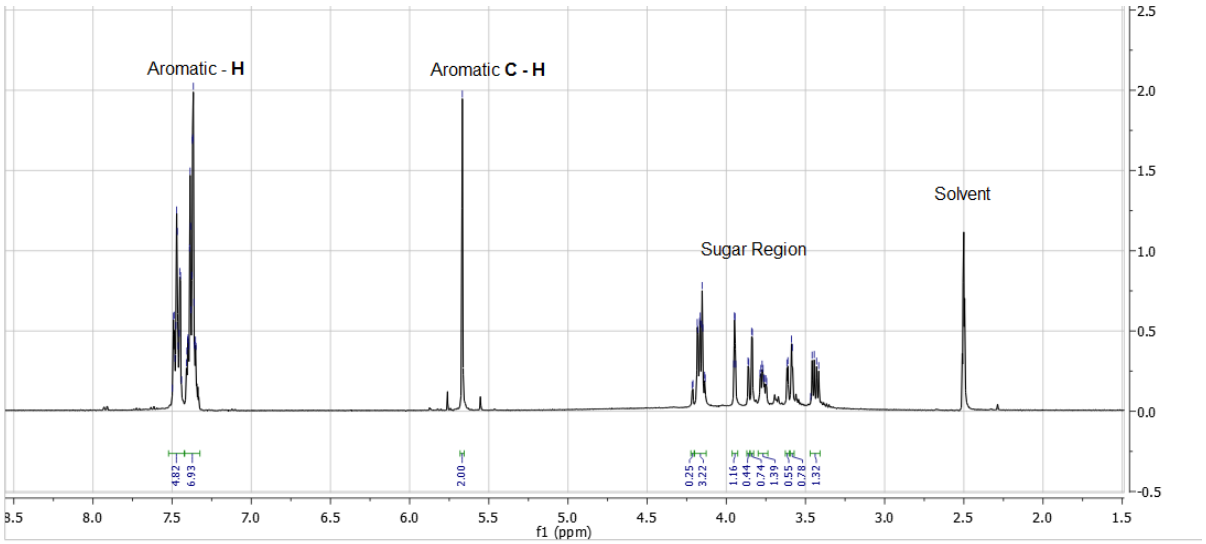

Figure 3.13 ^{1}H spectrum of a typical DBS based molecule in d_6-DMSO.

For each of the DBS derivatives there would also be additional peaks related to the additional functional group added to the aromatic ring in the para position. For DBS-CO_2CH_3 the additional CH_3 protons from the ester group could be seen at 3.85 ppm, the proton associated with the acid functionality on DBS-COOH appeared at 10.10 ppm, the CH_3 methoxy protons on DBS-OCH_3 were visible at 3.75 ppm, the ethoxy protons (DBS-OCH_2CH_3) could be observed at 4.01 (CH_2) and 1.32 ppm (CH_3), ^{n}propoxy protons were observed for DBS-$O(CH_2)_2CH_3$ at 3.91 (OCH_2), 1.72 (CH_2) and 0.97 ppm (CH_3), the methylthioether functional group CH_3 protons on DBS-SCH_3 were observed at 2.47 ppm, the methylsulfonyl CH_3 protons associated with this functional group on DBS-SO_2CH_3 were seen at 3.16 ppm and the protons associated with the hydrazide functional group on DBS-$CONHNH_2$ were observed at 9.81(NH) and 4.48 ppm (NH_2).

It can be seen from **Figure 3.12** that generally the compounds with high yields have electron withdrawing groups. The electron withdrawing groups make the carbon of the aldehyde more reactive hence, producing a high yield product. However, because they are so reactive you also get more of the tri–substituted by–product being produced, which as an impurity is difficult to remove. This badly affects the synthesis of DBS-NO_2. The opposite can be seen to be true with strongly electron donating groups, like DBS–$O(CH_2)_2CH_3$. The most notable property during the synthesis of these products is the reaction time. With electron withdrawing groups the reaction

proceeds much faster (approx. 2 h) compared to that of an electron donating group (approx. 4 h).

This synthesis described above compared to the two slightly different methods obtained from the literature and used within Chapter 2 dramatically improved the yield of DBS and of the derivatives. Not only did the yields improve but the reaction time reduced and the removal of the known by-products was now achievable through simple washing. This optimised synthesis, allows for a reproducible higher throughput of derivatives in a relatively short time, with potential recycling of the solvents used within the reaction.

To successfully synthesise all of the above listed derivatives, particularly DBS acid (DBS-COOH) and DBS hydrazide (DBS-$CONHNH_2$), the original DBS ester (DBS-CO_2CH_3) underwent further hydrolysis and /or hydrazination to yield the respective products.

3.2.1.1 Synthesis of DBS acid (DBS-COOH) from DBS ester (DBS-CO_2CH_3).

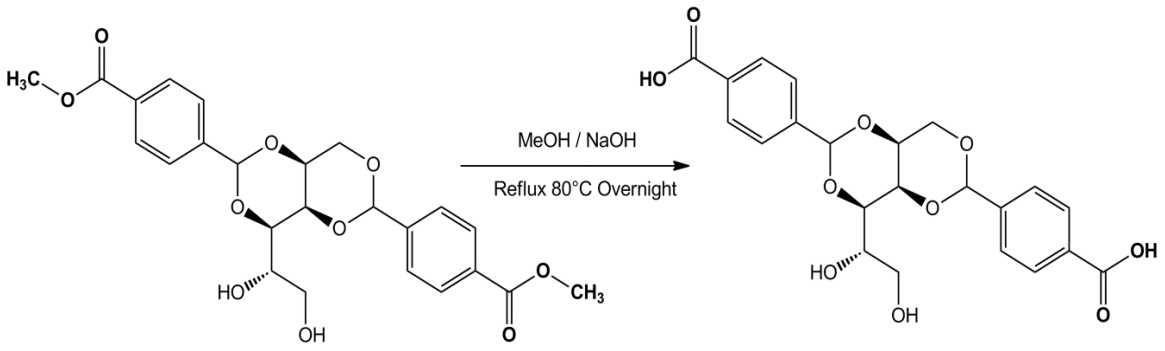

Scheme 3.2 Reaction scheme for the synthesis of DBS-COOH.

To form DBS-COOH, DBS-CO_2CH_3 was hydrolysed as shown in **Scheme 3.2**. DBS-CO_2CH_3 was added to a methanol/sodium hydroxide solution and refluxed at 80°C overnight. This white suspension dissolved to a colourless solution, suggesting the formation of the sodium carboxylate ion on the acid functional group, hence increasing its solubility in the salt form. The solvent was removed by rotary evaporation and the residue diluted with de-ionised water. This solution was then acidified to pH 3 using $NaHSO_4$ whereby the product could be seen to precipitate out of solution and form a white solid. The product was filtered, washed and dried. ^1H NMR characterisation confirmed the conversion of the ester functional group to an acid with the disappearance of the ester CH_3 peak at 3.85 ppm and a new peak at 10.10 ppm emerging from the carboxylic acid protons.

3.2.1.2 Synthesis of DBS hydrazide (DBS-$CONHNH_2$) from DBS ester (DBS-CO_2CH_3)

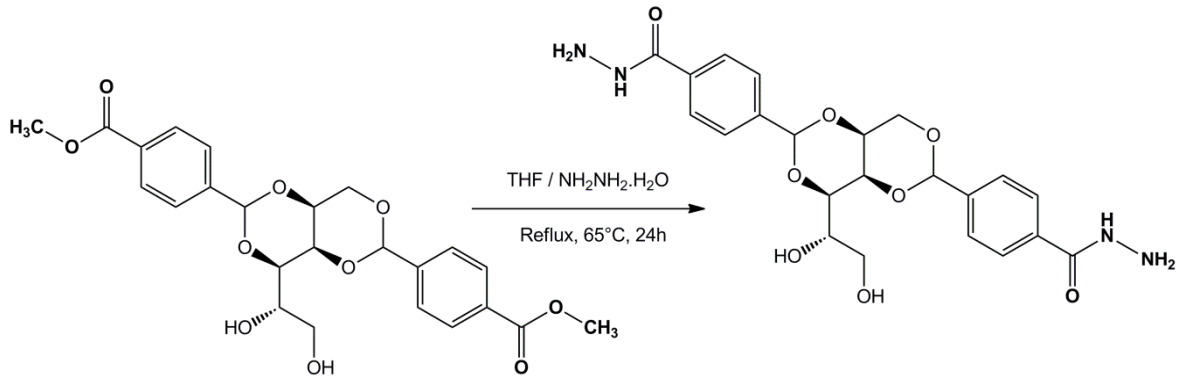

Scheme 3.3 Reaction scheme for the synthesis of DBS-$CONHNH_2$.

DBS-$CONHNH_2$ was synthesised from DBS-CO_2CH_3 as shown in **Scheme 3.3**. DBS-CO_2CH_3 was added to tetrahydrofuran (THF) along with an excess of hydrazine monohydrate and refluxed at 65°C for 24 hours, whereby a white solid formed. This solid was filtered, washed thoroughly with water to remove any remaining hydrazine monohydrate before being dried. Characterisation by ^1H NMR showed the disappearance of the CH_3 from the ester functional group at 3.85 ppm and the formation of two new peaks at 9.81 and 4.48 ppm corresponding to the 'amide' and 'primary amine' like sites within the acyl hydrazide functional group, confirming the conversion from the ester to the acyl hydrazide.

3.2.2 Synthesis of mono-benzylidene sorbitol (MBS) and tri-benzylidene sorbitol (TBS)

As well as synthesising the different derivatives of DBS, the known by-products of DBS that are formed in the synthesis were also synthesised independently. The same synthesis as described in **Section 3.2.1** was employed to synthesise the two by-products, MBS and TBS. The only differences made were the ratios of starting materials.

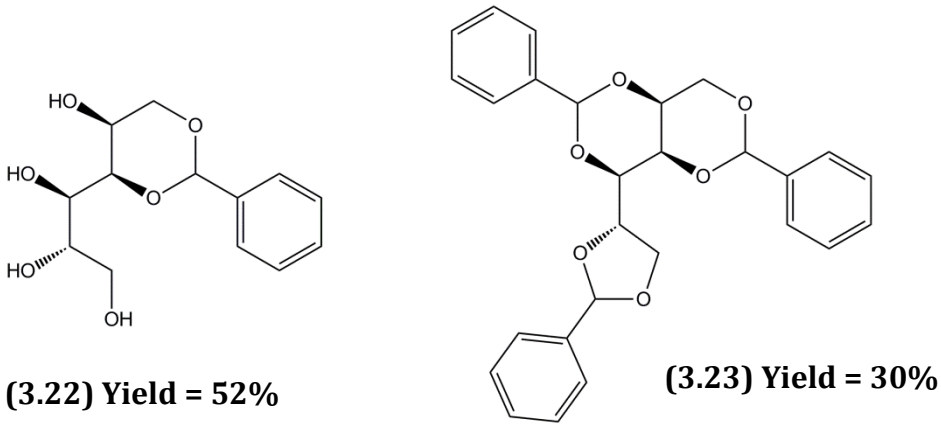

(3.22) Yield = 52% **(3.23) Yield = 30%**

Figure 3.14 By-products produced during the reaction. **Left**: MBS **Right**: TBS.

To form MBS, a 1:1 ratio of benzaldehyde and D–sorbitol was used to only allow the formation of the hemiacetal between the 1 and 3 position hydroxyl groups. Upon completion of the reaction the product was washed only with DCM and dried before being characterised. The product was obtained in a yield of 52%.

To form TBS, a 3:1 ratio of benzaldehyde to D–sorbitol was used. An excess of benzaldehyde was used to try and force the reaction to the formation of the triacetal (TBS) rather than the diacetal (DBS), however this proved to be difficult as the synthesis favours the formation of the diacetal. Therefore the DBS was formed as normal and the product washed with water to remove the MBS and starting materials, and then washed with DCM. The filtrates from the DCM washings were collected as it is known that washing DBS with DCM removes the TBS. The filtrate was rotary evaporated and dried before being characterised. This gave rise to a TBS yield of 30%.

3.2.3 Additional DBS derivatives

In addition to para-substituted benzaldehydes being used to create a library of DBS derivatives, benzaldehydes substituted with more than one functional group and branched groups were investigated. From the benzaldehydes available commercially we selected 2,4,6–trimethoxybenzaldehyde, 4–^{iso}propoxybenzaldehyde and 4–dimethylaminobenzaldehyde, see **Figure 3.15**.

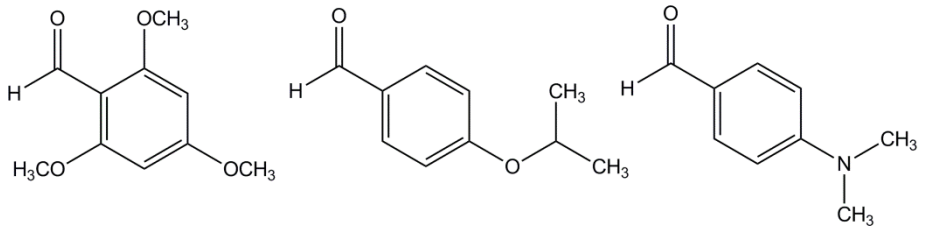

2,4,6 - (Trimethoxy) Benzaldehyde 4 - (^{iso}propoxy) Benzaldehyde 4 - (dimethylamino) Benzaldehyde

Figure 3.15 Additional benzaldehydes used to synthesise DBS derivatives.

Each of these substituted benzaldehydes shown in **Figure 3.15** underwent the same synthesis as described previously in **Section 3.2.1** with D–sorbitol. However, unlike the other derivatives, the use of the benzaldehydes shown in **Figure 3.15** did not form any type of solid. Instead they formed oils. 2,4,6–trimethoxybenzaldehyde when mixed in methanol with the catalyst turned red which proceeded to form a red oil upon addition to the sorbitol mixture. 4–^{iso}propoxybenzaldehyde formed a pink/ purple oil and 4–dimethylaminobenzaldehyde formed a green oil based product. These three benzaldehydes all reacted very similarly to one another, unlike the other benzaldehydes that were used throughout to create the library of DBS derivatives.

Initial thoughts were that the benzaldehydes were self-polymerising and not reacting with the D–sorbitol. It was thought that the aromatic rings are very electron rich due to their functional groups and can hence act as a nucleophile resulting in the benzene ring attacking the carbon on the aldehyde rather than the sorbitol reacting with the carbon of the aldehyde. However, no evidence of this occurring could be found on analysis via mass spectroscopy. Burkett and Schultz[341] conducted a study into the acid catalysed decarbonylation of 2,4,6–trimethoxybenzaldehyde. Through their research they also recorded the formation of a red solution and precipitate when high concentrations of 2,4,6–trimethoxybenzaldehyde react with an acid. They state that there are two possibilities of how the final product is formed. The first route, see **Figure 3.16**, involved 2,4,6–trimethoxybenzaldehyde **(I)** undergoing decarbonylation in the presence of an acid to yield 1,3,5–trimethoxybenzene **(II)**, then with the subsequent condensation reaction of one mole of **(I)** with two moles of **(II)** to yield **(IV)**. After washing with water, giving rise to a white solid, they determined the structure of the product to be 2,4,5,2',4',5',2'',4'',5''–nonamethoxytriphenylmethane. **(IV)**, and through titration experiments were able to determine that the red product was in fact a 1:1 molar adduct of **(IV)** and the acid. The second route they proposed was the reaction of **(I)** with acid to produce **(III)** with the condensation happening prior to the loss of the aldehyde group to yield **(IV)**.

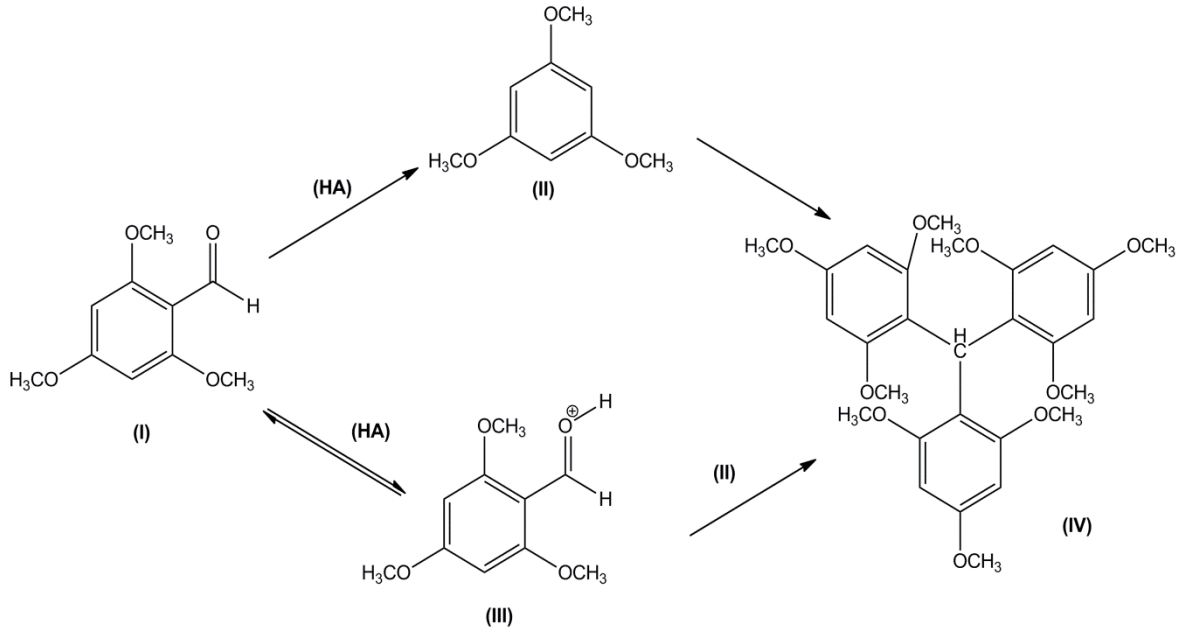

Figure 3.16 2,4,6-trimethoxybenzaldehyde adduct formation.[341]

Therefore within our reactions this explanation would also be plausible where the red oil formed is in fact an adduct of the benzaldehyde with the acid catalyst that was used throughout the synthesis. This result was also observed with branched electron donating groups such as 4–dimethylaminobenzaldehyde and 4–^{iso}propoxybenzaldehyde. We suggest that the electron rich nature of these particular examples facilitates this process.

3.2.4 Rika - Commercial DBS

During the course of this research there was no known commercially available source of 1,3:2,4–Dibenzylidene–D–sorbitol. Milliken and Co used to be the only manufacturer, but at the point of starting this research they had stopped all manufacture. Then in 2013, a commercially available form of 1,3:2,4–Dibenzylidene–D–sorbitol became available from RiKA International, known by the brand name "Geniset D". RiKA International and RiKAmerica were subsidiaries of New Japan Chemical Company. RiKA International and RiKAmerica now exist as NJC Europe and NJC America as of late 2014, but are still owned by New Japan Chemical Company. Within this study this commercially available version of DBS will be referred to as "Rika" for identification purposes and to separate it from the laboratory synthesised DBS. This is important as the synthetic route, purity and polymorphic forms of the two types of DBS are different.

Each of the successfully synthesised DBS and DBS derivatives were screened for their gelation ability within de-icing and anti-icing solvent systems. By derivatising DBS

with hydrophilic substituents we hoped to increase the solubility of these types of molecules within de-icing and anti-icing solvent systems which can include significant amounts of water on dilution.

3.2.5 Gelation Ability

Each of the DBS (synthesised & commercially available forms) and DBS derivatives were screened for their gelation ability in de/anti-icing solvent systems. In Chapter 2 we looked at three different types of glycols, however we now focussed on just the use of monopropylene glycol (MPG) and its aqueous mixtures. This was primarily due to the environmental toxicity of monoethylene glycol (MEG) being unfavourable and the industry-wide efforts to phase it out. Furthermore, 1,3–propanediol (PDO) although thought of as being more environmentally favourable, as it is bio-derived, is much more expensive than MPG and MEG. As such this has reduced the demand for this type of 'green' product at this point. Most manufacturers have now ceased production of such products and are seeking alternatives. De/anti-icing products are generally very cheap when composed of MPG and MEG but when substituted for PDO, the cost rises too much for it to be a viable asset to the end customers, therefore our intention was to make use of MPG which is cheap, readily available and still has a low environmental impact to produce a system which is cost- effective to end users of de/anti-icing products.

Each DBS and its derivatives were screened for their gelation ability in 100% MPG, 75:25% MPG: H_2O, 50:50% MPG: H_2O and 100% H_2O. The samples used for screening were made by weighing out a known amount of gelator into a glass vial. To the glass vial, 1ml of solvent was added. Each sample was sonicated for 1 hour before being heated to just below the boiling point of the solvent (90°C) to create a clear homogenous solution. Temperature was used as a trigger as this would be the stimulus used within the de-icing industry to achieve gelation. **Table 3.1** demonstrates the results of gelation testing of each molecule at 1 % w/v. Unlike Chapter 2 where duplicate samples were made of each molecule, only one set of samples were created for each molecule in each of the different solvents which were left overnight to cool on the bench at room temperature. This was because the results from Chapter 2 showed us that DBS forms gels at room temperature and above, therefore there was no need to test for the gelation capability at lower temperatures, unless no gels formed at room temperature. Results were recorded the next day.

The tube inversion method[286] was used to determine if a gel had formed. Samples were deemed a gel if when the vial was inverted there was no flow of the contents under gravity for a period of several minutes.

Table 3.1 demonstrates the gelation ability of the various DBS and its derivatives at 1% w/v. From **Table 3.1** it is clear that the commercially available DBS (Rika), has the same gelation performance as the laboratory synthesised DBS, which confirms our results from Chapter 2. When the gelation ability of the derivatives was investigated, it was apparent that one particular derivative, DBS-OCH_3, compared well to the original DBS gelator and the other derivatives, outperforming them all. DBS-OCH_3 at 1% w/v was able to form gels in all of the required solvent systems apart from water. Therefore with the addition of a methoxy ether group onto the DBS structure we have been able to demonstrate that this can increase the gelation ability in solvents such as 100% MPG at 1% w/v to create favourable interactions between the molecules to form fibres that create a 3D gel structure, unlike DBS which requires much higher concentrations to achieve this.

As a result of the success of modifying the DBS structure to incorporate a methoxy ether group on the para position we wanted to identify if other ether groups would have similar behaviour in these solvent systems. To investigate this, we considered the ethoxy ether and ^{n}propoxy ether substituents. With the addition of these substituents onto the DBS structure we can see from **Table 3.1** that we achieved the reverse effect compared to that of DBS-OCH_3. By increasing alkyl chains on both the ethoxy ether and ^{n}propoxy ether substituents we increase the hydrophobicity of these molecules, hence preventing them from dissolving and assembling in these solvent systems.

Table 3.1 Gelation ability of DBS and its Derivatives at 1% w/v.
G = Gel, PG = Partial Gel, S = Soluble, I = Insoluble, ***I*** = Insoluble but gels below 1%w/v.

	Solvents			
Molecules	**100% MPG**	**75:25 MPG:H_2O**	**50:50 MPG:H_2O**	**100% H_2O**
DBS	S	**G**	**G**	I
Rika (DBS)	S	**G**	**G**	I
DBS-OCH_3	**G**	**G**	**G**	I
DBS-OCH_2CH_3	S	I	I	I
DBS-$O(CH_2)_2CH_3$	I	I	I	I
DBS-SCH_3	***I***	***I***	***I***	I
DBS-NO_2	I	***I***	I	I
DBS-CF_3	S	***I***	***I***	I
DBS-CO_2CH_3	S	I	**G**	I
DBS-COOH	I	I	I	I
DBS-SO_2CH_3	I	**G**	**G**	I
DBS-$CONHNH_2$	I	**G**	**G**	***I***
TBS	I	I	I	I
MBS	S	S	S	S
Sorbitol	S	S	S	S

DBS with a methylthioether substituent was considered similar to the methoxy ether substituent, however changing the oxygen to a sulphur atom proved detrimental and at 1% w/v showed to be incapable of forming gels in the required solvents. Once again the solubility of this compound was just too low for gelation to be favoured. It is well known that thioethers are less polar than oxyethers.[342,343]

Next we tried to determine if including an electron withdrawing group on the DBS structure improved the gelation ability of DBS in the required solvents for de/anti-icing aircrafts.

A range of DBS derivatives with electron withdrawing substituents were examined. These substituents included nitro, trifluoromethyl, ester, acid, methylsulfonyl and hydrazide groups. From **Table 3.1** we can see with the incorporation of electron withdrawing substituents on the DBS structure hinders the formation of gels, with the exception of the methylsulfonyl and hydrazide DBS derivatives which have the ability to gel aqueous glycol mixtures at 1% w/v. Clearly these two substituents are more hydrophilic and are therefore better able to dissolve and gelate. The carboxylic acid could perhaps have formed gels but would have required a pH change in order to dissolve.[143,155]

Of all of the DBS derivatives that were analysed we can see that through the use of temperature as a stimulus, and in these required solvents very few are capable of forming gels at 1% w/v. None of these derivatives were able to form a hydrogelator at 1% w/v in 100% water. Therefore changing and adding different substituents on to the DBS structure to try and increase the hydrophilicity of the molecule to encourage gel formation in water was unsuccessful.

The by-products produced throughout the synthesis of DBS were also examined for their gelation ability. Tri-benzylidene sorbitol (TBS), unlike DBS was incapable of forming gels in any of the solvents and remained insoluble, presumably owing to its non-polar nature, whilst the opposite was observed for the more hydrophilic monobenzylidene sorbitol (MBS) where it remained soluble. Although MBS did not have the capability to form gels, Dotson and Scrivens[344] have shown that a different configuration of MBS can form gels in solvents such as glycerine, propylene glycol and water. They showed the formation of gels in these solvents was possible through the use of 2,4–O–(3,4-dimethylbenzylidene)-D-sorbitol, see **Figure 3.17.** However the ability of this molecule to form gels in these solvents was only observed at high concentrations of 2-3% w/v.

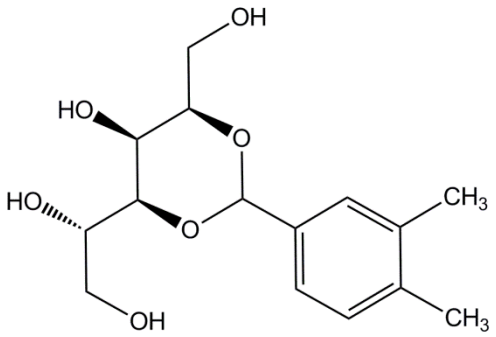

Figure 3.17 Structure of 2,4-O-(3,4-dimethylbenzylidene)-D-sorbitol.[344]

Unmodified D-sorbitol was also tested for its ability to act as a gelator. If successful, this would be cheap to use and environmentally friendly, as shown by its extensive use in foods as a sweetener. Grassi et al[345] have demonstrated that D–sorbitol does have the capability to form gels in ethanol and aqueous mixtures of ethanol, but once again this requires much higher concentrations, (1.5–3.5% w/v) than what has been studied throughout this chapter as well as a secondary stimulus of sonication. When D–sorbitol was tested it showed the same behaviour as MBS, remaining soluble in all of the chosen solvents.

The difference in gelation ability between DBS and its by-products can be attributed to its molecular structure. TBS with the additional benzene ring compared to DBS

imparts too much hydrophobicity in the molecule's structure for it to form interactions with other gelator molecules in these solvents. However, the additional hydroxyl groups on MBS and D–sorbitol mean they are too hydrophilic and consequently soluble in MPG, water and aqueous glycol mixtures to actually self-assemble and gelate.

We have seen that the modification of a molecular structure, such as that demonstrated by Dotson and Scrivens, where they incorporated methyl groups on the MBS structure, can improve the gelation ability, whilst adding hydrophobic groups and or branched groups in other instances can hinder gel formation. Obtaining the correct structure of a molecule to act as a gelator is a difficult and challenging task and is a balancing act between the solvent compatibility of each molecule.[184,185]

Throughout this study we have only tested the gelation ability of each of the derivatives up to and including 1% w/v, as shown in **Table 3.1**. No further investigation into the gelation ability of each of the DBS and DBS derivatives were undertaken above this concentration. This is primarily because the current polymer technology used with de/anti-icing products is at levels below 1% w/v. Higher concentrations (>1% w/v) would potentially increase the cost to manufacture such a product and hence reduce profit margins, therefore it is important that the molecules used can be used at similar concentrations and be of similar price.

Screening of the DBS and DBS derivatives below 1% w/v showed no change to the gelation ability for DBS-OCH_2CH_3 (Ethoxy), DBS-$O(CH_2)_2CH_3$ (^{n}propoxy), DBS-CO_2CH_3 (Ester), DBS-COOH (acid) or TBS, they all remained insoluble as they were at 1% w/v in the chosen solvents. Likewise with MBS and sorbitol they remained soluble at all lower concentrations and showed no signs of gel formation.

The molecules which were capable of forming gels at 1% w/v when tested at lower concentrations (**Table 3.2**) showed the same results for 100% MPG and water, except for DBS-OCH_3 and DBS-$CONHNH_2$, with their gelation performance improving in glycol aqueous mixtures. **Table 3.2** indicates that when compared to the original DBS and Rika molecules in aqueous glycol mixtures the derivatives have similar gelation ranges with DBS-$CONHNH_2$ requiring slightly higher concentrations than the other molecules. DBS-OCH_3 has the same gelation ability and range throughout the different glycol-containing solvents.

Table 3.2 Gelation range of DBS and DBS derivatives in monopropylene glycol and aqueous glycol mixtures.

Molecules	**Gelation Range in % w/v**			
	100% MPG	**75:25 MPG:H_2O**	**50:50 MPG: H_2O**	**100% H_2O**
DBS	S	0.1-1.0	0.07-1.0	I
Rika (DBS)	S	0.1-1.0	0.07-1.0	I
DBS-OCH_3	0.2-1.0	0.1-1.0	0.1-1.0	I
DBS-SO_2CH_3	I	0.3-1.0	0.2-1.0	I
DBS-$CONHNH_2$	I	0.7-1.0	0.8-1.0	0.2-0.35

Only one molecule when tested had the ability to act as a pure hydrogelator, DBS-$CONHNH_2$. This molecule could form gels at low concentrations but had a smaller gelation range. This molecule generally had a smaller concentration range than the other derivatives in the chosen solvents. This derivative is known to form hydrogelators through the use of heat-cool cycles as published elsewhere by the Smith group,[155] who noted that it can form gels across a range of different pH values, which may potentially be useful in applications such as environmental remediation.[155,267,268]

Some of the derivatives tested changed their behaviour at lower concentrations. As we can see from **Table 3.1**, at 1% w/v DBS-SCH_3, DBS-NO_2 and DBS-CF_3 were all insoluble. However, when the concentration was reduced for each of these derivatives it was noted that gels could be formed across quite a large concentration range similar to that of native DBS, see **Table 3.3**. DBS-NO_2 only showed the ability to form gels in 75:25 MPG:H_2O and no other solvent. DBS-CF_3 showed the same gelation ability as DBS with no changes observed when in 100% MPG or water. However, the most notably improved derivative was DBS-SCH_3. Not only does it have similar gelation ability to DBS but can also gel 100% MPG unlike DBS. This derivative was also the only molecule capable of forming gels below 0.1% w/v. Clearly, 1% w/v was just over the solubility threshold for DBS-SCH_3, and below this level it performs as a highly effective gelator – competitive with, or even better than DBS-OCH_3.

Table3.3 Comparison of DBS gelation range with DBS derivatives.

Molecules	Gelation Range in % w/v			
	100% MPG	**75:25 MPG:H_2O**	**50:50 MPG: H_2O**	**100% H_2O**
DBS	S	0.1-1.0	0.07-1.0	I
Rika (DBS)	S	0.1-1.0	0.07-1.0	I
DBS-SCH_3	0.3-0.9	0.03-0.9	0.02-0.4	I
DBS-NO_2	I	0.2-0.9	I	I
DBS-CF_3	S	0.1-0.9	0.1-0.9	I

From the gelation screening of the various DBS derivatives it is apparent that some derivatives are more successful than others in our chosen solvents. The majority of these derivatives struggle to form gels in 100% MPG and water but when incorporated into aqueous mixtures of glycol their ability to gel improves with increasing water content. This indicates that in partial water solvent systems the correct balance between insolubility and solubility for interactions to occur between the gelator molecules and solvent to form fibres can be achieved. Therefore it is noted that the substituent attached to the butterfly-like wings of DBS can play a key role in tuning gelation ability. Assembly for this class of compound occurs due to hydrophobic effects, hydrogen bonding and π-π stacking of the rings. These molecules therefore clearly demonstrate solvent mixture tuning effects of solubility / assembly.[105,163,183,189,346,347]

3.2.6 Minimum Gelation Concentration (MGC).

Each of the derivatives was tested to identify their minimum gelation concentration. From **Table 3.4** we can see that the derivatives capable of forming gels in 100% MPG, DBS-OCH_3 and DBS-SCH_3 require similar concentrations to form a gel regardless of the substituent. When each of the derivatives were tested in the aqueous glycol mixtures, DBS-SCH_3 operated at significantly lower concentrations presumably because its greater hydrophobicity helps to encourage the self-assembly.

Table 3.4 Minimum gelation concentration for each of the DBS molecules and their derivatives.

	Solvents			
Molecules	**100% MPG**	**75:25 MPG:H_2O**	**50:50 MPG:H_2O**	**100% H_2O**
DBS	S	0.1	0.07	I
Rika (DBS)	S	0.1	0.07	I
DBS-OCH_3	0.2	0.1	0.1	I
DBS-OCH_2CH_3	S	I	I	I
DBS-$O(CH_2)_2CH_3$	I	I	I	I
DBS-SCH_3	0.3	0.03	0.02	I
DBS-NO_2	I	0.2	I	I
DBS-CF_3	S	0.1	0.1	I
DBS-CO_2CH_3	S	I	0.2	I
DBS-COOH	I	I	I	I
DBS-SO_2CH_3	I	0.3	0.2	I
DBS-$CONHNH_2$	I	0.7	0.8	0.2
Tri-DBS	I	I	I	I
Mono-DBS	S	S	S	S
Sorbitol	S	S	S	S

For the majority of the derivatives, however, we note that MGC values are reasonably independent of solvent composition.

3.2.7 Thermal Stability

The thermal stability of each gel formed by the different gelator molecules was measured by finding the T_{gel} of the sample. This is measured using the tube inversion test as described in Chapter 2. The temperature at which the gel sample collapses was recorded as the T_{gel} value.

Each of the DBS derivatives which could form gels across a concentration range in each of the different solvents was tested to determine whether by modifying the original DBS structure would have any effect on the molecules thermal stability. All of the DBS analogues that were tested showed the same general behaviour, as concentration increases the T_{gel} increases, as would be expected and is typical for many gelators due to the gel network becoming more extensive on increasing the concentration of the gelator.

In Chapter 2 we found that as we changed the composition of our solvent system to include more water, the thermal stability of 1,3:2,4–Dibenzylidene–D–sorbitol i.e. if we increased the ratio of water from 0% (100% glycol) to 50% (50% glycol) the

thermal stability of each gel increased. Therefore by incorporating more water into the solvent system increases the hydrophobic effects which become more dominant and drives the self assembly of these molecules within our chosen solvents to produce gels which are more thermally stable.

Of all of the DBS derivatives tested only two molecules showed similar thermal stability profiles to that of DBS. These were DBS-OCH_3 and DBS-SCH_3. Both of these derivatives were able to gel all of the chosen solvents except water, like DBS. However, unlike DBS which required concentrations above 1% w/v to produce gels both of these derivatives could produce gels well below 1% w/v. Each of these derivatives clearly show the effects of increasing the water content through their thermal stability profiles, and hence the effects of the hydrophobic effects, with the 50:50 MPG:H_2O producing the most thermally stable gels, see **Figure 3.18 and 3.19**.

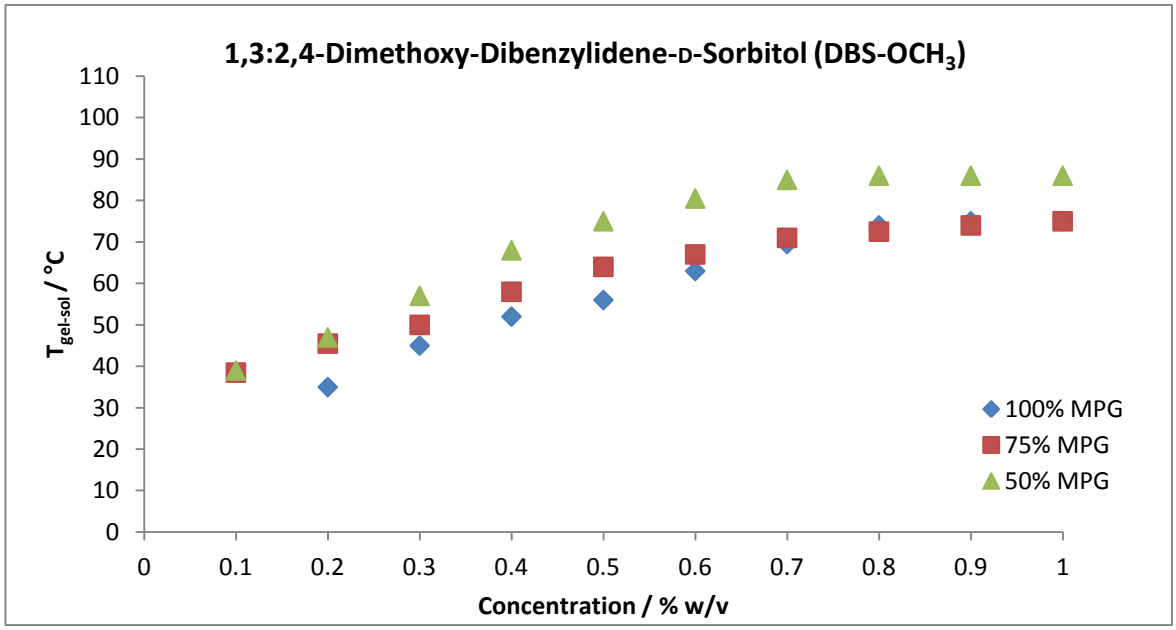

Figure 3.18 Thermal stability behaviour of 1,3:2,4-Dimethoxy-Dibenzylidene-D-sorbitol in MPG and aqueous mixtures of MPG.

This effect was particularly marked for DBS-SCH_3 on addition of water, supporting the previous view that this system becomes a highly effective gelator owing to its greater hydrophobicity–indeed it can be considered as a supergelator, with a MGC <0.1% w/v.

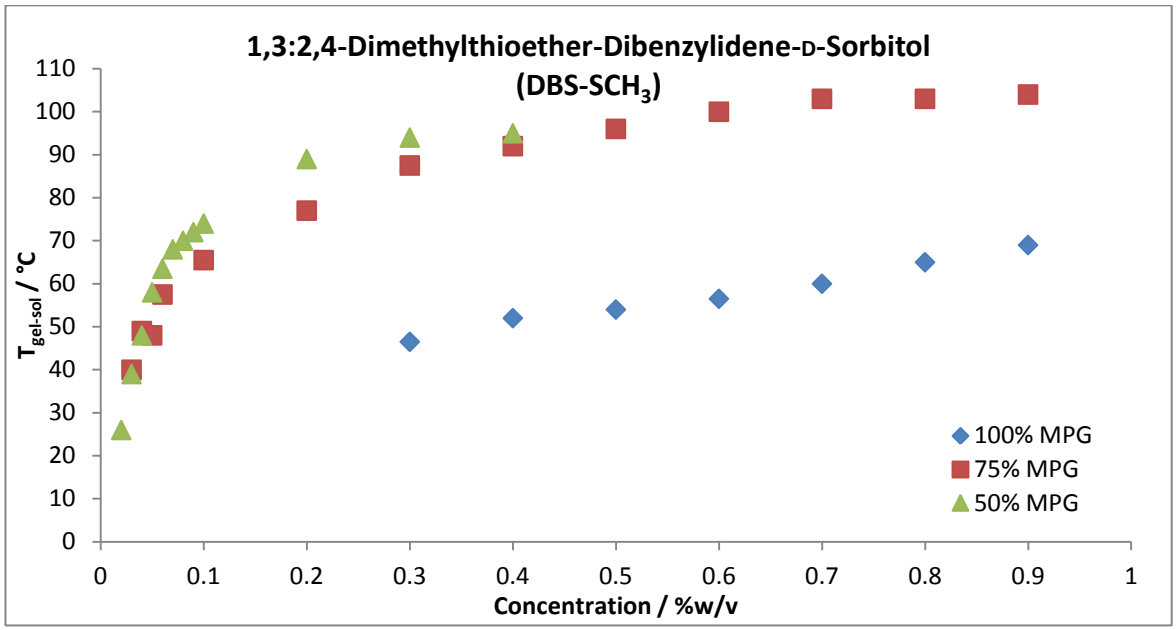

Figure 3.19 Thermal stability of 1,3:2,4-Dimethylthioether-Dibenzylidene-D-sorbitol in MPG and aqueous mixtures of MPG.

To understand if the DBS derivatives were creating more or less thermally stable gels these results were compared to those of DBS. Both of the DBS molecules tested during this study, the laboratory synthesised DBS and the commercially available DBS (Rika), had the same thermal stability profiles, therefore only DBS is shown for comparison purposes. Comparing the DBS derivatives DBS-OCH_3 and DBS-SCH_3 in aqueous glycol mixtures we can see from **Figures 3.20 and 3.21** that adding these groups to the structure of DBS enhances the thermal stability quite significantly. Therefore by changing the substituent to H on the benzene ring to OCH_3 and then SCH_3 we can double the thermal stability of a gel. This can clearly be observed in **Figure 3.20** when comparing all three molecules at the different concentrations, for example at 0.1% w/v the thermal stability increases from 30°C (DBS) to 38°C (DBS-OCH_3) to 64°C (DBS-SCH_3).

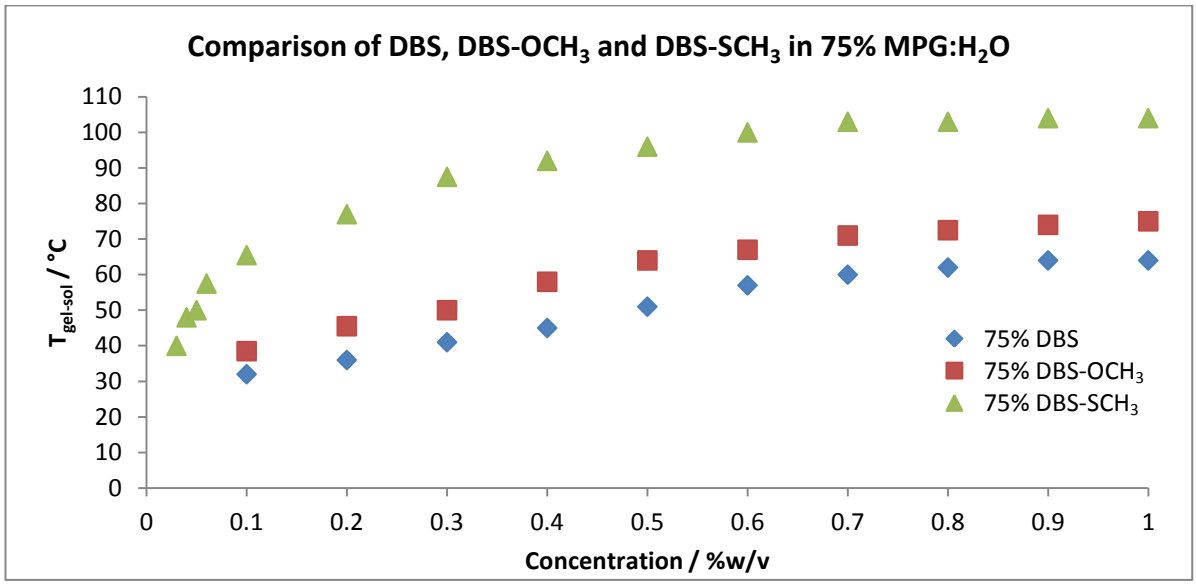

Figure 3.20 Thermal stability of DBS compared to DBS-OCH_3 and DBS-SCH_3 derivatives in 75:25 MPG:H_2O.

In 50:50 MPG:H_2O we can also see the same effects as with 75:25 MPG:H_2O solvent system. Again we note that as the water ratio increases the thermal stability increases due to the hydrophobic effects, with the most thermally stable gels being formed in 50% aqueous glycol mixtures and DBS-SCH_3 showing the greatest increase.

Comparing DBS to these derivatives it is clear that each of the derivatives can increase the thermal stability with DBS-SCH_3 performing the best. DBS-SCH_3, also demonstrates that by making a small simple change to the structure we can create gels which operate at much lower concentrations than the minimum concentration required for DBS, but still remains thermally stable.

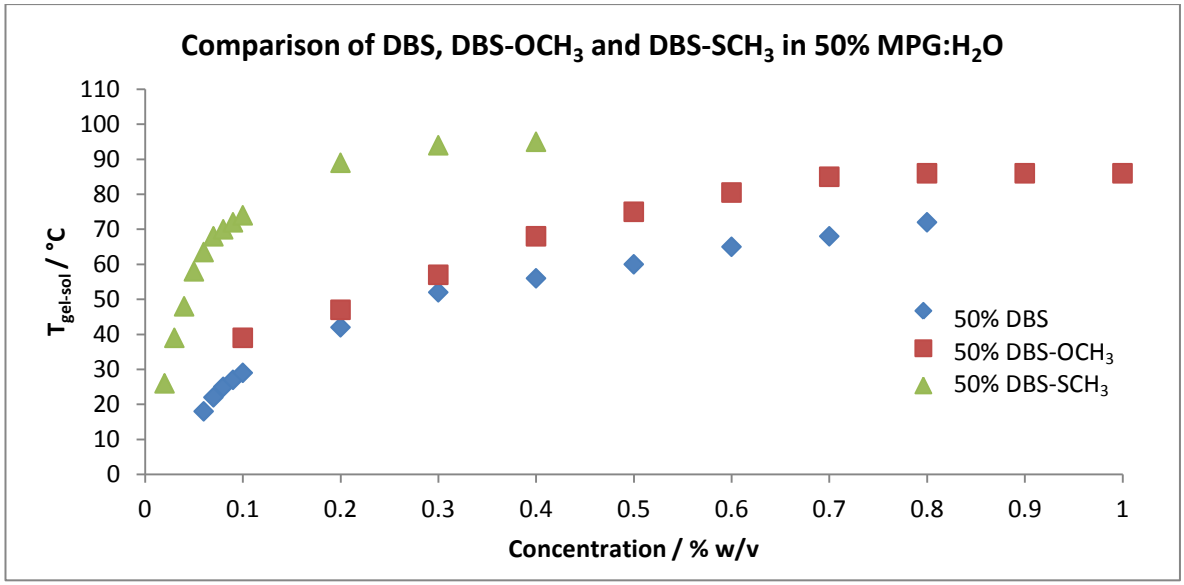

Figure 3.21 Thermal stability of DBS compared to DBS-OCH_3 and DBS-SCH_3 derivatives in 50:50 MPG:H_2O.

DBS derivatives with NO_2, CF_3, SO_2CH_3 and $CONHNH_2$ groups were also compared to DBS to identify if these types of substituents have similar effects. Unlike the DBS derivatives with OCH_3 and SCH_3 groups where we saw the thermal stability increase as a result of the structure modification, DBS derivatives with electron withdrawing groups such as NO_2, CF_3, SO_2CH_3 and $CONHNH_2$ do not show the same behaviour for all of the derivatives. Instead we observe that groups such as NO_2 and CF_3 increase the thermal stability relative to DBS whilst groups such as SO_2CH_3 and $CONHNH_2$ decrease the thermal stability when in aqueous glycol mixtures see **Figure 3.22**. This difference in the thermal stability of each of the DBS derivatives is potentially due to the hydrophilicity of the substituent. Substituents such as NO_2 and CF_3 are obviously interacting more effectively than SO_2CH_3 and $CONHNH_2$ groups which are more hydrophilic and hence less able to self assemble in these relatively polar hydrophilic media therefore do not form a more thermally stable gel than derivatives such as NO_2 or CF_3.

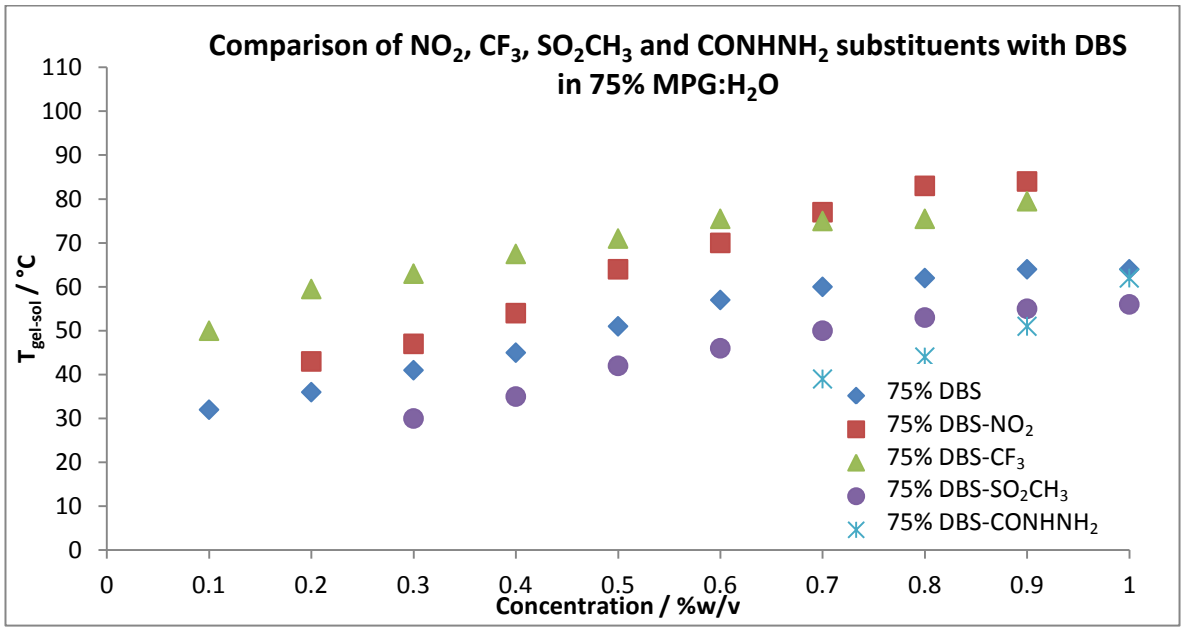

Figure 3.22 Thermal stability of DBS compared to DBS derivatives with NO_2, CF_3, SO_2CH_3 and $CONHNH_2$ groups in 75:25 MPG:H_2O.

As we already know DBS and its derivatives self assemble through hydrophobic effects in our chosen solvent systems and like the DBS derivatives with OCH_3 and SCH_3 groups, DBS derivativeS with CF_3 groups on produce the most thermally stable gels when there is 50:50 MPG:H_2O, see **Figure 3.23**. However, DBS-NO_2 is unable to form gels in 50:50 MPG:H_2O unlike the other derivatives and remains insoluble. This reflects the fact this is the most hydrophobic of these derivatives and just cannot

dissolve in this more polar solvent. As such, although it formed the best gel in 75:25 MPG:H_2O it becomes just too insoluble in 50:50 MPG:H_2O.

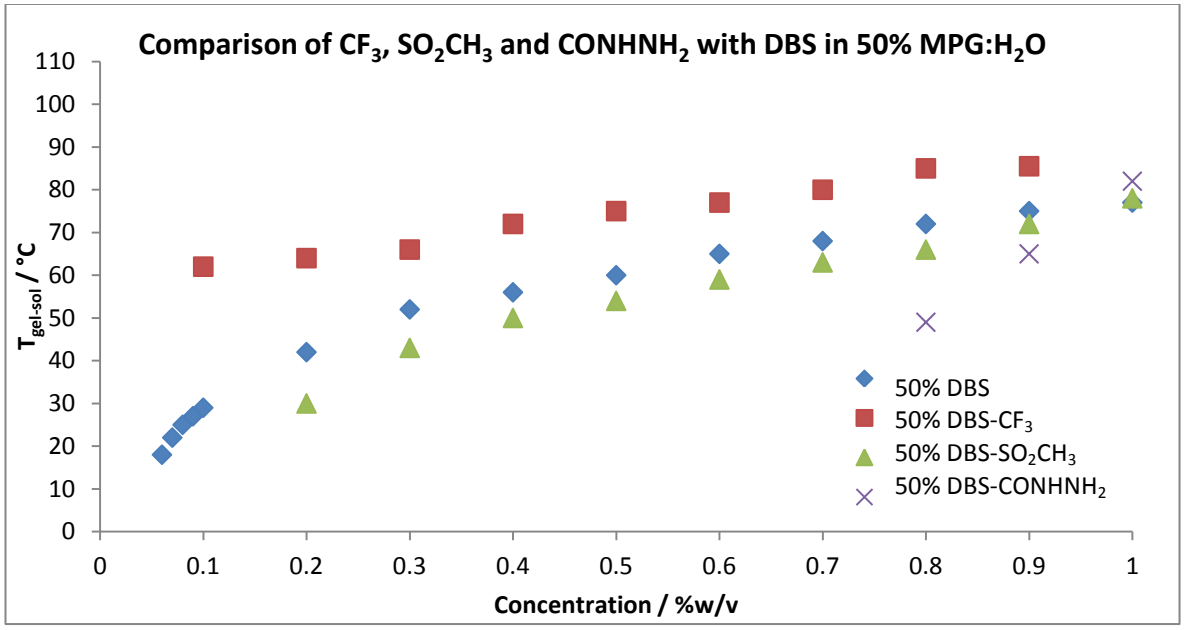

Figure 3.23 Thermal stability of DBS compared to DBS derivatives CF_3, SO_2CH_3 and $CONHNH_2$ groups in 50:50 MPG:H_2O.

From consideration of all of the different DBS analogues that have been screened within each of the different solvent systems it is clear that they predominantly self-assemble through hydrophobic effects which become more prevalent as the water ratio increases. All of the DBS derivatives have good thermal stability with some molecules exceeding the original DBS thermal stability profile and only a minority of the molecules, specifically the more hydrophilic ones having reduced thermal stability. Therefore it is also evident that the type of substituent added to the DBS structure can have significant effects in relation to a molecules thermal stability. DBS–SCH_3 had the best thermal stability amongst the analogues and also formed gels at ultra low concentrations. We suggest this compound has optimal hydrophobicity.

3.2.8 Environmental Concerns

The library of DBS derivatives which have been synthesised have very good gelation ability in the required de/anti-icing solvent. They have proven that gels can be formed at much lower concentrations than the original DBS molecule while also possessing higher thermal stability. However, although each of the DBS derivatives performance could work well within the de/anti-icing application, there are environmental concerns with regards to some of the different substituents that have been attached.

DBS itself is known to be used commercially and therefore does not pose any significant environmental concerns. DBS derivatives with groups such as OCH_3 and SCH_3 also pose no immediate concerns. However, some of the DBS derivatives with electron withdrawing groups do. DBS-CF_3, the performance of which could match that of the DBS-OCH_3 and DBS-SCH_3 derivatives is an environmental concern due to the CF_3 substituent. Fluorocarbons are very stable and have very long half-lives, therefore disposal/dispersal of such a molecule with this substituent may prove difficult. The industry is also very wary about the use of any chemicals containing nitrogen, therefore DBS-NO_2 and DBS-$CONHNH_2$ were ruled out from further analysis. This is primarily due to the use of urea-based chemicals that were historically used to clear runways. Through the use of urea-based products, it became apparent that the production of nitrosamine based by-products was causing environmental concerns. When trials were conducted by environmental bodies, they decided to ban the use of any nitrosating ingredient in general due to the fact nitrosamine based products could penetrate the skin and cause cancers. Therefore any risk of associating nitrosamine products into aviation is avoided at all costs.

DBS-SO_2CH_3 poses no environmental concerns to the aviation industry, however due to its lower thermal stability profile and inability to form gels at low concentrations of 0.1% w/v it has been ruled out for further analysis from this point forwards.

Therefore of all the DBS derivatives synthesised DBS and DBS derivatives, DBS-OCH_3 and DBS-SCH_3 will be investigated further, due to their expected low environmental toxicity, good thermal stability profiles and ability to form gels even below 0.1% w/v.

3.3 Conclusions

A library of DBS derivative low molecular weight gelators was created by structurally modifying DBS. This was achieved through the use of an acid catalysed condensation/dehydration synthetic procedure which was published in the literature and was modified by us. A number of DBS derivatives as well as DBS itself were successfully synthesised including DBS-CO_2CH_3, DBS-OCH_3, DBS-OCH_2CH_3, DBS-$O(CH_2)_2CH_3$, DBS-SCH_3, DBS-SO_2CH_3, DBS-CF_3, DBS-NO_2 as well as the known by-products MBS and TBS, produced during the synthesis of DBS. DBS-CO_2CH_3 was further converted with an additional synthetic step to yield two more DBS based gelators, DBS-COOH and DBS-$CONHNH_2$.

Additional derivatives of DBS with more than one substituent and or branched substituents were also investigated, however their synthesis proved to be unsuccessful and showed signs of polymerisation and the formation of adducts with the catalyst and benzaldehyde throughout the reaction. Therefore this may indicate that incorporating these types of substituents would require a modified synthesis.

Each of the successfully synthesised DBS derivatives, by-products and the commercially available DBS (Rika) were tested for their gelation ability in solvent mixtures (MPG and aqueous MPG mixtures), important for the de/anti-icing industry. The commercially available DBS (Rika) and the laboratory synthesised DBS showed the same gelation ability when tested at high concentration (1% w/v) and showed the capability of forming gels in aqueous MPG mixtures whilst remaining soluble in the 100% MPG. The other derivatives when tested at higher concentration (1% w/v) showed variable ability to gel the required solvents. The majority of the derivatives were incapable of gelling the required solvents with the exception of DBS-OCH_3, DBS-SO_2CH_3 and DBS-$CONHNH_2$. However, when tested at lower concentrations than 1% w/v, the gelation ability of the derivatives improved significantly. At concentrations of 1% w/v and below it became apparent that two of the DBS derivatives could perform better than the original DBS gelator. These were DBS-OCH_3 and DBS-SCH_3. Both of these gelators could gel all of the required solvents with the exception of water.

Due to the success of the DBS derivatives containing ether and thioether substituents, additional ether substituents were investigated with longer alkyl chains. However, it was shown that by adding additional carbons to the alkyl chain of the substituent made the molecule too hydrophobic so that they could not form gels in these solvent systems. Branched ether substituents, however, could not be synthesised.

Each of the derivatives with substituents which were electron withdrawing groups successfully formed gels in aqueous glycol mixtures with the exception of DBS-COOH and DBS-CO_2CH_3 which remained insoluble throughout. These molecules may require different stimuli to form gels in these solvent systems. Through the investigation of these derivatives with electron withdrawing substituents we then found the first DBS gelator with the ability to form gels in water, DBS-$CONHNH_2$. However, the concentration range in which hydrogelators could be formed was very small and could prove difficult to handle when scaled up.

The by-products, MBS and TBS produced through the synthesis of DBS when tested for the gelation ability showed to be unsuccessful, where MBS remained soluble and TBS insoluble. The structure of MBS is too hydrophilic and TBS too hydrophobic to successfully form gels in these solvents. Therefore this shows us the correct balance of hydrophilicity with hydrophobicity is important for a molecule's ability to form a gel.

The thermal stability of each of the successful gelators was tested which demonstrated that the self-assembly of these types of molecules is primarily driven through hydrophobic effects whereby the thermal stability of each of the molecules increase as the ratio of water increases with 50% MPG: H_2O being the most thermally stable. Effects of the differing substituents were also notable. With the two most successful gelators DBS-OCH_3 and DBS-SCH_3 having the best thermal stability compared to the original DBS with DBS-SCH_3 being particularly improved owing to its greater hydrophobicity. Derivatives with electron withdrawing groups showed differing effects with more hydrophobic DBS-CF_3 and DBS-NO_2 having greater thermal stability than DBS and more hydrophilic DBS-SO_2CH_3 and DBS-$CONHNH_2$ having lower thermal stability. Therefore this study has demonstrated that simple structural derivatisation of a molecule can significantly affect the solubility and the ability of a molecule to act as a gelator. In this way gelators can be optimised for specific interactions.

The de/anti-icing industry is becoming more and more environmentally driven and as a consequence, although the majority of the synthesised DBS derivatives performed well, some will not be further investigated due to their environmental concerns. Derivatives such as DBS-NO_2 and DBS-$CONHNH_2$ have the potential to form nitrosamine by-products which are detrimental to the environment and health. We also rejected DBS-CF_3 which may have a long half-life and environmental persistence. Although DBS-SO_2CH_3 has no immediate environmental concerns, this molecule did not show any improved performance compared to the original DBS molecule and it was therefore decided that no further investigation of this molecule will be undertaken at this time.

The next steps are therefore to further investigate the DBS derivatives which performed the best within the chosen de/anti-icing solvents. These molecules have the potential to be used across a large concentration range, they can form gels at very low concentrations below 0.1% w/v, have improved thermal stability compared to

DBS and potentially have little environmental impact. These molecules are DBS-OCH_3 and DBS-SCH_3. In the following chapters these molecules will be investigated and compared to the original DBS to gain a better understanding of how they self-assemble, their internal structure and how they respond to different stresses and strains that would be experienced throughout the de/anti-icing application, to gain a greater insight into the formation of their nanoscale structures at varying temperatures which simulate the real-life de/anti-icing application.

Chapter 4

DBS, Methoxy and Methylthioether Derivative Gelators

Chapter 4 DBS, Methoxy and Methylthioether Derivative Gelators

4.1 Introduction

In Chapter 3 we highlighted three main compounds, DBS, DBS-OCH_3 and DBS-SCH_3 which proved to be successful at forming gels in the required de/anti-icing solvents. These molecules were able to form gels across large concentration ranges and perform as supergelators, with gels formed at <0.1% w/v, with good thermal stability. As a result of the success of these three molecules we wanted to investigate them further to try and understand how they assemble, and explore the rheological properties of gels assembled using these molecules.

Within this chapter, each of the molecules in each of the different de/anti-icing solvents will be investigated through the use of circular dichroism (CD) to gain a better understanding of how these molecules self-assemble and disassemble when temperature is applied and how the kinetics affect gel formation. Rheological analysis of these molecules allow us to gain a greater understanding of the stability, strength and stiffness that can be achieved by each gel, and how each of the gels responds to changing temperatures. Finally within this chapter we will then try to determine if information obtained from these techniques can be related to the morphologies of the nanostructures observed through SEM. This combination of techniques therefore probes molecular-scale organisation, nanoscale morphology and macroscopic behaviour.

4.2 Results & Discussion

4.2.1 Effects of substituent on the chiral assembly of DBS and DBS derivative gelators

Each of the three gelators DBS, DBS-OCH_3 and DBS-SCH_3 was analysed using circular dichroism spectroscopy. It was decided that since the laboratory synthesised DBS and the commercially available DBS (Rika) showed the same properties, with regards to gelation ability and thermal stability in the previous chapter, that we would use commercial Rika (DBS) for all future studies. Should this molecule be successful for

use in de/anti-icing applications it would be more readily available commercially than needing to synthesise it within a laboratory setting.

Circular dichroism is one of the best methods available to investigate the nanoscale chiral aggregation of molecules and hence can provide detailed information about the solvated gel.[103,286] This is a solution-phase technique which measures the difference between the absorption of left and right handed circularly polarised light across a range of wavelengths.[286,348] For a molecule to exhibit circular dichroism it must contain a chiral centre. An achiral molecule will absorb both the left and right handed polarisations and give a zero spectrum. A chiral molecule can however absorb the two different polarisations differently giving rise to a positive or negative spectrum. Normally signals for individual molecules will have different absorptions to aggregates.[286,348,349] Therefore the intensity of the CD signal provides an indication of the extent of self-assembly. A CD absorption signal will only be observed at wavelengths where the molecule can absorb UV light, hence circular dichroism can be thought of as a type of 'chiral UV' spectroscopy.[348] Therefore the samples must be studied in a solvent which has a UV-Vis absorption spectrum that does not overlap with that of the sample itself.

Samples used for circular dichroism testing were prepared by weighing out a known amount of gelator (below the MGC) into a 2 ml glass vial with 1 ml of solvent (100% MPG, 75:25 MPG:H_2O or 50:50 MPG:H_2O). Each sample was then sonicated for 1 hour before being heated to below the boiling point of the solvent until a clear homogeneous solution was formed. Samples were then left to cool at room temperature before being tested the next day. Each sample (400 µl) in turn was transferred into a quartz cell with a path length of 1 mm and placed into the instrument at 20°C with the circular dichroism spectrum being measured between 200–320 nm.

All solvents used to prepare the samples were first tested on their own. Each of the solvents used were shown to have no active chromophore within their spectra, and hence the results obtained for each sample would be representative of the chromophore within each sample. Each of the three different gelators were then tested individually in the different solvent mixtures and compared with one another. From **Figure 4.1** we can see when we compare the samples containing Rika (DBS) in the different solvents of 100%, 75% and 50% MPG we see notable differences between the three samples. Rika (DBS) in 100% MPG, as shown in Chapter 3 does not

form gels, therefore we see no absorbance from a chromophore within this sample agreeing with the argument that the molecules are too solvated to interact with one another and hence cannot propagate self-assembly. However, Rika (DBS) can form gels in 75 or 50% aqueous glycol mixtures. Therefore we would expect to see a CD band to suggest chiral nanoscale self-assembly of these molecules in these samples.[143,180,350] For each of these samples an absorbance at λ=210.5 nm is detected. We suggest this is associated with the aromatic rings on DBS. The intensity of the CD signal shown in **Figure 4.1** is solvent dependent, which may indicate that the self assembly of this compound is more sensitive to solvent changes, with the absorption shown in 100% DBS being representative of the molecules signal and upon dilution representing the self organised assemblies.

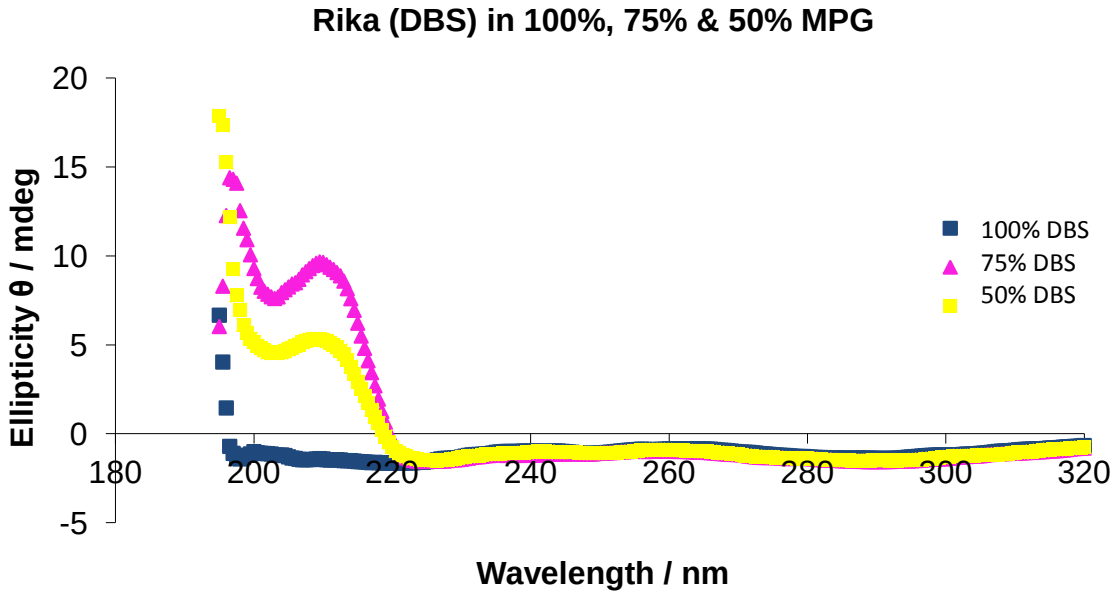

Figure 4.1 Circular dichroism for DBS in the different solvent mixtures.

Samples of DBS-OCH_3 and DBS-SCH_3 in 100% MPG, 75 and 50% MPG were also tested as above. However, unlike Rika (DBS) which cannot form gels in 100% MPG, these two molecules can. From **Figure 4.2** we see that all three of the DBS-OCH_3 samples in the different solvents show the presence of a CD band at λ=230 nm which is representative of the aromatic ring containing the methoxy substituent in the para position.

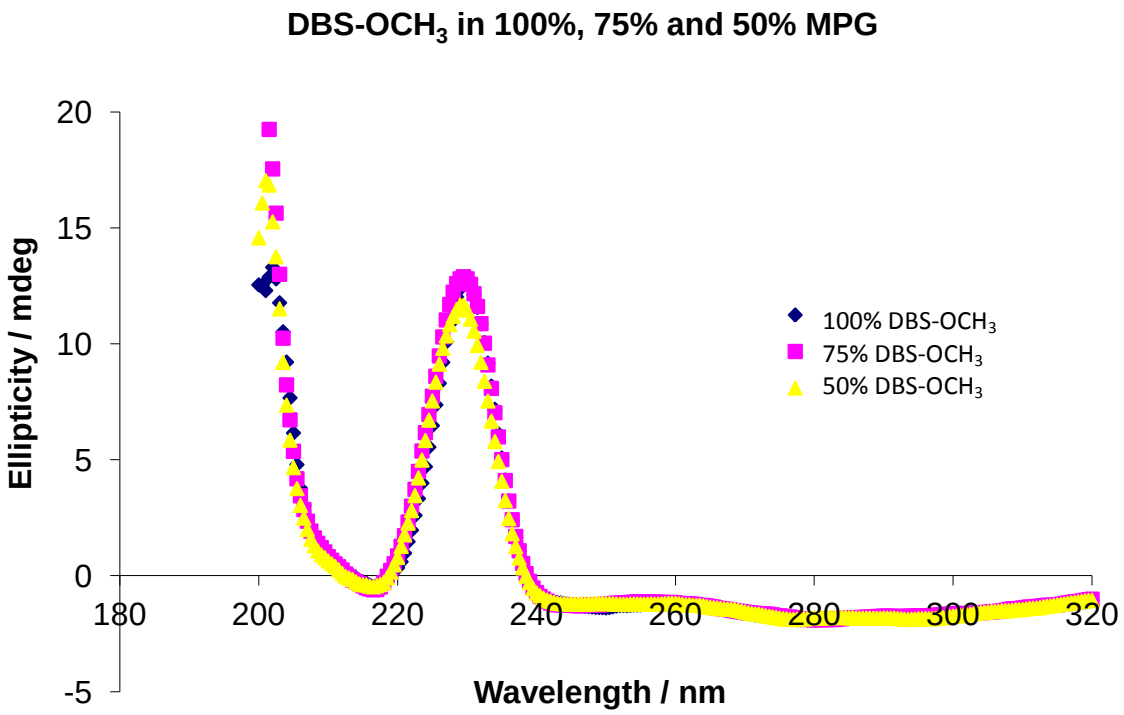

Figure 4.2 Circular dichroism for DBS-OCH_3 in the different solvent mixtures.

Likewise from **Figure 4.3** we see that all three samples in the different solvents with DBS-SCH_3 show the presence of a number of peaks at λ=205, 248 and 264 nm, with λ=264 nm being representative of the aromatic ring with a methylthioether substituent in the para position.

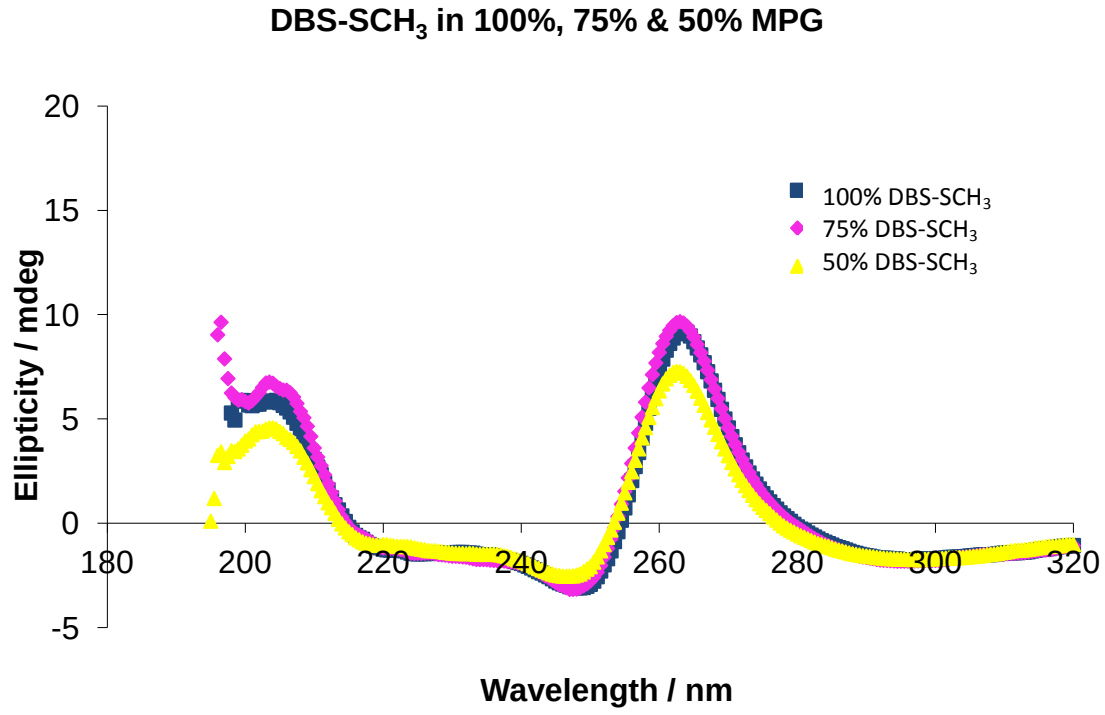

Figure 4.3 Circular dichroism of DBS-SCH_3 in 100%, 75% and 50% MPG.

From the data obtained for all three molecules we can see that the peak shifts in wavelength are in relation to the substituent which is attached to the aromatic ring. Therefore as the molecules become more electron rich by including electron donating substituents on their structures, H<OCH_3<SCH_3, the molecules absorb at longer wavelengths, which would be expected for the increased conjugation in the system. DBS has shown in these solvents that CD intensity is dependent on the solvent, however, DBS-OCH_3 and DBS-SCH_3 shows that the change in solvent has no effect on the peak intensities. Therefore changing the solvent for these molecules does not significantly change the chiral mode of assembly and we would therefore expect DBS-OCH_3 and DBS-SCH_3 to have similar assembly modes in all solvents due to their similar CD profiles. Although the assembly of DBS-OCH_3 and DBS-SCH_3 are similar they also have different shaped spectrums which may be an indication that different types of nanostructures are created for each of these molecules.[351,352]

4.2.2 Variable Temperature CD – Identification of Self Assembly Mode

Variable temperature circular dichroism (VT-CD) is an ideal approach for demonstrating the assembly/disassembly of nanoscale chiral aggregates in response to changes in temperature and can therefore act to confirm the presence of chiral nanoscale structures.[286,348-350,353] Samples for VT-CD were prepared as described above however the samples were placed into the instrument which was set to 100°C and left to reach temperature for 15 minutes before starting the test. Thereafter the instrument was reduced in 10°C increments every 20 minutes until 20°C was reached. Each of the three molecules in each of the solvents was tested. From **Figure 4.4** we can see when Rika (DBS) was tested in 50% MPG that the self-assembled form of the structure can be seen to reach the maximum when the temperature is at its lowest i.e. 20°C, with the peak height of the CD signal reducing as the temperature increases indicative that the nanoscale structure is disassembling. This behaviour was also observed for Rika (DBS) in 75% MPG.

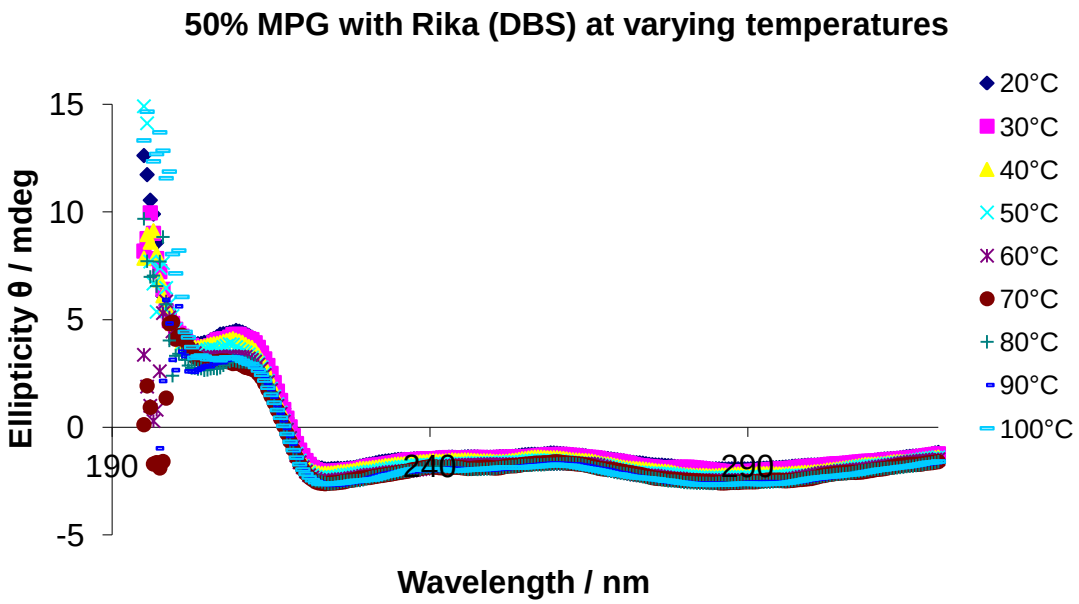

Figure 4.4 Response of CD signal to temperature for Rika (DBS) in 50% MPG.

Likewise when DBS-OCH_3 was tested in the different solvents they all showed the same general behaviour (see **Figure 4.5** for example) as described for Rika (DBS) where the self-assembled structure CD signal is at its maximum at the lowest temperature and then reduces somewhat on the application of higher temperatures.

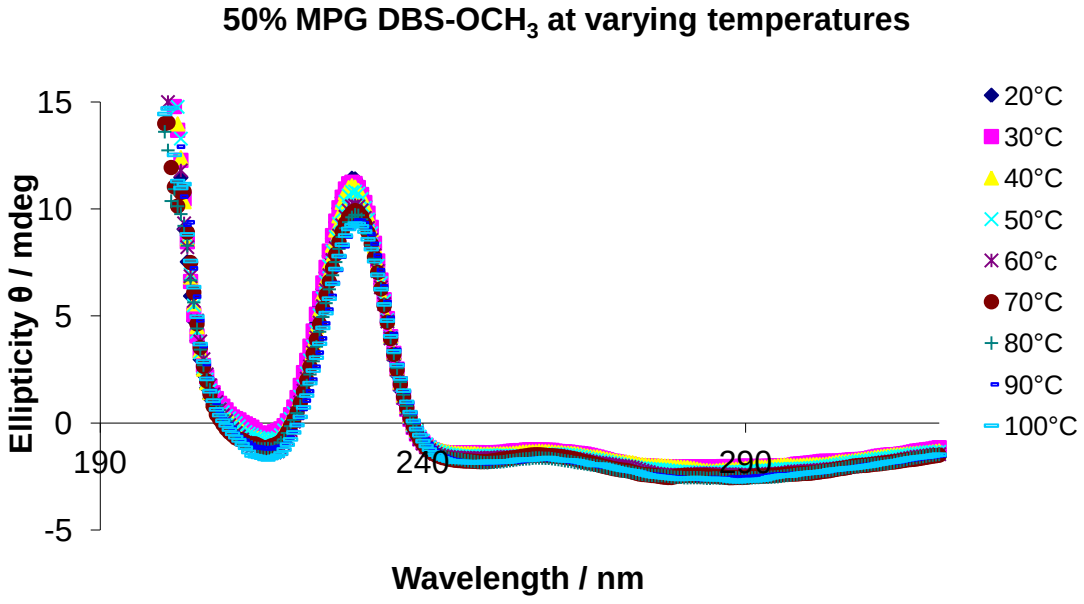

Figure 4.5 Response of CD signal to temperature for DBS-OCH_3 in 50% MPG.

The behaviour mentioned above for both Rika (DBS) and DBS-OCH_3 was also observed for DBS-SCH_3 in 100% MPG and 75% MPG however, in 50% MPG the results were markedly different. Instead a significant change in the CD spectrum on changing the temperature was observed. In particular, changing the temperature led to an

inversion of the CD signals. Furthermore above 70°C the chiral signal once again inverted (see **Figure 4.6**). The behaviour of this molecule in this solvent system clearly has different responses to temperature which may indicate the presence of different nanoscale chiral structures as the temperature is changed. Given the test is done by cooling, this may suggest that one chiral nanostructure forms first and then on cooling further it inverts to a different chiral nanostructure. It is well-known that self-assembled nanostructures, can be metastable.[116,121,122,177,354,355]

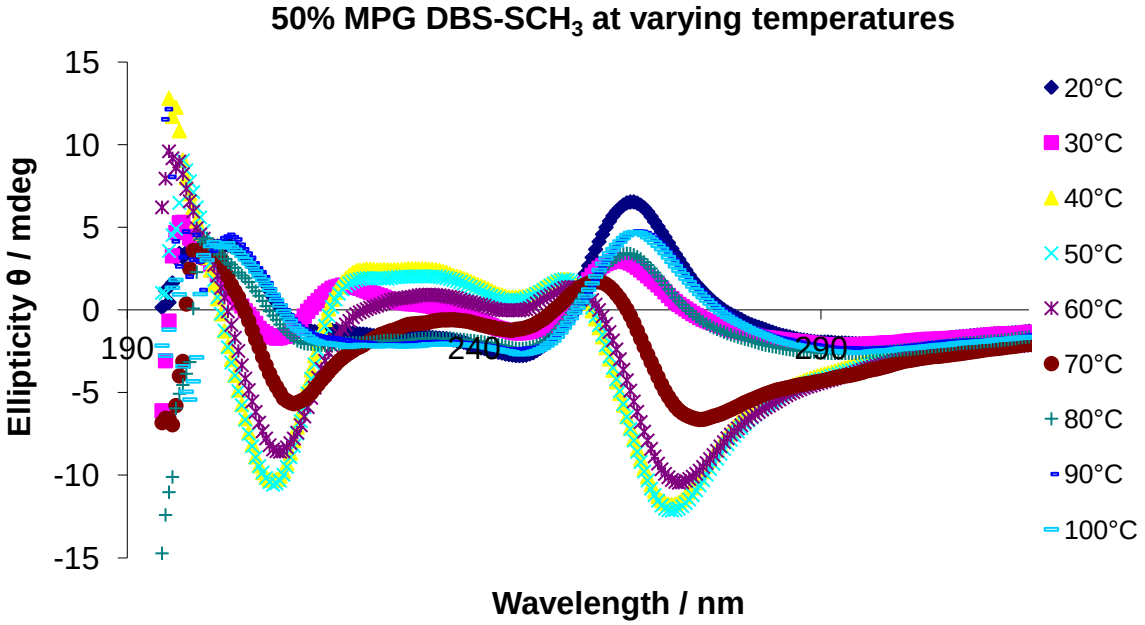

Figure 4.6 Changing CD signal in response to changing temperature.

4.2.3 Kinetics of gelation

Circular dichroism was also used in an attempt to identify the kinetics of gelation for the three different molecules. Samples were prepared as previously described however, this time the cell was placed into the instrument at a temperature of 100°C and then the sample was applied hot into the hot cell and the instrument ramped down to 20°C as quickly as possible. An interval scan method was then used across a wavelength range of 180-320 nm at 1 minute intervals. However, even after the first minute interval it was noted that the CD signal for each of the molecules in the different solvents had reached its maximum. Therefore we reduced the measurements to intervals of every 30 seconds (**Figure 4.7**) and finally 15 second intervals (**Figure 4.8**). Again we observed that even after 15 second intervals the CD signal had reached its maximum. Therefore we can only conclude that the assembly kinetics are very fast and could not achieve any quantitative data for the kinetics of gelation for these molecules.

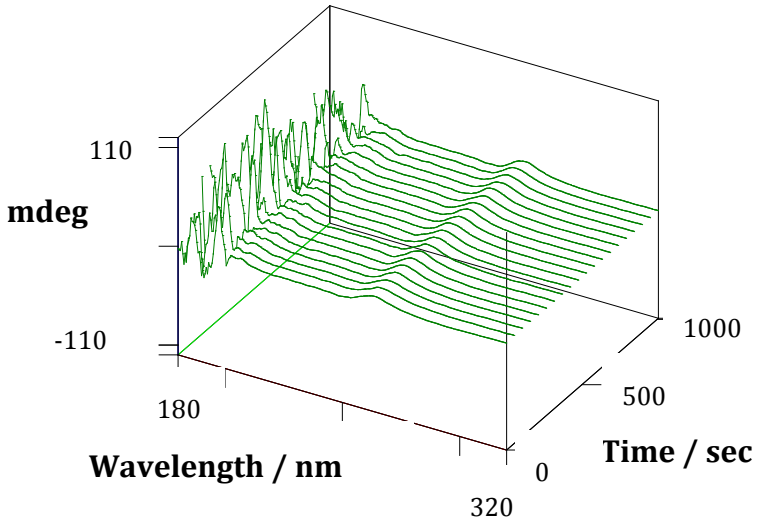

Figure 4.7 Kinetic analysis of DBS-SCH_3 in 100% MPG at 30 second intervals. Data below 200 nm should be ignored as they correspond to noise.

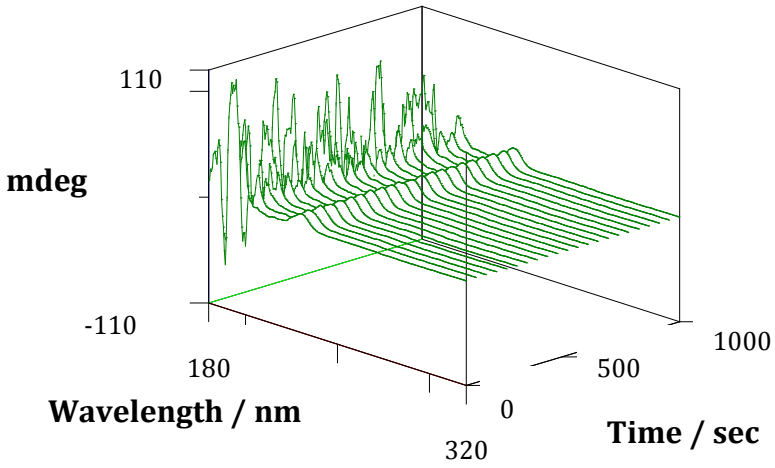

Figure 4.8 Kinetic analysis of DBS-OCH_3 in 100% MPG at 15 second intervals. Data below 200 nm should be ignored as they correspond to noise.

4.2.4 Rheology

The flow properties and the way in which fluids change under stress and shear is very important for de/anti-icing fluids in the aviation industry. A greater insight into how a fluid will flow, react and perform can be achieved through rheology. Rheology is the science of deformation and flow of materials in response to an applied stress. Through the use of a rheometer a more detailed insight into the structure and the effects put on a structure can be investigated.

Typical rheology testing is split into two categories, flow (viscosity) and deformation (oscillation).[356,357] Flow testing allows for measurement of the viscosity of a sample hence its resistance to flow and mimics processing conditions. Deformation quantifies

viscoelasticity by determining the samples properties and how a sample may behave before it flows.[358]

Rheological testing involves some standard variables such as shear stress (force (F) per area (A)), shear strain (displacement (u) divided by height (H)) and shear rate (change in strain with time).[359] To measure these variables a sample is sandwiched between two plates, the top plate known as a geometry which is dependent on the type of sample and test you are carrying out. **Figure 4.9** demonstrates the different types of geometries that are available depending on the type of sample.[360] Gels are commonly measured using cone and plate or parallel plate geometries.

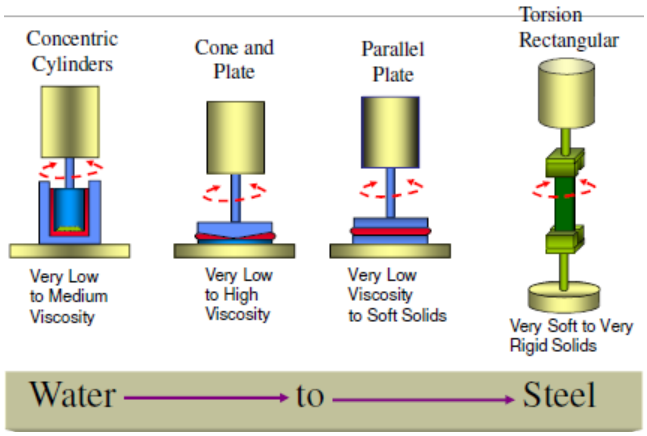

Figure 4.9 Different types of geometries based on sample types.[361]

When a sample is sandwiched between the two plates the top geometry rotates with force which displaces the sample creating a shear profile as shown in **Figure 4.10**.[362] From the shear profile typical material properties can be calculated such as the viscosity and deformation.

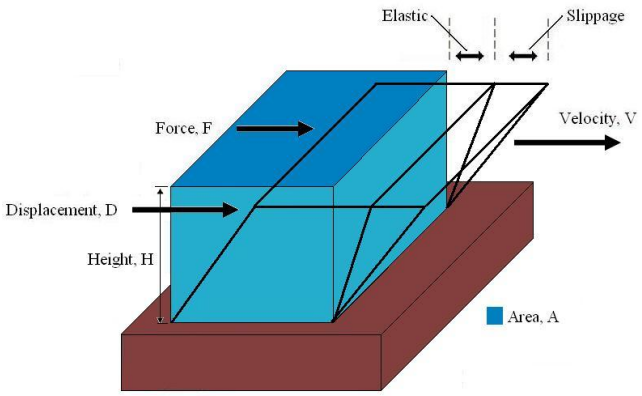

Figure 4.10 Standard variables of rheological testing.

This study will focus on deformation (oscillation) testing to determine the viscoelastic properties of gels. Viscoelastic materials such as gels can be measured

through oscillatory test methods. Dynamic oscillation testing applies a sinusoidal stress or strain to the sample in a back - and -forth motion which is non-destructive. For a pure elastic material the sinusoidal stress applied would produce a strain that is exactly in phase with the applied stress indicating there is no lag between the measured and applied signals and would give rise to a phase angle (δ) of 0° **see Figure 4.11(i)**.

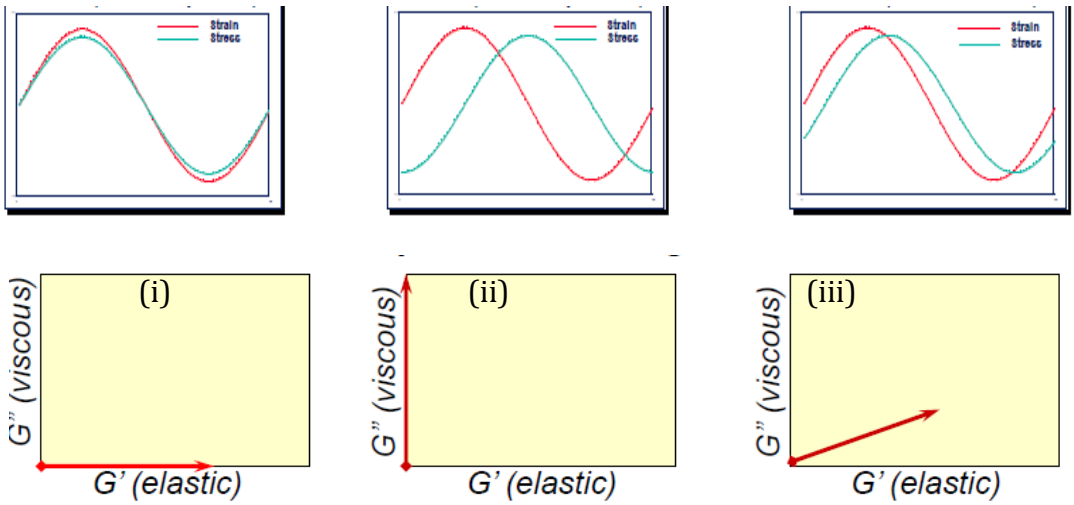

Figure 4.11 Sinusoidal responses of different types of materials[363]

For a pure viscous material the stress applied would produce a strain signal which is out of phase and show a phase angle of 90° see **Figure 4.11 (ii)**. Viscoelastic materials have a phase angle between 0 to 90° (measure of fluidity) with gels typically showing a phase angle of 45° see **Figure 4.11 (iii)**.[359]

From the stress and strain signals applied to a material the complex modulus (G*) can be derived which is a measure of the stiffness of a material. The higher the modulus the tougher the material. The complex modulus is made up of signals from both the elastic and viscous components of a material. The elastic component known as the storage/elastic modulus (G') and the viscous component known as the viscous/loss modulus (G''). Normally for gels, G'>G'' indicating the gel structure is more elastic and solid-like.[103,286]

A variety of dynamic oscillatory tests can be performed on gels.[361,364-366] The most important test which must be completed first is an amplitude sweep. Amplitude sweeps are used to determine the linear viscoelastic region (LVR/LVER) of a sample which is the region in which the stress/strain and modulus remain constant. As G' is a measure of structural integrity, any drop in G' indicates a breakdown of the structure and the onset of non-linearity. The LVR is also an indication of how stable and robust

a sample is, the longer the LVR the more stable the structure is towards shear forces.[123,361] **Figure 4.12** shows two examples of different structures, although the sample with a small LVR has a higher G* and is stiffer, the sample with a longer LVR has a more stable and robust structure which is stronger and requires higher strains to breakdown the structure. A value from the LVR is used in all subsequent tests to provide non destructive testing.

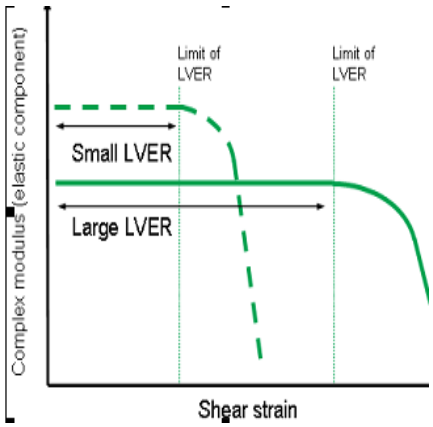

Figure 4.12 Example of an amplitude sweep indicating LVR/LVER regions and critical strains.[367]

A frequency sweep can then be performed to identify a micro structural fingerprint of a material. Since frequency is essentially the inverse of time it is possible to evaluate the time-dependent viscoelastic properties of a material by using a strain within the LVR and varying the oscillation frequency.[361,363,366,368]

Oscillation tests can also be performed to identify how fast a samples structure forms with time, by testing with a known strain value in the LVR, a set frequency and temperature. Similarly temperature analysis can also be performed to identify how a structure is affected by temperature, similar to table-top rheology which is used to characterise thermal stability of gels in a simple way.[367,369]

Rheological analysis of Rika (DBS), DBS-OCH_3 and DBS-SCH_3 were carried out on a Kinexus Pro+ stress controlled rheometer. Amplitude sweeps were determined for each sample at 20°C to determine the linear viscoelastic region (LVR) where the internal structure is not disrupted, and to find out what strain needs to be exerted on the samples before the internal structure breaks down. A value from the LVR was then used in subsequent tests to ensure when the sample is tested the internal structure is not broken down. The critical strain value denotes the strain which the sample must exceed before the structure breaks down. The critical strain value is

when the average G' value of the LVR drops by 5%, and is considered to indicate the point at which the internal structure breaks down.

Samples for rheological testing were prepared by weighing out a known amount of gelator into a glass vial with solvent added. Each of the samples was scaled up to 10 ml. The samples were sonicated for 1 hour before being heated to just below the boiling point of the solvent until a clear homogeneous solution was formed and the samples left overnight at room temperature to form gels. The next day, upon formation of the gels, they were placed in an oil bath at temperatures just above their T_{gel} values to form the solution phase. This is primarily because gels can be fragile if placed onto the instrument as a gel. Therefore using the hot solution phase of each sample they were placed onto the rheometer plate using a spoon to reduce any unnecessary damage to the sample which was set to 20°C. Upon application of the sample the geometry was brought down to the designated gap size (1 mm) and left to equilibrate for 15 minutes to allow the formation of the gel. From **Figure 4.13** and **Table 4.1** we can see that samples of 0.5% w/v Rika (DBS) in both aqueous glycol mixtures have the same LVR regions with critical strain values of 0.03% and very similar G' values. Therefore these samples are independent of solvent in relation to their stability and robustness as well as how stiff the resulting gel is.

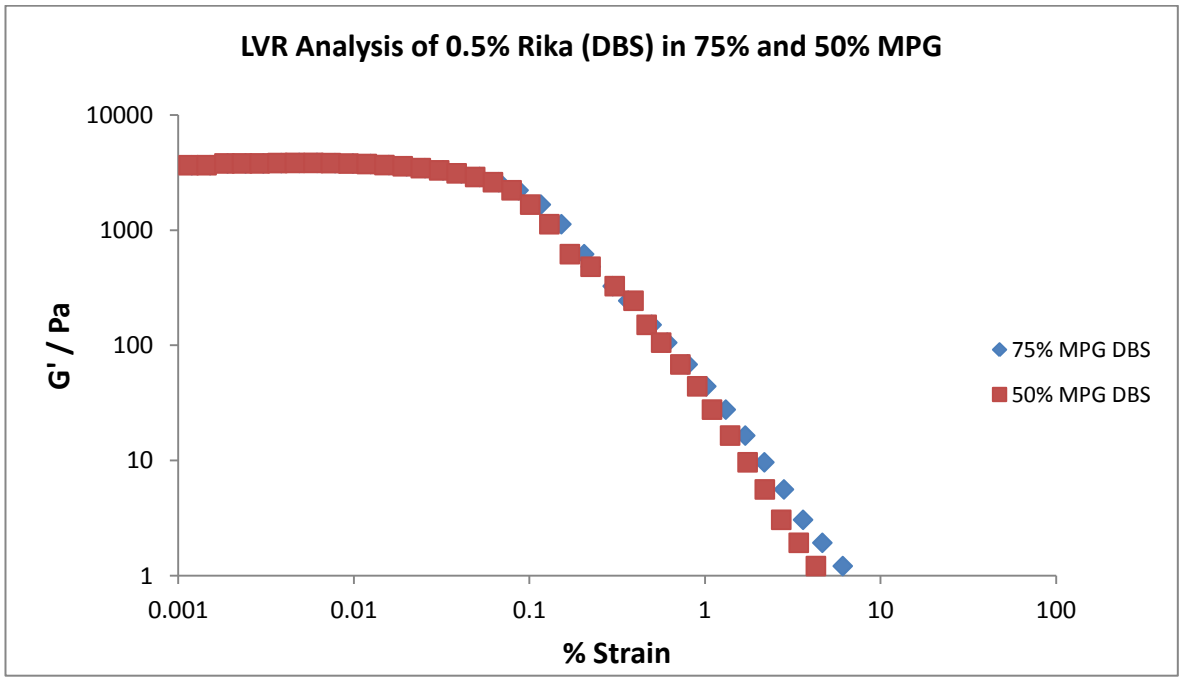

Figure 4.13 Amplitude sweep of 0.5% Rika (DBS) in 75% and 50% MPG solvent mixtures.

Table 4.1 Critical strain and stiffness (G') values for 0.5% Rika (DBS) in aqueous glycol mixtures.

Solvent	G' (Pa)	Critical Strain %
75% MPG	3679	0.03
50% MPG	3983	0.03

Amplitude sweeps were run for 0.5% w/v DBS-OCH_3 in glycol and aqueous glycol mixtures and, like the Rika (DBS) above, it was noted that DBS-OCH_3 in 75% and 50% aqueous glycol mixtures had similar strengths with critical strain values of 0.02 and 0.014% and similar stiffness values (see **Figure 4.14** and Table **4.2**). However 75% MPG with Rika (DBS) does have a slightly higher G' value suggesting that this gel is stiffer and may be a consequence of the molecules being able to interact better in this solvent. In 50% MPG, we note the G' value is lower which may suggest it is reaching its saturation point where the fraction of water is affecting the ability of the gelator molecules to interact to form a stiff tough network. When we look at DBS-OCH_3 in 100% MPG we can see that the stiffness of the gel is dramatically reduced compared to the other solvent mixtures containing water however, it is still able to form gels which can resist the same strain. Therefore it appears that the solvent in this case affects the ability of gelator molecules to interact to create stiff gels, where in 100% MPG the molecules may be more solvated and hence more dynamic than when in 75% MPG, which may be the optimum conditions for interactions to occur between the molecules, which in turn produce a stiffer gel.

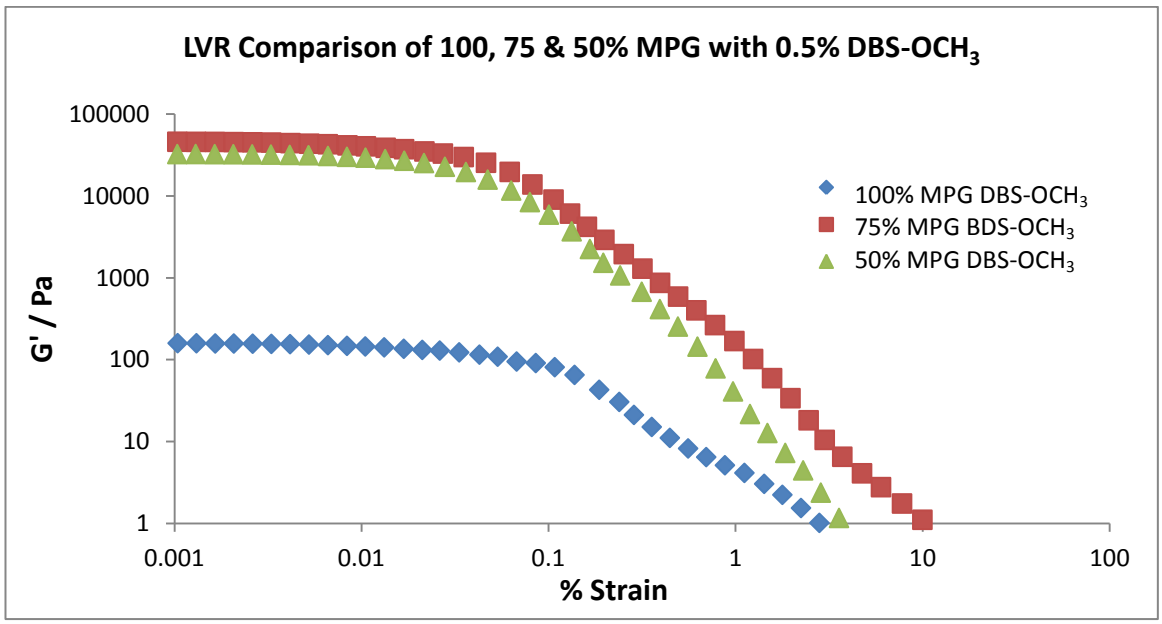

Figure 4.14 Amplitude sweep of 0.5% DBS-OCH_3 in 100%, 75% and 50% MPG solvent mixtures.

Table 4.2 Critical strain and stiffness values for 0.5% DBS-OCH_3 in glycol and aqueous glycol mixtures.

Solvent	G' (Pa)	Critical strain %
100% MPG	132.5	0.02
75% MPG	39717	0.02
50% MPG	28804	0.014

Each of the DBS-SCH_3 samples in the different solvents were also tested using amplitude sweeps to determine their LVR regions. However, unlike the Rika (DBS) and DBS-OCH_3 samples which were tested at 0.5% w/v concentrations DBS-SCH_3 was only tested at 0.1% w/v. This was because when DBS-SCH_3 was scaled up, it had solubility difficulties and could not form gels at 0.5% w/v in all of the solvent mixtures. Therefore like the Rika (DBS) and DBS-OCH_3 we selected a concentration range that was in the middle of the gelators ability to form gels. From the results in **Figure 4.15** and **Table 4.3** we can see that DBS-SCH_3 has very similar behaviour to DBS-OCH_3 in the different solvents where the stiffness achieved by each gel is dependent on the solvent. 75% MPG samples show the greatest G' value indicating that this sample is the stiffest, with 50% MPG and 100% MPG samples reducing in stiffness.

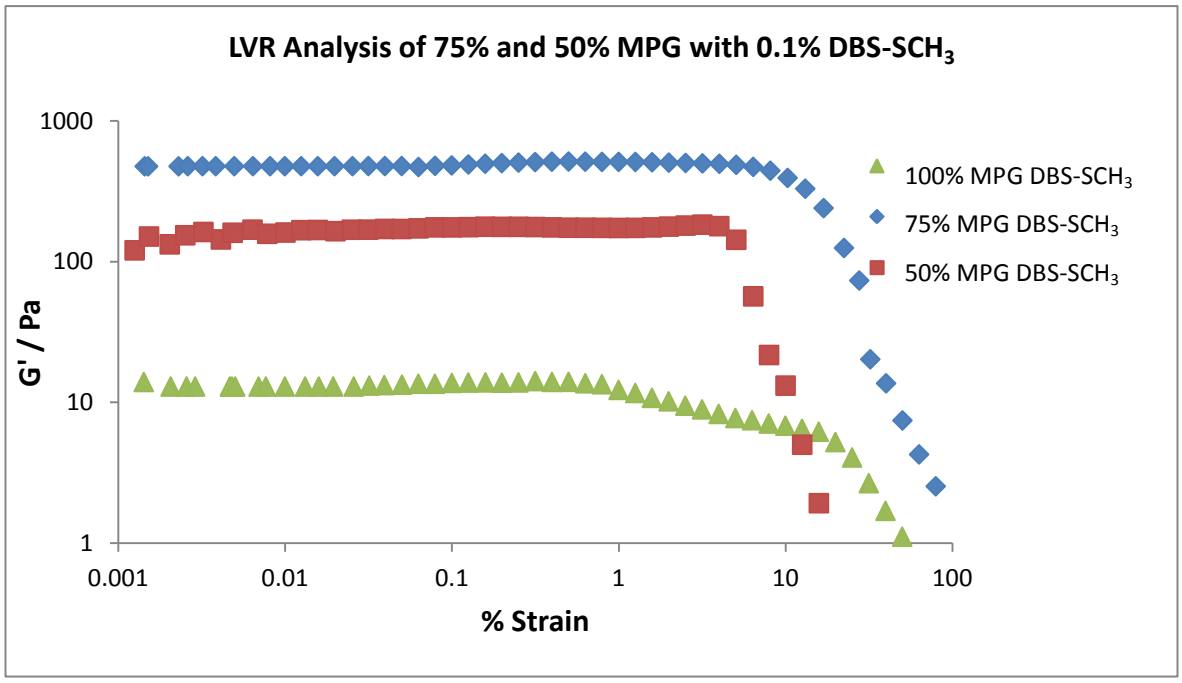

Figure 4.15 Amplitude sweep for 0.1% DBS-SCH_3 in 100% MPG, 75% and 50% MPG solvent mixtures.

Table 4.3 Critical strain and stiffness values for 0.1% DBS-SCH_3 in glycol and aqueous glycol mixtures.

Solvent	G' (Pa)	Critical strain %
100% MPG	12.69	0.99
75% MPG	452.47	7.8
50% MPG	158.81	4.3

Unlike the two molecules, DBS and DBS-OCH_3, where regardless of the stiffness that a gel could achieve, all samples had similar resistance to strain. DBS-SCH_3 shows a different behaviour. DBS-SCH_3 in the different solvents indicates that the stiffer the gel the stronger the gel, with 75% MPG being the stiffest and strongest and 100% MPG the weakest and hence least stable gel. Therefore it is evident, like with DBS-OCH_3, that solvent has an effect on the stiffness of the gel structure that is formed. With the inclusion of water it is also evident that this molecule can interact more effectively and produce stiff strong gels however, it reaches a point between 75–50% MPG where the interactions between the molecules are not at the optimum and hence weaker gels that are not as tough are formed. As such DBS-SCH_3 exhibits nice solvent-induced optimisation of rheological performance.

Putting these values into perspective of the de/anti-icing application we note that these samples could be compared to an anti-icing fluid which contains a thickener in the form of a polymer to give it structure and hence protective properties whereas de-icing fluids are Newtonian fluids with no structure and as a result cannot be compared to these samples. Anti-icing fluids provided by Kilfrost and our competitors when tested, produce G' values of 1-10 Pa with % strains of 1-10 %. From our results we have obtained for these gelators we can see that gel systems can produce much higher G' values than what is obtained for anti-icing fluids which could potentially create thicker films which could protect the aircraft for longer. However, they are very weak in comparison in terms of strain resistance. Having the ability to form very stiff gels that are weak would work really well in this application, as the gels could protect the aircraft for longer but be completely removed upon take-off, an important requirement in this application in order to not affect the aerodynamics of an aircraft.

Frequency sweeps of the same samples were then performed at 20°C to determine the behaviour of networks within the solvents. G' (storage modulus) and G'' (loss modulus) for each sample were determined and the response to increasing frequency recorded. If G' is dominant over G'', the material is elastic and solid-like. If G'' is

dominant over G' the sample is more viscous and liquid-like. If a sample is a gel, G' will be dominant over G'' and be independent of frequency. From **Figure 4.16** showing an example of a frequency sweep of Rika (DBS) in 75% MPG we noted that all samples regardless of concentration and/or solvent, are solid like with phase angles below 45° and shown to be independent of frequency with G'>G''. Santos and Abiad[370] have conducted a study into the viscoelastic properties of DBS at much higher frequencies than we tested within this chapter. From their findings they showed that although DBS is independent of frequency when tested at higher frequencies, DBS still showed the same behaviour. However, they noted that the G' values can change as a result of solvent polarity and/or gelator concentration.

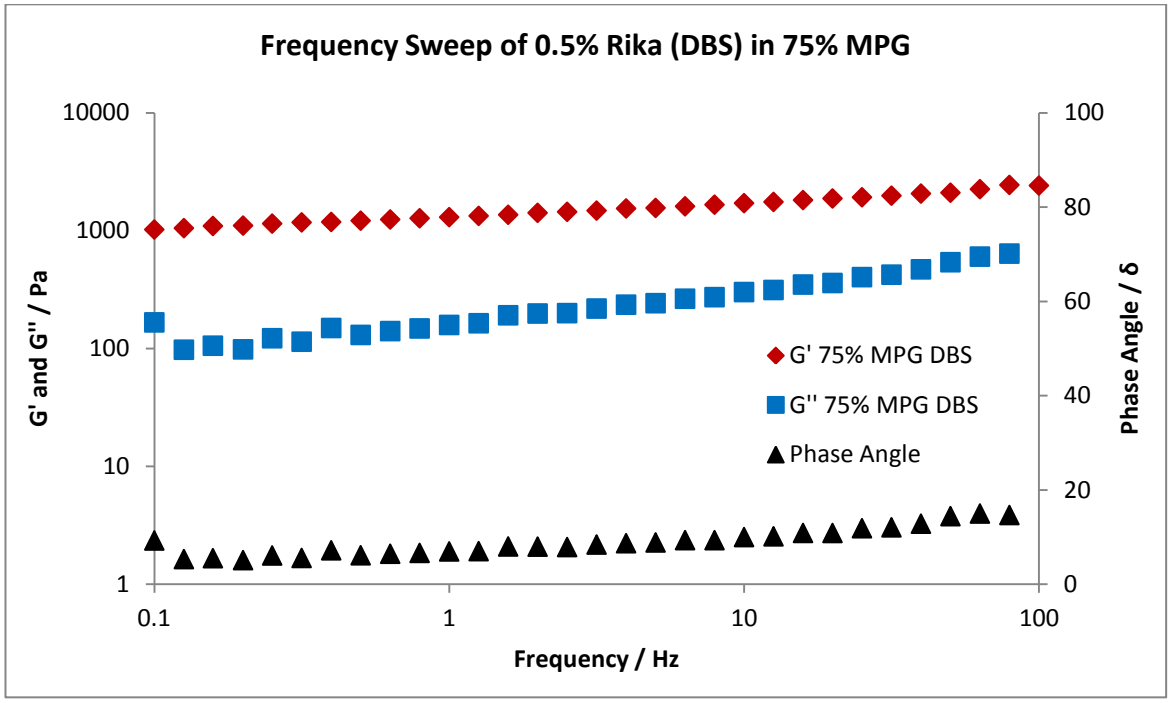

Figure 4.16 Frequency sweep of 0.5% Rika (DBS) in 75% MPG:H_2O

One molecule did change its behaviour on increasing frequency. This was DBS-SCH_3. What we observed when DBS-SCH_3 was tested in all of the different solvents was that G'>G'' and the samples were independent of frequency up to approximately 10 Hz. Above frequencies of 10 Hz the samples then showed to act as visco-elastic solids with the phase angle increasing (**Figure 4.17**). Therefore these samples are frequency dependent above 10 Hz. This may reflect the fact that these gels were tested at lower concentrations and have lower G' values or the possibility that two different structures are present as suggested from CD.

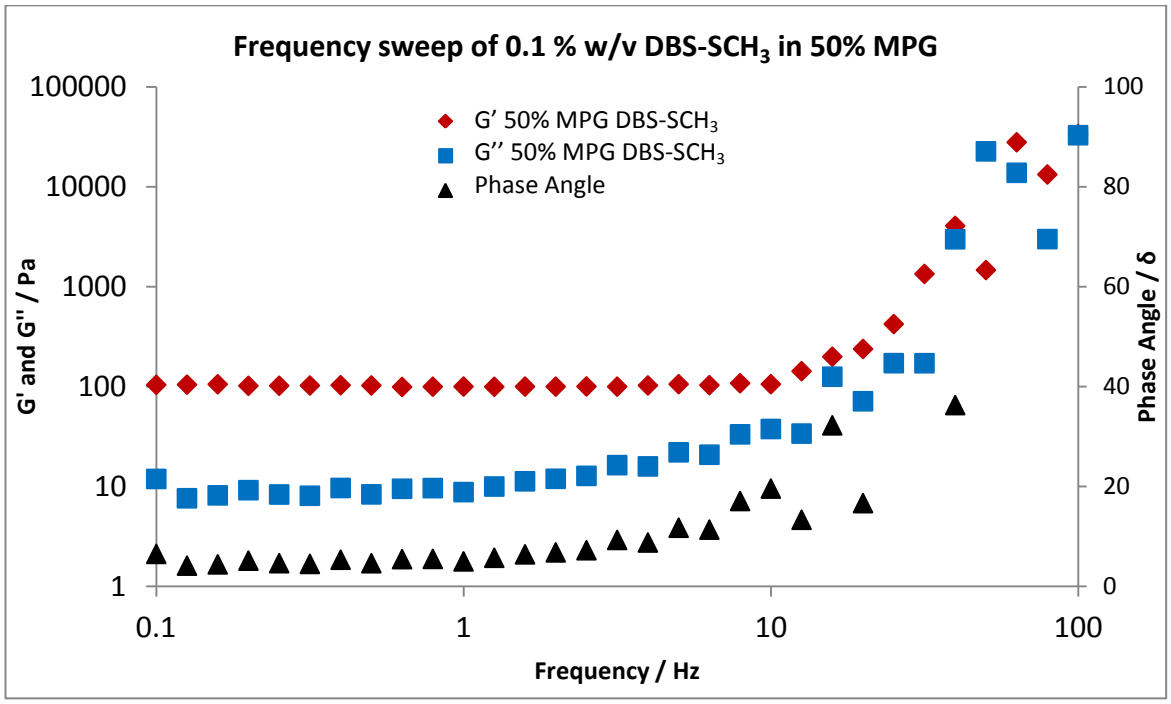

Figure 4.17 Frequency sweep of 0.1% DBS-SCH_3 in 50% MPG showing changes in structure as frequency increases

Each of the three molecules in the different solvents was then tested to identify their response to increasing and decreasing temperatures. Unlike the sample application described above where the samples were applied to a cold plate on the rheometer, to conduct thermal analysis they were applied in the same way but the rheometer plate set to 85-90°C. The plate was then slowly cooled down. Using this method of application, the temperature at which a gel forms (T_f) can be measured. The temperature at which the G* (complex modulus) increases sharply is denoted T_f. This is a poorly defined term within rheology and therefore within this study we are defining it as the point at which the G* reaches its maximum. Furthermore, on heating, the temperature at which the gel disassembles (T_d) into the solution phase can also be detected. **Figure 4.18** shows an example of a temperature ramp obtained on the rheometer for Rika (DBS) in 75% MPG. In **Figure 4.18** as the test begins at high temperatures of 80-95°C the sample is in its solution phase and hence above its T_{gel}, and as a result the data is scattered representative of the solution state. Then on cooling to approximately 44°C, the gel structure begins to form and the structure continues to build as noted by the increase in G*. The gel structure continues to build until it reaches its maximum G* and this is the temperature which is recorded as the T_f, denoting the formation of the full gel (T_f = 18.7°C). When the cycle is reversed from low to high temperatures, as the temperature increases the gel disassembles from the gel state into the solution state denoted by the reduction in G*, until it eventually

reaches the point where the data becomes scattered again. The temperature at which the gel returns to solution and hence disassembles is recorded as the T_d.

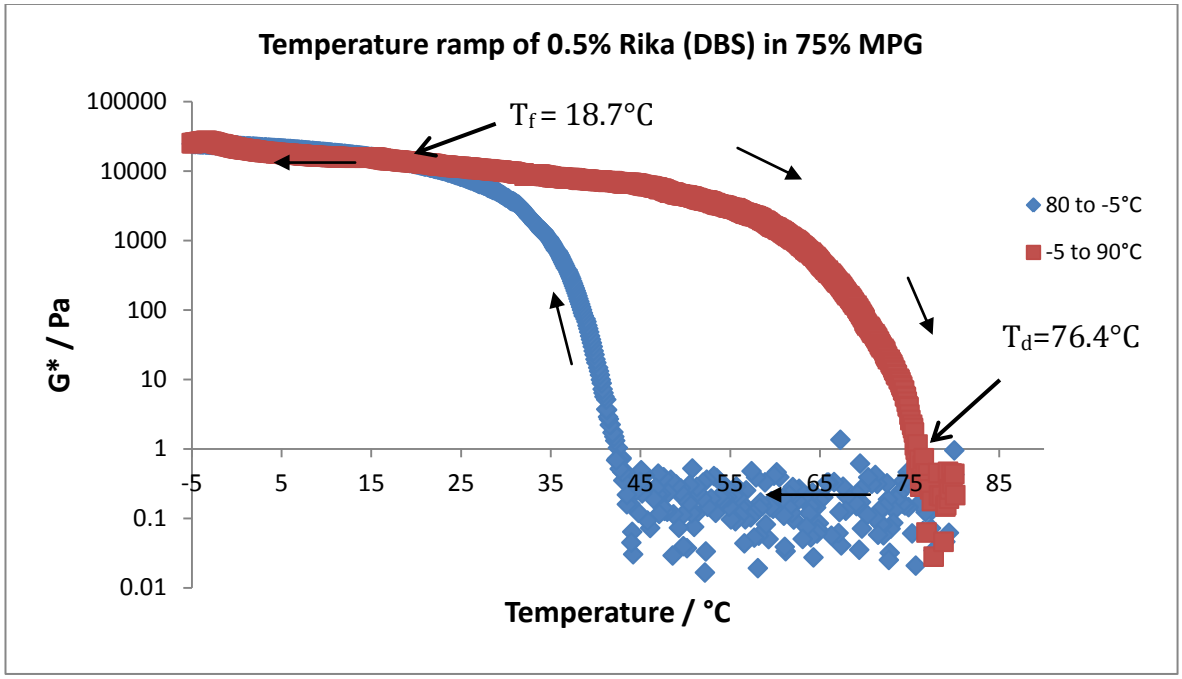

Figure 4.18 Temperature ramp of 0.5% Rika (DBS) in 75% MPG showing the temperatures at which the gel fully forms (T_f) and when it is disassembled (T_d)

Each of the three molecules Rika (DBS), DBS-OCH_3 and DBS-SCH_3 were tested in the different solvent mixtures to determine their behaviour in response to increasing and decreasing temperatures. All of the molecules showed the same general trend, as temperature decreased samples containing more water (50:50 MPG:H_2O) would form gels more easily with 75% MPG and 100% MPG gels forming at lower temperatures. Likewise when the temperature cycle was reversed from low to high they all showed the same general trend with gels disassembling at lower temperatures when there was less water present (**Table 4.4**). This supports the view that water content and hydrophobicity is important in controlling the gelation event.

Table 4.4 Gel formation and disassembling temperatures obtained from temperature ramp analysis for 0.5% Rika and DBS-OCH_3 and 0.1% DBS-SCH_3.

	Molecule					
Solvent	**Rika (DBS)**		**DBS-OCH_3**		**DBS-SCH_3**	
	T_f/(°C)	T_d/(°C)	T_f/(°C)	T_d/(°C)	T_f/(°C)	T_d/(°C)
100% MPG	S	S	18.8	83.8	0.3	63.2
75% MPG	18.7	76.4	35.7	95.6	6.2	70.8
50% MPG	19.8	89.7	45.5	96.9	20.9	84.8

Therefore gels containing 50% MPG are the most thermally stable with 100% MPG samples being the least thermally stable. This is in agreement with the T_{gel} measurements made in Chapter 3 which also showed samples containing 50% MPG to be the most thermally stable. Although the T_{gel} and temperature ramp conducted on the rheometer provide the same trends, their values are somewhat different and as a result cannot be directly related. This is primarily due to the differences which we are measuring. The inversion tube test measures the macroscale gel collapsing whereas the rheometer is measuring the complete material phase change. It is worth noting that the thermal properties are different to the rheological properties – which are actually optimal for 75% MPG. As such, we can conclude that the most thermally stable gels do not necessarily have optimised nanostructures for rheological performance.

Considering the rheometer temperature data in terms of de/anti-icing it would allow customers to apply or store the fluids at much higher temperatures than what we currently advise (60-80°C). Customers currently overheat our current products and as a result reduce the protective properties they can achieve from the fluids, as such this would potentially supply a remedy for such occurrences. The customers would potentially be able to spray these gelators in the de/anti-icing solvents between 65-100°C depending on the gelator, with the gels forming very quickly on the surface thereafter.

4.2.5 SEM - room temperature and crash cooled

Each of the three potential gelator molecules was imaged using scanning electron microscopy (SEM) in each of the glycol and aqueous glycol mixtures to try and identify the supramolecular structures formed in the gel state and understand what may be happening on the microscopic scale.

Two methods of preparing SEM samples were carried out to try and determine if simulating application temperatures would have an effect on the nanoscale structures that could be formed. The first method involved spreading a small amount of a gel sample on an aluminium stub at room temperature. These samples were left to dry in a dessicator until the solvent was removed and a dried film was present on the stub. The second method involved placing the formed gel sample into an oil bath set to 98°C to form the solution state. During which time the aluminium SEM stubs were placed into the freezer at -21°C for 5 minutes to cool. One drop of the hot gel solution was then pipetted onto the cold aluminium stub and spread over the surface. The

stubs were then placed back into the freezer for 2 hours to allow the gel to set at freezing temperatures. After 2 hours the stubs were removed from the freezer and placed into a dessicator at room temperature to dry and leave the xerogel. To ensure the samples are conductive, they were then coated with a thin layer of Pd/Au using a sputter coater. Therefore the sample being viewed is a dried, collapsed, coated form of the gel network within each of the samples. It is important to recognise that the images obtained for each of the samples here is not how the gel network would exist in the solvated state, but can give an indication of the type and size of the supramolecular structures that are formed, and is useful for comparative analysis.

Gels formed by each of the methods described above were compared to try and determine if changing the temperature affects the supramolecular structure that each of these gelator molecules can create. Preparing samples from hot solutions which form gels upon contact with cold surfaces will give us a better idea how these systems may form gels when used in the de/anti-icing application. When solutions are used as de/anti-icers for aircrafts they are typically sprayed at high temperatures on to freezing surfaces, therefore by identifying how these systems will form in these conditions can allow us to identify how they can be best used for this application.

Images for Rika (DBS) in 75% and 50% MPG at both of the different preparatory temperatures were successfully obtained, however the samples which were prepared by using gels formed at room temperature degraded under the electron beam and as a result was difficult to obtain clear images (**Figure 4.19**). What can be observed from the samples prepared at room temperature are that Rika (DBS) in 75% MPG produces very small fibres ca. 5 nm that appear straight with no obvious shape i.e. twists. However they do appear to create a fibrous network of fibre bundles although from the images is difficult to determine their sizes. When we compare this to the sample produced at freezing temperatures, we see that the latter image is much clearer. This shows very similar sized fibres (ca. 5 nm) but it is much clearer that these fibres appear twisted in a helical order as suggested by the circular dichroism results. These fibres appear to create an expansive network with many fibre bundles being observed ranging from ca. 200-300 nm, however it is unclear where one fibre or fibre bundle begins and ends as they all intertwine.

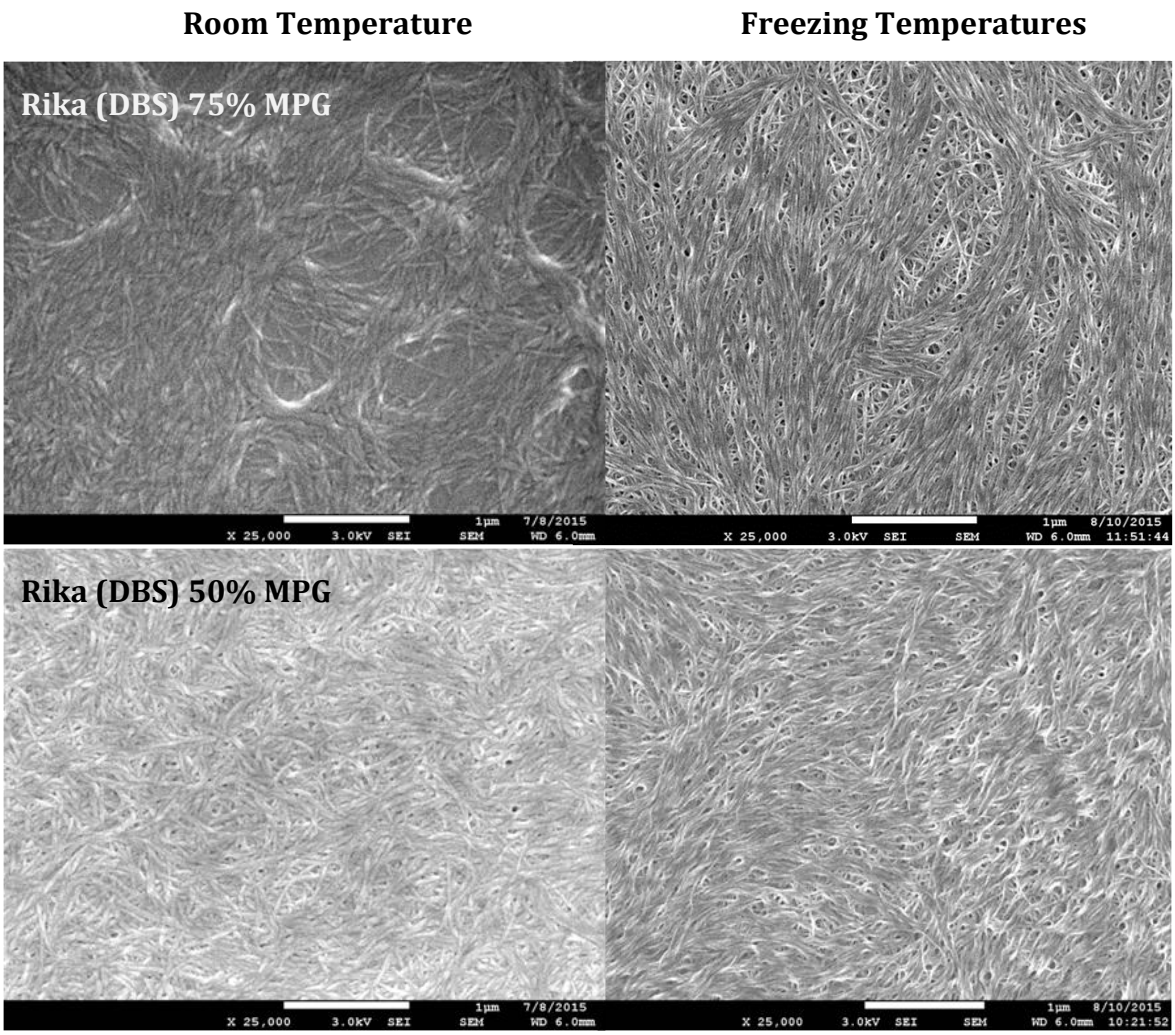

Figure 4.19 Comparison of gels prepared at room temperature and freezing temperatures imaged using SEM for Rika (DBS) in 75% and 50% MPG.

Similarly with Rika (DBS) when in 50% MPG, we observed the same size ca. 5 nm fibres which have helical twists, agreeing with the CD results. However it is difficult to clearly see these fibres due to the reaction with the electron beam, but it is evident that an expansive entangled fibre network is formed that is throughout the whole sample. When samples prepared at low temperatures were viewed we can see the fibres a bit more clearly. The fibres appear to be of similar size with a definite helical twist however it is difficult to determine any individual fibre bundles. The fibres seemed to be tightly packed together creating one overall large bundle of fibres throughout the whole sample.

Comparing the preparation method at the two different temperatures it appears that regardless of the temperature this molecule creates the same size fibres that are helical in nature which extend throughout the whole sample to create entangled gel networks. However, because this molecule shows no change to the size, type or physical structure of these fibres regardless of the temperature, gives us an indication

that these fibres form extremely rapidly, supporting the kinetic results of the CD studies.

Samples of DBS-OCH_3 were imaged in the same way, however DBS-OCH_3 is also able to form gels in 100% MPG (**Figure 4.20**). Images for DBS-OCH_3 in 100% MPG at room temperature formed long thin fibres ca. 5-8 nm in diameter, these potentially could be smaller as it is difficult to identify just one single fibre, they have a helical twist and are seen throughout the sample creating an entangled network. Fibre bundles within the images are also present with sizes ca. 10-100 nm, but again it is difficult to distinguish a single fibre and where it starts and ends. When comparing this image to the freezing temperature images it is clear that very similar fibres are created with similar sizes and shapes. Although it appears as if there are more longer fibres or fibre bundles throughout this sample, these are also present in the room temperature sample.

Images for DBS-OCH_3 in 75% MPG at both different preparation temperatures show very similar structures. They appear to form long thin twisted fibres ca. 3-5 nm in diameter that span the whole sample creating a fibrous network. Regardless of temperature this gelator in this solvent system appears to form the same structure of fibres and hence gel network.

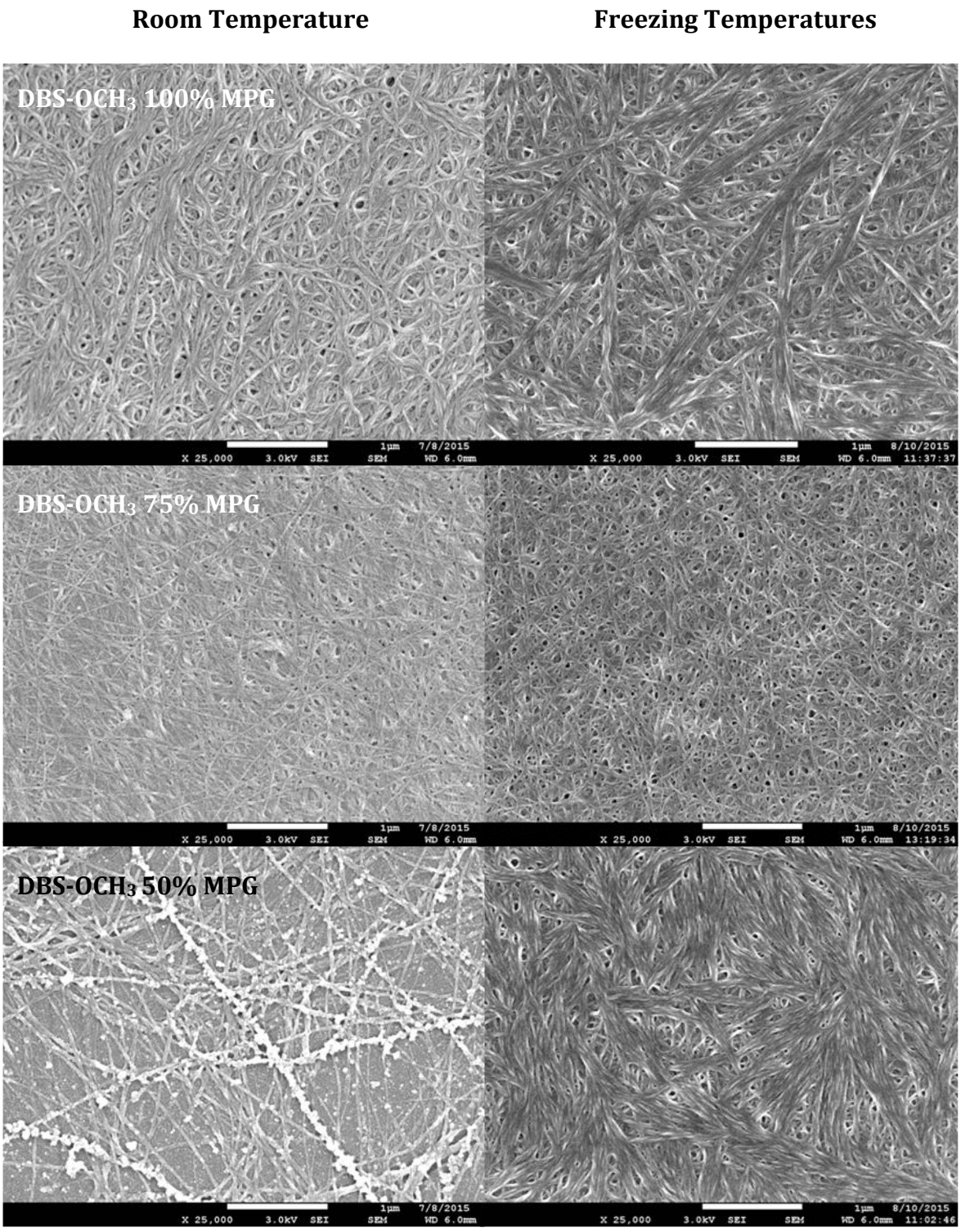

Figure 4.20 Comparison of DBS-OCH_3 in glycol and aqueous glycol mixtures at room temperature and freezing temperatures using SEM.

DBS-OCH_3 in 50% MPG shows slightly different morphologies on preparation at the different temperatures, unlike the other two solvents tested. At room temperature we can see that long straight rigid fibres are formed which appear twisted and helical, measuring ca. 5 nm in diameter however there are also signs that these fibres show the starting point of crystal formation.[371-374] Some fibre bundles are also evident measuring between 10-100 nm in diameter. However, the samples imaged at freezing

temperatures shows a more expansive entangled network compared to the room temperature samples which suggests the solvent is having some effect on fibre formation at lower temperatures. Lots of fibre bundles can be observed in the freezing temperature sample which all seem to amalgamate into one large network made from bundles ranging from 100-300 nm in diameter with some appearing as large as 500 nm in diameter. We suggest that the increased water content drives the self assembly to differ under the different cooling rates.

DBS-SCH_3 was also imaged in the three different solvents and as we can see from **Figure 4.21** samples prepared at room temperature and at freezing temperatures for DBS-SCH_3 in 100% MPG are very similar to one another. In 100% MPG DBS-SCH_3 creates long slightly larger fibres of 10-15 nm than the other molecules.

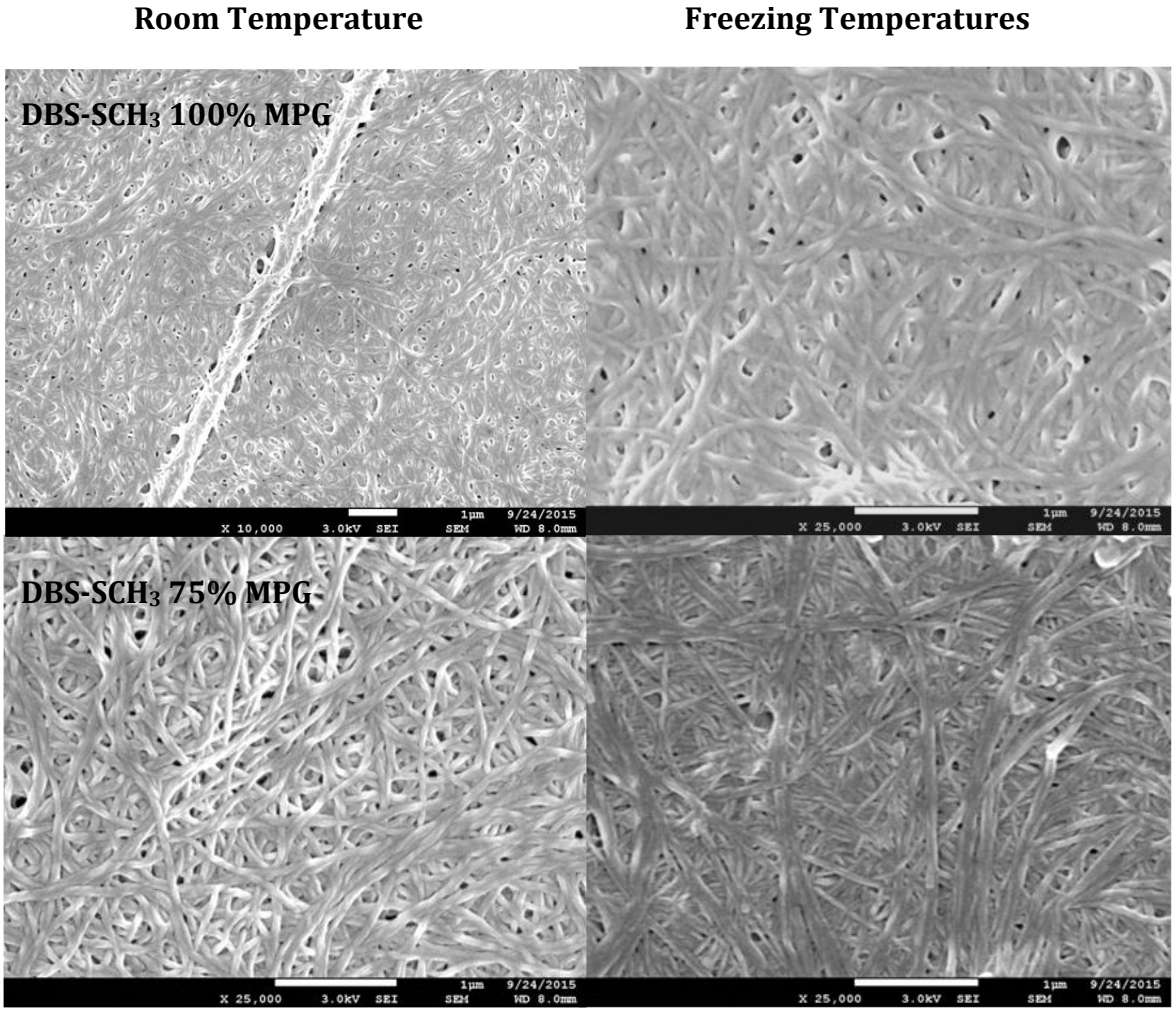

Figure 4.21 Comparison of SEM images obtained for DBS-SCH_3 in 100% MPG and 75% MPG mixtures at room temperature and freezing temperatures.

These appear long and twisted in nature, however it is unclear where one fibre ends and one begins and therefore the size of the fibres could potentially be smaller, and

what we are seeing is lots of small fibres bundled together creating small fibre bundles.

DBS-SCH_3 in 75% MPG at room temperature appears to have more of a porous network compared to the 100% MPG samples viewed previously. It is made up of small fibres ca. 5-8 nm which are seen to be twisted together forming fibre bundles of ca. 100 nm. When viewed at freezing temperatures long ca. 100 nm fibre bundles are more obvious throughout the gel structure with what appears a network of singular fibres creating a network throughout these. However it is difficult to determine if temperature has had any real effect on this sample, as the differences are small.

DBS-SCH_3 in 50% MPG however showed some interesting and very significant differences. Unlike both 100% MPG and 75% MPG where we noted there were fibres formed that create bundles which create the overall gel network which appeared twisted and helical DBS-SCH_3 in 50% MPG creates a completely different structure. At room temperature in **Figure 4.22** it is clear at low magnification x 5000 the structure created by this sample is not helical and in fact appears flat with a tape-like structure. These flat fibres can be seen to form quite large fibre bundles ca. > 1 μm in diameter in some cases. This structure appears to be much more nano/micro crystalline in nature. At higher magnification x 25000 it is clear these are flat structures but they are potentially 200-300 nm in diameter and have defined edges which appear broken. However it is impossible to find the other end of the fibre to determine the length of a single fibre. When the temperature is reduced to freezing conditions, we see the same type of flat fibre being formed throughout the whole sample creating an entangled network. In some areas these flat fibres appear to stack one on top of the other to create bundles. However, at lower temperatures the fibres that are formed appear much smaller ca. <100 nm in diameter compared to the 200-300 nm fibres that are formed at room temperature. At higher magnifications it appears that not only are the flat tape-like structures present but there are also signs of twisted fibres, possibly suggesting that two types of fibres are formed at lower temperatures. This is in direct agreement with the effects we observed when testing this sample using circular dichroism where two different chiral signatures were present. Therefore in this solvent system at low temperature we observe that the faster a gel forms the smaller the fibres, and the more slowly a gel forms larger fibres form, which show distinctive flat tape-like structures. This is in agreement with the other studies which have reported the nucleation of more small fibres under fast cooling conditions and the

formation of more crystalline systems at slower cooling rates.[146,213,214,375-379] We suggest this greater crystalline behaviour occurs as the solubility decreases in the presence of more water.

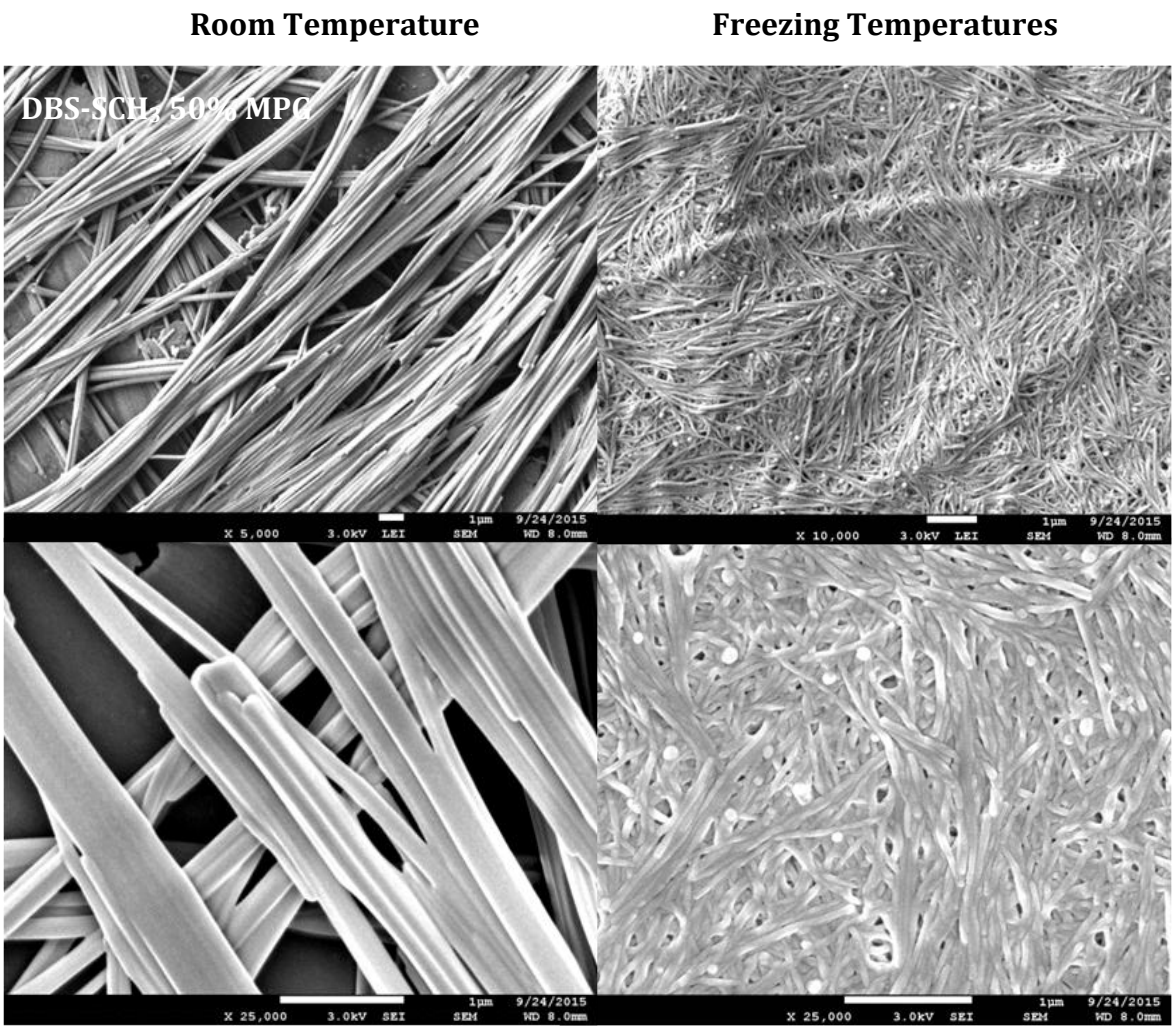

Figure 4.22 Comparison of DBS-SCH_3 gels prepared in 50% MPG at room temperature and freezing temperatures.

This behaviour may also explain why DBS-SCH_3 shows gelation at lower concentrations. From the SEM analysis of the three molecules it is clear they create very similar supramolecular nanostructures in glycol and aqueous glycol mixtures. We note that all three molecules have very similar fibre sizes and helical structure as suggested by the initial CD results, except DBS-SCH_3 in 50% MPG. However, changing the temperature with regards to preparing the gel seems to have little difference in the end structure that is formed apart from DBS-SCH_3 in 50% MPG. The rate of gel formation in 50% MPG DBS-SCH_3 suggests that this system is affected by temperature. At higher temperatures we saw larger flat fibres were formed but at

freezing temperatures the fibres changed and became smaller in size and showed the presence of flat and helical like fibres.

From the SEM imaging of the three different gelator molecules it is possible that the types of fibres that are formed are producing the different properties that each of the gelator molecules possess when in the different solvent mixtures. In all images of the three different molecules with 100% MPG we noted that long fibres are primarily produced and make up the gel network. This type of fibre may therefore give rise to the low thermal stability profile we obtain, and hence contribute to the low G* values we see which are weaker as a result of lower critical strain values. These long fibres are possibly not interacting enough with one another, and are perhaps in the balance of being more soluble in 100% MPG than gel-like. However, when we look at the type of fibre produced in the 50% MPG samples we see that they are the opposite. Small fibres are created which appear gathered together creating bundles which ultimately create expansive networks are tree like in nature and appear less porous as a result. Therefore this type of fibre may be creating the higher thermal stability profiles we obtain as a result of the fibres being packed very tightly together. These types of fibre produce very high G* values and are strong as a result. However, in terms of rheology the 75% MPG samples perform the best. It is suggested this is a result of combining these two effects of long and small fibres to create a more effective overall structure. In 75% MPG samples it is clear that there is a combination of the long fibres observed in the 100% MPG samples with the small compacted dense fibre networks seen in the 50% MPG samples. As a result of the 75% MPG containing both these types of fibres, the long fibres may contribute to the lowering of the thermal stability, which is in line with the thermal stability results obtained for 100% MPG samples, while the smaller fibres contribute to the creation of a very stiff network which is ultimately stronger. Therefore we obtain an overall combinatorial effect from the different nanostructures that are formed. As such, the structure of these samples are dependent on the volume of water that is present and hence the solvent.

The results of the SEM images at the varying temperatures would suggest that overall these type of gel systems are more than capable of creating the same type of structures whether at room temperature or at freezing temperatures and as a result would allow these systems to be sprayed at high temperatures as would be performed in the de/anti-icing application with their properties being predetermined at room temperature. However, there are clearly morphological differences for DBS-

SCH_3 and DBS-OCH_3 under certain conditions which would need careful consideration. Although it should be noted that the rapid cooling typical of an aircraft wing gives the more effective inter-penetrated small nanofibre network.

4.3 Conclusions

Within this chapter we have further investigated the three most successful gelator molecules, DBS, DBS-OCH_3 and DBS-SCH_3 highlighted in Chapter 3. From further investigation using circular dichroism we identified that each of the molecules absorb at specific wavelengths denoted to the substituent attached to the aromatic ring of the structure. This indicated that the more electron rich the molecule becomes by including electron donating groups onto the aromatic rings the more each molecule absorbs at longer wavelengths in the order SCH_3>OCH_3>H. DBS has showed us that it is potentially solvent dependent with the intensity of the CD peaks decreasing with increasing water and this agrees with the fact that the solubility of this molecule lowers upon the addition of more water. Whilst the other two molecules produced very similar spectra. Through the use of variable temperature circular dichroism we have demonstrated that each of these molecules self assemble and disassemble through the use of temperature with the highest peak being observed at the lowest temperature and the decrease in intensity as temperature increases. All molecules in the different solvents tested had the same behaviour except DBS-SCH_3 in 50% MPG. This sample responded differently when increasing temperature was applied to the sample, with evidence of two different nanoscale assemblies which could interconvert.

Kinetic experiments were attempted using circular dichroism but unfortunately due to the very rapid self assembly of these molecules, we could not detect the gradual growth of supramolecular fibres.

Each of the gelator molecules was also examined using rheology. Through rheology we showed that Rika (DBS) regardless of the solvent had very similar stabilities and strength up to 0.03% strain, where after the gel gradually breaks down. DBS-OCH_3 and DBS-SCH_3 showed similar G' value patterns showing that their stiffness is dependent on solvent, with 100% MPG producing the least stiff gels and 75% MPG producing the stiffest gels. However regardless of the stiffness of DBS-OCH_3 gels formed they still all showed similar strain resistance. Unlike the other molecules, DBS-SCH_3, showed different behaviour, with the stiffest gel being the strongest gel,

hence as the strength reduced the stiffness reduced. However, the DBS-SCH_3 samples were tested at much lower concentrations (0.1%) than Rika and DBS-OCH_3 and this explains the lower G' values, hence less gel network. Therefore as a result of this lower concentration it has shown to have a greater capacity to assemble with lower solubility. However, due to its better capacity to assemble it forms gels which are more resistant to strain than the other gel systems. The gel samples we have created in all of the selected solvents are very weak in comparison to standard additives used in aviation and would be easily removed at the point of take-off. However they do possess the ability to achieve higher G' values with results achieving 2-3 magnitudes greater G' values than measured for thickened fluids. This property is also an advantage as the higher the G' the thicker the film, and the thicker the film the greater the potential holdover protection time.

This type of material therefore possesses the perfect properties in relation to achieving good holdover protection to an aircraft to protect it from winter conditions with the ability to provide very good aerodynamics with the easy removal of fluid.

Rheology has also shown us that the self-assembly and disassembly of each of the gels can be detected and has a hysteresis effect with higher temperatures being required to break down the gel than form it. Like the thermal stability results achieved in Chapter 3 by the inversion test we again note samples with increasing water content are more thermally stable. Therefore these samples could potentially be sprayed at high temperatures between 60-100°C without degrading the molecules ability to form gels, unlike what happens to the current polymeric thickened fluids, which degrade with high temperatures and over time lose their ability to provide any holdover protection.

SEM analysis of these molecules showed us that all three molecules create similar types of gel networks regardless of differing temperatures which would represent spraying in the de/anti-icing application. Each of the molecules forms long twisted helical nanostructures, with the exception of DBS-SCH_3 when in 50% MPG, which formed flat tape-like fibres which were more crystalline in nature if the sample was cooled slowly. DBS-OCH_3 also showed signs of crystallisation at room temperature but the effect is not as marked as for DBS-SCH_3. However, this fits with the view that the oxy-ether is more soluble in the presence of water than the thio-ether as a result of the oxy-ethers potential to form better hydrogen bonds. It has been shown that as the samples incorporate more water and hence create a more hydrophobic

environment, the self assembly of these gels produce smaller fibres which create more densely packed entangled networks compared to the longer fibres observed in 100% MPG samples. This is presumably because the presence of water lowers the solubility and causes more fibres to be nucleated which can then[146,374,380] grow large. The size of these fibres that create the entangled networks is potentially one explanation to the differing properties we observe through rheology. With long fibres giving rise to less stiff networks and lower thermal stabilities and smaller fibres creating very stiff structures with good thermal stability. It is thought that because the 75% MPG samples for all molecules contain both long and small fibres that this has a combination effect which creates very stiff gels with increased strength i.e. this is the mechanism of solvent optimisation.

The next steps within this study are to demonstrate that these molecules can be incorporated and used within a known Type I de-icing fluid that is currently on the market and provided by Kilfrost Ltd. Using a de-icing fluid which is an unthickened fluid and therefore contains no polymeric thickener, potentially allows us to change the behaviour of a Type I de-icing fluid to a Type II or IV anti-icing fluid providing additional holdover. The gelation ability, thermal stability, rheological profiles and imaging of networks created in these systems will be obtained and analysed to try and understand if this type of molecule can actually be incorporated into a de/anti-icer for aircrafts and whether the resulting product can meet or exceed key product specification criteria.

Chapter 5

Introduction of DBS into a Type I De-Icing Aviation Product

Chapter 5 Introduction of DBS into a Type I De-Icing Aviation Product

5.1 Product Introduction

De-icing is the process of removing frozen contamination from surfaces. This is extremely important in the aviation industry to allow an aircraft to taxi and take-off safely.[3,7,28,29,51,62,63] A number of techniques are commonly used to de-ice an aircraft including the use of simple brooms,[2] storing aircraft in hangars,[2,381] forced and pressurised air,[2,7,28] as well as hot water and in newer technologies through the use of infrared[5,31] as discussed in the introduction. However, the most common way of de-icing an aircraft is through the use of de-icing fluids, known as Type I fluids.[32]

Type I de-icing fluids[32] are commonly composed of high concentrations of monopropylene glycol (MPG) and water as well as other additives. In the undiluted form a de-icing fluid contains 80% MPG with the remaining 20% being made up of water and other additives including surfactants, corrosion inhibitors, pH-adjusters, water softeners and dyes. A Type I de-icing fluid is orange in colour, which allows for identification upon spraying and contains no thickeners, therefore has low viscosity. A de-icing product is never used in its original undiluted form, due to the effects that can be incurred to the aerodynamics and is always diluted depending on the outside air temperature (OAT). Dilutions as low as 10% can be used which would contain 8% MPG, however care must be taken especially where water is only used with regards to the freeze protection that is required relative to the outside temperature.

De-icing fluids are applied hot (70-90°C)[4,54,60] and should provide a minimum of 3 minutes holdover time.[32,33] Holdover time is the amount of time a fluid can protect the surface of an aircraft before further frozen contamination can build up.[2,32,382] This short 3 minute holdover time allows enough time for an aircraft to have the frozen contamination removed before an anti-icing fluid is applied.

Anti-icing is the means to protect an aircraft from future build up of frozen contamination.[39,44,63,383,384] There is currently no other means to anti-ice an aircraft other than through the use of anti-icing fluids. Anti-icing fluids are commonly composed of lower concentrations of MPG compared to Type I de-icing fluids of 50% MPG with the remaining 50% being made up of water, polymeric thickeners and

other additives. The additives can include corrosion inhibitors, pH-adjusters, viscosity modifiers as well as dyes. There are three types of anti-icing fluids known as Type II, Type III and Type IV fluids.[33] Type II and Type IV fluids are the most commonly used, with Type III being a rarity. Anti-icing fluids contain polymeric thickeners which create thickened films. Anti-icing fluids are commonly sprayed cold after de-icing but can also be applied hot to act as a de-icer and anti-icer together. Type II and Type III fluids are commonly coloured yellow or straw with Type IV fluids being coloured green, to aid with identification when being applied. An anti-icing fluid therefore is expected to provide longer holdover times than a de-icing fluid. Type II fluids can provide holdovers of a minimum of 30 minutes, Type III a minimum of 20 minutes and Type IV fluids having the greatest holdover of 80 minutes[33] in their undiluted form. Anti-icing fluids can also be used diluted, with the lowest dilution being 50% which has a 25% MPG content.

Normally customers using such fluids would apply a two step regime when de/anti-icing an aircraft where the first step makes use of a de-icing fluid and the second an anti-icing fluid. However, customers also apply just anti-icing fluids which when heated can act to remove the frozen contamination and protect from further frozen contamination build up.[37]

Within this chapter we hope to identify if the three successful gelators highlighted in previous chapters could be incorporated into a complex fluid such as a Type I de-icing fluid and still form gels. We then hoped to explore the properties of these gels to understand the thermal stability profiles to identify if the de-icing fluid with gelators can still be applied at high temperatures. We planned to investigate the rheological profiles of these gels to determine if incorporating gelators into a de-icing fluid can improve and/or exceed the current fluid properties as well as identify if the gel structure formed within a de-icing fluid changes on the nanoscale before testing the holdover and aerodynamic performance of a potentially new anti-icing formulation.

5.2 Results & Discussion

5.2.1 Screening of gelation ability

The three gelator molecules that were highlighted within Chapters 3 and 4, Rika (DBS), DBS-OCH_3 and DBS-SCH_3, have all been demonstrated to have ideal gelation behaviour in the required solvents (1,2–monopropylene glycol (MPG) and aqueous mixtures of it) used in the de/anti-icing industry. As they are able to form gels in

these solvents it is now of interest to identify if the same behaviour and effects can be seen when the gelators are incorporated into a finished de-icing product which also contains other additives. The de-icing product used for testing was supplied by Kilfrost Ltd and is known by the brand name DF Plus (DF+). Each of the three gelators was screened in various dilutions of DF Plus with water. The dilutions that were selected reflect the maximum and minimum glycol concentrations that would be found and potentially used within a Type I de-icing fluid. The three gelators have all been screened at 1% w/v, 0.5% w/v and 0.1% w/v in a range of dilutions of DF Plus and water. The percentages shown on the Figures indicate the percentage of MPG each sample contains. To prepare the samples, a known weight of gelator was added to a 2 ml glass vial and 1 ml of DF Plus-based solvent added (See Experimental for preparation of solvent), each sample was sonicated for 30 minutes before being heated in an oil bath to below the boiling point of water until a clear homogenous solution was formed, if after 1 hour a clear solution was not formed, the sample was removed from the heat. All samples were then left on the bench at room temperature overnight to allow gelation to occur and results recorded the next day.

Initially it was unknown whether the gelator would be soluble in the finished de-icing product due to other additives being present, but surprisingly the gelators were soluble in the majority of the solvent dilutions depending on the concentration used. From **Figure 5.1** we can see when Rika (DBS) was incorporated into the undiluted DF Plus (80% MPG) and dilutions of DF Plus, at high concentrations (1% w/v) it showed good solubility down to 64% MPG where clear gels are seen to form, thereafter the gelator existed as a precipitate. As the concentration was reduced Rika (DBS) had good solubility down to 48% MPG at 0.5% w/v and down to 16% MPG when 0.1% w/v gelator was used. Comparing these results to those obtained in Chapter 3, we can see at 1% w/v that the solubility of Rika has been reduced. Gels were able to form in 50% MPG when previously tested. Therefore the additional additives seem to be having a slight negative effect on the ability of this molecule to dissolve within this de-icing product. Nonetheless, overall the solubility is generally good.

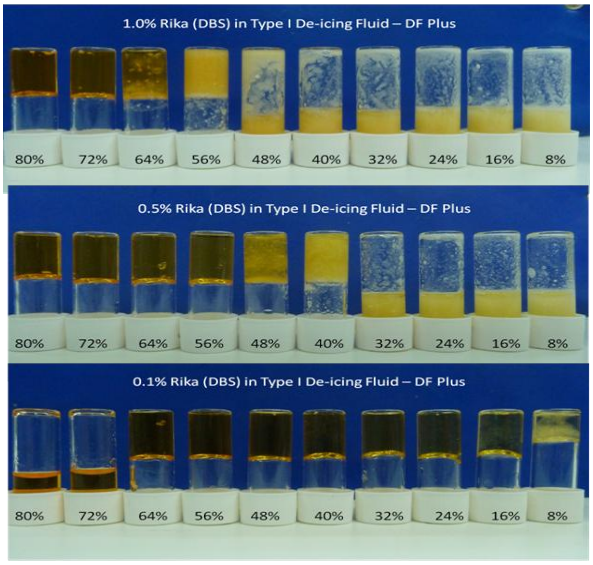

Figure 5.1 Screening of Rika (DBS) in Type I DF Plus dilutions at high, medium and low concentrations.

For DBS-OCH_3 the same general behaviour was observed as for Rika (DBS), i.e. as the concentration decreases the solubility increases. However, even at high concentrations the solubility has increased across the range of dilutions compared to Rika (DBS) at 1% w/v shown above. At 1% w/v DBS-OCH_3 was soluble down to 48% MPG, 40% MPG at 0.5% w/v and down to 8% MPG at 0.1% w/v, see **Figure 5.2**. However at 0.1% w/v the samples appear as solutions in **Figure 5.2**, when in fact they are actually very weak gels and/or partial gels that collapsed upon inversion when photographed. These all have improved solubility compared to Rika (DBS) in DF Plus and this can be attributed to the substituent on the para position of the benzene rings of the molecule increasing the hydrophilicity making it more soluble as the % MPG goes down and the degree of water content increases.

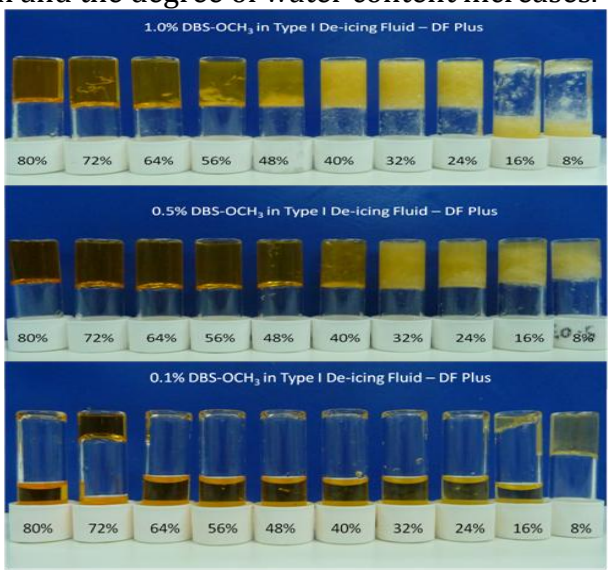

Figure 5.2 Screening of DBS-OCH_3 in Type I DF Plus dilutions at high, medium and low concentrations.

DBS-SCH_3 was also screened in the same way as described above but showed slightly different results, see **Figure 5.3**. At high concentrations although it looks like a gel is formed at 80% and 72% MPG, the samples actually contain precipitate and the remaining samples exist as an insoluble precipitate in solution. At 0.5% w/v concentration the same effect was observed. However, when the samples were at low concentration clear homogenous gels were formed and are shown to be soluble down to 48% MPG. This gelator therefore has similar gelation behaviour to the other gelators when at low concentration, but lacks the ability to be used across a larger concentration range.

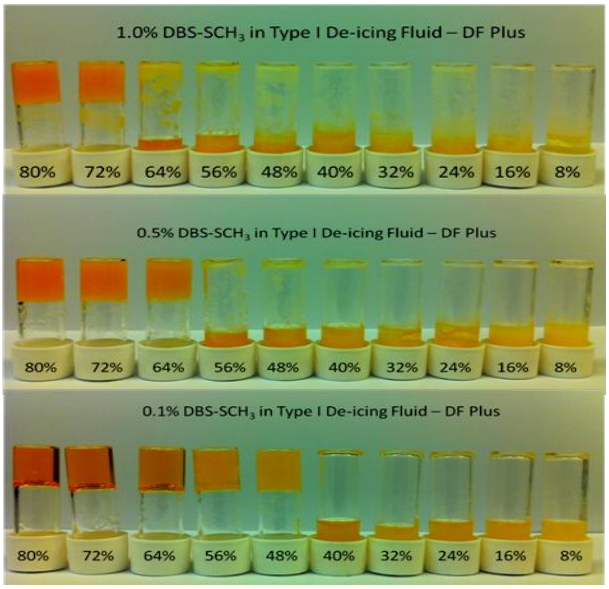

Figure 5.3 Screening of DBS-SCH_3 in Type I DF Plus dilutions at high, medium and low concentrations.

Each of the three gelators were tested at concentrations lower than 0.1% w/v however, none of the molecules showed the ability to form gels at lower concentrations except DBS-SCH_3. DBS-SCH_3 acted as a supergelator with gels being formed as low as 0.02% w/v in dilutions of DF Plus containing 56% and 48% MPG. Gels could also be formed in DF Plus dilutions containing 72% and 64% MPG at 0.04% w/v however the undiluted DF Plus (80% MPG) could not form gels below 0.1% w/v.

5.2.2 Minimum Gelation Concentration (MGC)

Each of the three gelators in DF Plus was then tested to determine what the minimum gelation concentration required to form a gel in the various dilutions of DF Plus.

Table 5.1 Minimum gelation concentration of the three gelator molecules in DF Plus and DF Plus dilutions.

% MPG in DF Plus Dilution	Gelator / % w/v		
	Rika (DBS)	**DBS-OCH_3**	**DBS-SCH_3**
80%	0.2	0.2	0.1
72%	0.2	0.2	0.04
64%	0.1	0.2	0.04
56%	0.1	0.2	0.02
48%	0.1	0.2	0.02
40%	0.1	0.2	*I*
32%	0.1	0.2	*I*
24%	0.1	0.2	*I*
16%	0.1	0.2	*I*
8%	*I*	0.2	*I*

From **Table 5.1** it is clear to see that DBS and DBS-OCH_3 have very similar MGC values across the range of DF Plus dilutions with increased solubility being observed with DBS-OCH_3. This is most likely due to the additional substituent the DBS-OCH_3 possesses compared to that of DBS which would aid increased solubility by making the molecule more hydrophilic. DBS-SCH_3 is slightly different in the fact it can form gels at much lower concentrations and act as a supergelator. This might be attributed to the polarity of the SCH_3 substituent allowing the fibres to form more easily in this solvent system hence, requiring lower concentrations of gelator. Similar effects were considered in pure solvents in Chapter 3.

5.2.3 Thermal stability

The thermal stability for each of the three gelators in the various DF Plus dilutions was determined using the tube inversion method as described previously. Gels were only tested when a range of concentrations could be formed in the same solvent mixture. Gels that could only be formed at one concentration were not tested.

From **Figure 5.4** it is evident that gels formed in DF Plus and its dilutions follow the general behaviour observed for all gels in that as the concentration increases the thermal stability of the gel increases. It is also evident from **Figure 5.4** that as the solvent system becomes more dilute with water the thermal stability increases. This can be accounted for by the hydrophobic effect. This becomes more dominant as the solvent becomes more dilute, which encourages the gelator molecules to interact and aggregate more effectively, producing more thermally stable gel networks with

higher T_{gel} values and hence becoming increasingly difficult to disassemble into its individual molecules. This is in agreement with the results obtained previously when each of the molecules was tested only in MPG:water mixtures.

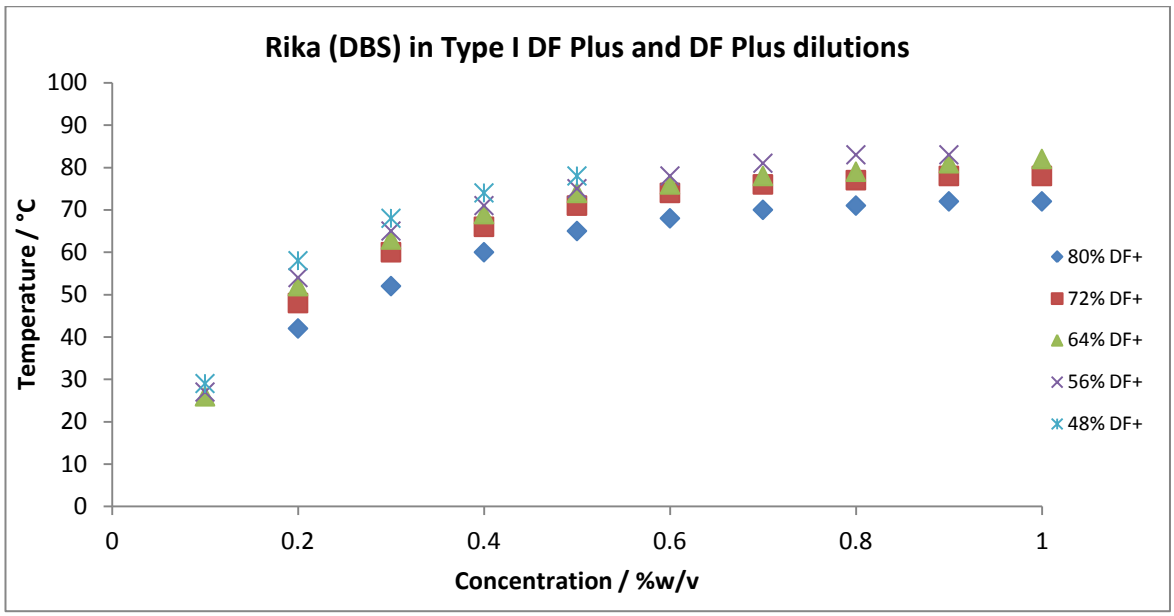

Figure 5.4 Thermal stability of Rika (DBS) in DF Plus and DF Plus dilutions.

Like Rika (DBS) above the same trend is demonstrated by DBS-OCH_3 in the different dilutions of DF Plus, see **Figure 5.5**. As concentration increases the thermal stability increases, which is expected as a denser network with more entangled fibres is formed when higher concentrations are present. The same behaviour is also noted when the solvent becomes more dilute, the gel network becomes more thermally stable resulting in higher T_{gel} values. However, DBS-OCH_3 is soluble down to 40% MPG content (i.e. 60% water and additives) but we can note that it is also starting to show that this may be the limit at which this gelator can form gels as the effective concentration range of this gelator in 40% MPG in DF Plus halves to 0.5% w/v and lower. Above this concentration range, the gelator exists as a precipitate in solution.

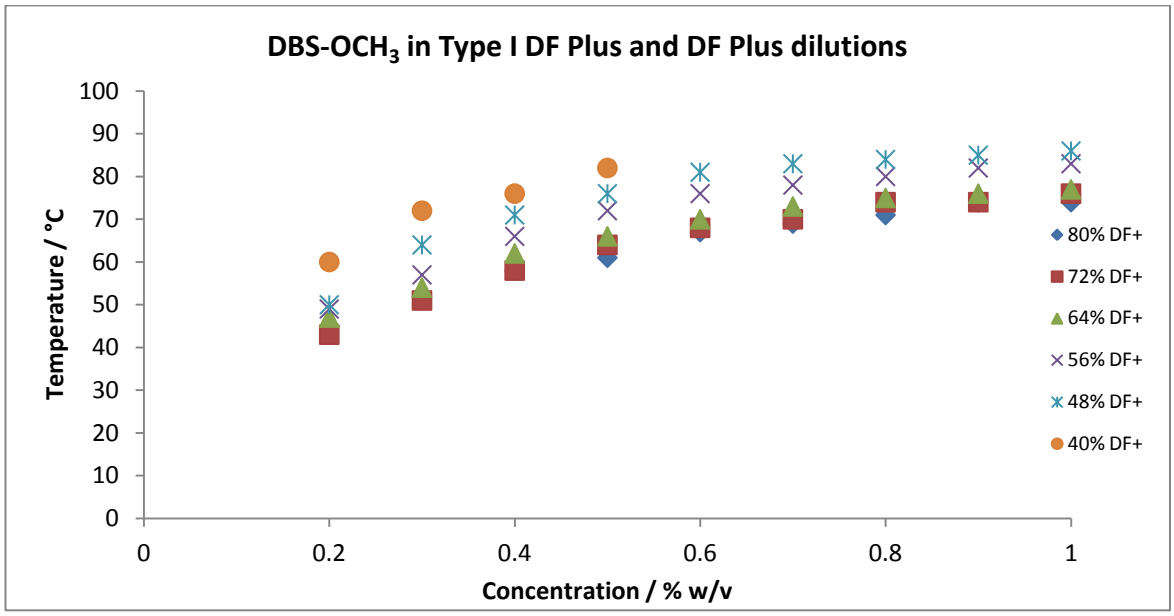

Figure 5.5 Thermal stability of DBS-OCH_3 in DF Plus and dilutions of DF Plus.

From **Figures 5.4** and **5.5** we can see that although the two gelator molecules, Rika (DBS) and DBS-OCH_3 are different structurally they both show similar T_{gel} values and hence thermal stability in the solvent dilutions where they both form gels. Overall however, DBS-OCH_3 gelator performs better in this chosen solvent and evidently shows better solubility across the range of dilutions with a large concentration range. As de-icing fluids are used diluted, using DBS as an additional additive may potentially be unsuitable in this product as it cannot form and or support a gel network when there is 40% MPG or less, whereas DBS-OCH_3 can form gels in 40% MPG and therefore appears more versatile for use in de-icing products.

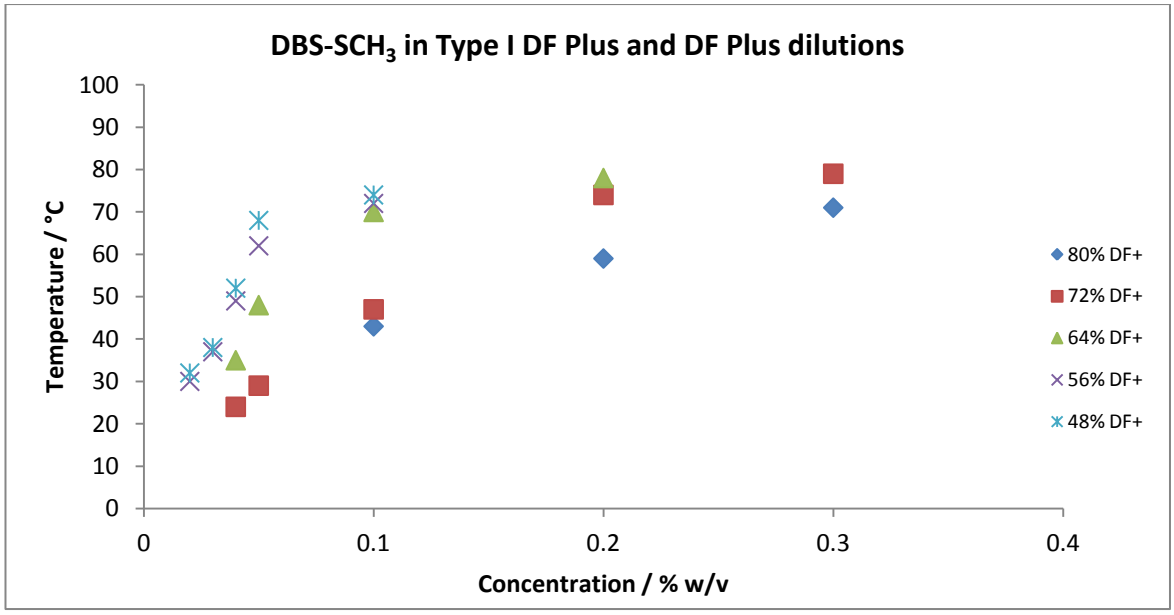

Figure 5.6 Thermal stability of DBS-SCH_3 in DF Plus and DF Plus dilutions.

DBS-SCH_3 is different from the other gelators in that it can form gels in this solvent but the concentrations are much lower and the range is narrow compared to the other gelators. It generally follows the expected trend for T_{gel}, as concentration increases thermal stability increases, **Figure 5.6**. Once again the hydrophobic effect is evident with this analogue. However, at 48% MPG we are reaching the saturation point where the ability of the gelator to form a gel is reduced further to very low concentrations. Use of this gelator for this type of application may be limited as it only has a very small functional concentration range and cannot form gels when the solvent is diluted to 40% MPG and below.

5.2.4 Scale up effects

Each of the gelators in the differing DF Plus dilutions were then scaled-up to 200 ml, similar size samples are used when performing the industry standard testing to identify if any changes occur when on larger scale. It is important once a test has been successfully identified on small scale to scale it up and identify if the sample properties or if its effects change, which would alter or change the way in which it could be used in a real life application. Obviously this required large-scale synthesis of each of these derivatives – as outlined in Chapter 3.

Gels were prepared as mentioned previously but to 200 ml scale in glass Schott bottles, and instead of being heated for 1 hour, the samples were heated in an oil bath overnight to achieve clear homogenous solutions. The samples were removed from the heat and placed on the bench to reach room temperature to allow gelation to occur, with results recorded the next day. From **Figure 5.7** below of Rika (DBS) in DF Plus dilutions it is clear that when this gelator is scaled up its performance is in agreement with the small scale samples and shows no significant differences except when there is 0.1% w/v concentration. Large scale samples of 0.1% w/v Rika (DBS) indicate that gels can only be formed down to and including 24% MPG but when tested on small scale showed that gels also could be formed when there was only 16% MPG present. It is also evident that these gels are weaker than first thought and form partial gels which collapse upon inversion of the bottles. Therefore when Rika (DBS) is scaled up, it has reduced solubility in this solvent system at low concentration.

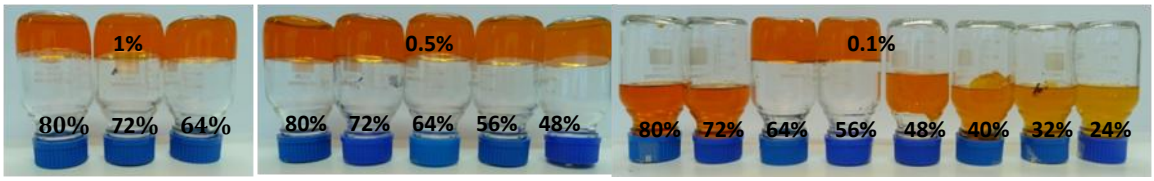

Figure 5.7 Scale up samples of Rika (DBS) at high, medium and low concentration in DF Plus and DF Plus dilutions.

When DBS-OCH_3 was scaled up at 1% w/v we can see from **Figure 5.8** that clear gels were formed down to 64% MPG. Upon further dilution all samples appear insoluble in solution. This does not agree with the small scale samples where gels could be seen to form when there was 48% MPG present. At 0.5% w/v concentration, gels could be formed between 80% MPG and 48% MPG, but again gels could be formed in more dilute systems of 40% MPG when smaller samples were made. However after a further day of heating the 40% MPG sample it could actually form clear gels, like in the small scale samples. At 0.1% w/v partial gels in solution were formed down to 24% MPG whereafter the gelator is insoluble in the solvent. However, like the other concentrations, when tested at small scale this gelator showed it could form gels when there was as little as 8% MPG present. Overall, this gelator's solubility in this de-icing product has been shown to reduce upon scale up.

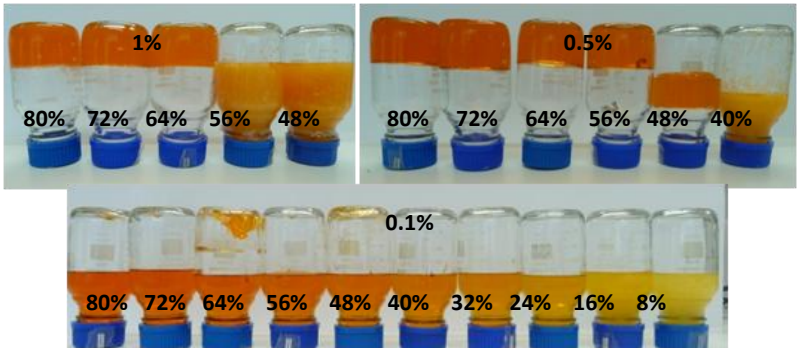

Figure 5.8 Scale up samples of DBS-OCH_3 at high, medium and low concentrations in DF Plus and DF Plus dilutions.

DBS-SCH_3 unlike the other two gelators was not scaled up at 1 % w/v and 0.5% w/v concentrations. This is because they were insoluble across the full range of DF Plus dilutions on small scale. Therefore only samples which could form gels that could be potentially used in further tests were scaled up. Like the others tested above, DBS-SCH_3 had reduced solubility when scaled up. At 0.1% w/v when tested on smaller scale, gels could be formed when DF Plus was diluted and contained 48% MPG, however once scaled up, gels could not be formed in samples containing 56% MPG or

lower unless they were heated for a further day at which point clear gels were then seen to form as the small scale samples indicated, see **Figure 5.9**.

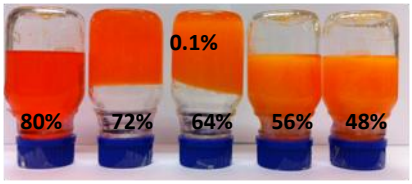

Figure 5.9 Scale up samples of DBS-SCH_3 at 0.1% w/v in DF Plus and DF Plus dilutions.

Therefore by scaling up these gelators, it clearly demonstrates that small samples do not always portray what will happen when scaled up and in this instance it has highlighted that all three gelators have reduced solubility than expected or would require prolonged periods of heating. This becomes very important if the gelator has to be used on large scale.

Each of the scale-up samples was used for further testing to identify their rheological profiles and properties, as well as their properties within industrial relevant test methods. This would allow us to understand if these types of fluids could be potentially used as a de/anti-icing fluid for aircrafts.

5.2.5 Rheology

Rheological analysis of each of the gelators in Type I DF Plus and DF Plus dilutions were carried out on a Kinexus Pro+ stress controlled rheometer using a 20 mm parallel plate. To understand how each of these gelators when in DF Plus respond to differing stresses and strains a full rheological profile was carried out to determine their strength, stiffness and robustness through amplitude sweeps. Each of the tests were conducted at 20°C and the LVR determined for each sample, with a value from the LVR then being used for all further testing.

Samples prepared in **section 5.2.4** above were used for rheological testing. Upon testing each of the samples were placed into an oil bath at temperatures just above their T_{gel} values to form the solution phase. This is primarily because gels can be fragile if placed directly onto the instrument as a gel. Therefore using the hot solution phase of each sample they were placed onto the rheometer plate using a spoon to reduce any unnecessary damage to the sample which was set to 20°C. Upon application of the sample the geometry was brought down to the designated gap size (1 mm) and left to equilibrate for 15 minutes to allow the formation of the gel. From **Figure 5.10** and **Table 5.2** we can see that samples of 0.5% w/v Rika (DBS) in both

DF Plus and dilutions of DF Plus were very stable, robust and strong with long linear LVR regions, and critical strain values of 0.4-1%, compared to what was observed in Chapter 4 (0.03% strain) when tested in MPG:water mixtures. Therefore by incorporating this gelator into a pre-formulated de-icing fluid with additional additives we have increased the resistance to strain of the system by between 10-30 times. This may be a result of the additives having interactions with the gelator molecules which are creating a stronger and stiffer network. From **Figure 5.10** we can also see that for Rika (DBS) when there is a 72% MPG content compared to the other dilutions has the greatest stiffness. Comparing this to the 75% MPG results achieved in Chapter 4 shows us that the G' values have increased 10 fold. Therefore knowing that the MPG:water mixtures do not possess such high G' values or strengths, this must be a direct result of the different additives incorporated within the de-icing product. When Rika (DBS) was in DF Plus in its original form we see from **Figure 5.10** that high G' values are also achieved with high critical strain values (similar to that observed when anti-icing fluids are tested which include a polymer gel network) and the same is seen to be true when Rika (DBS) is in 64% MPG. However, we also note that at 64% MPG content the G' value has reduced and continues to reduce upon further dilution. As well as the stiffness of the gel network reducing, the strength of the gel also reduces to almost half of that obtained for the higher MPG content samples. Therefore we note that the optimum conditions for interactions to occur in this system to produce stiff strong networks in DF Plus requires dilutions which incorporate between 20-36% water (80-64% MPG). In more dilute systems such as 56% and 48% MPG, we see that similar G' values are obtained as was shown in Chapter 4 when tested in MPG:water mixtures however they are much stronger. Therefore these gels like in Chapter 4 may also be reaching a saturation point where the presence of water is affecting the ability of the gelator molecules and additives to interact to create a stiff network.

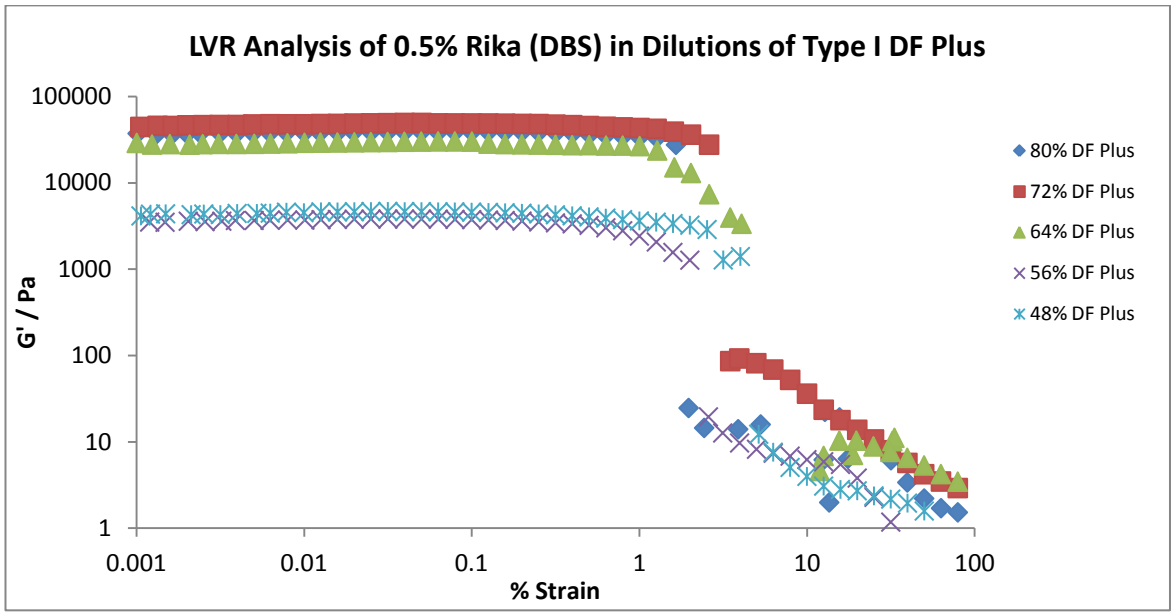

Figure 5.10 Amplitude sweeps of 0.5% w/v Rika (DBS) in DF Plus (80% MPG) and DF Plus dilutions (percentages represent the MPG content).

Table 5.2 Critical strain and stiffness (G') values of 0.5% w/v Rika (DBS) in DF Plus (80% MPG) and DF Plus dilutions.

% MPG	G' (Pa)	Critical Strain %
80%	35401	0.6
72%	43810	0.8
64%	26657	1.0
56%	3344	0.4
48%	3975	0.5

Amplitude sweeps were also run for 0.5% DBS-OCH_3 in DF Plus and aqueous mixtures like Rika (DBS) above, see **Figure 5.11** and **Table 5.3**. DBS-OCH_3 showed that as the water ratio increased the stiffness of the gel network reduced, with the stiffest gel being formed in the original undiluted product. DBS-OCH_3 also shows that the stiffer the gel the stronger the gel network is towards strain with the exception of DBS-OCH_3 in 40% MPG. Therefore from the amplitude analysis we note that like Rika (DBS) above, when this molecule is incorporated into the de-icing fluid the strength of the gels that are formed are 20-60 times stronger than when they are in MPG:water mixtures however the stiffnesses of the gels that are formed are very similar. This is potentially a result of the additional substituent on the periphery of the gelator molecule tuning the interactions with the additives within the de-icing fluid which in turn creates a stronger gel.

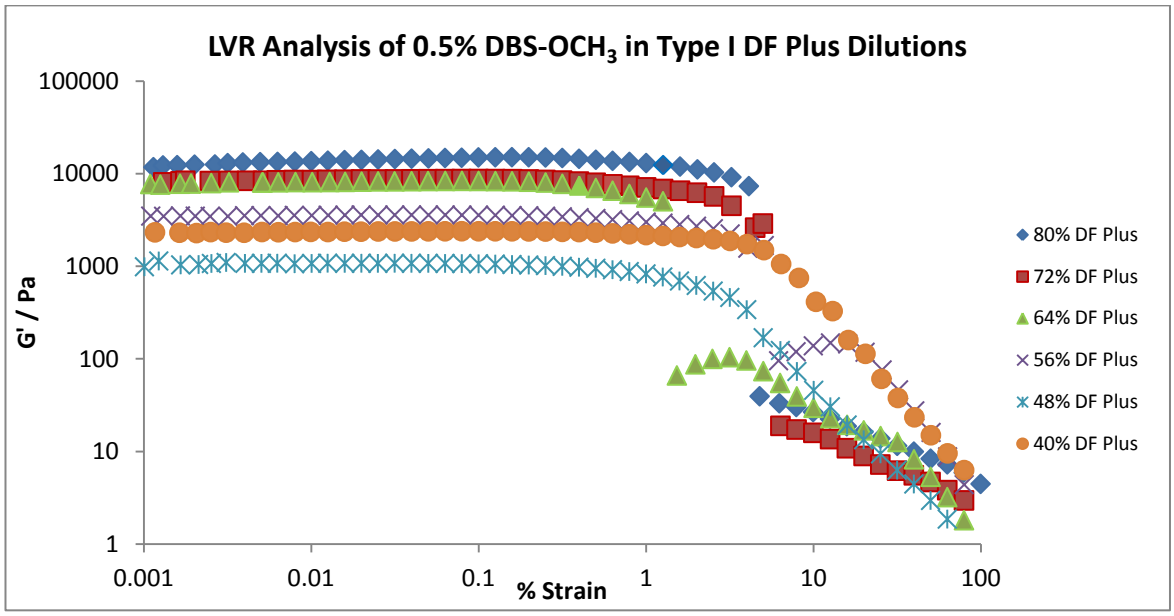

Figure 5.11 Amplitude sweeps of 0.5% w/v DBS-OCH_3 in DF Plus (80% MPG) and DF Plus dilutions (Percentages represent the MPG content).

Table 5.3 Critical strain and stiffness (G') values of 0.5% DBS-OCH_3 in DF Plus (80% MPG) and DF Plus dilutions.

% MPG	G' (Pa)	Critical Strain %
80%	12672	1.3
72%	7677	0.7
64%	7392	0.4
56%	3154	0.6
48%	933	0.5
40%	2120	1.3

DBS-SCH_3, when tested to determine the LVR region, showed a different behaviour compared to the other two molecules above. Unlike Rika (DBS) and DBS-OCH_3 that were tested at 0.5% w/v concentrations, DBS-SCH_3 was tested at 0.1% w/v concentration. From **Figure 5.12** and **Table 5.4** we can see that DBS-SCH_3 shows that as the water ratio increases the stiffness of the gel network increases, which is indicative of the self assembly mechanism due to hydrophobic effects. This pattern was also observed when tested in Chapter 4 with MPG:water mixtures. This suggests that interactions with additives may be less significant for DBS-SCH_3 than for Rika (DBS) or DBS-OCH_3. The stiffness values (G') obtained for the gels when in DF Plus and aqueous mixtures show similar values to when in MPG:water mixtures. However, the incorporation of the gelator into the de-icing fluid has affected the strength of the gels which are formed, with the strength almost being halved compared to when tested in MPG water mixtures. From **Figure 5.12** we note that the stiffest gel is the

strongest gel but upon dilution the gel becomes weaker. When the gelator is in the undiluted (80% MPG) DF Plus we also can see that the gel networks produced are weaker, and the stiffness of the gel structure is the lowest. This is most commonly due to the fact that as this molecule assembles through the use of hydrophobic effects, the 80% MPG content is making the gelator molecules more soluble and dynamic unlike the gels formed when there is 64% and 56% MPG. Therefore the optimum solvent composition for gels to form with this molecule lie between 64% and 56% MPG, thereafter the gel networks become weaker and less stiff as a result of increasing water content and lower solubility.

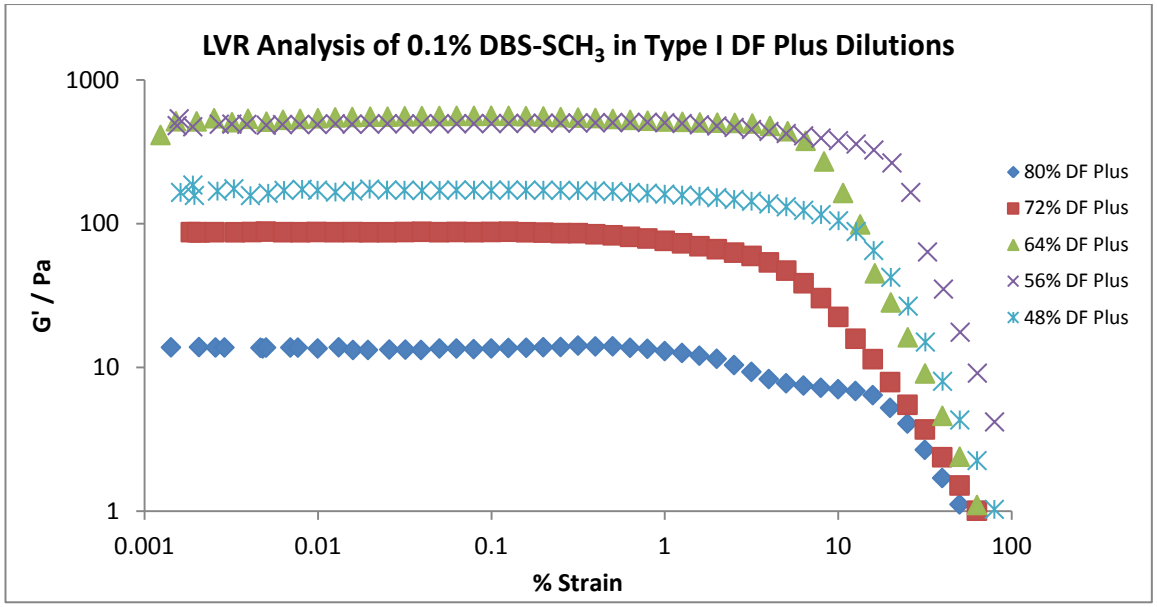

Figure 5.12 Amplitude sweeps of 0.1% w/v DBS-SCH_3 in DF Plus (80% MPG) and DF Plus dilutions (Percentages represent the MPG content).

Table 5.4 Critical strain and stiffness (G') values of 0.1% w/v DBS-SCH_3 in DF Plus (80% MPG) and DF Plus dilutions.

% MPG	G' (Pa)	Critical Strain %
80%	13.0	1.3
72%	83	0.5
64%	498	3.2
56%	448	3.2
48%	151	2.0

Unlike Rika (DBS) and DBS-OCH_3, which in DF Plus and aqueous mixtures of DF Plus show to have increased stiffness and strengths due to the possible interactions with the additional additives that are within a de-icing fluid, DBS-SCH_3 does not show the same behaviour. The additional additives in this case do not affect the stiffness of the

gel networks that are formed, however, they do appear to have a detrimental effect on the strength of the gels that are formed where they are seen to half. Where it is thought that the additional additives may be beneficially interacting with the gelator molecules with Rika (DBS) and DBS-OCH_3 it is clear that the substituent on DBS-SCH_3 may not be able to make or create further interactions like the other molecules which therefore hinders the ability of the gel network to become stronger.

By incorporating these molecules into a Type I de-icing fluid which under normal circumstances is a Newtonian fluid with no gel structure, we have potentially created a new type of thickened fluid which could potentially protect an aircraft from further frozen contamination. As gels have been able to be formed within a finished de-icing product it allows for direct incorporation which requires no additional equipment, they could also potentially provide holdover protection due to the stiff gel networks that are formed, with G' values (1-10 Pa) in some cases exceeding what is normally observed for anti-icing fluids. These gelators are also as strong as anti-icing fluids (1-10% strain), with the added benefit of being reversible upon application of temperature which does not affect the gel structure unlike the polymer gels currently used in anti-icing fluids. As such our gelators may be able to convert a de-icing fluid into an anti-icing fluid in one simple step.

Frequency sweeps of the same samples were performed at 20°C to determine the behaviour of networks within DF Plus and aqueous mixtures of DF Plus. G' (storage modulus) and G'' (loss modulus) for each sample were determined and the response to increasing frequency recorded. If G' is dominant over G'' the material is elastic and solid-like. If the G'' is dominant over G' the sample is more viscous and liquid-like. If a sample is a gel, G' will be dominant over G'' and independent of frequency. From **Figure 5.13** of 0.5% Rika (DBS) in DF Plus and aqueous mixtures of DF Plus we noted that all samples, regardless of solvent, were solid-like and show to be independent of frequency with G'>G'', characteristic of gels.

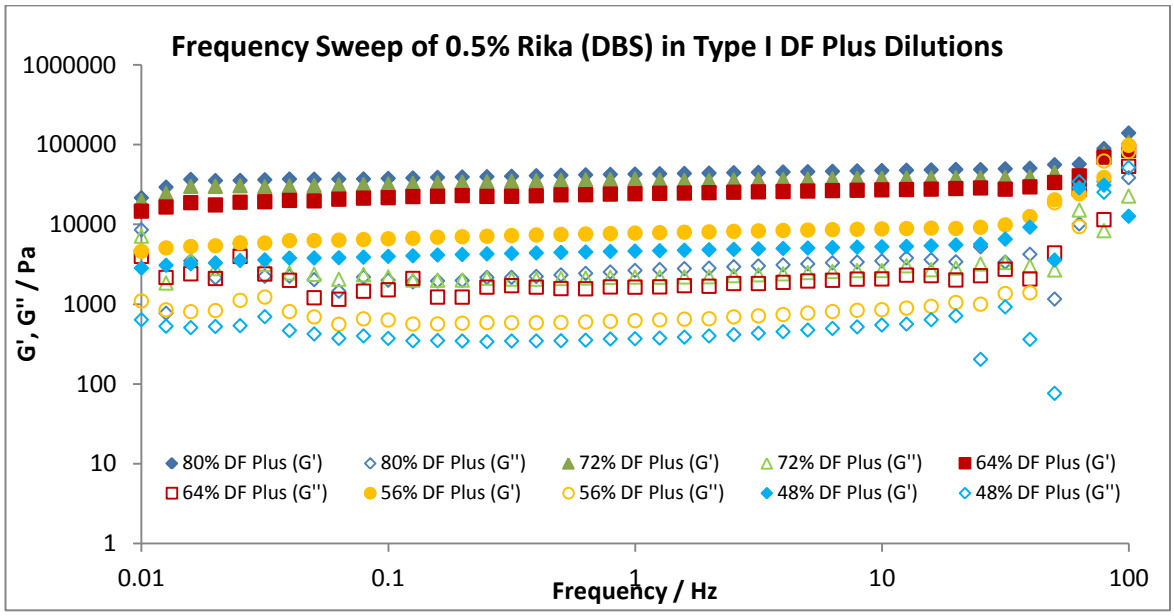

Figure 5.13 Frequency sweep of 0.5% w/v Rika (DBS) in DF Plus and DF Plus dilutions.

However, unlike Rika (DBS) that is independent of frequency, DBS-OCH_3 and DBS-SCH_3 behaviour changes at high frequencies, above 10 Hz for DBS-OCH_3 and 5 Hz for DBS-SCH_3. Below these frequencies they are independent of frequency with G'>G'', see **Figures 5.14** and **5.15**. Therefore DBS-OCH_3 and DBS-SCH_3 are frequency dependent and act as visco-elastic solids where G' increases with increasing frequency. The fact that DBS-SCH_3 is more frequency dependent than the other gelators may reflect the fact that these gels were tested at lower concentrations, and as a result have lower G' values.

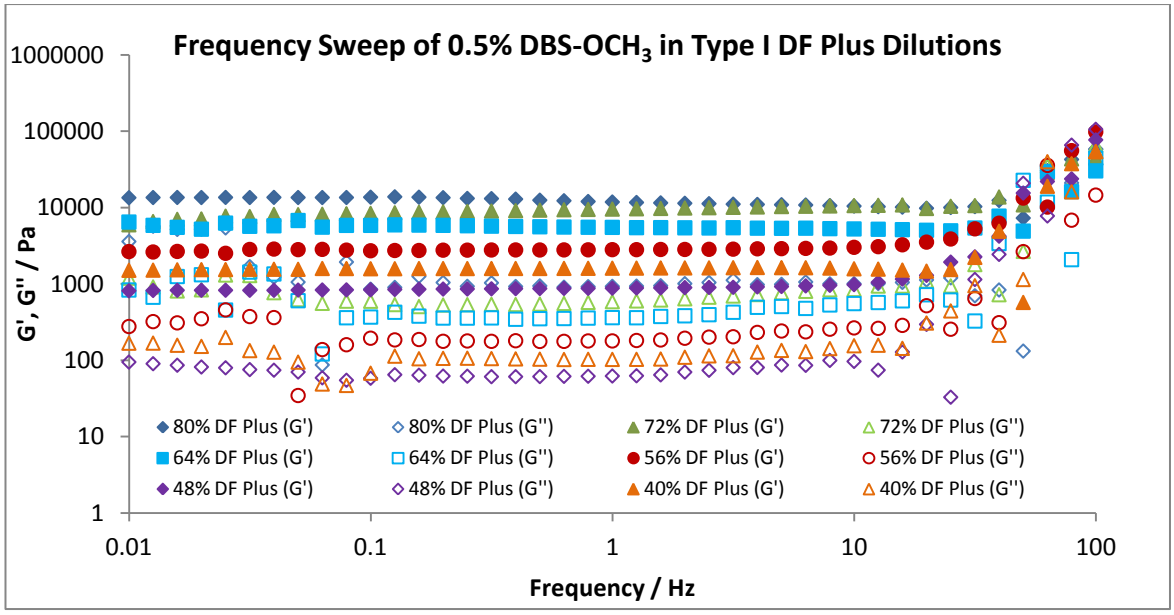

Figure 5.14 Frequency sweep of 0.5% w/v DBS-OCH_3 in DF Plus and DF Plus dilutions.

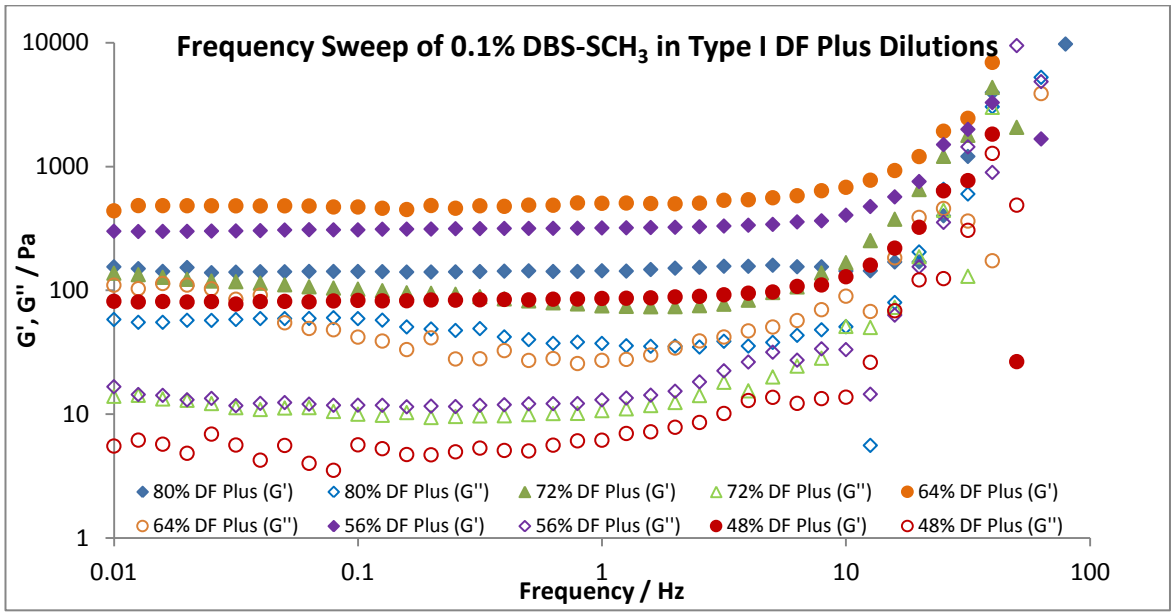

Figure 5.15 Frequency sweep of 0.1% DBS-SCH_3 in DF Plus and DF Plus dilutions.

Each of the three molecules in the different DF Plus dilutions was then tested to identify their response to increasing and decreasing temperature. Unlike the sample application described above where the samples were applied to a cold plate on the rheometer, to conduct thermal analysis they were applied in the same way but with the rheometer plate set to 85-90°C. The plate was then slowly cooled down. Using this method of application the temperature at which a gel forms (T_f) can be detected, this is measured as the temperature at which the G* (complex modulus) increases sharply. This is a poorly defined term within rheology and therefore within this study we are defining it as the point at which G* reaches a maximum value. Furthermore, on heating, the temperature at which the gel disassembles (T_d) into the solution phase can also be detected.

All of the molecules showed the same general trends. As the temperature decreased samples containing more water would form gels at higher temperatures with undiluted DF Plus requiring the lowest temperatures. Likewise when the temperature cycle was reversed from low to high temperatures they all showed the same general trend with higher temperatures being required to disassemble gels which contained more water (**Table 5.5**). This supports the view that water content and hydrophobicity are important in controlling the gelation event.

Table 5.5 Gel formation (T_f) and gel dissolution (T_d) temperatures for 0.5% w/v Rika (DBS) and DBS-OCH_3 as well as 0.1% w/v DBS-SCH_3 in DF Plus and DF Plus dilutions (*I* = Insoluble)

	Molecule					
Solvent / % MPG	**Rika (DBS)**		**DBS-OCH_3**		**DBS-SCH_3**	
	T_f/(°C)	T_d/(°C)	T_f/(°C)	T_d/(°C)	T_f/(°C)	T_d/(°C)
80	31.8	73.5	32.9	62.1	9.5	67.9
72	46.5	61.4	42.5	68.1	32.0	72.8
64	51.2	72.1	44.9	71.4	44.1	76.7
56	65.0	79.5	48.6	76.1	54.1	84.1
48	63.9	76.1	61.6	82.1	68.6	88.1
40	*I*	*I*	71.9	86.8	*I*	*I*

Therefore gels containing 48% MPG for Rika (DBS) and DBS-SCH_3 and 40% MPG for DBS-OCH_3 are the most thermally stable, with the undiluted DF Plus (80% MPG) samples being the least thermally stable. This is in agreement with the T_{gel} measurements in **Section 5.2.3** which also showed samples containing the most water to be the most thermally stable. Although the T_{gel} and temperature ramp conducted on the rheometer provide the same trends, their values are somewhat different and as a result cannot be directly related as they are measuring different phase behaviours.

Although rheology has demonstrated that incorporating these three different gelators into a de-icing fluid such as DF Plus can create stronger and stiffer gels compared to gels formed in only MPG:water mixtures, they still require the same temperatures to form and breakdown their structures. Therefore this allows for customers to use these fluids between 65-100°C as highlighted in Chapter 4 but with the potential of longer holdover protection times due to the increased G' values which would create thicker films upon application to cold surfaces.

To try and identify the behaviour if these types of gels were applied to an aircraft at low temperatures, we wanted to identify how fast a gel would be formed upon application from a hot solution onto a cold surface.

As before, the samples used were the scaled-up samples prepared in **Section 5.2.4**. These were placed into an oil bath at temperatures above their T_{gel} value to form the solution phase. Each of the samples in turn were then applied to the rheometer sample plate set to 20°C using a spoon with the geometry brought down to the designated gap size (1 mm) and the test started immediately. The test was run over 1

hour. The time at which the complex modulus (G*) reaches a plateau is recorded as the length of time it takes for a gel to form. From **Figure 5.16** we can see an example of 0.5% DBS-OCH_3 in DF Plus and DF Plus dilutions. Generally the higher the glycol content the longer it takes the gel to form and likewise the higher the water content the faster the gel forms with 40% MPG samples forming the most quickly.

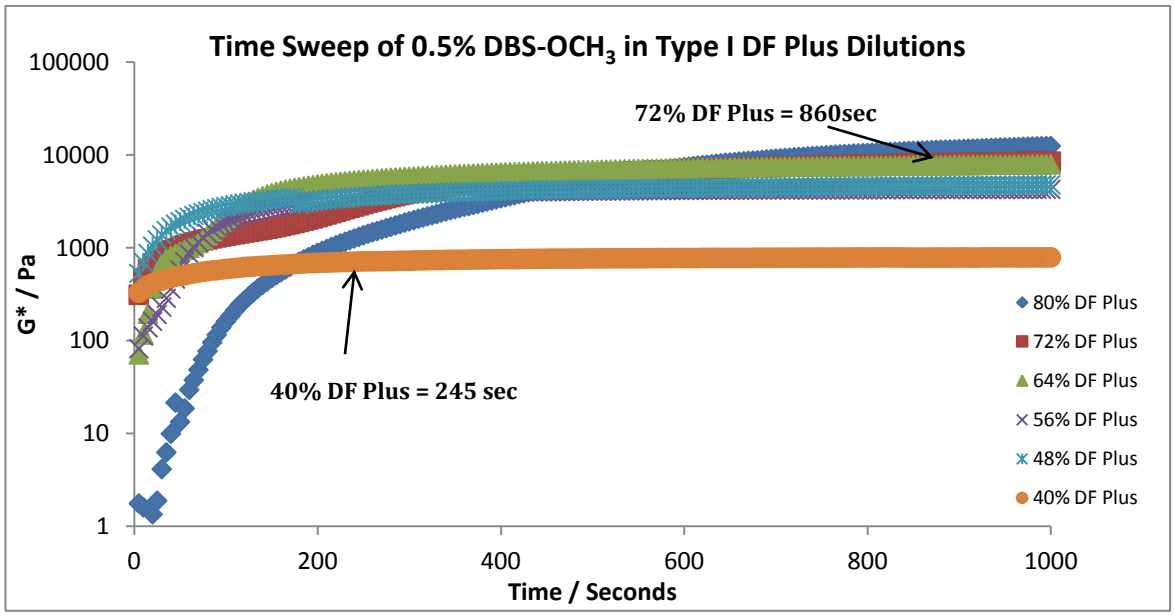

Figure 5.16 Time sweep analysis of 0.5% w/v DBS-OCH_3 in DF Plus and DF Plus dilutions.

From **Table 5.6** it is evident that all three gelator molecules show the same behaviour. As the water content increases the gel networks form more quickly, taking between 4-10 minutes to fully form. However, unlike the diluted DF Plus samples, values could not be obtained for DF Plus in its undiluted state for any of the gelators. Each of the gelators showed their G* values continually growing even after 1 hour.

Table 5.6 Time taken to form a gel with 0.5% w/v Rika (DBS) and DBS-OCH_3 as well as 0.1% w/v DBS-SCH_3 in DF Plus and DF Plus dilutions.

Solvent / % MPG	**Time of Formation / seconds (minutes)**		
	Rika (DBS)	**DBS-OCH_3**	**DBS-SCH_3**
80	N/A	N/A	N/A
72	475 (7.9mins)	860 (14.3 mins)	N/A
64	380 (6.3 mins)	660 (11 mins)	2540(42 mins)
56	295 (4.9 mins)	435 (7.3 mins)	525(8.8 mins)
48	275 (4.6 mins)	435 (7.3 mins)	265 (4.4 mins)
40	*I*	245 (4.1 mins)	*I*

Therefore by incorporating gelators into a de-icing fluid we can potentially create a thickened fluid which creates a film on an aircraft relatively quickly, especially when using dilute systems. However, this test was conducted at 20°C for instrumental reasons and for uniformity across all testing. Of course, in real life these types of gels would be being applied to surfaces which would be at 0°C and below, therefore the gels would potentially form even more quickly.

5.2.6 Scanning Electron Microscopy (SEM)

To understand the morphology of the gel networks created when gels are formed in DF Plus and dilutions of DF Plus, we conducted scanning electron microscopy (SEM) for each of the gelators. Analysis of the gels formed in undiluted DF Plus (80% MPG) and on the most dilute gel sample for each gelator were collected and compared to identify any obvious morphological changes when the water content increased as well as giving an insight into how the gel network forms at differing temperatures, representative of de-icing an aircraft.

Samples for SEM analysis were prepared by two different methods to identify if gels formed at room temperature compared to gels formed at high temperatures which simulate application temperatures and then crash-cooled at freezing temperatures would affect the morphology of the gel network. The first method involved spreading a small amount of a gel sample on an aluminium stub that was left to form at room temperature. These samples were left to dry in a dessicator until the solvent was removed and a dried film was present on the stub. The second method involved placing the formed gel sample into an oil bath set to 98°C to form the solution state, during which time the aluminium SEM stubs were placed into the freezer at -21°C for 5 minutes to cool. One drop of the hot gel solution was then pipetted onto the cold aluminium stub and spread over the surface. The stubs were then placed back into the freezer for 2 hours to allow the gel to set at freezing temperatures. After 2 hours the stubs were removed from the freezer and placed into a dessicator at room temperature to dry and leave the xerogel. To ensure the samples are conductive, they were then coated with a thin layer of Au/Pd using a sputter coater. Therefore the sample being viewed is a dried, collapsed, coated form of the gel network within each of the samples. It is important to recognise that the images obtained for each of the samples here is not how the gel network would exist in the solvated state, but can give an indication of the type and size of the supramolecular structures that are formed, and is useful for comparative analysis.

Images for Rika (DBS) in undiluted DF Plus (80% MPG) and diluted DF Plus containing 48% MPG were obtained in both preparatory conditions (**Figure 5.17**). What can be observed from the samples prepared at room temperature are that Rika (DBS) in undiluted DF Plus produces very small fibres ca. 5 nm that appear straight with no obvious shape i.e. twists. However they do appear to create a fibrous network throughout the whole sample. Within the images it is also evident that crystalline structures are present in certain areas of the gel network but it is unclear whether they are part of the gel network. These potentially could be created from the additional additives present in DF Plus. When we compare this to the sample produced at freezing temperatures, we see that similar types of fibres are produced which measure ca. 5 nm in diameter with fibre bundles being formed measuring ca. 100-200 nm in diameter. Again we see the same crystalline structures present but it is still unclear whether they are on the surface of the fibrous gel structure or entangled within it indicating the possibility of further interactions with what may be the structures formed from the additives. When the diluted DF Plus samples containing 48% MPG with Rika (DBS) were viewed under the microscope they were seen to react with the electron beam creating unclear images, however it is evident that similar types of fibres are formed, ca. 5 nm in diameter, that span the whole sample creating an entangled network with crystalline structures appearing on the surface at room temperature. When the diluted DF Plus Rika (DBS) sample prepared at freezing temperatures was imaged, no evidence of fibres or a gel network could be found.

Room Temperature **Freezing Temperatures**

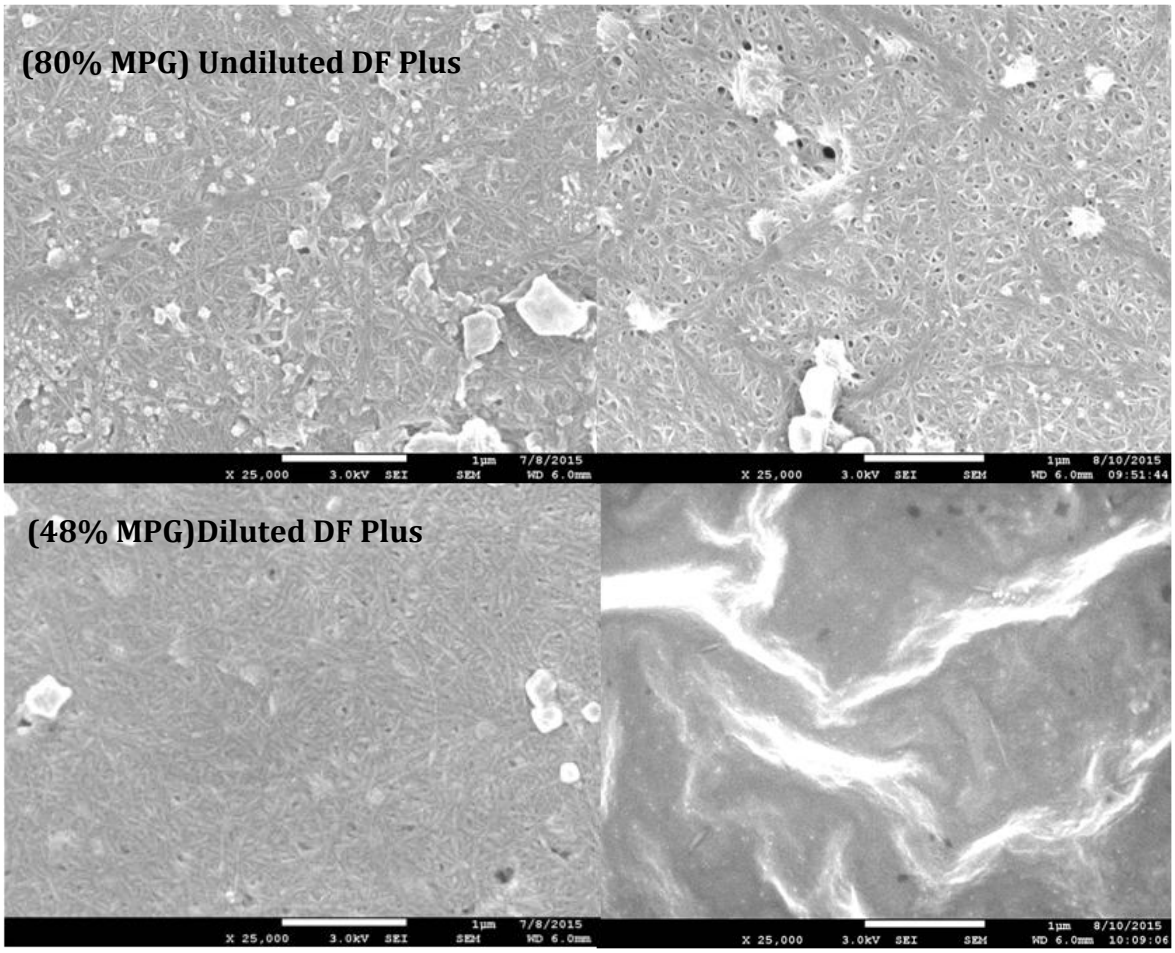

Figure 5.17 SEM analysis of Rika (DBS) in (80% MPG) DF Plus at room temperature (Top left), and freezing temperatures (Top right) as well as diluted DF Plus (48% MPG) at room temperature (Bottom left) and freezing temperatures (Bottom right).

Samples of DBS-OCH_3 were imaged in the same way, however DBS-OCH_3 is able to form gels in more dilute solvent systems containing 40% MPG. Images for DBS-OCH_3 in undiluted DF Plus at room temperature formed long thin fibres ca. 5-10 nm in diameter, these potentially could be smaller as it is difficult to identify just one single fibre. They have a helical twist and are seen throughout the sample creating an entangled network. Fibre bundles within the images are also present with sizes ca. 10-100 nm in diameter, however unlike the images obtained for Rika (DBS) above their seems to be no evidence of the crystalline structures (**Figure 5.18**). This suggests these may have resulted from Rika (DBS) rather than from the presence of additives. When comparing this image to the freezing temperature images it is clear that very similar fibres are created with similar sizes and shapes. The fibres at freezing temperatures appear to create more fibre bundles than at room temperature

and span the whole sample. They also appear more tightly packed together creating a porous fibrous structure.

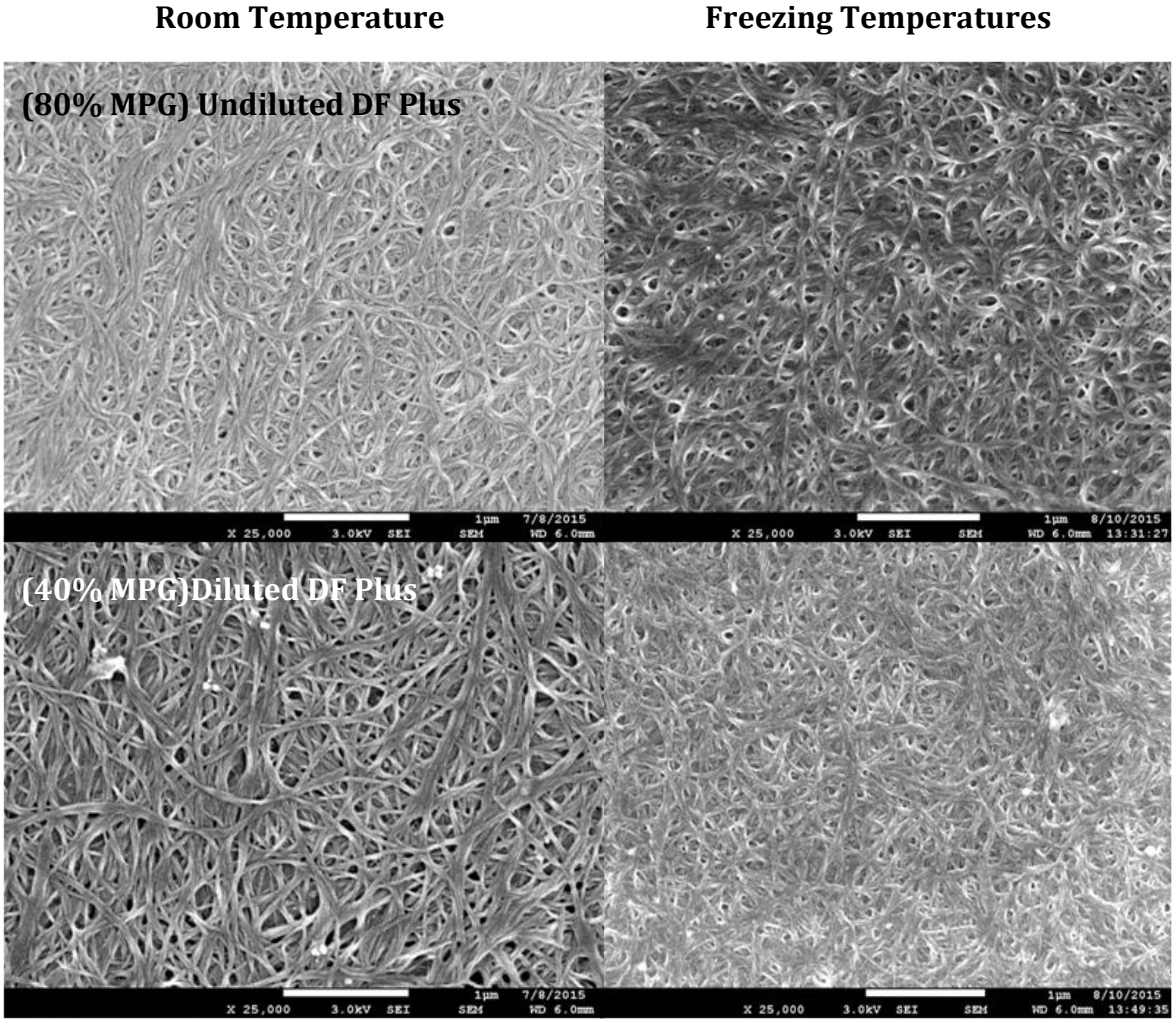

Figure 5.18 SEM analysis of DBS-OCH_3 in DF Plus (80% MPG) at room temperature (Top left) and freezing temperatures (Top right) as well as and DBS-OCH_3 in diluted DF Plus (40% MPG) at room temperature (Bottom left) and freezing temperatures (Bottom left).

DBS-OCH_3 unlike the other two gelators, Rika (DBS) and DBS-SCH_3 can form gels in DF Plus when it is diluted to contain 40% MPG. When imaged at room temperature (see **Figure 5.18**) DBS-OCH_3 appears to form similar sized fibres as when in undiluted DF Plus ca. 5-10 nm in diameter with large long fibre bundles being formed measuring between ca. 100-200 nm in diameter throughout the whole sample appearing as an entangled fibrous network. When imaged at freezing temperatures similar sized fibres appear to form however the presence of the longer fibre bundles is no longer evident and the smaller fibres are seen to create one overall fibrous network structure with smaller pores. This may suggest that low temperatures lead to rapid nucleation of a larger number of smaller fibres.

DBS-SCH_3 was imaged as the other gelators mentioned above. Only images at x 5000 magnification could be obtained and all other images at higher magnifications such as x 25000 magnification shown above for the other gelators appeared blurry with no defined structures being present.

When imaged at room temperature in DF Plus (80% MPG), DBS-SCH_3 was very difficult to image (see **Figure 5.19**). However, from the image it is evident that small fibres are present which are so entangled with one another it appears as if a meshed network is present underneath what appears to be large bundles of fibres measuring ca. 100-500 nm in diameter. The fact that the images appeared very unclear maybe due to the fact that the fibres are very solvated in the DF Plus de-icing fluid with such high MPG content and the solvent may not have been removed as much as was thought. When imaged at freezing temperatures again large fibre bundles could be observed in the centre of the image with what appears as a very dense tightly packed fibrous structure underneath. As well as this it is also evident that the crystalline structures are present as was observed when Rika (DBS) was imaged in DF Plus. Again it is unclear whether they actually form part of the fibrous gel network or are just present on the surface.

However when DBS-SCH_3 is imaged in diluted DF Plus containing only 48% MPG, different morphological nanostructures are formed (see **Figure 5.19**). At room temperature they appear to form long straight rigid flat tape-like structures measuring > 500 nm in diameter, but it is unclear where one fibre starts and ends therefore the individual fibres could be smaller in size and the size quoted above is more representative of the fibre bundles that are formed.

When imaged at freezing temperatures it appears that similar types of fibres are formed which are straight and rigid in nature with the same flat tape-like appearance however they appear much smaller ca. 100 nm in diameter. Fibre bundles of these flat fibres can be seen to form where the flat tape-like fibres stack one on top of the other, and span the whole sample creating one structure which appears less porous than what is produced for the other gelators. Therefore in this solvent system at low temperature we observe that the faster a gel forms the smaller the fibres, and the more slowly a gel forms the larger fibres form, which show distinctive flat tape-like structures. These structures were also evident when tested in MPG:water mixtures shown in Chapter 4, and indicate that nanofibres nucleation is controlled by temperature for this system.

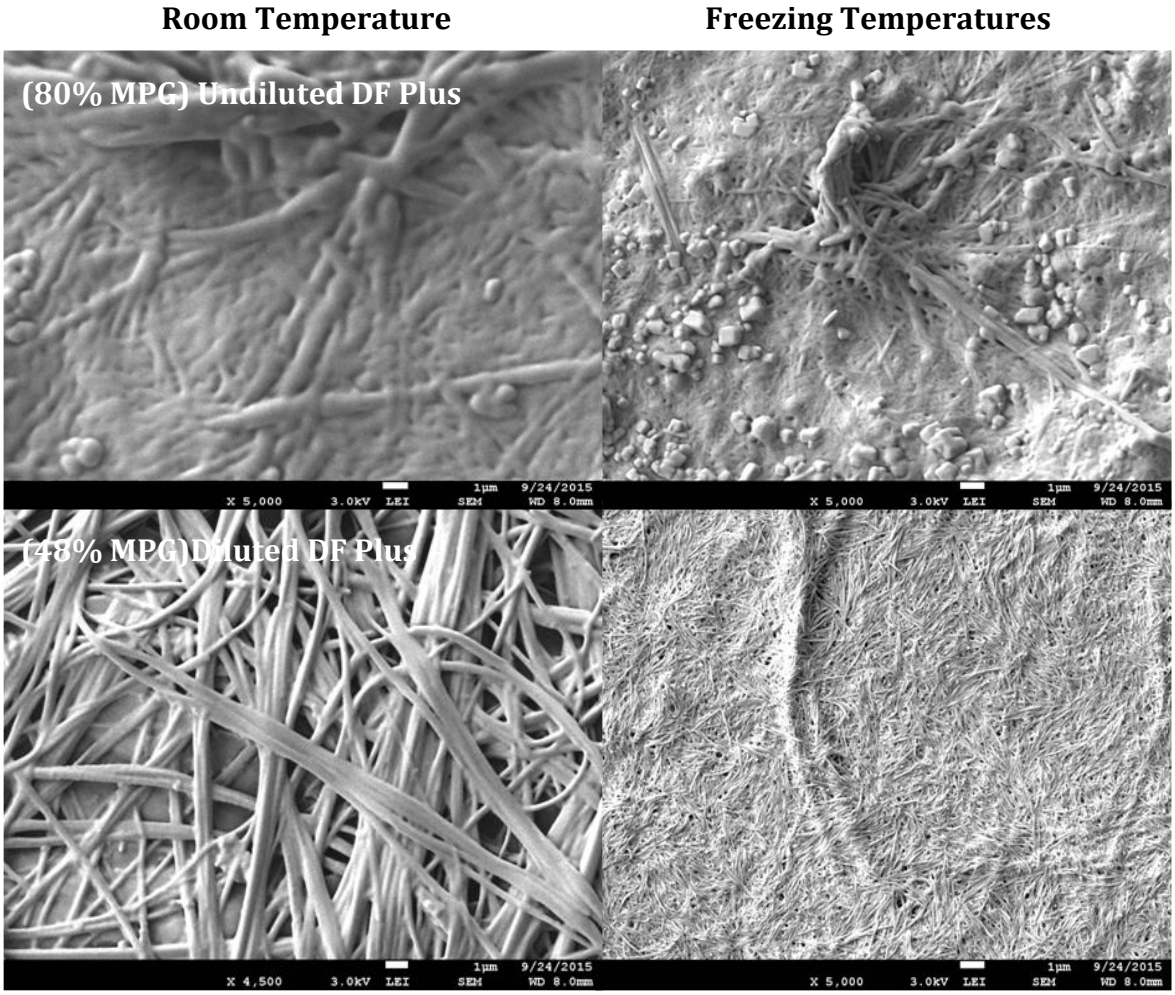

Figure 5.19 SEM analysis of DBS-SCH_3 in DF Plus (80% MPG) at room temperature (Top left) and at freezing temperatures (Top right) as well as DBS-SCH_3 in diluted DF Plus (48% MPG) at room temperature (Bottom left) and freezing temperatures (Bottom right).

SEM analysis of these molecules showed us that all three molecules create similar types of fibrous gel networks. Each of the gelators forms long straight or helical fibrous nanostructures, with the exception of DBS-SCH_3 when in diluted DF Plus, which formed flat tape-like fibres which were more crystalline in nature if the sample was cooled slowly. Rika (DBS) at both temperatures and DBS-SCH_3 at room temperature also showed signs of crystallisation with differing structures being present on the surface of the gel network. However, no evidence of these crystalline structures was found in the DBS-OCH_3 samples.

There was no obvious evidence from the images obtained by SEM that would help us identify why gels formed in undiluted DF Plus compared to diluted DF Plus have greater G' values with the same strengths as found through rheology, other than the

importance of the solvent composition for each of these gelators to form interactions with one another to create stiff strong networks.

To obtain a better insight to how these gelator molecules would form gels on an aircraft wing, where they are applied at hot temperatures to freezing surfaces we next conducted the water spray endurance test (WSET). This is an industry standard test method that is conducted on every de-icing and anti-icing fluid to determine how long a fluid can protect an aircraft from frozen contamination experienced in winter conditions known industrially as the holdover time (HOT).

5.2.7 Water Spray Endurance Test (WSET)

For a fluid to be used as a de-icing fluid or anti-icing fluid it must pass certain specifications set by the SAE.[33,382,385] One of these specifications involves the water spray endurance test (WSET). The water spray endurance test is a laboratory-based test developed to evaluate the holdover performance of de-icing and anti-icing fluids under differing weather conditions.[4,37,61] This test determines the length of time an aircraft has between application of a de/anti-icing fluid to taxiing and take-off before reapplication is required due to further ice contamination.

The standard WSET test is defined in AS5901[382,385] and SAE AMS1428.[33] This test is performed within a temperature-controlled climatic chamber where the air temperature is controlled at -5°C. Within this chamber an aluminium frosticator plate (**Figure 5.20**), representative of an aircrafts leading edge on a wing is set to -5°C and tilted at an angle of 10°. The frosticator plate consists of 6 test panels; four panels are used for test samples whilst the two outer most panels are used as controls. A motor is suspended above the frosticator plate which holds a spray nozzle. This nozzle travels back and forth across the frosticator plate spraying a fine mist of water (see **Figure 5.20** for the setup of the instrument) which upon freezing produces 5±0.2 $gdm^{-2}h$ of ice also known as the “catch”. This is designed to replicate typical freezing conditions.

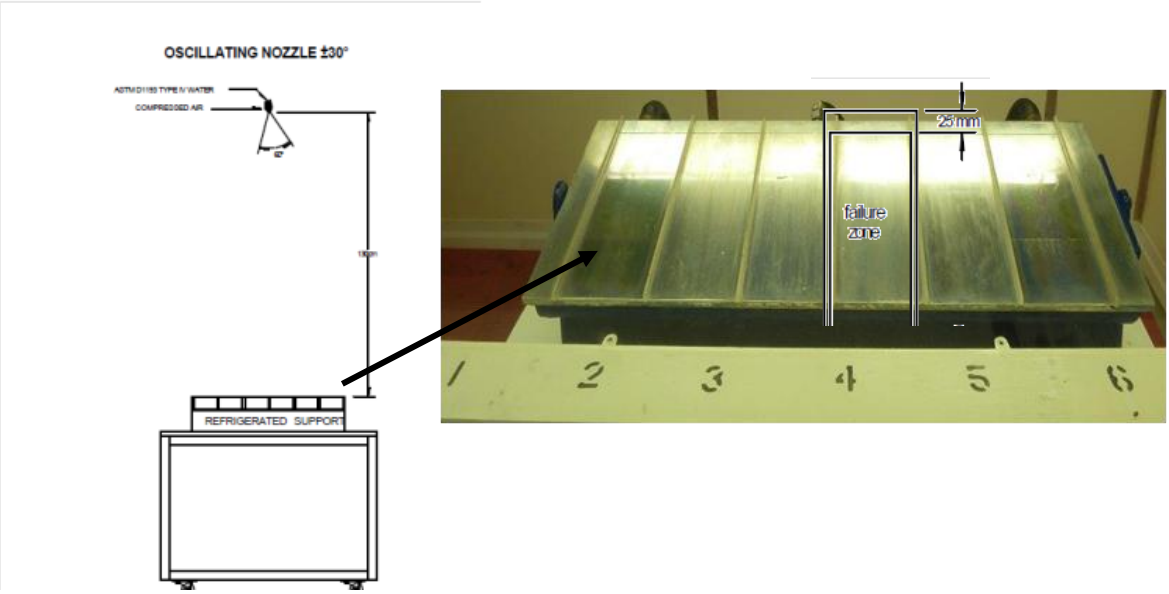

Figure 5.20 Left: Instrumental setup of WSET as set out in SAE guidelines. Right: the actual frosticator plate representative of an aircraft wing with the test and failure zones highlighted that is used for WSET.

To ensure the instrument is producing the correct "catch", square aluminium plates are placed onto the top edge of the control panels of the frosticator which are weighed before and after the completion of each test and run alongside each sample tested. Application of each sample to each test panel is achieved by pouring across the top of the panel in a backwards and forwards motion ensuring the top of the panel (leading edge) is fully covered. Gravitational forces cause the fluid to run down the inclined panels which decreases the thickness of the de/anti-icing fluid. The fluid is the thinnest at the top of the panel and thicker at the bottom. Consequently ice formation initiates at the top of the panels edge and progressively moves downward. The WSET time correlates to the time taken for the ice front to reach a distance of 2.5 cm from the top of the plate also known as the test zone for each of the samples. As soon as the first shard of ice touches this line the time is recorded and is used to calculate the holdover time (HOT) for each sample relative to the catch.

This industry standard test method normally applies samples that are at room temperature to the instrument set at -5°C,[33,382] however because each of the gels formed by the inclusion of gelators into DF Plus and dilutions of DF Plus are solid gels at room temperature and hence cannot be poured, each of the samples were placed into an oil bath set to 95°C to form the solution phase until applied onto the instrument for testing. To ensure accurate comparisons could be made between the original de-icing product (DF Plus) and its dilutions to samples including the gelator

molecules the original de-icing product was also prepared with the same dilutions and placed into the oil bath at 95°C. For a de-icing fluid to be effective the SAE ASTM1424[32] and SAE ASTM1428[33] state that a de-icing fluid must be able to sustain a holdover time (HOT) of 3 minutes regardless of the dilution. De-icing fluids are used depending on the outside air temperature (OAT) and always used diluted. Therefore the particular dilution used by a customer will be based on the OAT and freeze point that they require. A Type I de-icing fluid will also never be used in its undiluted state, as MPG is known to thicken at low temperatures, and AEA guidelines recommend that dilutions do not exceed 69% (~55% MPG) DF Plus in order to not affect the aerodynamics of the aircraft. Dilutions as low as 10% DF Plus (8% MPG) have been known to be used but for this to be possible the OAT must be sufficiently high enough. As well as very high dilutions of MPG being used as de-icing fluids, in some cases water on its own is also used. However this can only be conducted safely if the temperature is high enough to prevent the water from freezing on the wing.

Table 5.7 Holdover times for Type I DF Plus and DF Plus dilutions (**X** = no holdover recorded as sample froze on application).

% MPG in DF Plus	Holdover Time (mins:sec)	Type I Pass/Fail
80	7.07±0.16	Pass
72	6.35±0.16	Pass
64	6.13±0.13	Pass
56	5.51±0.13	Pass
48	5.41±0.13	Pass
40	4.37±0.10	Pass
32	3.15±0.07	Pass
24	2.13±0.05	Fail
16	0.36±0.01	Fail
8	**X**	Fail

From **Table 5.7** we can see that when DF Plus is tested using the WSET each of the holdover values for a de-icing fluid is based on the composition of MPG and water that is present. Upon dilution of DF Plus the holdover reduces, and at 24% MPG the fluid can no longer act as a de-icer as the holdover does not meet the minimum requirement of 3 minutes.[32] At 8% MPG the sample froze before the test started and no holdover time could be determined.

Previous gelation screening and rheological testing means we know that when gelators are incorporated into DF Plus and its dilutions it forms thickened gels. As de-icing fluids are not thickened we therefore also have to consider a comparison with

anti-icing fluids known as Type II, III and Type IV fluids which are thickened fluids containing polymeric gels. As anti-icing fluids are thickened they are required to meet higher holdover protection times compared to de-icing fluids which are stated in SAE AMS1428[33] and shown in **Table 5.8.**

Table 5.8 Minimum WSET holdover times as specified by the SAE.

Dilution	**Minimum WSET Holdover Time (minutes)**		
	Type II	*Type III*	*Type IV*
100%	30	20	80
75%	20	Report	20
50%	5	Report	5

Each of the gelator molecules in DF Plus and dilutions of DF Plus were tested at high (1% w/v), medium (0.5% w/v) and low (0.1% w/v) concentrations. Only samples that formed cleared gels as demonstrated in **Section 5.2.4** when the samples were scaled up were used. Using **Table 5.7** as a control of DF Plus, we can see from **Table 5.9** when Rika (DBS) is incorporated into DF Plus at the various dilutions, the ability of Rika (DBS) to provide holdover protection improves greatly at high and medium (1% and 0.5%) concentrations. With 1% Rika (DBS) loading the holdover time increases to more than 3 times the value of the standard DF Plus and continues to increase as DF Plus becomes more dilute. This effect is also evident at 0.5% and 0.1% concentrations. At 0.1% w/v we can also see the effect water has on the gel network. From 80% MPG to 56% MPG the gelator's ability to provide holdover protection increases as the gel network becomes more effective, but after this starts to slowly decline as the lack of glycol begins to become problematic.

Table 5.9 Holdover times achieved for Rika (DBS) at high, medium and low concentrations in DF Plus and aqueous dilutions of DF Plus.

% MPG in DF Plus	**Holdover Time (mins:sec)**		
	1% w/v	**0.5% w/v**	**0.1% w/v**
80	22.57±0.52	14.49±0.35	7.21±0.17
72	25.46±0.54	15.53±0.37	8.35±0.20
64	38.24±1.28	16.46±0.39	9.05±0.20
56	X	22.38±0.53	9.49±0.23
48	X	27.32±1.04	7.59±0.17
40	X	X	6.55±0.16
32	X	X	5.18±0.13
24	X	X	3.23±0.08
16	X	X	X
8	X	X	X

DBS-OCH_3 in DF Plus also provides an increase in holdover protection through the use of the gel networks formed inside the de-icing product (**Table 5.10**). DBS-OCH_3 produces more than 4 times more holdover protection compared to the DF Plus standard in its undiluted form but also continues to improve with increased dilution with water. At 0.5% w/v the same effects as shown with Rika (DBS) is evident for DBS-OCH_3, as the dilution increases the holdover increases to 48% MPG. For DBS-OCH_3, the increased solubility compared to DBS allows us to also operate at 40% MPG, but the holdover then is seen to reduce with increasing water. The effects seen with DBS-OCH_3 at 0.1% w/v are the same as those seen for Rika (DBS).

Table 5.10 Holdover times achieved for DBS-OCH_3 at high, medium and low concentrations in DF Plus and diluted DF Plus.

% MPG in DF Plus	Holdover Time (mins:sec)		
	1% w/v	0.5% w/v	0.1% w/v
80	31.50±1.14	13.06±0.30	4.50±0.11
72	33.54±1.19	13.28±0.31	6.59±0.16
64	46.41±1.47	15.53±0.37	7.52±0.18
56	X	18.56±0.44	8.11±0.19
48	X	25.07±0.58	7.34±0.18
40	X	23.49±0.56	6.44±0.16
32	X	X	4.55±0.11
24	X	X	3.08±0.07
16	X	X	X
8	X	X	X

DBS-SCH_3, as shown previously, has reduced solubility at higher concentrations than the other two gelator molecules and as such only samples containing 0.1% w/v concentrations were tested. DBS-SCH_3 has the capability of providing holdover times which are twice the values of undiluted DF Plus. Like the other molecules, it shows the same holdover behaviour, see **Table 5.11**. As the water increases in the solvent mixture the holdover increases up to 56% MPG, whereafter the holdover reduces and acts similarly to the original DF Plus de-icing fluid with holdover reducing relative to the MPG water mixture. It is noteworthy that at 0.1% w/v loading DBS-SCH_3 significantly outperforms Rika (DBS) and DBS-OCH_3.

Table 5.11 Holdover times achieved for DBS-SCH_3 at 0.1% w/v in DF Plus and dilutions of DF Plus.

% MPG in DF Plus	Holdover Time (mins:secs)
	0.1% w/v
80	12.02±0.28
72	14.20±0.33
64	18.26±0.43
56	19.03±0.44
48	18.11±0.42
40	X
32	X
24	X
16	X
8	x

Comparing all of the gelators together at 0.1% w/v, **Figure 5.21**, we see that there is a clear distinct pattern which each of the gelators follow. Generally as the % MPG reduces the holdover increases down to 56% MPG, thereafter the holdover decreases, similar to the behaviour of the DF Plus control.

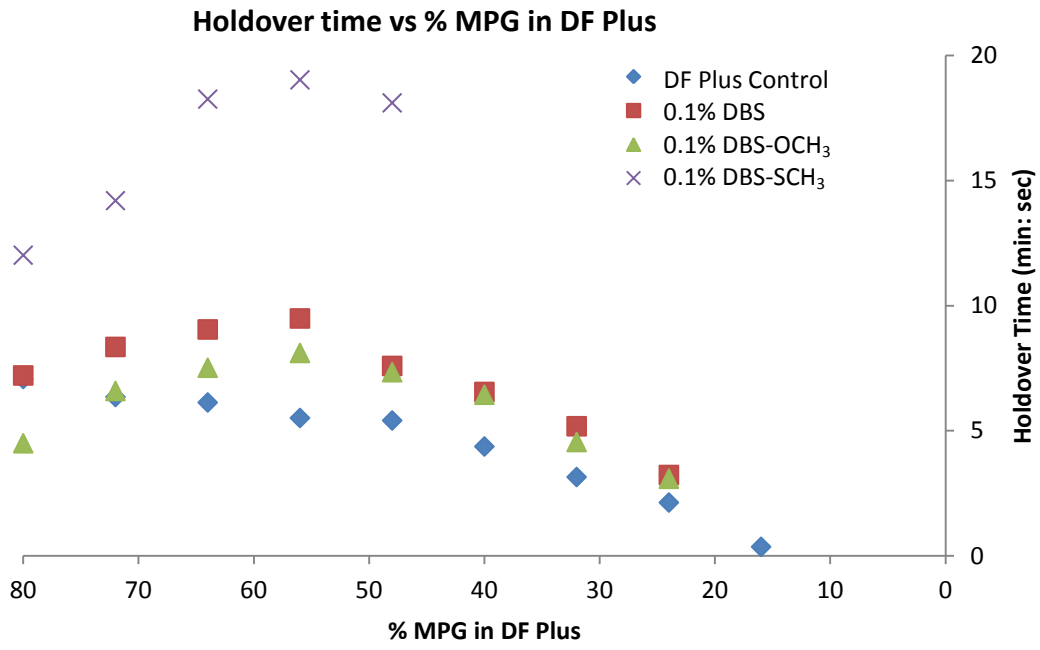

Figure 5.21 Comparison of Holdover times achieved for DF Plus control, Rika (DBS), DBS-OCH_3 and DBS-SCH_3 at 0.1% w/v in the varying dilutions of DF Plus (% MPG).

For each of the gelators, it is evident they possess the ability to change the holdover behaviour of a de-icing fluid to that more like a thickened anti-icing fluid, whereby the minimum holdover time of 3 minutes is more than exceeded. Each of the gelators

show the same behaviour when tested with holdover increasing as the samples become more dilute. As concentration is reduced and gels are formed at increased dilutions with water it becomes evident that there is a pivotal point where the holdover capability of each of the samples reverses and reduces, most commonly when the samples are diluted to contain 48% MPG and lower. Although we noted from rheology that the stiffest gels for each of the gelator molecules most commonly contained 80-64% MPG and therefore thought that this might be related to the length of holdover each gel may provide, we can see that this is not the case. This is most likely because the conditions are very different compared to what was tested on the rheometer. Unlike de-icing fluids where we see the holdover reduce as the MPG is reduced, this is reversed when gelators are incorporated and samples containing lower amounts of glycol are seen to protect for longer, a result of hydrophobic interactions which underpin the gel network found on the model aircraft wing.

Within the WSET due to water being constantly sprayed onto the gels this potentially allows for the gelator molecules in the various dilutions to further interact as the water increases and dilutes the film layer. As we know these types of gelators interact through hydrophobic interactions, therefore the increased water creates a more hydrophobic environment which would encourage more gelator-gelator interactions to produce a gel layer which increases in strength and hence is able to protect for longer. However there is a point at which the gel network becomes saturated with regard to solvent dilution and loses its effect. Thereafter the product acts as the normal de-icing product and the holdover times are based simply on the ratio of MPG and water present.

From all of the samples tested we can note that at all concentrations and dilutions tested, we have improved the performance of the Type I de-icing fluid, DF Plus. However, for these samples to act as an anti-icing fluid like that of a Type II, III or IV fluid it must have much higher holdover protection times, see **Table 5.8**. Therefore from the holdover times achieved from each molecule at 1% w/v we can see that from the required limits that these samples could potentially act as Type II or Type III fluids when diluted. However, at concentrations of 0.5% w/v these gels made from Rika (DBS) and DBS-OCH_3 could only be classified as Type III fluids upon dilution. At 0.1% w/v although the differences in holdover time produced by Rika (DBS) and DBS-OCH_3 were similar compared to the original de-icing product they could not be classified as an anti-icing fluid. However, DBS-SCH_3 at 0.1% w/v could potentially act

as a Type III, anti-icing fluid whereby holdover of almost 20 minutes could be produced. Although these gelators could potentially be used as anti-icing fluids their use would be limited to specific solvent dilutions and MPG content.

5.2.8 Aerodynamics

The second important specification that each de-icing and anti-icing fluid must meet specified by the SAE is an aerodynamic acceptability test. The aerodynamic acceptance of an anti-icing fluid is based on its ability to flow from the surface of an aircraft during takeoff acceleration to leave an acceptable thickness of wet film, known as the Boundary Layer Displacement Thickness (BLDT).[385] Normally as the temperature drops the viscosity of an anti-icing or thickened fluid will increase. An increase in viscosity can have a deleterious effect on the aerodynamics and the ability of the fluid to be sheared from an aircraft during acceleration. This can also limit the lowest operational temperature of a fluid (LOUT).

There are two separate aerodynamic tests. One for fast large transport jet aircraft which have takeoff rotation speeds of 100 to 110 knots and acceleration times of 23 seconds, and one for slower aircraft whose takeoff rotation speeds exceed 60 knots with acceleration times of 16 seconds.

Both of these tests are carried out in the laboratory using a temperature controlled wind tunnel according to AS5900[385] and SAE AMS 1428.[33,61] The climatic chamber is temperature controlled and can allow fluids to be tested as low as -40°C. Fluids are tested by pouring a sample of a fluid onto a perspex surface which is then spread out to a thickness of 1.5 mm, see **Figure 5.22**. The fluid is left to reach temperature for 5 minutes before a fan is started which represents the shear experienced by a fluid when the acceleration is started during takeoff of fast and slower rotational speed aircraft. The thickness of the wet film remaining on the surface is calculated and identified to how it affects the aerodynamics.

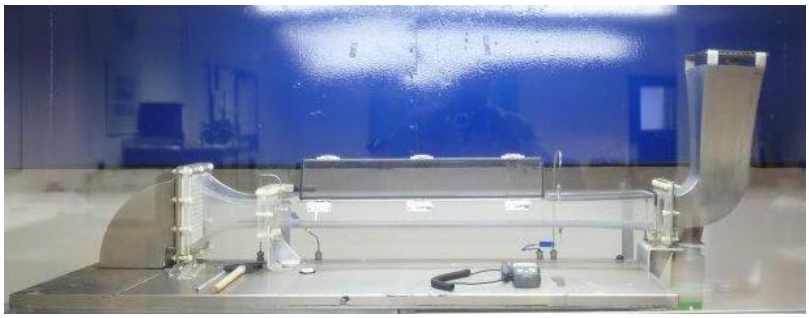

Figure 5.22 BLDT instrumentation located within a temperature controlled wind tunnel.

Unfortunately due to the nature of the gels formed within the de-icing fluid, DF Plus, this test could not be performed. Normally samples tested using this instrument are applied at room temperature but because the gels produced with gelators are solid at room temperature they cannot be poured and or spread evenly. Samples also cannot be applied hot as it affects the shape of the Perspex box and there are currently no standards that apply to testing aerodynamics at elevated temperatures. However we have tried to demonstrate the breakdown of these gels by similar means on the rheometer. The AS9000 standard states that for an anti-icing fluid to be used effectively and not affect the aerodynamics of an aircraft it must be able to demonstrate that the fluid can be broken down by 74% of its original viscosity value.

Using this as a means to determine if gels formed in DF Plus and its dilutions with gelators can be broken down and removed effectively we have performed oscillatory time sweeps. Three time sweeps within the same test have been carried out where each sample is applied to the rheometer plate as a hot solution above its T_{gel} value and allowed to set on the rheometer plate to form the gel. The first time sweep is performed using a strain value within the LVR to ensure the structure is not damaged and the stiffness of the original gel determined. Within the second step increasing strains outside of the LVR are applied similar to what would be experienced during take-off, and finally the third step allows us to determine if these gels would rebuild by again applying a low strain value as in step one which is in the LVR over a longer period of time.

From **Figure 5.23** and **Table 5.12** we can see an example of 0.5% Rika (DBS) in 80% MPG at increasing strain values of 10, 50 and 100% compared to DF Plus which has no gel structure. From **Figure 5.23** it is clear that although these gelator networks that are formed have very large G' values and hence are very stiff with only 10% strain applied, the structure can be broken down completely, where it is seen to only

leave 0.53% of the original fluid behind and this consequently increases as strain increases. This was also evident for DBS-OCH_3. However, what is noted is that upon removal of the increasing strain values the gel networks slowly rebuild and have thixotropic behaviour

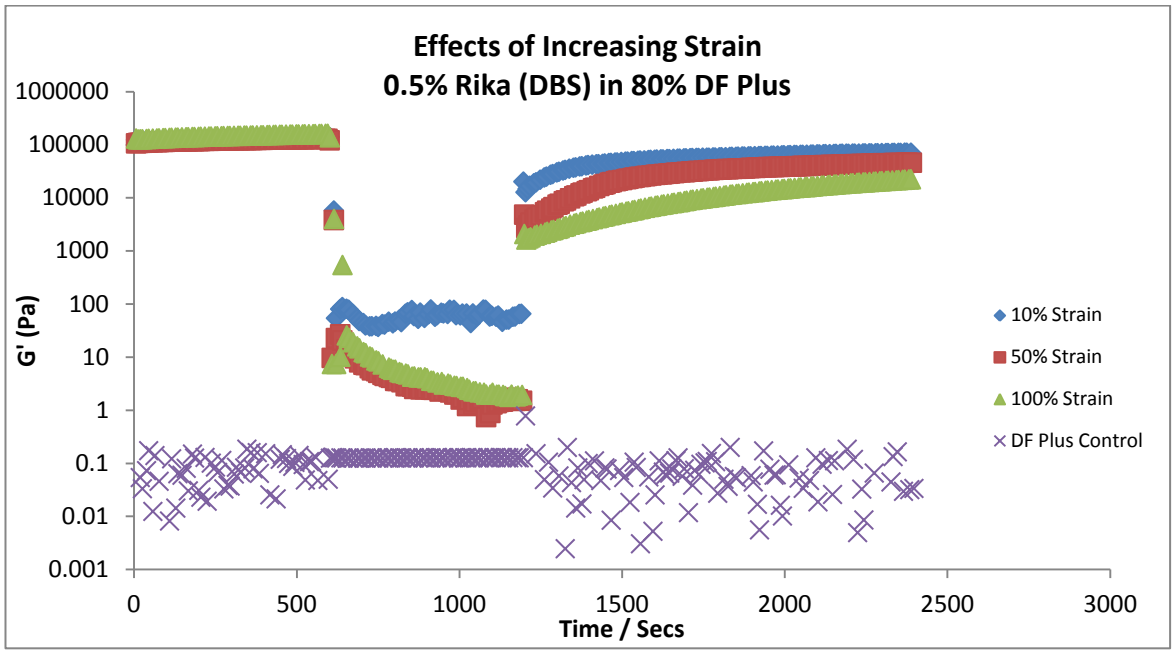

Figure 5.23 Effects of increasing strain on the gel structure of 0.5% w/v Rika (DBS) in 80% MPG DF Plus to simulate aerodynamic effects.

Table 5.12 Percentage of fluid remaining after increasing strain on 0.5% w/v Rika (DBS) and DBS-OCH_3 in 80% MPG DF Plus.

% Strain	% of Fluid remaining after Increasing Strain	
	Rika (DBS)	***DBS-OCH_3***
10	0.53	1.19
50	0.15	0.15
100	0.09	0.01

From **Table 5.13** we can see that when only small strains of 10% are applied to each of the Rika (DBS) and DBS-OCH_3 networks the gel can recover between 40-60% of its original stiffness. However the greater the strain applied the more difficult it becomes for the gel structure to recover. Therefore these gel structures are very weak and shear rates experienced at take off are most similar to what the gel experiences when 100% strain is applied. As the gel structure has shown to be thixotropic this may potentially be a problem should the gel not be fully removed at the point of take off. Due to the thixotropic nature of the gels they could rebuild once airborne and continue to build up in aerodynamic quiet areas which may affect the aircrafts ability to land safely.

Table 5.13 Percentage recovery of gel networks of 0.5% w/v Rika (DBS) and DBS-OCH_3 on increasing strain.

% Strain	% Recovery of Gel Network compared to original G' value	
	Rika (DBS)	***DBS-OCH₃***
10	42	59
50	25	49
100	7	14

When we tested DBS-SCH_3 at 0.1% w/v in 80% MPG (**Figure 5.24),** this gelator shows the same behaviour as the two shown above. Almost all of the gel structure was broken down (0.18-1.3% remaining). However like the other molecules even at lower concentrations than tested for Rika (DBS) and DBS-OCH_3 we can see that the gel has thixotropic behaviour upon removal of the increased strain. DBS-SCH_3 regains ~80% of its original structure even at very high strains see **Table 5.14**.

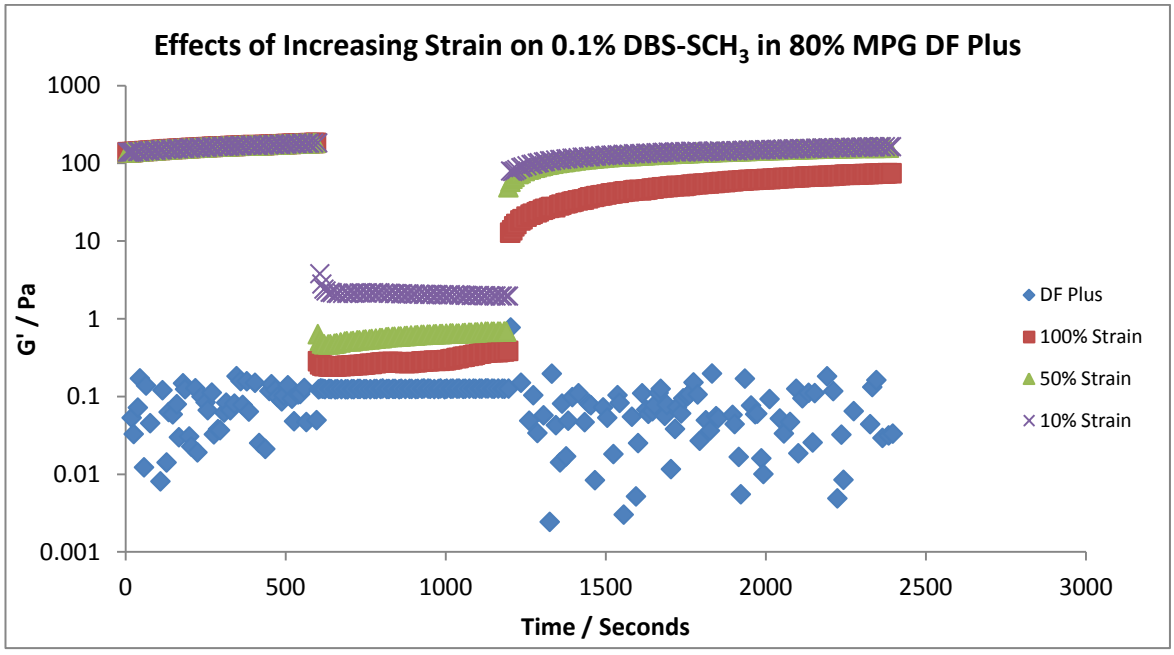

Figure 5.24 Effects of increasing strain representative of aerodynamic effects of an aircraft on 0.1% w/v DBS-SCH_3 in 80% MPG DF Plus.

Table 5.14 Effects of increasing strain on 0.1% w/v DBS-SCH_3 in 80% MPG DF Plus.

% Strain	% of Fluid remaining after Increasing Strain	% Recovery of Gel Network compared to original G' value
	DBS-SCH₃	***DBS-SCH₃***
10	0.18	31
50	0.17	80
100	1.3	84

Each of the gelator molecules forms very stiff gel structures which become weak upon application of increasing strain representative of the shear rates that an aircraft would experience during takeoff. The weak non-covalent interactions that form the gel structure, allow the structures to be broken down easily. However, these systems show to possess thixotropic behaviour upon the removal of high strain, this potentially can lead to the obstruction and build up of the gel structures in aerodynamic quiet areas preventing an aircraft from operating effectively if all of the gel network is not removed upon take-off.

5.3 Conclusions

Within this chapter we have demonstrated the potential of the three most successful gelators Rika (DBS) DBS-OCH_3 and DBS-SCH_3 highlighted in the previous chapters, ability to not only form gels in MPG water mixtures, but to have the ability to form gels within complex fluids such as de-icing fluids which are available commercially.

The gelation ability of each of the molecules was tested and demonstrated that gels could be formed at high (1% w/v) medium (0.5% w/v) and low (0.1% w/v) concentrations for Rika (DBS) and DBS-OCH_3, with gels formed being dependent on the solvent mixture. The number of gels that could be formed for each of the molecules increased as a result of decreasing concentration. As the solvent mixture (de-icing fluid) became more dilute gels could be seen to form as low as 48% MPG at 0.5% w/v for Rika (DBS) and 40% MPG for 0.5% w/v for DBS-OCH_3. DBS-OCH_3 had slightly better solubility due to the OCH_3 substituent on the benzene ring making the structure more hydrophilic. DBS-SCH_3 however struggled to form gels at high and medium concentrations like the other molecules, and could only form gels at low concentrations down to 48% MPG content. As a result of the gelation ability of each of the gelators these can be thought of alternative thickeners which like polymers found in anti-icing fluids may give rise to additional properties which could protect an aircraft in winter.

The thermal stability of each of the gelators were tested which demonstrated that the self assembly of these types of molecules is primarily driven through hydrophobic effects whereby the thermal stability of each of the molecules increased as the ratio of water increased, with 48%MPG being the most thermally stable for Rika (DBS) and DBS-SCH_3, whilst 40% MPG was the most thermally stable gel produced from DBS-OCH_3.

We have also demonstrated the possibility of using these gelators within a de-icing product on a larger scale. Although the results are comparable on larger scale it was noted that some samples especially the more dilute samples e.g. 48-40% MPG required longer heating times to produce the same clear gels that was noted when tested on a smaller scale. This demonstrates the fact that care needs to be taken to understand not only experiments on small scale but also large scale, should one of these gelators become industrially-relevant for manufacture in the future.

Rheological testing indicated that regardless of solvent, gels of Rika (DBS) and DBS-OCH_3 have similar strengths. Solvent affected the stiffness of the gels produced, with samples containing 80-72% MPG producing the stiffest gels and samples containing 48% MPG the least stiff gels. However unlike the other gelators DBS-SCH_3 showed a different behaviour, with strengths almost double that of the other two molecules. The stiffness of the gels produced was also solvent dependent, however with this molecule, as the de-icing fluid became more dilute, the gel became stiffer up to 56% MPG whereafter, it is seen to reduce. DBS-SCH_3 samples were tested at much lower concentrations (0.1%) than Rika and DBS-OCH_3 and this explains the lower G' values, (less gel network). As a result of this lower concentration, it has shown greater capacity to assemble with better solubility. However, due to its better capacity to assemble it forms gels which are more resistant to strain than the other gel systems. Each of the gels produced using DF Plus has greater strengths than when just in MPG:water mixtures as tested in Chapter 4 with values similar to the lower end of the strengths expected for anti-icing fluids. This may be down to the additional additives that are incorporated into the finished de-icing product creating a gel which potentially interacts further with the gelators to give a stronger structure. Each of the gels produced in DF Plus and its dilutions acted as gels where G' > G'' and were independent of frequency. However, both DBS-OCH_3 and DBS-SCH_3 became frequency dependent at frequencies greater than 5 Hz acting as visco-elastic solids.

Rheology allowed us to determine what temperatures are required for each of the gels in the various de-icing fluid dilutions to be formed as well as disassembled. Like the thermal stability studies conducted through the use of the tube inversion test rheology shows the same behaviour. As the water increased in each dilution the temperature required to breakdown the gel increases. Gels with the most water content also formed at higher temperatures than gels containing higher MPG contents. Rheology also demonstrated that these gelators in DF Plus de-icing fluid can form gels relatively quickly. Gels were seen to form as quickly as 4 minutes when the fluid is most dilute, and in 7-14 minutes with higher MPG (72%) content. Therefore this potentially allows for the use of each of these gelators in a de-icing fluid such as DF Plus to be sprayed at temperatures between

40-90°C which will then set up very quickly when applied to cold surfaces to provide a gel film which will potentially protect an aircraft in winter conditions.

SEM analysis of each of the differing gelators in DF Plus was performed under different sample preparation conditions which emulate how the gels would potentially form when used within the de-icing application. Each of the gelators in the undiluted de-icing product either formed very similar straight or helical fibres which entangle with one another forming a 3D gel network with similar structures being observed at room temperature in the differing dilutions. At lower temperatures the gel networks for each of the gelators are seen to be more densely packed. In previous chapters it has been shown that as the samples incorporate more water and hence create a more hydrophobic environment, the self assembly of these gels produce smaller fibres which create more expansive networks. Also within the SEM images it is evident there are signs of crystalline structures on the surface of the gel networks for both Rika (DBS) and DBS-SCH_3 which may be a result of the additional additives within the de-icing fluid, however it is unclear whether these are part of the gel network or separate and exist on top of the gel structure. DBS-SCH_3, as was also shown in Chapter 4, creates different nanostructures when in dilute solvent mixtures which are more crystalline in nature. Unlike the other gelators, this molecule forms straight, rigid flat tape-like structures. Therefore should these gelators be applied to an aircraft wing within a de-icing fluid it would potentially form a denser gel network which is less porous at freezing conditions. These morphologies were also different depending on whether they were formed by rapid cooling or not.

To understand the industrial relevance of these gels formed within the de-icing fluids we conducted WSET and similar BLDT aerodynamic industrials test methods. WSET testing showed us that unlike a de-icing fluid, which is primarily made up of MPG and water, and has a minimum holdover of 3 minutes, is determined by the ratio of MPG water. When we add each of the gelators to a de-icing fluid they act as alternative thickeners similar to the behaviour expected of an anti-icing fluid. At high concentrations Rika (DBS) and DBS-OCH_3 have the same holdover capability as that required for a Type II or Type III anti-icing fluid with holdover values of 20-45 minutes. With the addition of gelator, the holdover ability increases as the water ratio within the solvent mixture increases. At lower concentrations of 0.5% w/v the holdover again is also increased from that of a de-icing fluid but is only comparable to an anti-icing fluid upon high dilutions with water. At low concentrations all three

gelators show the same behaviour, as water increases the holdover increases, this is primarily due to the nature of the self assembly mechanism of these types of gelator through hydrophobic effects. DBS-SCH_3 at low concentrations compared to the other gelators has the potential to form similarly to a Type III fluid unlike the other gelators which marginally improve the holdover performance of the de-icing fluid However, what is also evident is that between 48-40% MPG the holdover behaviour reverses and declines similar to the behaviour of the original de-icing fluid. Solvent mixtures must therefore be carefully suited to these gelators to achieve maximum holdover protection. It is clear that holdover performance in the WSET tests is a combination of gel strength (increasing with dilution) and glycol content (decreasing with dilution).

Aerodynamically although these gelators produce very stiff gels with high G' values and are strong, they can be easily broken down exceeding the >74% removal of fluid from the surface to be aerodynamically accepted. However, these gels also exhibit thixotropic behaviour which is not ideal for this application due to the risk that the gel structure could rebuild with time in aerodynamically quiet areas where removal is less effective.

Therefore we have potentially created a new type of fluid that could be used as an anti-icing fluid for aircrafts. It has stiff structures with strengths that match current anti-icing fluids, they can be heated to high temperatures whilst not destroying the gel structure, provide high holdover times, depending on concentration and solvent and be easily removed preventing any aerodynamic effects.

The next steps within this study are to identify if these gelators that have been highlighted as potential alternative thickeners can be further used within existing anti-icing fluids such as Type II and Type IV anti-icing fluids, which contain polymeric thickeners and known by the brand names ABC 3, ABC K Plus and ABC S Plus and can in this way increase their properties further, and potentially increase their already long holdover times. The gelation ability, thermal stability, rheological profiles as well as their performance in the industrially relevant testing of holdover and aerodynamics will be determined to identify if potential hybrid gel networks between low molecular weight gelators and polymers can be used to create a new improved anti-icing fluid.

Chapter 6

Introduction of DBS into Type II and Type IV Anti-Icing Aviation Products - Hybrid Gel Systems

Chapter 6 Introduction of DBS into Type II and Type IV Anti-Icing Aviation Products

6.1 Introduction to Hybrid Gel Systems

Hybrid materials are a relatively new area of research which is gaining momentum very quickly in gel chemistry. Hybrid materials are normally made up of two or more components or networks and can be thought of as materials which have enhanced performance or ability. There are a number of different types of gel systems which combine polymeric and low-molecular-weight components out there which have been recently reviewed by Cornwell and Smith.[145] Within this review the authors categorised the different hybrid gels into five classifications including:

(i) Polymerisation of LMWG
(ii) Capture of LMWG fibres in a polymer matrix
(iii) Addition of a non-gelling polymer in solution to supramolecular gels
(iv) Directed interactions between LMWGs and polymers
(v) Hybrid gels combining low-molecular-weight and polymer gelators

We are focussing here on type (v) gels. Type (v) gels have only recently emerged in the literature. These hybrid gels combine polymers and LMWG both of which are capable of individually forming a self-supporting gel network. By combining a polymer gel with a LMWG it is thought that the properties of both of the gel networks can be combined to create multi-responsive smart gels. Cornwell et al have[143] demonstrated the creation of a hybrid gel by using 1,3:2,4-Dibenzylidene-D-sorbitol-p,p'-dicarboxylic acid (DBS-CO_2H) which is pH responsive with a polymer gel, agarose, which is thermally responsive. Using these two gels they created a gel which is responsive whereby the LMWG could be assembled and disassembled by changing the pH, whilst the agarose gel remained unchanged. Cornwell et al[144] also then demonstrated the ability of hybrid gels to form multi-domains within one material by photopatterning. By combining DBS-CO_2H (LMWG) with poly (ethylene glycol) dimethacrylate (PEGDM) which is photo-inducible they noted they could form the LMWG and then with additional photo-irradiation using a mask to target a specific area they could form a hybrid between the LMWG and polymer gel with the hybrid showing noticeable transparency and strength, with differences in diffusion being

noticeable in the different domains due to the interactions between both networks that create the hybrid gel regions, see **Figure 6.1**.

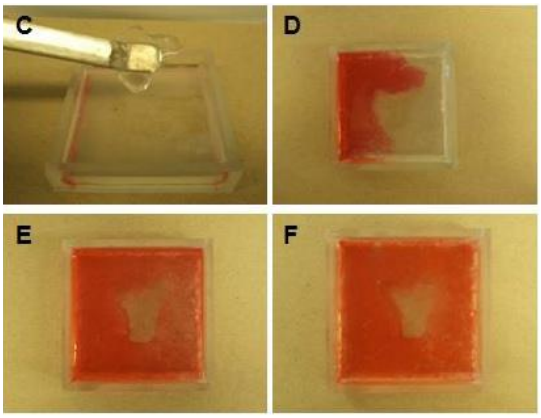

Figure 6.1 Hybrid hydrogel. Y shaped region is formed from both the polymer and LMWG gel networks whilst the remainder of the gel is only formed from the LMWG where diffusion of a dye can be seen to easily transfer through the gel but not enter the hybrid gel.[144]

Yang and co-workers have shown that hybrid hydrogels can be created whereby additional components can be incorporated. To show the potential in drug delivery they used congo red as a model drug.[386] Through investigation they showed that interactions between the model drug and the LMWG nanofibres were present and depending on the type of LMWG the rate of release of the model drug could be varied. In other research they managed to demonstrate that a similar hybrid could work the opposite way, where a dye molecule could be extracted from aqueous solutions[387] more efficiently when a hybrid gel was used compared to the individual gels on their own.

Cornwell *et al* have also made advancements towards different types of hybrid hydrogels formed through the use of two differing LMWG instead of a polymer gel. In their work they have demonstrated that this type of hybrid is also responsive like the polymer hybrid gels, depending on the trigger used for gel formation. They have demonstrated that these responsive hybrid hydrogels can in fact be photo-patterned (**Figure 6.2**) and hence may find uses in biomedical sciences.

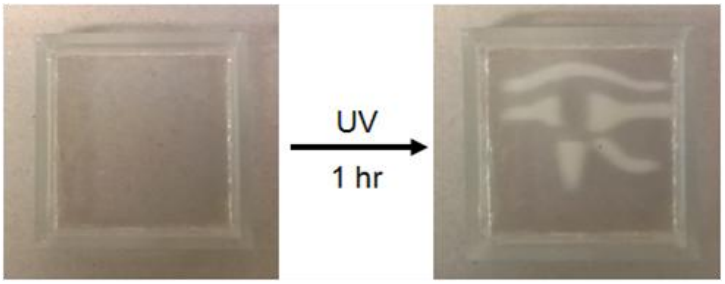

Figure 6.2 Photo-patterned multi-domain gels using two LMWG networks to form a hybrid gel.

Creating hybrid gels can ultimately allow for the creation of gels which have improved performance and enhanced properties when compared to the original gel networks on their own. Hybrid gels have been shown to impart greater gel strength, mechanical, thermal and temporal stability compared to simple gels.[117,150,172,388-390] As hybrid gels can be tuned, hence molecularly programmed they have potential use in a number of applications. Already we have seen from current research that hybrid gels are smart responsive multifunctional materials which can be used in dentistry,[303,391,392] controlled release and delivery of drugs,[386,387,393] to increase biological activity, as well as evolution and control over biological systems. With advancements underway it will be potentially possible to use such gels for tissue engineering,[394] disease modelling and drug release which will be more controlled and responsive with self healing properties.[143,144]

Considering DBS and its derivatives as low molecular weight gelators, we find this molecule already has prevalent use in industry as a hybrid gel where it is used within polymers as a nucleating and clarifying agent in plastics and thermoplastics.[395-398] Research predominantly focuses on the use of DBS and its derivatives in polyolefins such as polypropylene[395-401]/polyethylene glycol[402] etc as well as polydimethylsiloxanes[205,403,404] and block and graft co/terpolymers.[205,405-407] These polymers receive such a great deal of interest due to their use in everyday items such as foodstuff,[399] cosmetics containers,[399] children's toys, medical devices[400] and electrical components[398] see **Figure 6.3** for some examples.

Figure 6.3 Plastic items formed from using a clarifying / nucleating agent.

Their widespread use, allows customers to demand a certain quality, and in most cases this is clarity and transparency of the plastic/thermoplastic that is produced. However, because most of these polymers have a degree of crystallinity they ultimately produce hazy end products. The haze is thought to be produced as a result of the size and number of crystals that are formed, with larger crystals reducing clarity, an effect due to diffraction and scattering of light. Therefore to increase the clarity and optical transparency additives in the form of clarifying and nucleating agents have been added to polyolefin compositions.[404,408-412] DBS and its derivatives act as nucleating agents in these types of polymers by being dissolved in the molten form of the polymers and homogeneously dispersed throughout the polymer matrix. These melts can then be heated to high temperatures. Upon cooling, the DBS and/or its derivatives form a thermoreversible 3D network within the polymer, which results in the fast nucleation of the polymer to organise more uniform, small crystal growth which ultimately creates plastics which are optically transparent.[206,413-415] Using DBS and its derivatives as clarifying/nucleating agents provides improved mechanical strength and chemical resistance, increased resistance to shrinkage and heat deterioration as well as shorter processing times at lower temperatures providing an overall combination of reduced costs with increased performance[401,412,416-418] pleasing both the manufacturer and consumers.

Within this chapter we will attempt to create a hybrid gel between a polymer gel and a low molecular weight gelator, each on their own, can create self supporting networks. However, unlike the use of DBS and its derivatives in the plastics industry with bulk polymer samples, we will be incorporating Rika (DBS), DBS-OCH_3 and DBS-SCH_3 into a finished complex anti-icing product which contains only a very small concentration of polymer (0.2-0.4% w/v), a small concentration of each of the

gelators (<0.1% w/v) in a bulk solvent of glycol and water. The polymer within each of the three different types of anti-icing fluids that will be tested is based on polyacrylic acid (PAA), see **Figure 6.4**.

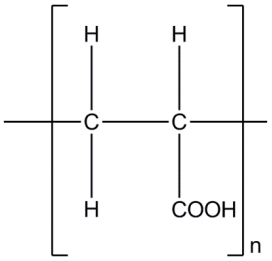

Figure 6.4 Generic structure of polymer used within each of the anti-icing fluids.

However, in general very little is actually known about the polymers within the anti-icing fluids due to the information being proprietary to the manufacturer. However, it is known that all three products contain a version of PAA. In ABC 3 the polymer has less cross-linking and more hydrophobic modification when compared to the other products. ABC S Plus polymer has the greatest amount of cross-linking between the polymer chains and has the least amount of hydrophobic modification. ABC K Plus polymer lies between the two extremes of the other products.

Therefore because we have both polymer and LMWG at similar concentrations but in a bulk solvent it is unknown whether a gel or a hybrid gel will be formed. However, from Chapter 5 we showed that these types of gelators could immobilise a de-icing fluid which is primarily just solvent similar to the bulk solvent within an anti-icing fluid. Therefore the gelator should, in principle gel the bulk solvent with the potential of further interactions being created between the polymer and LMWG networks to make a hybrid gel. Each of the gelators, in each of the different products, will be tested for the potential gelation ability, thermal stability and scalability before investigating each of the potential new hybrid gels for rheological performance to identify if these types of gels can further enhance or improve an anti-icing fluid. If successful, their industrial relevance in terms of their ability to provide holdover and effects incurred to the aerodynamics of an aircraft will be determined to identify their suitability in this type of application.

6.2 Results & Discussion

6.2.1 Gelation ability

Due to the successful gelation of the three gelators, Rika (DBS), DBS-OCH_3 and DBS-SCH_3 in de-icing fluids we wanted to identify if it was possible to form gels in an even more complex fluid; an anti-icing fluid. However, unlike de-icing fluids which have high MPG content (80%) anti-icing fluids have only 50% MPG in their finished product. As we have seen in Chapter 5 with the de-icing product, as the concentration of MPG is reduced the solubility of the gelator decreases. As well as low MPG concentrations anti-icing products also contain thickeners in the form of a polymer. Therefore we initially have to identify if the gelators can be directly incorporated into an anti-icing product or if a bottom up approach through formulation should be undertaken.

Each of the three gelators was screened in three different anti-icing products. Each of the anti-icing products was supplied by Kilfrost Ltd. Two of the anti-icing products classified as Type II anti-icing fluids, known by the brand names ABC 3, which is straw in colour and ABC K Plus which is yellow in colour as well as one Type IV anti-icing fluid, known by the brand name of ABC S Plus and is green in colour was used for testing. Anti-icing products are commonly used in their original undiluted form (100%), but can be diluted to 75% and 50%. Anti-icing fluids are not used below 50% dilutions in order to achieve the correct holdover and or freeze point protection. For screening purposes only the original product in its 100% undiluted form has been tested due to the low starting MPG content of 50% MPG. When anti-icing fluids are diluted to 75% and 50% the MPG content drops to 37.5% MPG and 25% MPG respectively, which could give rise to potential solubility issues as found in previous chapters.

Gels were prepared by weighing out a known amount of gelator into a 2 ml glass vial and 1 ml of solvent (anti-icing fluid) added. Each sample was sonicated for 30 minutes before being heated in an oil bath to below the boiling point of the water until a clear homogenous solution was formed. If after 1 hour a clear solution was not formed, the samples was removed from the heat and left on the bench to cool to room temperature overnight. Results were recorded the next day.

From **Figure 6.5** we can see that fortunately, by adding Rika (DBS) straight into the anti-icing products, clear homogenous gels can be formed. At high concentrations of

2% and 1% it was not possible to form gels and the gelator remained insoluble and showed to contain precipitate, but at lower concentrations of 0.5% to 0.1% clear gels could be formed. At very low concentrations of 0.05% w/v only partial gels in solution were formed, which collapsed upon inversion. Control samples of each product were tested and treated in the same way for comparison purposes and all remain clear viscous solutions.

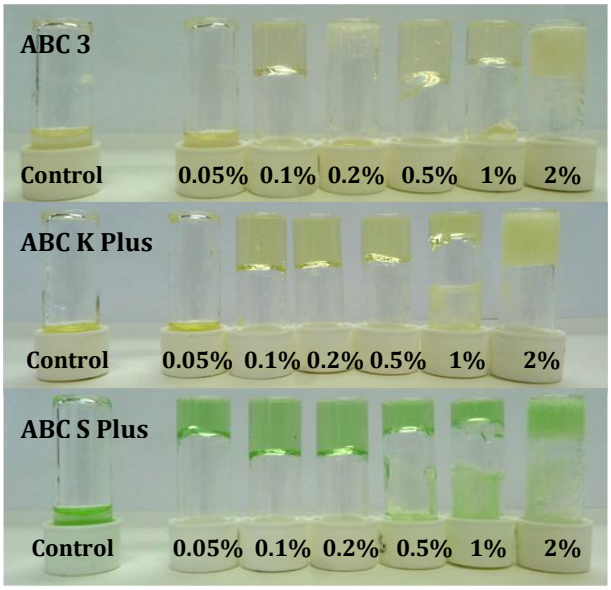

Figure 6.5 Gelation ability of Rika (DBS) in Type II (ABC 3 and ABC K Plus) and Type IV (ABC S Plus) anti-icing fluids.

DBS-OCH_3 was also screened in the three anti-icing products in the same way as Rika (DBS) above, excluding the higher concentration of 2% w/v, (**Figure 6.6)**. As with Rika (DBS) we can see that DBS-OCH_3 produces the same gelation results. At high concentrations the gelator remains insoluble and contains precipitate, with gels being formed between 0.5% and 0.1%w/v and partial gels in solution at lower concentrations of 0.05% w/v.

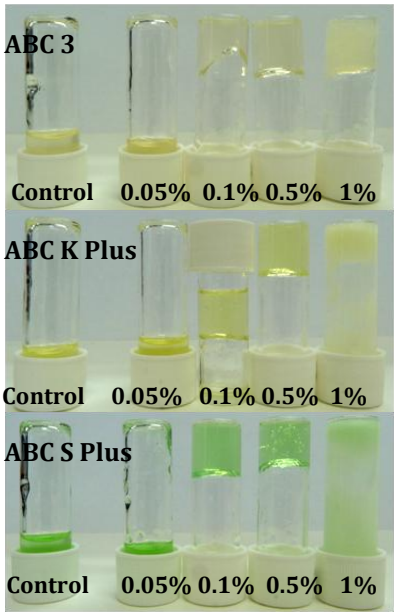

Figure 6.6 Gelation ability of DBS-OCH_3 in Type II (ABC 3 and ABC K Plus) and Type IV (ABC S Plus) anti-icing products.

Like the other two gelators, when DBS-SCH_3 was screened for its gelation ability in anti-icing fluids, (**Figure 6.7)** it was also incapable of forming gels at high (1% w/v) and medium concentrations of 0.5% w. However, clear gels were formed between 0.1% to 0.04% w/v (for ABC 3 and ABC K Plus these were weak gels and collapsed upon photographing) with partial gels being formed at much lower concentrations (0.025% w/v).

This molecule therefore has similar gelation behaviour to the other two molecules however can only form gels within a narrow, and lower concentration range.

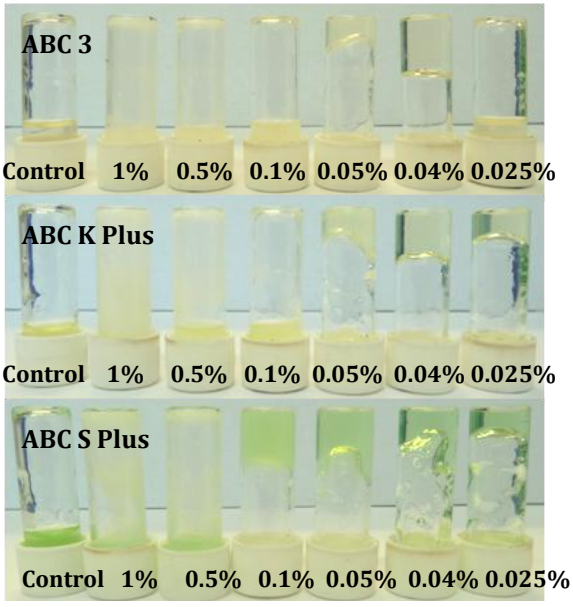

Figure 6.7 Gelation ability of DBS-SCH_3 in Type II (ABC 3 and ABC K Plus) and Type IV (ABC S Plus) anti-icing fluids.

6.2.2 Minimum gelation concentration (MGC)

Each gelator in the three different anti-icing products was tested at descending concentrations to identify the lowest concentration at which a gel could be formed.

Table 6.1 MGC range of the three gelators in Type II and Type IV Anti-icing products.

Gelator	**Minimum Gelation Concentration % w/v**		
	ABC 3	***ABC K Plus***	***ABC S Plus***
Rika (DBS)	0.06	0.06	0.05
DBS-OCH_3	0.06	0.06	0.06
DBS-SCH_3	0.04	0.04	0.04

From **Table 6.1** we can observe that regardless of the choice of gelator or anti-icing product the minimum gelation concentrations (MGCs) are very similar. These MGC values are very low when compared to the gelators in de-icing products in Chapter 5. A gel is formed when the concentration is half of that needed for a gel to form in a de-icing product.

The low concentrations required to form a gel may be attributed to the fact that these products also contain a polymer. Therefore the gel may not only be because of the LMWG but may also benefit from the polymer network, potentially creating a hybrid system where there are two interacting networks. Consequently, there may be two different networks forming separately and co-existing together in the same sample. This must be an effect from the presence of polymer as these effects are not seen at such low concentrations when in de-icing products.

6.2.3 Thermal stability

Each gelator was then tested to determine its thermal stability in each of the anti-icing products through the use of the tube inversion test as described previously.

From **Figure 6.8,** Rika (DBS) in anti-icing products (like the de-icing products in Chapter 5) showed the expected trend for gels, as concentration increases thermal stability increases. However, surprisingly from the graph, regardless of the type of product and concentration, the thermal stability was very similar across all products. When we compare this to the thermal stability of Rika (DBS) in DF Plus (de-icing product) with 50% MPG content we see that the thermal stability across the concentration range has increased. Therefore we can deduce that the increased thermal stability must be from the synergy between the LMWG and polymer within the anti-icing products, creating a more thermally stable gel.

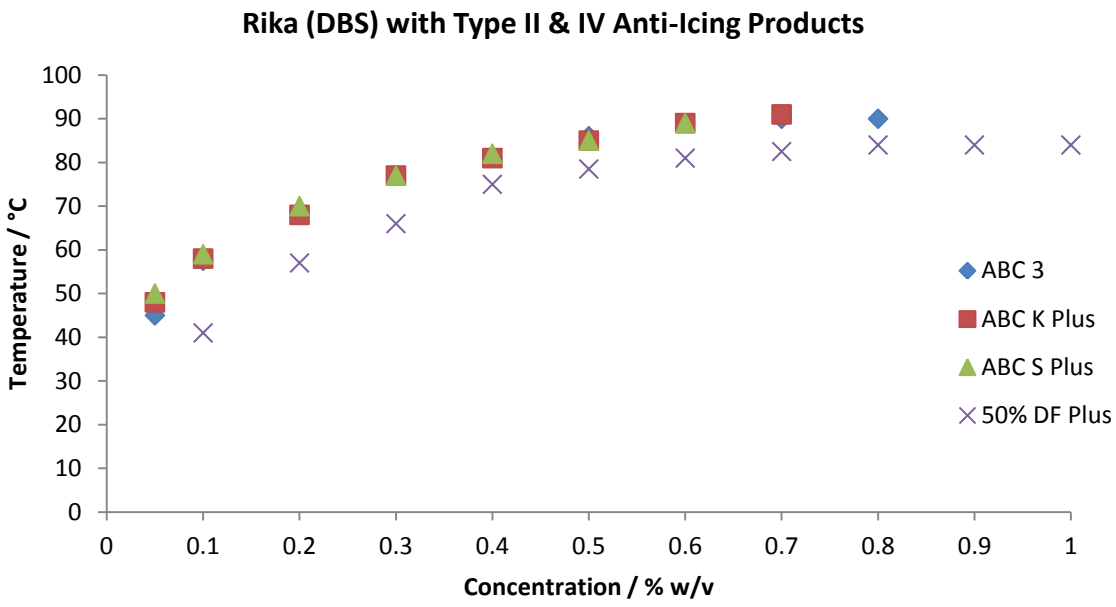

Figure 6.8 Thermal stability of Rika (DBS) in Type II and Type IV anti-icing products.

DBS-OCH_3 also shows the same general trend (**Figure 6.9)**. As concentration increases the thermal stability increases. Once again, this seems to be independent of the product type and concentration. When we compare these values to DBS-OCH_3 in DF Plus with 50% MPG content, again we can see that although they have similar MPG content the thermal stability of the gels has increased.

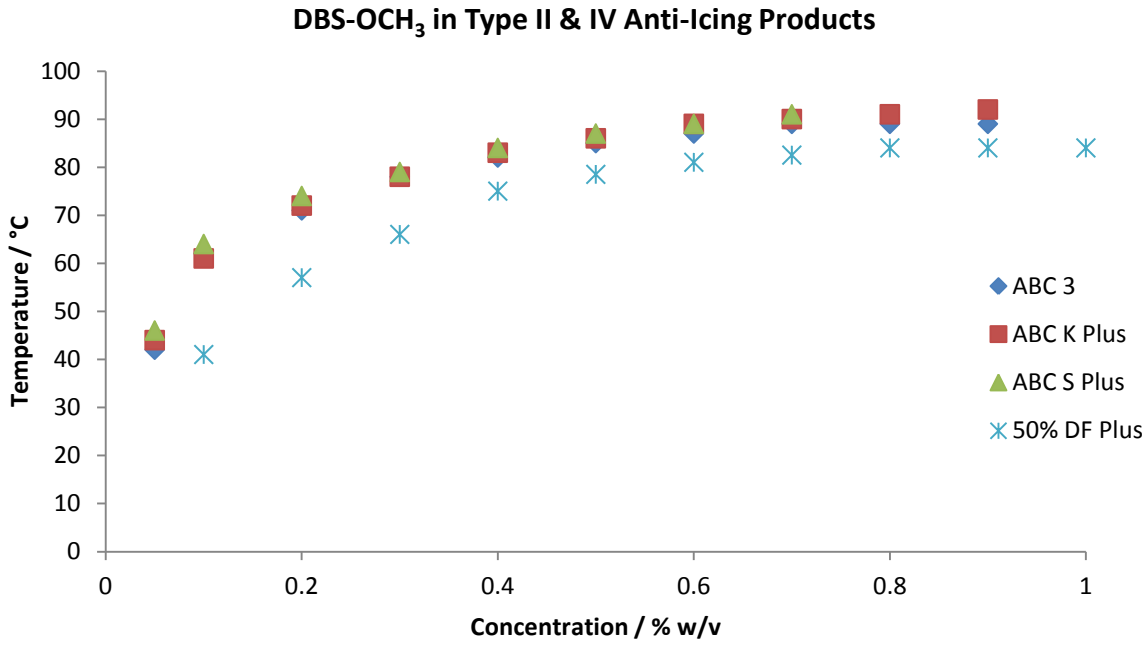

Figure 6.9 Thermal stability of DBS-OCH_3 in Type II and Type IV Anti-icing products.

From **Figure 6.10** we can see that DBS-SCH_3 also follows the same general trend as identified for the two gelators above. As concentration increases the T_{gel} increases.

However, this molecule is different from the other gelators in that it can only form gels in very low concentrations therefore the range is narrow compared to the other gelators. Regardless of the narrow concentration range, this molecule still has the ability to produce similar and higher T_{gel} values.

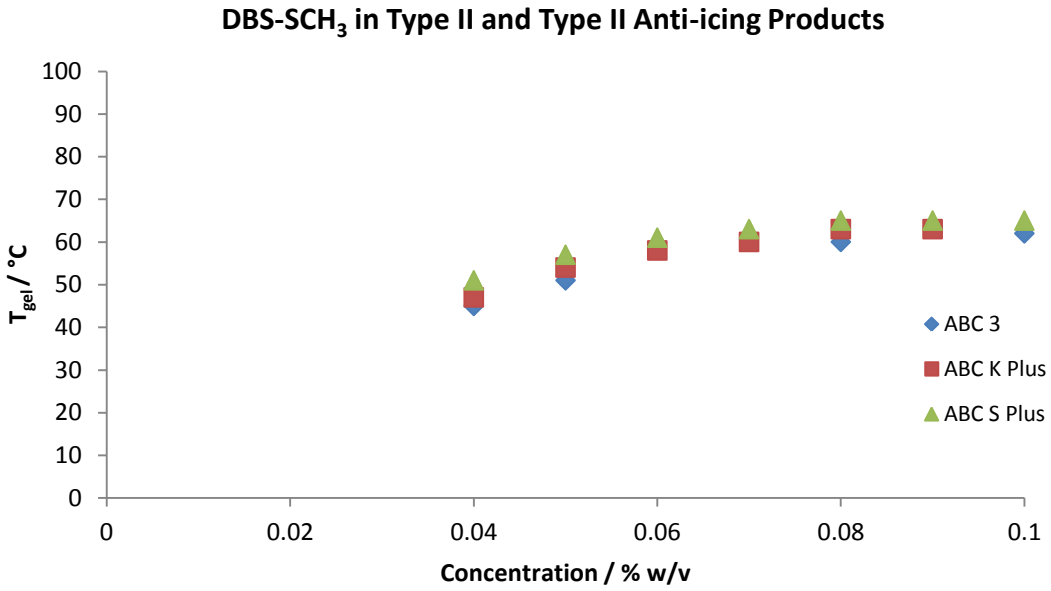

Figure 6.10 Thermal stability of DBS-SCH_3 in Type II and Type IV Anti-icing products.

Thermal stability analysis of each of the different gelators in the anti-icing products demonstrates that the thermal stability increases as a result of the polymer being present. The increased thermal stability and MGC values are a potential result of synergistic interactions occurring within the sample between the polymer and the gelator networks.

6.2.4 Scale-up Samples

We then wanted to identify if the same effects would be observed when these samples were scaled up for industrial testing. Unlike the de-icing products where we prepared high, low, and medium concentration samples in Chapter 5, it was thought since these products already contain a polymer network we should aim for a similar concentration already used for the polymer with the gelator. With Type II products ABC 3 and ABC K Plus, the polymer concentration in a finished product is approximately 0.2% w/v increasing to 0.4% w/v for a Type IV product (ABC S Plus). Therefore by potentially trying to keep costs low should the gelator prove to be successful within these products, a low concentration of 0.1% w/v was selected as the high concentration similar to the current polymer levels, with 0.05% and 0.025% w/v also being tested as lower concentrations.

As well as cost being a reason for selecting the concentration range, we were also trying to identify a sample which would have similar behaviour to the original anti-icing product at room temperature i.e. a viscous solution or partial gel. This would allow for ease of handling, avoid any unnecessary heating that could potentially cause degradation to the polymer and be representative of how we currently test and apply fluids to an aircraft (applied cold).

Samples of the three gelators were prepared as in **Section 6.2.1** but scaled up to 200 ml, and instead of heating for 1 hour required heating overnight to produce clear homogenous solutions. When Rika (DBS) was scaled up in the three different anti-icing products at room temperature we can see from **Figure 6.11** that all 0.1% w/v samples were gels which did not flow upon inversion. However, when the concentration was reduced to 0.05% w/v the samples existed as partial gels, in agreement with the gelation ability results we obtained on smaller scale. We also made scale up samples containing 0.025% w/v to identify if partial gels would also be formed on larger scale with very low concentrations of gelator, however they showed to be very similar to the original anti-icing products without gelator and appeared as viscous solutions.

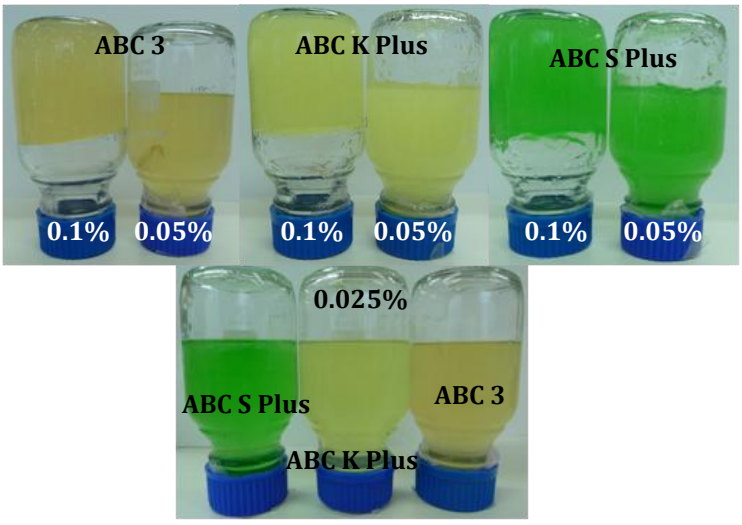

Figure 6.11 Scale up samples of Rika (DBS) in Type II and Type IV Anti-icing

Similar effects were also observed for DBS-OCH_3. However, from **Figure 6.12** it appears the 0.1% w/v samples are in fact partial gels when scaled up and do not agree with the smaller scale results which showed them as self supporting gels, whilst partial gels was created at 0.05% w/v which agreed with the small scale samples. Like Rika (DBS) above when DBS-OCH_3 was tested at 0.025% w/v again we see from **Figure 6.12** that all samples appeared as viscous solutions similar to the original product.

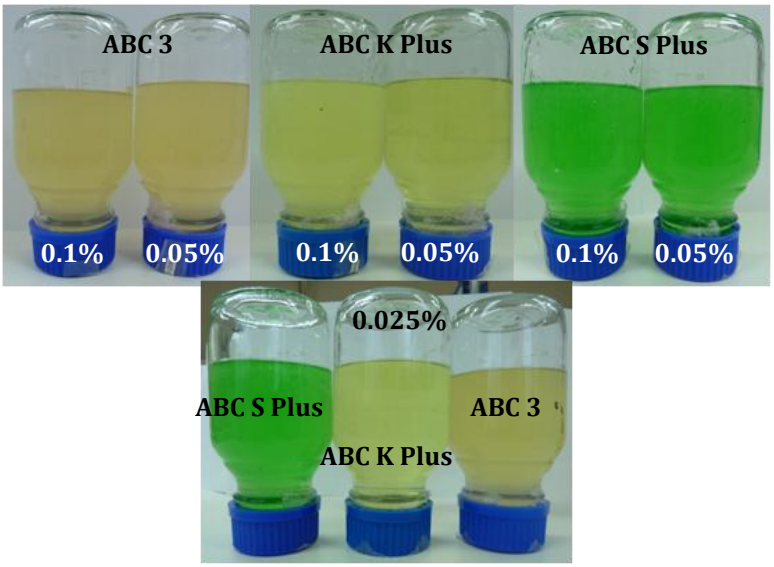

Figure 6.12 Scale up samples of DBS-OCH_3 in Type II and Type IV Anti-icing products.

When DBS-SCH_3 was scaled up in the anti-icing products we can see from **Figure 6.13** that at all concentrations when in ABC 3 all samples appeared to create partial gels, this agrees with the observation that when tested on small scale the gels appeared weak and collapsed upon photographing. However, when in ABC K Plus and ABC S Plus unlike the small scale samples which showed us that gels could be formed from 0.1-0.05% w/v we also observe that on large scale gels can also be formed when there is only 0.025% w/v of gelator present.

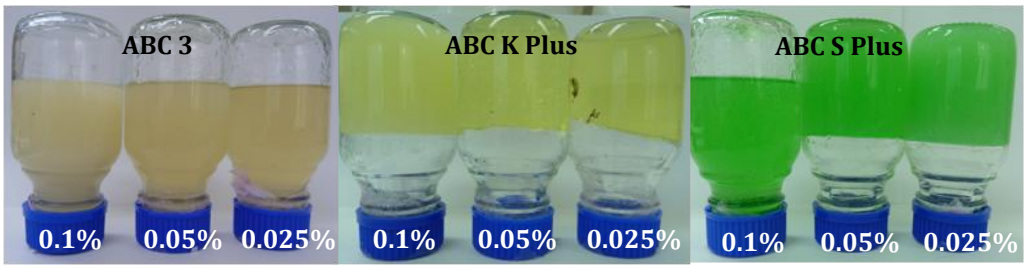

Figure 6.13 Scale up samples of DBS-SCH_3 in Type II and Type IV Anti-icing products.

From the above samples it therefore appears that scaling up samples can in fact in some instances such as DBS-SCH_3 change the behaviour. By scaling up DBS-SCH_3 we found that gels can in fact be formed with very low concentrations of 0.025% w/v which was not possible for any of the gelators on small or larger scale. Therefore from the scale-up results we chose to use a sample containing gelator within each of the anti-icing products similar to the original anti-icing products at 0.05% w/v. Using this concentration would allow us to apply the samples in the industrial test methods without applying heat hence, preventing any unwanted degradation of the network. Samples of 0.1% w/v were not tested further due to their formation of solid gels at room temperature and the difficulty of application within the industrial test method.

The above scaled up samples for each for the gelators were tested further to identify their strength, stability and robustness using rheology before being subjected to the WSET industrial test method to identify if incorporating a gelator into a thickened polymeric anti-icing product can enhance the existing performance of an anti-icing product.

6.2.5Rheology

Rheological analysis of each of the gelators in the Type II (ABC 3 and ABC K Plus) and Type IV (ABC S Plus) anti-icing products were carried out on a Kinexus Pro+ stress controlled rheometer using a 20 mm parallel plate. To understand how each of the gels responds to differing stresses and strains a full rheological profile was carried out to determine their strength, stiffness and robustness through amplitude sweeps. Each of the tests were conducted at 20°C and the LVR determined for each sample, with a value from the LVR then being used for all further testing.

Samples prepared in **Section 6.2.4** above were used for rheological testing. The samples were placed into an oil bath at temperatures just above their T_{gel} values to form the solution phase and the hot solution was placed onto the rheometer plate set to 20°C using a spoon to limit any unnecessary damage to the sample. The sample geometry was corrected to the designated gap size (1 mm) and left to equilibrate for 15 minutes to allow the formation of the gel. From **Figure 6.14** and **Table 6.2** we can see that samples of each of the gelators at 0.1% w/v in ABC 3 were stable, robust and strong with long linear LVR regions. However, adding the gelators to ABC 3 does not increase the resistance to strain, it remains similar to the original product, however the G' values increase in the order of DBS-OCH_3<DBS-SCH_3<Rika (DBS). Therefore the increased stiffness of the gel networks that have been created are a result of incorporating the LMWGs into the polymeric thickened product, as a result we have potentially created a hybrid network between both the polymer and gelator.

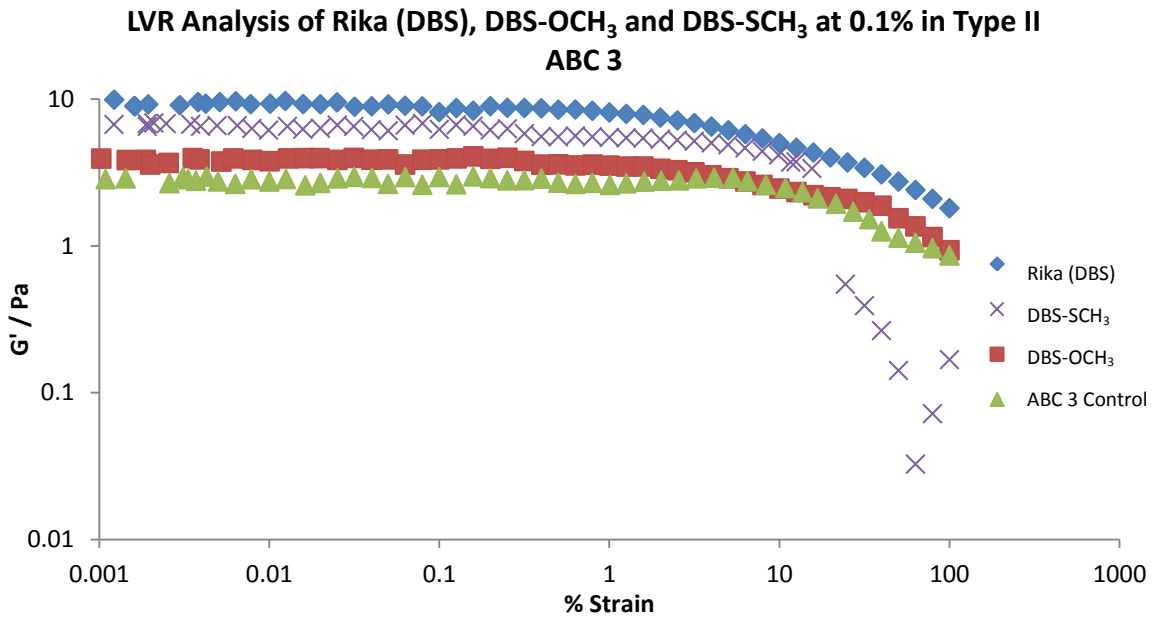

Figure 6.14 Amplitude sweep of Rika (DBS), DBS-OCH_3 and DBS-SCH_3 at 0.1% w/v in Type II Anti-icing product ABC 3.

Table 6.2 Critical strain and stiffness (G') values of each gelator at 0.1% w/v in ABC3.

Sample	G' (Pa)	Critical Strain %
Rika (DBS)	8.56	0.63
DBS-OCH_3	3.61	0.50
DBS-SCH_3	5.75	0.63
ABC 3 Control	2.66	0.63

When we incorporate the three different gelators into ABC K Plus, see **Figure 6.15** and **Table 6.3**, we observe that unlike in ABC 3, the strength, (i.e. resistance to strain) and the stiffness (G') of the gel networks have both dramatically increased compared to the original products, with the exception of DBS-SCH_3 which has halved the resistance to strain of the gel network. This may be due to the fact that DBS-SCH_3 performs better at much lower concentrations than 0.1% w/v as shown in Chapters 3 and 5 and at 0.1% w/v may be too close to being insoluble that it weakens the formation of the gel network when incorporated into the anti-icing product.

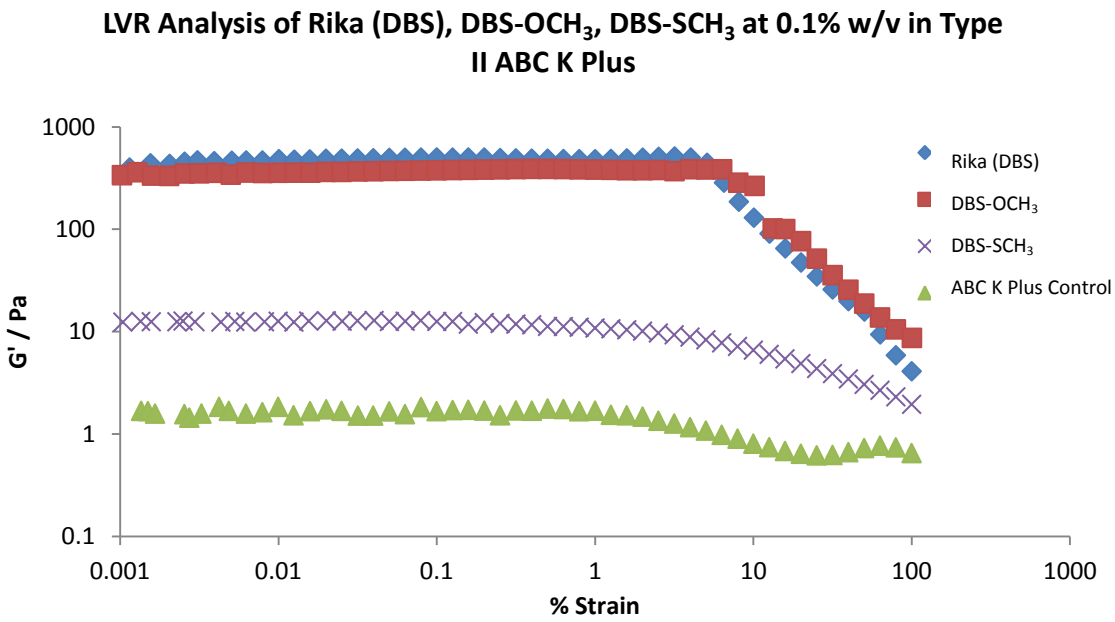

Figure 6.15 Amplitude sweep of Rika(DBS), DBS-OCH_3 and DBS-SCH_3 in Type II Anti-icing product ABC K Plus at 0.1% w/v.

Table 6.3 Critical strain and stiffness (G') values of each gelator in ABC K Plus.

Sample	G' (Pa)	Critical Strain %
Rika (DBS)	459.47	3.18
DBS-OCH_3	346.59	3.18
DBS-SCH_3	11.33	0.63
ABC K Plus Control	1.57	1.59

When we incorporate the different gelators into a Type IV anti-icing product, (**Figure 6.16** and **Table 6.4)** once again the stiffness of the gel network has increased significantly in the order of DBS-SCH_3<DBS-OCH_3<Rika (DBS). However we now observe that incorporating Rika (DBS) does not enhance the strength (i.e. resistance to strain) which remains the same. However, DBS-OCH_3 is able to increase the resistance to strain as well as the stiffness.

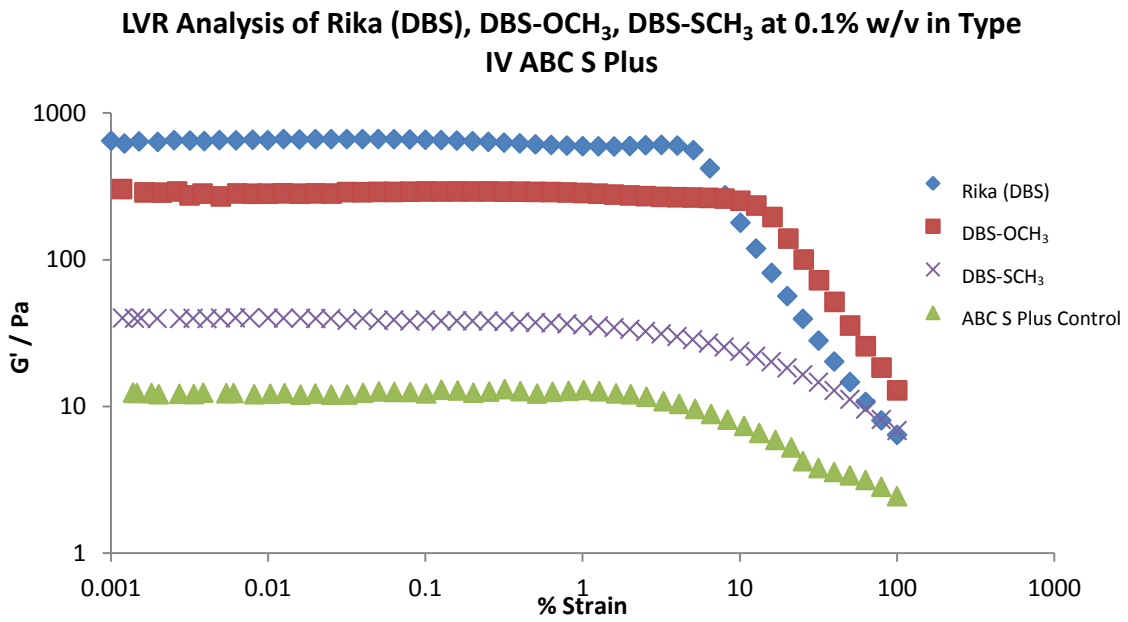

Figure 6.16 Amplitude sweep of Rika (DBS), DBS-OCH_3 and DBS-SCH_3 in Type IV Anti-icing product ABC S Plus at 0.1% w/v.

Table 6.4 Critical strain and stiffness (G') values of each gelator in ABC S Plus.

Sample	G' (Pa)	Critical Strain %
Rika (DBS)	603.40	2.52
DBS-OCH_3	268.23	3.17
DBS-SCH_3	36.67	0.79
ABC S Plus Control	11.70	2.55

Therefore from the amplitude sweeps of each of the gelators in each of the different anti-icing products we can see that the gelators are potentially interacting with the polymer within the anti-icing product. With Rika (DBS) and DBS-OCH_3 in all of the different products we notice a remarkable increase in both resistance to strain and stiffness of the gel networks that are formed which is more suggestive that the two different types of gel network are interacting with one another to form a hybrid gel network. DBS-SCH_3 has a smaller effect at 0.1 %w/v loading.

Frequency sweeps of each of the gelators in the different anti-icing products were performed at 20°C to determine the behaviour of each of the gel networks. The G' (storage modulus) and G'' (loss modulus) for each sample were determined and the response to increasing frequency recorded. If G' is dominant over G'' the material is elastic and solid-like. If the G'' is dominant over G' the sample is more viscous and liquid-like. All samples in ABC 3 regardless of gelator, were solid-like and

independent of frequency with G'>G'' characteristic of gels up to 1 Hz, thereafter they act as visco-elastic solids with G' increasing with increasing strain (**Figure 6.17**).

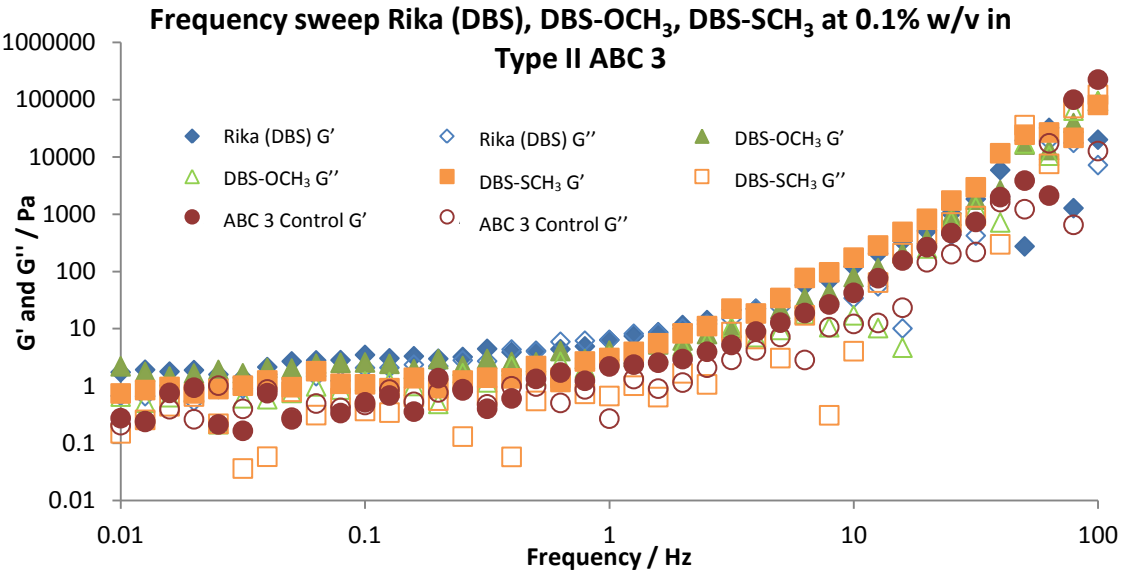

Figure 6.17 Frequency sweep of Rika (DBS), DBS-OCH_3 and DBS-SCH_3 at 0.1% w/v in ABC 3

In ABC K Plus, each of the gelators was independent of frequency (**Figure 6.18**), with G'>G'' up to 2.5 Hz for DBS-SCH_3 and up to 15 Hz for both Rika (DBS) and DBS-OCH_3 whereafter they act as visco-elastic solids with G' increasing with increasing frequency. When DBS-SCH_3 is incorporated into ABC K Plus, it is more frequency dependent than the other gelators. This may be due to the fact that it does not form stiff gels like the other gelators with lower G' values.

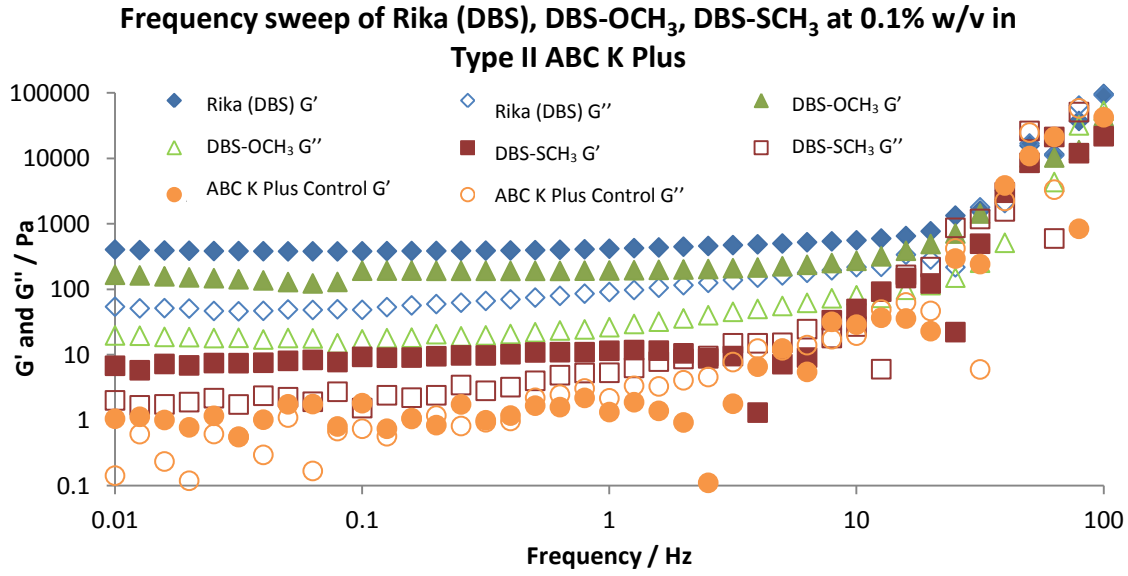

Figure 6.18 Frequency sweep of Rika (DBS), DBS-OCH_3 and DBS-SCH_3 at 0.1% w/v in ABC K Plus.

Each of the gelators when incorporated into ABC S Plus shows characteristic behaviour of a gel (**Figure 6.19)** with G'>G'' up to 8 Hz for DBS-SCH_3 and up to 15 Hz for Rika (DBS) and DBS-OCH_3, thereafter they become frequency dependent and act as visco-elastic solids.

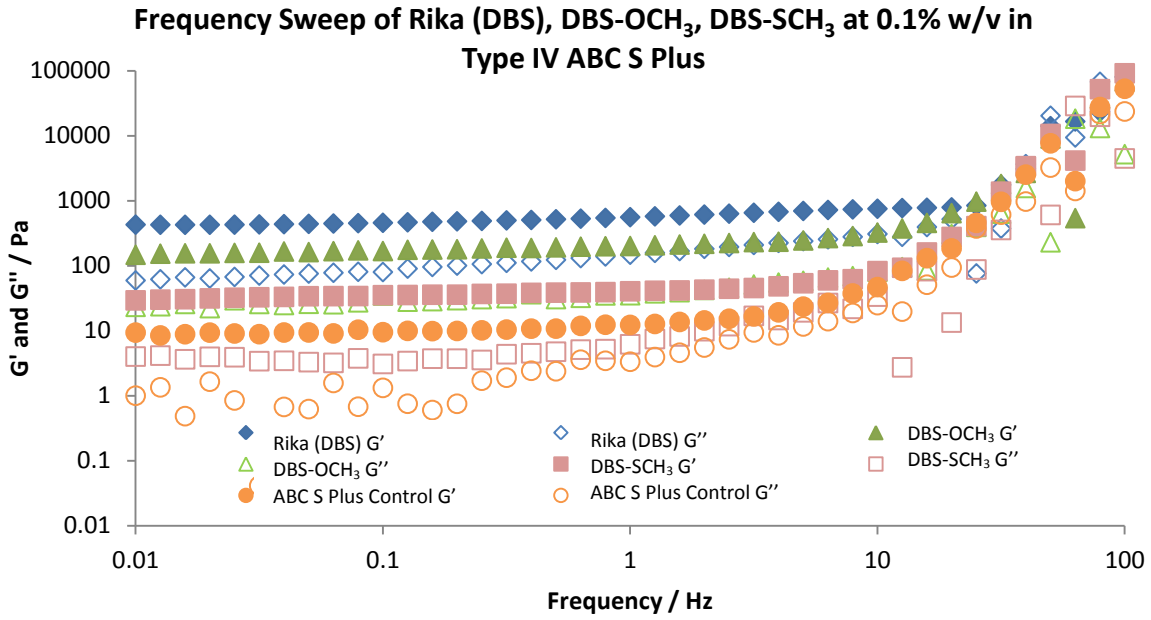

Figure 6.19 Frequency sweep of Rika(DBS), DBS-OCH_3 and DBS-SCH_3 at 0.1% w/v in ABC S Plus.

Therefore from the frequency analysis of each of the gelators compared to each of the original anti-icing products we can see that each of the samples show characteristic behaviour of gels but at increasing frequencies, turn into visco-elastic solids similar to the original anti-icing products.

Each of the gelators within each of the anti-icing products was also tested to determine their response to temperature. The scaled-up samples were heated in an oil bath to just above their T_{gel} in order to be able to be applied hot to the rheometer. Unlike when testing amplitude and frequency response, the rheometer plate was set to 90°C and the hot sample applied to the hot plate. The geometry was brought down to the required gap size (1 mm) and the temperature was ramped down slowly in 2°C increments per minute. Conducting testing in this way allows us to determine the temperature at which the gel network forms and the temperature on heating again at which it disassembles. From **Table 6.5** we can see that all of the three gelators show the same general trend, with gels forming in ABC S Plus at higher temperatures and ABC 3 requiring the lowest temperatures. Likewise when the temperature cycle was reversed ABC 3 required lower temperatures to disassemble the gel, with gels formed

in ABC S Plus requiring higher temperatures for all of the gelators. Therefore we can note that the most thermally stable gels are formed in ABC S Plus with all three gelators, and the least thermally stable gels are formed in ABC 3 with each of the gelators. This is in agreement with the impact on rheological performance described above.

Table 6.5 Gel formation (T_f) and gel dissolutions (T_d) temperatures of Rika (DBS), DBS-OCH_3 and DBS-SCH_3 at 0.1% w/v in ABC 3, ABC K Plus and ABC S Plus.

	Molecule					
Product	**Rika (DBS)**		**DBS-OCH_3**		**DBS-SCH_3**	
	$T_f/(°C)$	$T_d/(°C)$	$T_f/(°C)$	$T_d/(°C)$	$T_f/(°C)$	$T_d/(°C)$
ABC 3	13.5	49.1	17.1	55.2	19.8	73.4
ABC K Plus	28.9	53.8	29.1	56.6	32.9	77.4
ABC S Plus	31.5	57.9	34.7	66.1	39.1	82.1

These trends may be a result of the type of polymer contained within each anti-icing product. Although each product contains a similar type of polymer based upon polyacrylic acid they have different degrees of cross-linking and hydrophobic modification. ABC 3 is known to have the least amount of cross-linking and is the most hydrophobically modified, and ABC S Plus is the most cross-linked polymer with the least amount of modification. ABC K Plus is intermediate. Therefore the thermal stability we are observing probably suggests that the more hydrophilic cross-linked polymer network becomes more stabilised with ABC 3<ABC K Plus<ABC S Plus.

From the thermal stability analysis, we could maintain the recommended temperatures advised to the customer the same i.e. 60-80°C when being applied to an aircraft. As such, incorporating the gelators into these types of products would not require higher temperatures to break or apply the fluids to an aircraft and hence reduces any further costs that could be incurred by the customer if they had to change or replace equipment.

Since we have now incorporated gelators into anti-icing products we must also identify how long it takes for the gel to be formed, highly relevant in the real life application. Therefore samples of each gelator in the respective anti-icing products were placed into an oil bath just above the T_{gel} value to obtain the solution form. Each of the samples in turn was then applied to the rheometer plate set to 20°C and the test started immediately and ran over a period of 1 hour. The time the complex modulus (G*) takes to reach a plateau is the time recorded for the gel to form. From **Table 6.6** we can see that for each of the gelators they generally follow the same

trend, with the time required to form a gel reducing in the order of ABC 3>ABC K Plus>ABC S Plus. Therefore gels form most quickly in ABC S Plus and more slowly in ABC 3. However, no time was recorded for DBS-SCH_3 in ABC K Plus or ABC S Plus, as before the instrument could take the first measurement the gels had reached their maximum G* value.

Table 6.6 Time taken to form a gel with Rika (DBS), DBS-OCH_3 and DBS-SCH_3 at 0.1% w/v in ABC 3, ABC K Plus and ABC S Plus.

Product	**Time of Formation / seconds (minutes)**		
	Rika (DBS)	**DBS-OCH_3**	**DBS-SCH_3**
ABC 3	1210(20.2mins)	2675(44.6mins)	415(6.9mins)
ABC K Plus	810(13.5mins)	1185(19.8mins)	N/A
ABC S Plus	640(10.7mins)	1035(17.3mins)	N/A

Therefore we can see that gels can take between 10-45 minutes to form depending on the gelator and type of anti-icing product. Unlike the gels formed in Chapter 5 in de-icing products which formed within 5-8 minutes when there was 50% MPG we see just by having the presence of the polymer within a thickened product potentially increases the time the gel network takes to form, however this could be attributed to extra interactions potentially occurring between the gelators and polymer to create an overall hybrid gel network. In general terms the LMWG has to assemble its network around the polymer gel. In terms of the application of these gels onto aircrafts, the gels would potentially form more quickly when at lower freezing temperatures.

6.2.6 Imaging

We then carried out SEM analysis on each of the different gel samples to try and visualise the internal structures of these systems which would allow us to get a better in depth understanding of the network that is being formed. Samples of each of the original anti-icing fluids were prepared by adding one drop of the product onto an aluminium SEM stub. This was smeared over the surface to create a thin film and dried in a dessicator to leave the xerogel. Unfortunately when these were imaged using the scanning electron microscope no nanostructures were observed and the same held true when viewed using transmission electron microscopy (TEM). We then decided to image just the polymer dispersions that are added at the formulation stage to each of the anti-icing product to try and get an idea of what type of network the polymer would form on its own. Like the anti-icing products one drop of each of the

different polymer dispersions was placed onto an aluminium SEM stub and smeared across the surface before leaving to dry in a dessicator. The polymer dispersions dried very quickly (within 30 minutes) and formed a film on the stubs which became brittle and flaked off in areas. Each of the samples were then sputter coated with a 4 nm Au/Pd layer before being imaged. The polymers were very unstable under the microscope beam however we managed to obtain images to get an idea of how these polymers create a network within the products. The SEM images (**Figure 6.20)** indicate that the polymers may form micellar aggregated structures which clump together through the cross-linking and branched nature of the polymers and appear as globules. The polymers differ in each product by the degree of cross-linking however there are no obvious nanostructural differences between each polymer dispersion that is used within each of the different anti-icing products. However, these globules may result from drying processes.

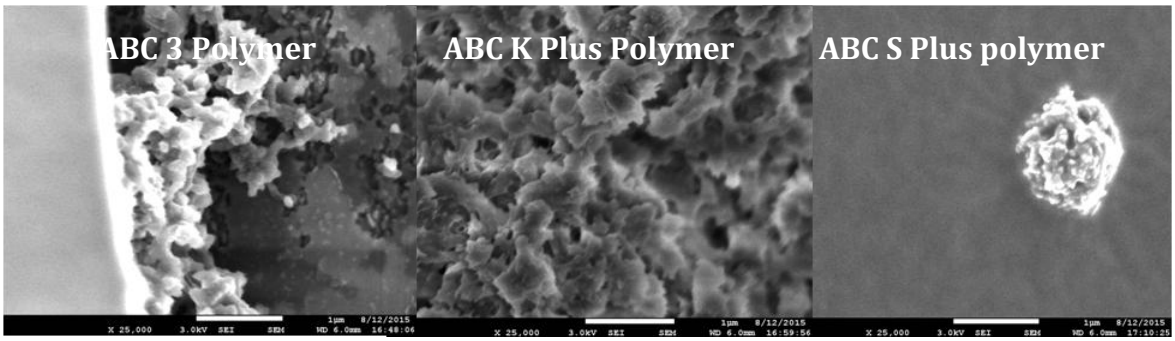

Figure 6.20 SEM imaging of the three different polymer dispersions found within each of the anti-icing products, ABC 3, ABC K Plus and ABC S Plus.

The polymers were also imaged using TEM to identify if there were any other structures formed. Samples for TEM analysis were prepared by placing one drop of each of the dispersions onto a copper backed TEM grid. The grid was then left to air dry overnight and imaged the next day. From **Figure 6.21** we can see that the samples are very unstable under the microscope and difficult to image. However it is clear that no fibres are formed from the polymer and what appear as small spherultic black (negative) regions with regions of high density where they are clumped together. The more dense darker regions can be observed most in the ABC S Plus polymer, and this is most likely because it has approximately double the concentration of polymer compared to the other two polymer dispersions.

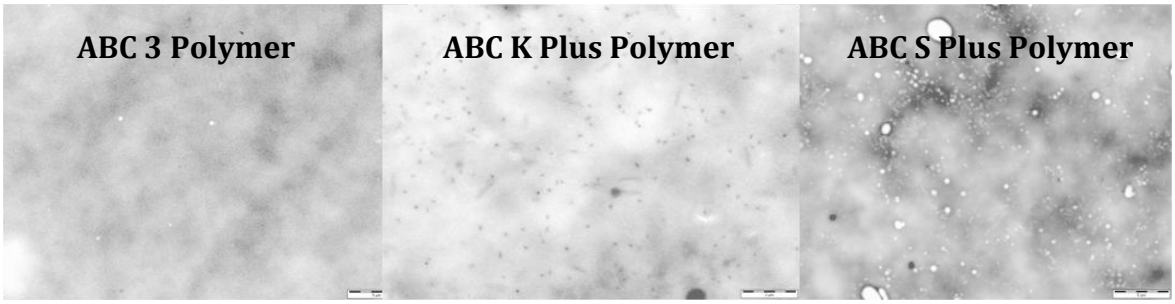

Figure 6.21 TEM analysis of the three different polymer dispersions used within anti-icing products ABC 3, ABC K Plus and ABC S Plus.

Therefore from the SEM and TEM analysis we now know that the polymers within anti-icing fluids do not form highly structured nanostructures unlike the three gelators being tested which have previously been shown to create networks through long helical or straight fibres (Chapter 4 and 5). Therefore if we have created a hybrid system it will potentially contain both the globular unstructured nature of the polymer and the fibrous nature of the gelator network.

Gel samples of each of the gelators in the three different anti-icing products were prepared by smearing a small sample of the gel onto an aluminium SEM stub to create a thin film. These were then left to dry in a dessicator before being sputter coated with a layer of Au/Pd. From **Figure 6.22** of Rika (DBS) in each of the anti-icing products we can see that the images appear very solvated. There unfortunately was no detail to the images and we could not identify if one or two networks were present together or separately. However, there were signs at the edges that some form of fibre was present. Therefore the solvent may not have been effectively removed or the structure that we observed for the polymers in **Figure 6.20** could be contributing to the effects we observe when imaging these samples. The polymer structure may potentially be masking the fibrous nature of the gelator network. Therefore this type of sample preparation did not achieve the desired information and showed the same effects when DBS-OCH_3 and DBS-SCH_3 were imaged.

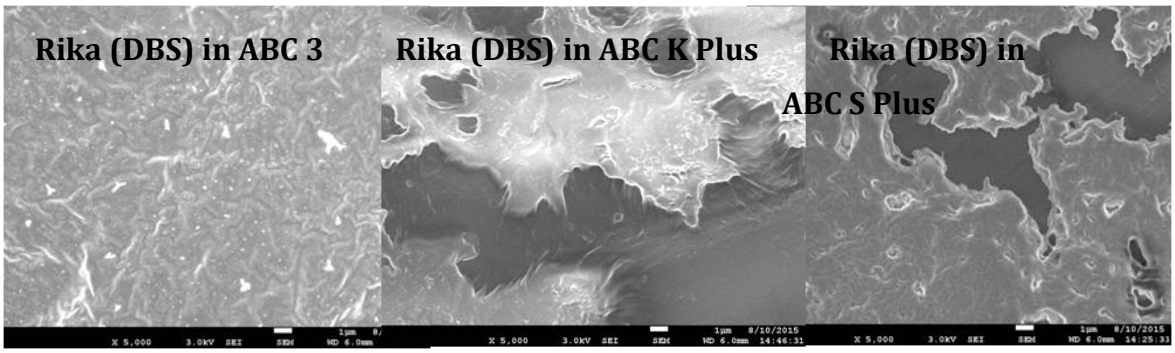

Figure 6.22 SEM analysis of Rika (DBS) in each of the anti-icing products, ABC 3, ABC K Plus and ABC S Plus.

We then prepared samples for SEM through using a freeze dryer to try and achieve the aerogel form of the internal structure. However, this means of preparation failed for these samples with this type of solvent system, due to MPG having a melting point of -49°C and the machine operating at -65°C. This unfortunately encouraged the solvent to bubble and boil instead of drying effectively.

Therefore, the samples were imaged using transmission electron microscopy (TEM).

Samples of the hybrid gels for each of the gelators were prepared by using a gel formed at room temperature. A small sample of the gel was removed with a spatula and brought very briefly into contact with a copper backed TEM grid. Each of the grids was then left to dry overnight before being imaged the next day.

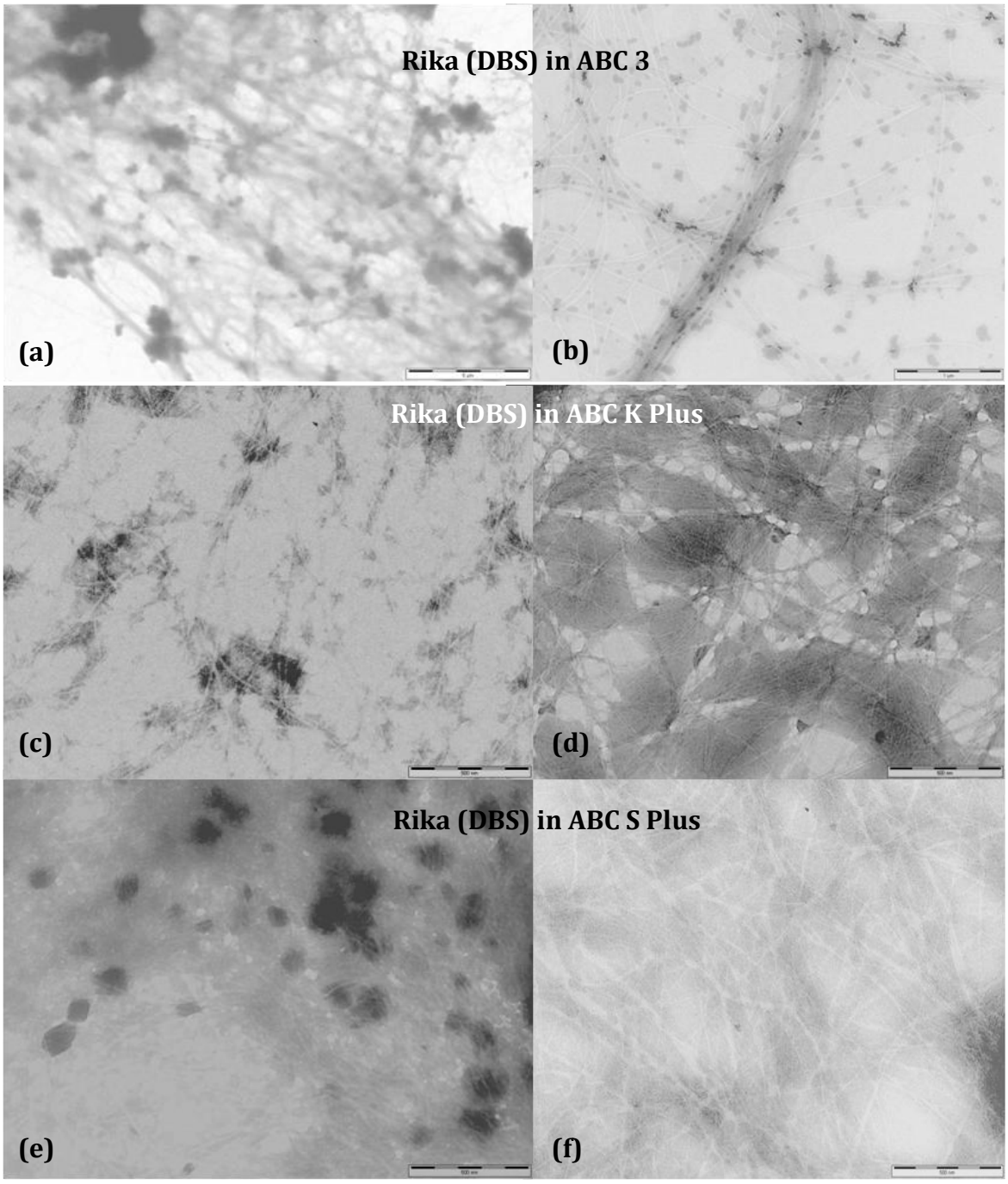

Figure 6.23 TEM analysis of Rika (DBS) in ABC 3((**a**) at 5μm, (**b**) at 1μm), ABC K Plus ((**c**) and (**d**) at 500nm) and ABC S Plus ((**e**) and (**f**) at 500 nm).

From **Figure 6.23** of Rika (DBS) in ABC 3 at low magnification (x4000) in **(a)** there appears to be a fibrous type network formed made up long thin fibres that are <100 nm in diameter with what appears as globular structures which are darker and denser in specific areas throughout the structure that range from ca. 500 nm to ca. 3 μm in diameter. At higher magnification **(b)** we can clearly see that this is indeed made up of long thin fibres that span throughout the whole of the sample measuring ca. 5-10 nm which are typical of Rika (DBS), with a large fibre bundle measuring ca. 250 nm in diameter. It is also much clearer at higher magnification that the black

dense globular structures are also present throughout the whole sample and are seen to be interconnected or attached to the length of the fibres and throughout the pores where the solvent would exist.

When we imaged Rika (DBS) in ABC K Plus and ABC S Plus we noted that no structures could be observed at low magnifications as for Rika (DBS) in ABC 3. Therefore images were only obtainable at higher magnifications. From **Figure 6.23** we can see for **(c)** and **(d)** when in ABC K Plus that the very small ca. 5-10 nm fibres are again present and span the whole sample creating a fibrous network. We also note that within these images there are areas of high density, darker regions which may be characteristic of the polymer structure. But it is unclear if the two structures are one complete network or if one is on top of the other. This was also true when Rika (DBS) was imaged in ABC S Plus see **(e)** and **(f)** in **Figure 6.23**.

Achieving images of these types of sample was very difficult because they were so unstable under the microscope. The images of Rika (DBS) in ABC 3 clearly show that there is potentially a hybrid gel network being created where the polymer (dark dense regions) is interacting along the length of the fibres. However, this is more difficult to determine in ABC K Plus and ABC S Plus. However it is clear that this gelator is able to form its own fibrous network within a complex fluid such as an anti-icing fluid, generating a hybrid material.

DBS-OCH_3 was also imaged in all three anti-icing products, but like Rika (DBS) we had trouble obtaining clear images to understand the make-up of the networks that are being formed. From **Figure 6.24** we can see that the images for DBS-OCH_3 unfortunately all appear very solvated or covered/masked by a secondary component within the samples, which is potentially the polymer network. However, in all cases we can clearly see that there are fibres present which span the whole sample measuring ca. 5-10 nm in diameter which are associated with the gelator. These appear to branch off and create fibre bundles. However, from the images obtained it is unclear whether there are two different networks or if both polymer and gelator are interacting which was suggested with the Rika (DBS) gelator above.

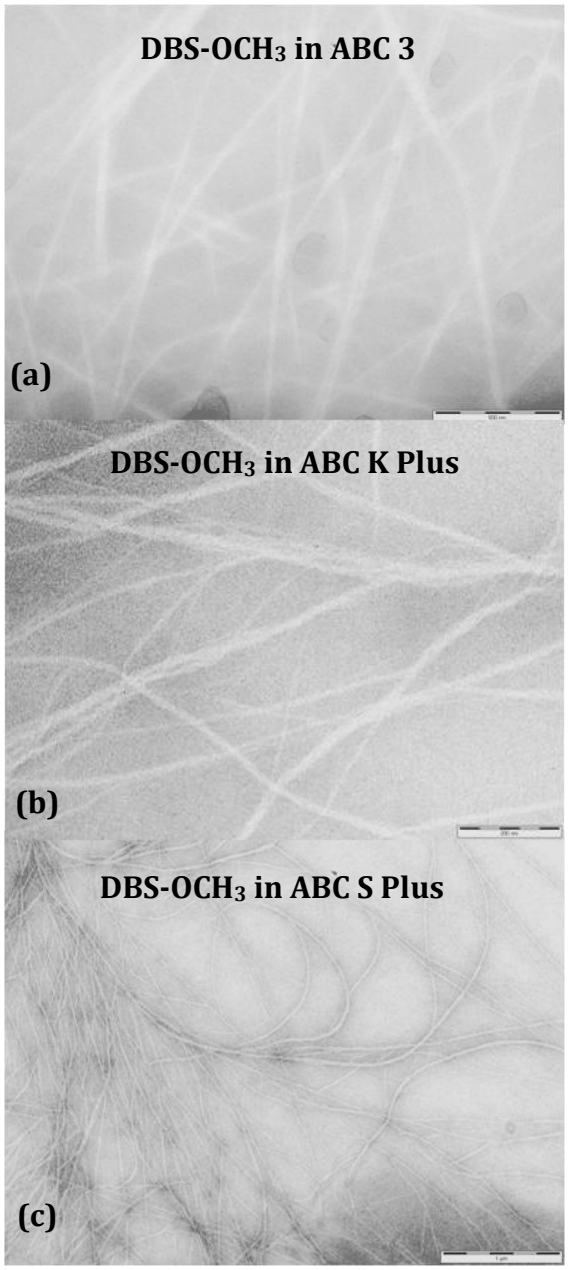

Figure 6.24 TEM analysis of DBS-OCH_3 in ABC 3**(a),** ABC K Plus **(b)** and ABC S Plus **(c)** anti-icing products.

Like the gelators above, DBS-SCH_3 in each of the anti-icing products was also imaged using TEM. However, unlike the other two gelators, gels formed using DBS-SCH_3 in the anti-icing products were able to produce very clear images that gives us a better insight into what is happening within the gel samples. In all products at low magnification of x 6000 it was clear that long thin fibres (< 100 nm in diameter) were formed that spanned throughout the networks, see **(a)**, **(c)** and **(e)** in **Figure 6.25**. Regardless of the type of anti-icing fluid, they formed very similar networks. As well as small long fibres being formed, circular globular type structures appended on to these fibres were observed. At higher magnification in **(b)**, **(d)** and **(f)** in **Figure 6.25** we can see that these globular structures measure between 200 nm and 1 μm where

they can be seen to clump together to create larger structures. This type of structure as we have seen previously in **Figure 6.20** and **6.21** is characteristic of the structures created by the polymers within the differing anti-icing products.

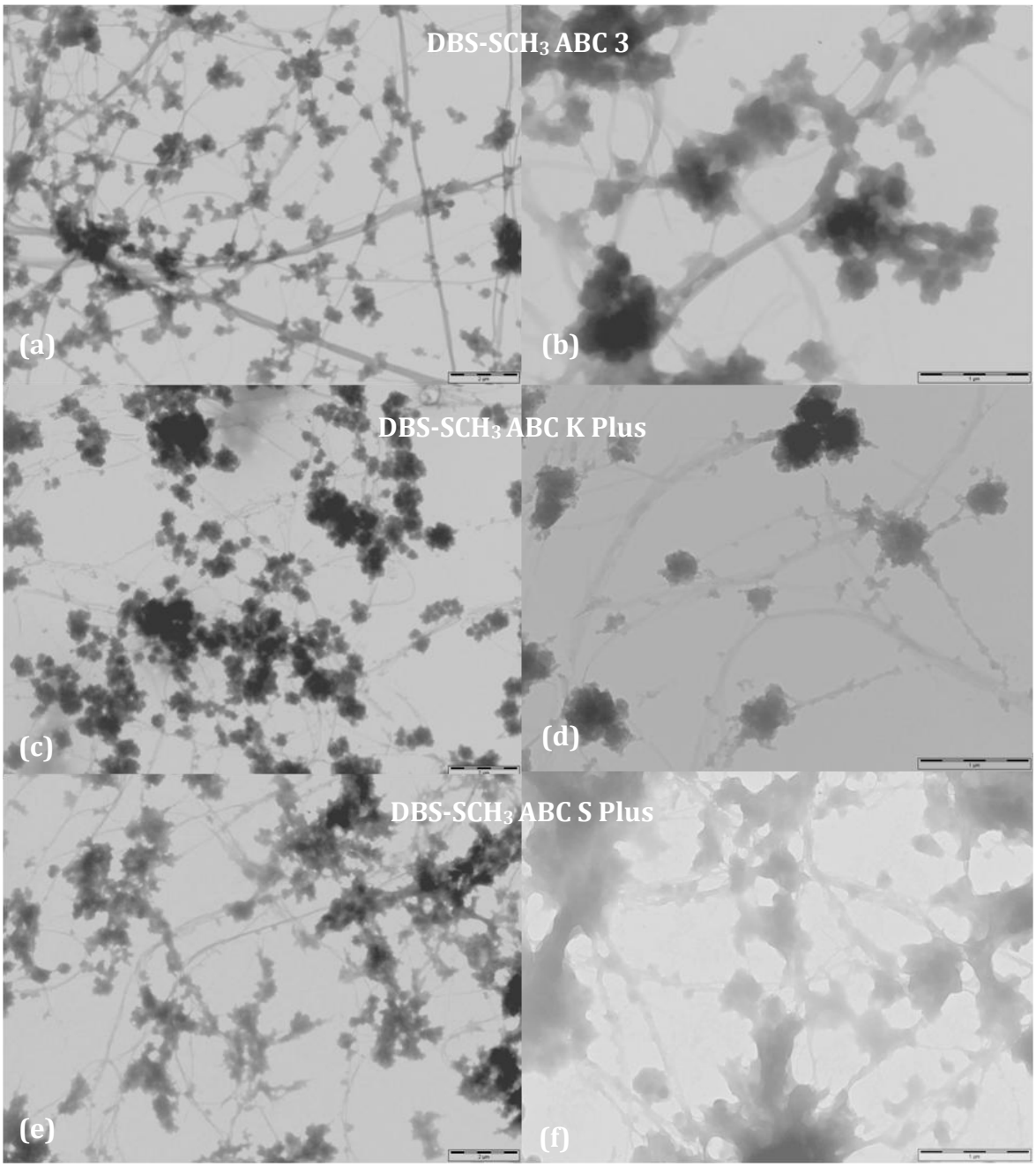

Figure 6.25 TEM analysis of DBS-SCH_3 in ABC 3 ((**a**) and (**b**)), ABC K Plus ((**c**) and (**d**)) and ABC S Plus ((**e**) and (**f**)) anti-icing products.

Therefore it appears as if the polymer structures interact on the periphery of the fibres created by the gelators in each of the different anti-icing products, and it would appear that the globular structure of the polymer can interact with itself to create dense concentrated areas of polymer network whilst also interacting with the fibres of the gelators, effectively pulling them together to create one extended hybrid gel network. These interactions on the periphery of the gelator fibres with the polymers

may be why we achieve stiffer gels, and in some cases more resistance to strain when tested by rheology.

Through the use of SEM and TEM imaging we have been able to get a better insight into what is happening when a gel is formed in anti-icing products. It is evident the gelator molecules form a fibrous network which can span the whole sample with the polymer interacting along the length of the fibres and throughout the sample as a whole. We have distinguished that both networks have completely different structures with polymer molecules appearing globular with no distinct shape and the gelator molecules forming long fibres. From imaging it would therefore suggest that we have in fact generated a structure made up of two different networks that interact with one another.

6.2.7 NMR Hybrids

To understand in more detail the behaviour of the gel networks from both the polymer and the LMWG in the anti-icing product, we carried out NMR spectroscopy. NMR spectroscopy can help identify what is immobilised within a gel phase. Using an internal standard allows for quantification of what is being immobilised hence the gel networks and what is mobile i.e. the solvent. When gelator molecules are assembled into a self supporting gel network they appear invisible when tested by NMR, whereas the solvent remains mobile and hence visible. Therefore using NMR, we can determine how much of the gelator is immobilised and forming a network which can be compared to the control samples

Within a two component gel such as the anti-icing fluid with additional gelator, we will potentially also be able to see if the polymer network is immobilised preferentially or if the gelator molecules are immobilised, or alternatively we will be able to identify how much they interact with one another to create a hybrid network by quantification with the internal standard, with the integrals associated with each of the polymer and gelator molecules.

Gel samples of each anti-icing fluid with each of the different gelators formed at room temperature were placed in an oil bath to just above their T_{gel} value to form the solution phase. 1 ml of the hot gel solution was then added to a 6 ml glass vial with 1 ml of stock solution added. The stock solution contained 5 ml of D_2O with 10 µl of either acetone or DMSO to act as an internal standard. Each sample was kept hot and mixed before being pipetted into an NMR tube using a Gilson pipette. Control samples

of each of the anti-icing products were also made in the same way. Each sample was then run using the JEOL ECX400 spectrometer and the ^1H spectra collected and integration values compared.

Figure 6.26 shows an example of testing ABC K Plus on its own and on addition of Rika (DBS). The ^1H NMR was run at 25°C but there is no evidence of the polymer which suggests it is immobilised at this temperature. What we do see is the peak at 4.79 ppm is associated with the D_2O as well as the internal standard DMSO, at 2.50 ppm. As well as these peaks we can also see between 3.65–3.16 ppm peaks associated with the CH_2 and CH groups on 1,2-monopropylene glycol structure as well as at 0.90-0.88 ppm the CH_3 group of the 1,2-monoproylene glycol structure. These peaks are apparent in both the original anti-icing product as well as when the Rika (DBS) gelator is incorporated. When the gelator is incorporated into the anti-icing product, this too is immobilised and not observed. Therefore because both polymer and gelator molecules are not observed it potentially suggests that both are incorporated into solid-like networks – in agreement with the TEM observations.

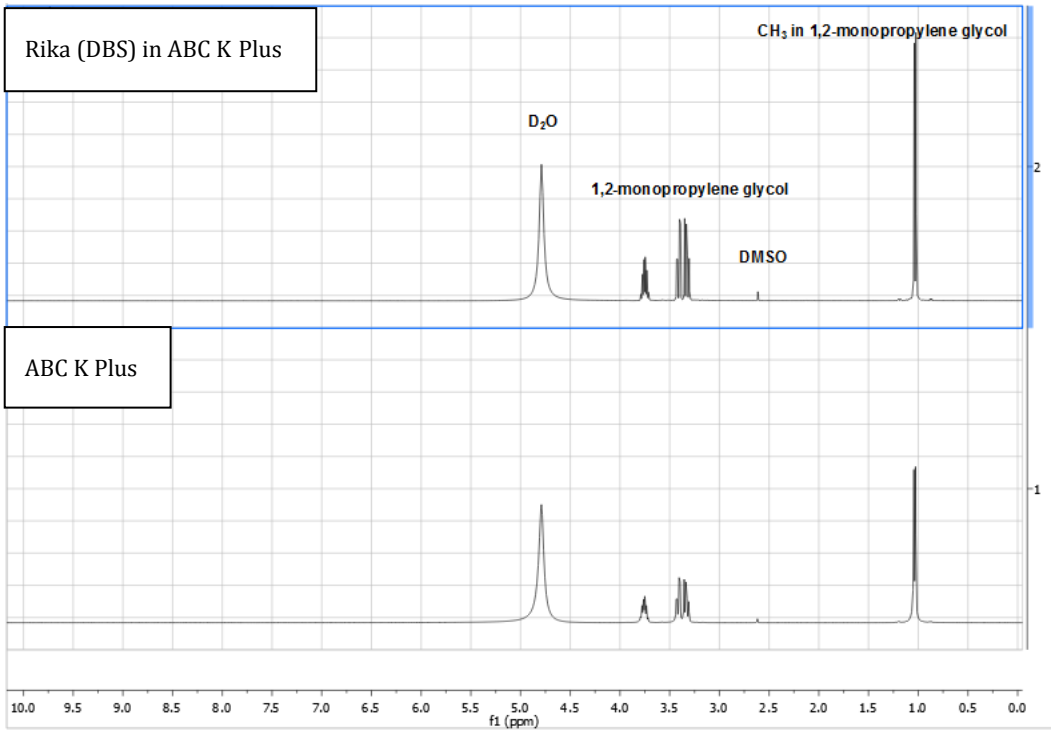

Figure 6.26 Comparison of ABC K Plus anti-icing product with ABC K Plus containing 0.1% w/v Rika (DBS)

Both DBS-OCH_3 and DBS-SCH_3 were tested in the same way in each of the anti-icing products and showed the same results as demonstrated in **Figure 6.26.**

6.2.8 Water Spray Endurance Test (WSET)

We then went on to perform water spray endurance testing (WSET). To try and simulate the same conditions in which anti-icing fluids are tested, we decided that due to samples containing 0.1% w/v gelator existing as solid gels at room temperature, they would not be tested further at this stage. Samples containing 0.05% w/v and 0.025% w/v of each of the gelators in each of the anti-icing fluids all existed as partial and/or weak gels and therefore were similar to the original anti-icing products which exist as viscous solutions at room temperature. Therefore these samples could be applied at room temperature without any further heating. Anti-icing fluids are commonly used undiluted which we describe as 100%, diluted with water, either 75:25 product:water or a 50:50 product:water dilution. Therefore, 100% undiluted samples will provide the longest holdover, due to the high content of MPG, with 50% dilutions providing the least, which after dilution actually only contains 25% MPG. For a fluid to be classified as an anti-icing fluid the SAE ASTM1428[33] standard states that it must be able to meet specific time limits for each dilution, see **Table 6.7**.

Table 6.7 Minimum holdover times as specified by the SAE for the undiluted and diluted products.

Dilution	**Minimum WSET Holdover Time (minutes)**		
	Type II	*Type III*	*Type IV*
100%	30	20	80
75%	20	Report	20
50%	5	Report	5

Samples created in **Section 6.2.4** were used for testing on the WSET. 100 ml of each sample in the undiluted anti-icing products with 0.05% w/v and 0.025% w/v gelator were used without further preparation whilst the remaining 100 ml of each sample was diluted with hard water to create a 50% dilution of the product. Only 100% and 50% dilution samples were tested as worst case scenario samples. To ensure comparisons could be made to the original 100% anti-icing fluids and 50% dilutions of each anti-icing fluid, control samples of each product were run alongside each sample.

Anti-icing fluids are selected based upon the outside air temperature (OAT) and hence the required freeze point protection they require as well as the length of holdover. Anti-icing fluids in the UK and throughout Europe are generally used in a

one step procedure where the anti-icing fluid is applied hot and acts to de-ice and then anti-ice all in one step. Therefore the anti-icing fluid that is selected will be based on how long the aircraft needs to be protected with anti-icing fluid for before it takes off, which allows the user to select the correct dilution of fluid that needs to be applied.

From **Table 6.8** we can see that all of the original undiluted anti-icing products meet the specified holdover requirements set by the SAE. ABC 3 and ABC K Plus are classified as Type II products and therefore in their undiluted state should have a minimum holdover of 30 minutes whilst, ABC S Plus is a Type IV product which should provide a minimum of 80 minutes. All products exceed the minimum requirements. When we add Rika (DBS) into each of the anti-icing products we can see from **Table 6.8** that adding just 0.05% w/v of gelator can increase the holdover by 19 minutes in ABC 3, 45 minutes in ABC K Plus and 7 minutes in ABC S Plus. When we reduce the concentration of Rika (DBS) to 0.025% w/v we again increase the holdover by 4 minutes in ABC 3, 48 minutes in ABC K Plus and 28 minutes in ABC S Plus. Therefore adding the gelator to an anti-icing product allows for the creation of a hybrid gel network which helps to improve the holdover time of each of the products. ABC 3 is most enhanced when 0.05% w/v Rika (DBS) is added and less so at lower concentrations.

Table 6.8 Holdover times achieved for Rika (DBS) at 0.05% w/v and 0.025% w/v in the original undiluted anti-icing products ABC 3, ABC K Plus and ABC S Plus.

Product	Control	Holdover Time (min:secs)	
		0.05% w/v	**0.025% w/v**
ABC 3	33:25±1:18	52:59±2:02	37:50±1:27
ABC K Plus	68:13±2:38	113:39±4:22	116:35±4:30
ABC S Plus	90:41±3:29	97:14±3:44	118:03±4:32

ABC K Plus shows, regardless of concentration, that the holdover times can be enhanced and are very similar. This polymer has a more cross-linked structure and it appears that the gelator and polymer are able to interact better to create a hybrid network which can almost double the holdover time of the original product. The polymer within ABC S Plus is the most highly cross-linked polymer however has the least amount of modification to its structure. Therefore this polymer is the most entangled and as a result generally provides higher viscosities. However, it appears that the hybrid gel network that can be created between the gelator and polymer within ABC S Plus provides the greatest holdover when there are small (0.025% w/v)

concentrations of gelator present. This may suggest that larger amounts of Rika (DBS) are not able to fully form and optimise their network.

When hybrid gels containing DBS-OCH_3 were tested in each of the anti-icing products we can see from **Table 6.9** that like Rika (DBS) the holdover times achieved within each product follow a similar pattern. At 0.05% w/v we note the holdover increases by 5 minutes in ABC 3, 16 minutes in ABC K Plus and 2 minutes in ABC S Plus. Whilst when 0.025% w/v of gelator is used within each of the anti-icing products the holdover again increases for each of the products with the holdover for ABC 3 increasing by 3 minutes, 19 minutes in ABC K Plus and 18 minutes in ABC S Plus. However this time, regardless of the concentration of gelator in ABC 3 we achieve similar holdovers, and the same is true in ABC K Plus. The main difference lies when there is only 0.025% w/v of gelator in ABC S Plus. This increase in holdover could be attributed to the correct balance of hydrophobicity of the polymer with the correct concentration of gelator being able to fit in between the entanglements of the polymer and hence interact with one another effectively to create a hybrid gel. In general DBS-OCH_3 is slightly less effective than Rika (DBS).

Table 6.9 Holdover times achieved for DBS-OCH_3 at 0.05% w/v and 0.025% w/v in the original undiluted anti-icing products ABC 3, ABC K Plus and ABC S Plus.

Product	Control	Holdover Time (min:secs)	
		0.05% w/v	**0.025% w/v**
ABC 3	33:25±1:18	38:23±1:28	36:10±1:24
ABC K Plus	68:13±2:38	84:37±3:15	87:04±3:21
ABC S Plus	90:41±3:29	92:23±3:34	108:34±4:10

From **Table 6.10** we can see that when DBS-SCH_3 was tested in each of the anti-icing fluids, it too could also create gel networks which provide longer holdover times than the original products. At 0.05% w/v the holdover in ABC 3 increased by 17 minutes, in ABC K Plus by 36 minutes and in ABC S Plus by 12 minutes. When we reduced the concentration by half to 0.025% w/v we again achieved higher holdovers with the holdover increasing by 13 minutes in ABC 3, 38 minutes in ABC K Plus and 31 minutes in ABC S Plus, significant improvements.

Table 6.10 Holdover times achieved for DBS-SCH_3 at 0.05% w/v and 0.025% w/v in the original undiluted anti-icing products ABC 3, ABC K Plus and ABC S Plus.

Product	Control	Holdover Time (min:secs)	
		0.05% w/v	**0.025% w/v**
ABC 3	33:25±1:18	50:41±1:57	46:11±1:46
ABC K Plus	68:13±2:38	104:47±4:01	106:07±4:05
ABC S Plus	90:41±3:29	102:41±3:57	121:35±4:41

From **Figure 6.27** we can see when we add any one of the three gelators into an anti-icing product, which potentially creates a hybrid network between the polymer network and gelator network, we can increase the holdover times of each product. In all products we see that the greatest increases in holdover are achieved with Rika (DBS) or DBS-SCH_3. DBS-OCH_3 also increases the holdover times of each product but not as much as the other two gelators. Generally we see with Rika (DBS) and DBS-SCH_3 we can increase the holdover by ~20 minutes in ABC 3, > 30 minutes in ABC K Plus and 5-10 minutes in ABC S Plus. Therefore the greatest increase in holdover performance is achieved in ABC K Plus. We suggest this is a result of the nature of the polymer. This polymer can be described as having a medium amount of cross-linking with medium hydrophobic modification when compared to the other polymers. Therefore this may create an ideal environment for interactions to occur between the gelator and polymer and with the increased hydrophobic nature of the polymer and solvent system in the product having 50% MPG may encourage self assembly and hence aggregation of gelator with the polymer. It is worth noting that the addition of these gelators to ABC K Plus converts a Type II anti-icing product into a Type IV product under these conditions.

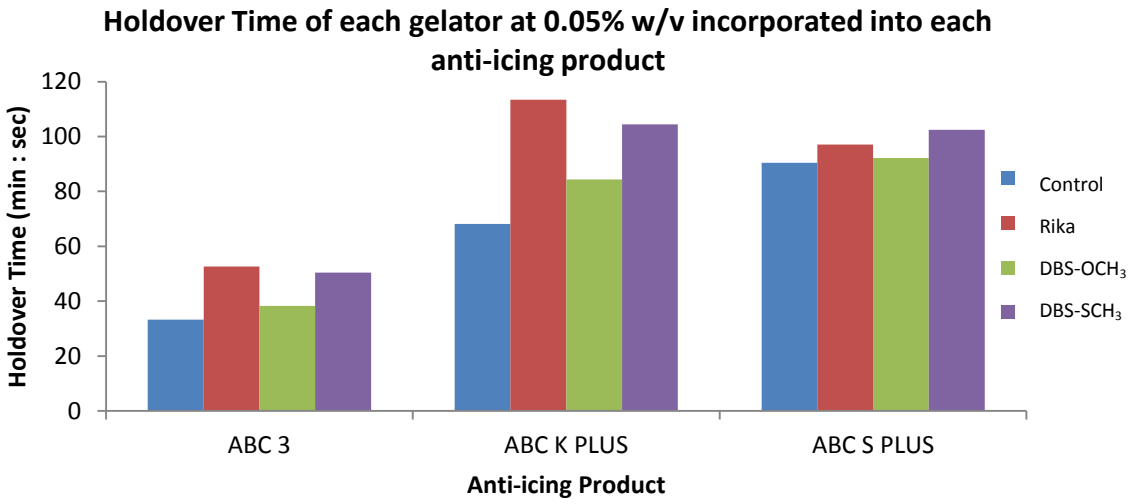

Figure 6.27 Comparison of holdover times achieved from the original 100% anti-icing products with samples containing 0.05% w/v of each gelator in the different anti-icing products.

We also tested them in their most dilute form of the product - 50%. 50% dilution of anti-icing fluid with water is the lowest dilution ever used in order to meet the correct freeze point and holdover time. Therefore, to identify if incorporating gelators into anti-icing fluids diluted to 50% and hence only containing 25% MPG could improve the holdover times, as in the undiluted products shown above, samples containing 0.05% w/v and 0.025% w/v of each of the gelators were tested in each of the anti-icing fluids and compared to control samples of each anti-icing fluid diluted to 50%.

From **Table 6.11** we note that each of the original anti-icing products all meet and/or exceed the minimum 5 minutes holdover required for a 50% diluted anti-icing product. With the incorporation of Rika (DBS) to ABC 3 at 0.05% w/v we see that the holdover obtained is very similar to the original product. In ABC K Plus, the inclusion of the gelator increases the holdover by 3 minutes and in ABC S Plus, by 5 minutes. However when we halve the concentration of gelator added to 0.025% w/v the holdovers for both ABC 3 and ABC K Plus remain similar to the original product, and a small increase of 2 minutes observed for ABC S Plus. Therefore incorporating Rika (DBS) into a 50% dilution of each of the anti-icing products does not give such big increases in holdover as were observed in the undiluted products and this may be due to the low MPG content and hence high water content. We know from previous chapters that the self assembly of the gelators is based upon hydrophobic effects, however they reach a point where self assembly is not favoured and they can no

longer build to create a stiff gel network. Therefore this solvent mixture may be at the maximum to which the gelators can self assemble.

Table 6.11 Holdover times achieved for Rika (DBS) at 0.05% w/v and 0.025% w/v in 50% dilution of each anti-icing product with water.

Product	Control	Holdover Time (min:secs)	
		0.05% w/v	**0.025% w/v**
ABC 3	6:13±0:15	6:43±0:15	6:52±0:16
ABC K Plus	5:22±0:13	8:27±0:19	6:43±0:15
ABC S Plus	9:36±0:22	14:52±0:35	11:14±0:25

When DBS-OCH_3 was tested in each of the anti-icing products at 50% dilution the findings were similar as for Rika (DBS) above, see **Table 6.12**. At 0.05% w/v gelator in ABC 3 we see no real increase in holdover, in ABC K Plus the holdover increases by 3 minutes and in ABC S Plus by 2 minutes. When we halve the concentration of gelator, again the holdovers achieved for both ABC 3 and ABC K Plus remain similar to the original product with ABC S Plus again showing an increase of 2 minutes.

Table 6.12 Holdover times achieved for DBS-OCH_3 at 0.05% w/v and 0.025% w/v in 50% dilution of each of the anti-icing products with water.

Product	Control	Holdover Time (min:secs)	
		0.05% w/v	**0.025% w/v**
ABC 3	6:13±0:15	6:52±0:16	6:40±0:15
ABC K Plus	5:22±0:13	8:19±0:19	6:09±0:14
ABC S Plus	9:36±0:22	11:05±0:26	11:10±0:26

DBS-SCH_3 in each of the 50% diluted anti-icing products showed the greatest increase in holdover across all products of all the gelators. When 0.05% w/v of DBS-SCH_3 was incorporated into each product we observed an increase of 2 minutes holdover in ABC 3, 4 minutes in ABC K Plus and 5 minutes in ABC S Plus. And when the concentration was halved we observed an increase of 1 minute for ABC 3, 1 minute for ABC K Plus and 10 minutes for ABC S Plus, see **Table 6.13**.

Table 6.13 Holdover times achieved for DBS-SCH_3 at 0.05% w/v and 0.025% w/v in 50% dilution of each anti-icing product with water.

Product	Control	Holdover Time (min:secs)	
		0.05% w/v	**0.025% w/v**
ABC 3	6:13±0:15	8:04±0:19	7:46±0:18
ABC K Plus	5:22±0:13	9:01±0:21	6:54±0:16
ABC S Plus	9:36±0:22	14:37±0:35	19:12±0:44

From **Figure 6.28** comparing all of the differing anti-icing products diluted to 50% with the anti-icing fluids containing each of the gelators we can see that generally in ABC 3 and ABC K Plus with both Rika (DBS) and DBS-OCH_3 we achieved a similar holdover compared to the original products, whilst DBS-SCH_3 gives the greatest improvement. However, in ABC S Plus we see that both Rika (DBS) and DBS-SCH_3 provide the same 5 minutes increase in holdover, effectively doubling the minimum holdover required for a 50% diluted anti-icing product. Overall the hybrid gel networks created using DBS-SCH_3 generally give the greatest improvement throughout all products.

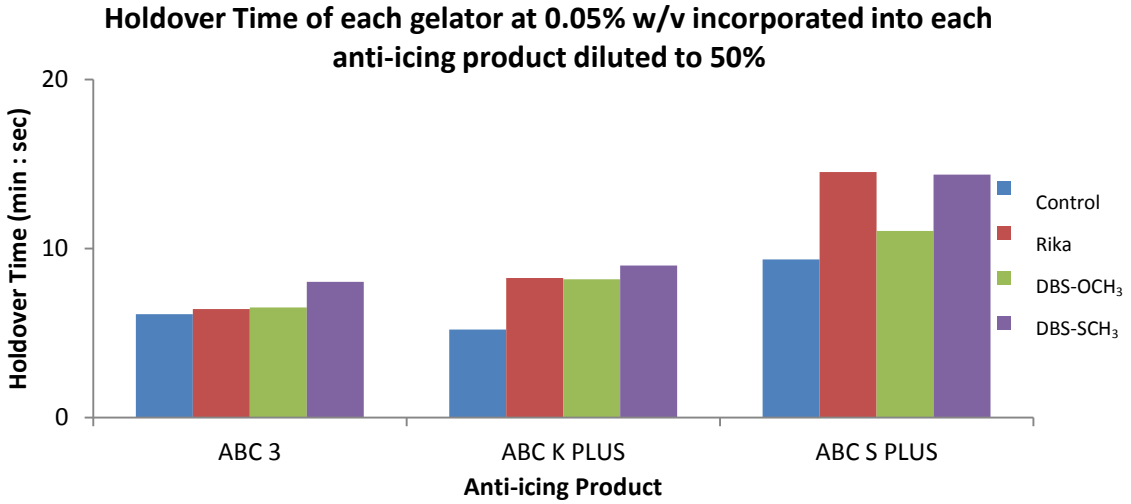

Figure 6.28 Comparison of holdover times of 50% dilution of each anti-icing product with samples containing 0.05% w/v of each gelator in each anti-icing product diluted to 50%.

From the WSET analysis of each of the gelators in each of the anti-icing products we have found that incorporating gelators into these types of fluids allows the formation of hybrid gel networks between the polymer and gelator. Through the formation of these networks we can improve the behaviour of an anti-icing product by increasing its holdover performance. Using low concentrations of gelator between 0.05% w/v and even 0.025% w/v combined with low concentrations between 0.2-0.4% w/v of polymer we can increase the holdover by 15-66 %. However upon further dilution we can improve the holdover by 20-55 %.

6.2.9 Aerodynamics

To understand the aerodynamic impact that anti-icing fluids with added gelator may have on an aircraft after application, we carried out a rheological analysis on each of the samples using a time sweep analysis with increasing strains as described in

Chapter 5. Samples were not tested using the industrial test method known as the boundary layer displacement thickness test (BLDT) as the gels cannot be applied hot and the gels could not be spread evenly on the surface of the instrument.

Using rheology allows us to identify how much of the gel structure can be broken down and removed from an aircraft with increasing strain, similar to what would be experienced during takeoff. The AS9000[385] (BLDT standard) standard states that for an anti-icing fluid to be used effectively and not affect the aerodynamics of an aircraft it must be able to demonstrate that the fluid can be broken down by 74% of its original viscosity value. Therefore if the gel structures created when gelators are incorporated into anti-icing fluids can be removed effectively they have the potential to be used as improved anti-icing fluids.

Three time-sweeps within the same test have been carried out where each sample is applied to the rheometer plate as a hot solution above its T_{gel} value and allowed to set on the rheometer plate to form the gel. The first time-sweep is performed using a strain value within the LVR to ensure the structure is not damaged and the stiffness of the original gel determined. Within the second step increasing strains outside of the LVR are applied similar to what would be experienced during take-off, and finally the third step allows us to determine if these gels would rebuild, by again applying a low strain value as in step one which is in the LVR over a longer period of time.

From **Figure 6.29** and **Table 6.14,** for each of the gelators when in ABC 3 compared to the original ABC 3 anti-icing product we can note that all of the samples have similar stiff networks, then as high strain is applied, in this case it is the worst case scenario of very high strain (100%) similar to the high stress that would be exerted onto an aircraft during takeoff, we see that all of the different gel networks break down. Each of the gel networks in ABC 3 as well as the control samples all break down by roughly 60-70% of their original G' values. Therefore if we compare this to the 74% accepted value that the AS9000 standard states we can see that the control product as well as the products with gelator in all do not quite reach the minimum requirement. This suggests that the structure of the gel networks have not broken down enough and removed from the surface of an aircraft that would allow an aircraft to take off safely. However, each of these products are certified and do indeed pass the actual BLDT when tested using that instrument, therefore using the 74% reduction of the original viscosity value within the rheological test method is not fully representative. This is primarily due to the different means of testing. The BLDT

instrument uses a fan to create a fast airflow representative of an aircraft taking off. The airflow across the surface of the fluid shears and hence applies stress to the fluid which in turn is removed from the surface. However on the rheometer we do not have the capability of representing the shear and stress that is exerted from a high speed fan instead high oscillatory movements of the geometry on top of each sample is applied at high strain under controlled temperature and timed conditions. However, we can deduce that with the incorporation of each of the gelators to ABC 3 they potentially have the ability to be removed effectively from an aircraft as the percentage of fluid that is removed compared to the control sample is very similar. Upon the removal of high strain to each sample, we see from each of these samples as well as the control sample that they exhibit thixotropic behaviour where the gel structure can be seen to rebuild over time. The anti-icing fluids are known to behave as thixotropic fluids, where after shearing, through the action of spraying the fluid on to an aircraft, the fluid can actually rebuild and form a thick layer of anti-icing fluid on the cold surfaces of an aircraft. Each of the gelator samples can effectively recover between 70-80% of their original structure. However this is lower than the recovery of ABC 3 alone (92%) and suggests these materials may be suitable for use on aircrafts.

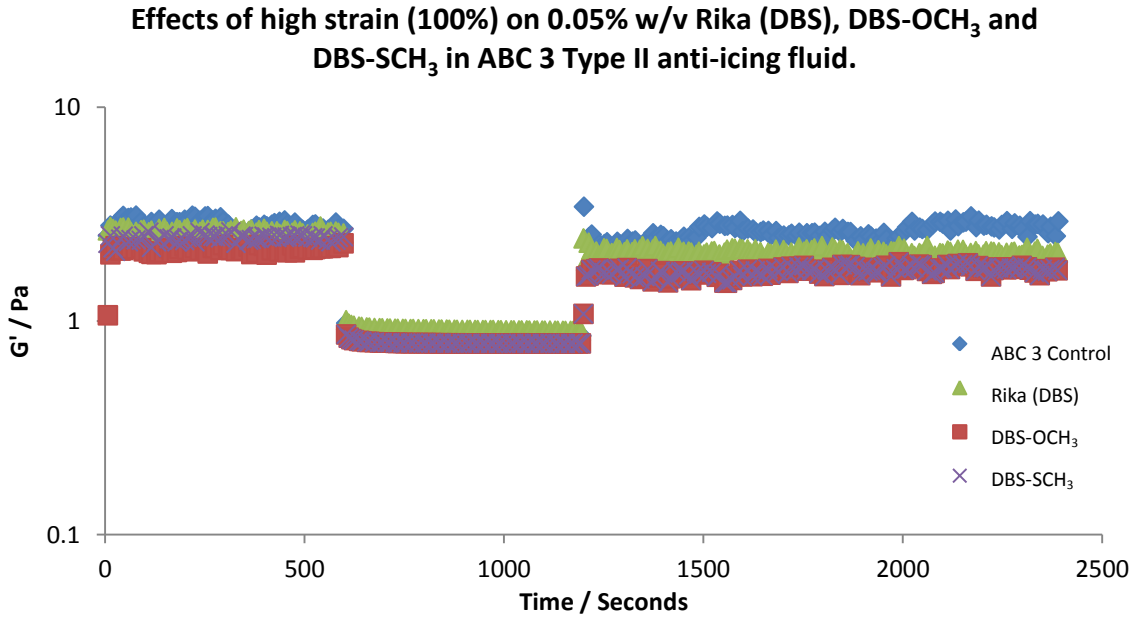

Figure 6.29 Effects of high strain (100%) on 0.05% w/v Rika (DBS), DBS-OCH_3 and DBS-SCH_3 in ABC 3 Type II anti-icing fluid.

Table 6.14 Percentage of fluid removed after high strain and the percentage recovery of each of the gel networks formed with each gelator in ABC 3.

Gelator	% Fluid removed after high strain	% Recovery of Gel network compared to original value
Rika (DBS)	66	80
DBS-OCH_3	63	80
DBS-SCH_3	68	70
ABC 3 Control	69	92

When we tested the gelators in ABC K Plus we can see from **Figure 6.30** that the gel networks formed within ABC K Plus produce much stiffer gels with higher G' values compared to the control ABC K Plus sample. However unlike the samples above in ABC 3, the samples containing each of the gelators were more fully broken down than the original product, with 76-80% of the original gel network stiffness being removed upon application of high strains, see **Table 6.15**. Therefore although the control sample shows that it is only capable of breaking down the polymer gel network by 57% the incorporation of the gelator molecules to the anti-icing fluid which creates the hybrid gels must introduce more sensitivity to strain. When these gelators in ABC K Plus have the strain removed the hybrid gel networks are able to regain 80-96% of their original structure, however the control sample can only regain ~50% of its original gel structure.

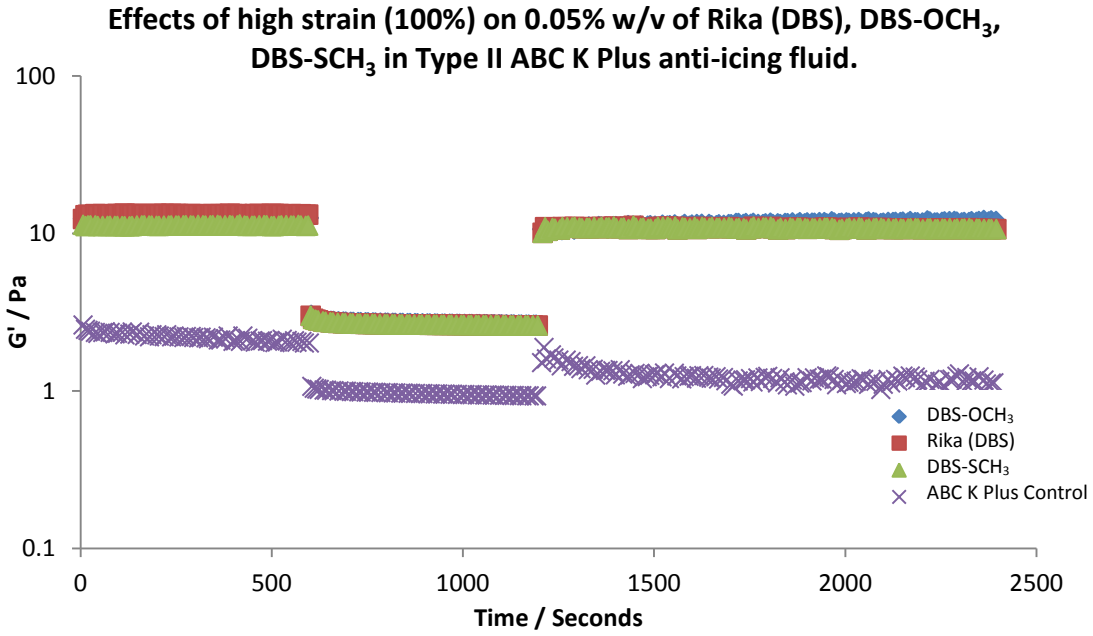

Figure 6.30 Effects of high strain (100%) on 0.05% w/v Rika (DBS), DBS-OCH_3 and DBS-SCH_3 in ABC K Plus

Table 6.15 Percentage of fluid removed after high strain and percentage recovery of each gel network for each gelator in ABC K Plus

Gelator	% Fluid removed after high strain	% Recovery of Gel network compared to original value
Rika (DBS)	80	82
DBS-OCH_3	78	93
DBS-SCH_3	76	96
ABC K Plus Control	57	56

Adding each of the gelators into ABC S Plus we see the same trend in behaviour as the other products. We note that with the incorporation of the gelators to the anti-icing fluids we create hybrid networks which have greater stiffness and hence higher G' values compared to the control sample, see **Figure 6.31**. Upon application of high strain to each of the samples all of the gel networks are reduced. The hybrid gel networks are much more easily broken down and hence removed by 80-90% whilst the control sample under high strain can only be removed by 77%, see **Table 6.16**. Once the strain is removed we see the same behaviour as before with the gel networks reforming. The hybrid gels containing Rika (DBS) and DBS-SCH_3 show to effectively almost regain their full structure ~90-96% whilst gels made using DBS-OCH_3 could only rebuild up to 70% of their original structure like the control sample.

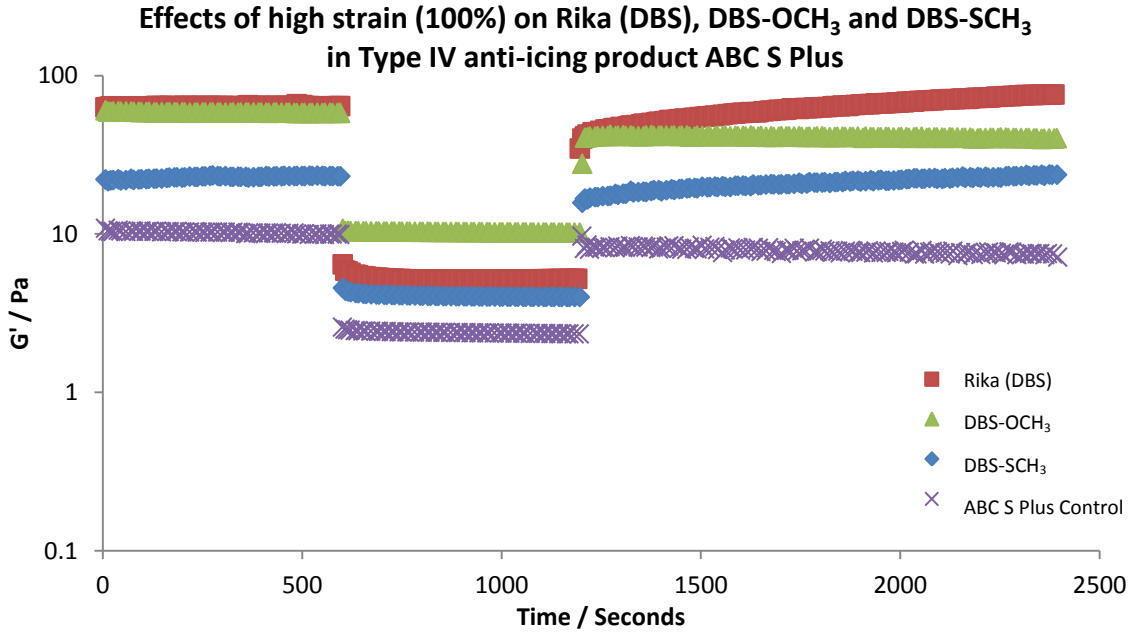

Figure 6.31 Effects of high strain (100%) on Rika (DBS), DBS-OCH_3 and DBS-SCH_3 in ABC S Plus

Table 6.16 Percentage of fluid removed after high strain and percentage recovery of each gel network formed by each gelator in ABC S Plus

Gelator	% Fluid removed after high strain	% Recovery of Gel network compared to original value
Rika (DBS)	92	96
DBS-OCH_3	83	70
DBS-SCH_3	82	91
ABC S Plus Control	77	77

By incorporating gelators into anti-icing products we have effectively created stiffer gels with higher G' values when compared to each of the control anti-icing fluids. Although the gels are stiffer they are still capable of being broken down easily by strain and in some cases, much more effectively than the original anti-icing fluids when they are subjected to high strains representative of an aircraft taking off. However they do exhibit thixotropy. Although each of the hybrid gels are thixotropic and can rebuild almost all of their original gel structure the anti-icing fluids are also somewhat thixotropic, so as long as all of the fluid is completely removed before take off the aircraft should potentially see no increased effects on the aerodynamics. However should some of the gel structure be left on the surface of the aircraft it could potentially build up over time in aerodynamic quiet areas preventing the aircraft from operating correctly.

6.3 Conclusions

In this chapter we have demonstrated the ability of the gelator molecules, Rika (DBS), DBS-OCH_3 and DBS-SCH_3 to form gels in very complex fluids such as anti-icing fluids which contain polymeric thickeners to create hybrid gel nanostructures with potential use as anti-icing fluids for aircrafts.

We have shown the gelation ability of each of the gelator molecules in three different commercially available anti-icing products known as Type II (ABC 3 and ABC K Plus) and Type IV (ABC S Plus) anti-icing fluids. Through the gelation screening it is evident that adding gelators to each of the anti-icing products we can create gel structures with very low concentrations of gelator. Concentrations of each gelator that are required are 4 times less the minimum concentration that was required to form gels in de-icing fluids demonstrated in Chapter 5.

The thermal stability of each of the anti-icing fluids containing each gelator appeared very similar. The gels had greater thermal stabilities than when the gelators where added to a de-icing fluid with no additional polymeric thickener.

Scale-up of each of the samples proved that gels formed on a smaller scale are not always fully representative of the effects on larger scale which can be used commercially. As a result we observed concentrations of only 0.1% w/v of each gelator formed stiff gels which were self supporting when inverted, whilst partial gels could be formed when lower concentrations were used.

Rheologically we found that when gelators are added to ABC 3 they can enhance the stiffness of the gel network a little but provide no extra strength, however when in ABC K Plus and ABC S Plus we could see both the stiffness of the gel and strength, hence resistance to strain increase significantly. DBS-SCH_3 had no change in resistance to strain in all of the different anti-icing products but could increase the stiffness of the gel structure formed. For the stiffness of the gel structure in each case to increase would suggest that the polymer and gelator molecules are cooperating to create a stiffer gel with increased strength in some cases.

When tested for their performance with increasing frequency, we found that in ABC 3 regardless of the gelator all samples showed characteristic behaviour of a gel where G' was independent of frequency and G'>G'' up to 1 Hz. At higher frequencies the samples become frequency dependent and were characteristic of visco-elastic solids similar to the original anti-icing product. In ABC K Plus, the gelators showed similar behaviour as in ABC 3 however they were more independent of frequency. DBS-SCH_3 was independent of frequency up to 2.5 Hz whilst Rika (DBS) and DBS-OCH_3 were more independent up to 15 Hz. At higher frequency they also showed to be dependent on frequency and change into visco-elastic solids. The same behaviour was also observed when in ABC S Plus but again the range of independence of frequency increased for each gelator up to 8 Hz for DBS-SCH_3 and 15 Hz for both Rika (DBS) and DBS-OCH_3.

Rheology has also demonstrated that these types of gel systems are temperature dependent. Gels formed in ABC 3 are the least thermally stable whilst gels formed in ABC S Plus are the most thermally stable, with ABC K Plus lying in between the two. This is most likely due to the nature of the polymer. Although the concentration of polymer in both ABC 3 and ABC K Plus is similar at 0.2% w/v and double in ABC S Plus (0.4% w/v) it is most likely the degree of cross-linking and hydrophobic

modification that creates the different thermally stable gels. ABC 3 has the least amount of cross-linking but has the highest degree of modification whilst ABC S Plus is the most cross-linked polymer with the least amount of modification and therefore as a result of the increased cross-linking in ABC S Plus this results in higher temperatures being required to breakdown the polymer-gelator network. This also agrees with the effects on G' in each of the anti-icing products.

Using rheology, we have been able to show that Rika (DBS) and DBS-OCH_3 in ABC S Plus form gels relatively quickly between 10-17 minutes whilst in ABC K Plus and ABC 3 gels require longer periods of time with ABC 3 almost requiring double the time (20-44 minutes). However, when DBS-SCH_3 was tested in each of the anti-icing products it was difficult to determine how quickly the gels formed, as before the test could start the gel showed to have reached its maximum G' and plateau. The time achieved for DBS-SCH_3 in ABC 3 however would suggest that of all the gelators formed with DBS-SCH_3 could form gels much more quickly.

SEM analysis of the polymers used within each of the anti-icing fluids suggested that the polymer molecules create globular structures that can amalgamate into larger structures which encompass the whole sample. TEM provided evidence of a fibrillar nanostructure from the DBS and the polymer network. With both Rika (DBS) and DBS-SCH_3 there was evidence to suggest that the polymer molecules were in fact interacting along the gelator fibres potentially creating a hybrid gel between the two. DBS-OCH_3 proved more difficult to image and as a result it was unclear if similar types of structures were being created.

Analysis using NMR suggested both the polymer and gelator molecules were immobilised into a gel network whilst the solvent remained mobile.

These type of hybrid gel systems showed that they may have potential to be used as a more advanced anti-icing fluid. WSET results showed us that when each of the gelators were incorporated into the different anti-icing products they could all increase the length of time (holdover) that a potential aircraft could be protected in winter conditions. The holdover values could be seen to increase by 55% in ABC 3, 66% in ABC K Plus and 13% in ABC S Plus in the undiluted products. Analysis was also carried out on the samples when they were diluted to 50%, simulating the lowest dilution that is possibly used within this application. The holdover times for each of the diluted products also showed to increase the holdover by 20-55%. Therefore the hybrid gel networks that are created show the best optimisation when in ABC K Plus

and this may be due to the degree of cross-linking the polymer possesses as well as the amount of hydrophobic modification. This medium balance of both may allow the ideal environment of interactions to occur between the gelator and polymer molecules to create a thick film which protects for longer.

Aerodynamically although the hybrid gels are very stiff in comparison to the original anti-icing products they have been shown to break down easily with high strain, similar to that experienced during takeoff. When gelators are incorporated into each of the products they are removed just as well as the original product, and in most cases they are removed better, with less of the sample remaining on the surface after they have been subjected to high strains. Each sample however does exhibit thixotropy, and the gel structures can rebuild by >90%. This potentially can lead to problems with the build up of gel in aerodynamically quiet areas should the gel structures not be fully removed before take-off.

Throughout this work we have demonstrated that it is not only possible to incorporate gelator molecules into a very complex formula such as an anti-icing fluid which contains polymeric thickeners, but that we can also enhance the existing properties of such a fluid retaining the advantages of both the polymer and the self-assembling gelator. This type of advance within the aviation industry is unheard of, and may help pave the way to investigate, develop, standardise and identify new classifications of de/anti-icing fluids for the future.

The next stages of this work would be to develop different types of hybrid gel systems to identify if by using two different gelator molecules together to create a hybrid would enhance the properties further than the polymer–gelator network investigated within this chapter.

Chapter 7

Preliminary Studies for Future Work

Chapter 7 Preliminary Studies for Future Work

7.1 Future Work

In Chapter 6 we demonstrated the ability of hybrid gels composed of a combination of a polymer network and a low molecular weight gelator network to improve the performance of an anti-icing fluid to provide greater protection to an aircraft during winter. As a result of this we have begun to look at the possibility of creating hybrid gels using a combination of two low molecular weight gelator species. Through this research we have shown that three molecules Rika (DBS), DBS-OCH_3 and DBS-SCH_3 have all been successful in their own right by either having the capability to form a gel in industrially relevant solvents or improving the performance of de-icing or anti-icing fluids. Rika (DBS) can be bought commercially and has no adaptations to its structure performed well across the board, while DBS-SCH_3 showed its performance was optimum at very low concentrations <0.1% w/v. Therefore to identify if gels could be made at low concentrations, preferably lower than our current polymer concentrations, with these two known gelators we combined them in some preliminary studies to make a potential hybrid nanostructure.

7.1.1 Gelation Testing

Initial tests were conducted using Rika (DBS) as the main constituent to form a gel. The reduction of Rika (DBS) by 10% and 50% would be replaced with 10% and 50% DBS-SCH_3 creating a potential hybrid system which could potentially operate at an overall lower concentration.

Samples were prepared at 0.5% w/v and 0.1% w/v only as we were trying to form gels that have similar or lower concentrations to the current polymers found in anti-icing fluids which use 0.2-0.4% w/v. Samples at 0.5% w/v were prepared by weighing out 90% (4.5 mg) of 0.5% w/v of Rika (DBS) into a 2 ml glass vial. To the same vial 10% (0.5 mg) DBS-SCH_3 was added. 1 ml of solvent was then added to each vial which was sonicated for 1 hour before being heated in an oil bath to just below the boiling point of the solvent until a clear homogenous solution had formed. Samples were removed from the oil bath and left to cool on the bench at room temperature overnight with results recorded the next day. The same procedure was also followed for concentrations of 0.1% w/v.

Samples containing the same concentrations of 0.5% w/v and 0.1% w/v were also prepared with 50% of each of the gelator making up the final concentration. All samples were prepared and treated in the same way as described above with results recorded the next day.

From **Figure 7.1** we can see that with just a 10% reduction of Rika (DBS) at 0.5 %w/v we can create gels not only in the different MPG mixtures but also in the more complex Type I de-icing fluid DF Plus. From Chapter 3 we note that with the incorporation of two different LMWG we have been able to increase the solubility of these molecules in industrially relevant solvents compared to when they were tested individually. In Chapter 3 we saw that when Rika (DBS) was added to 100% MPG it remained soluble whilst DBS-SCH_3 formed a gel, however combining them together we form a gel. In 75% MPG they both previously formed a gel and again show to form a clear gel. Previously in 50% MPG Rika (DBS) formed a gel whilst DBS-SCH_3 remained insoluble however when combined the solubility of DBS-SCH_3 increases and both molecules form a gel. When we then changed the solvent to a complex Type I de-icing fluid we see very different results. We see from **Figure 7.1** that clear gels are formed in both the original undiluted product (80% MPG) and when the product is diluted to 50% (40% MPG), however from Chapter 5 we saw that when in the original undiluted product, Rika (DBS) formed a gel whilst DBS-SCH_3 was insoluble and both of these molecules previously remained insoluble when tested in 50% product (40% MPG) whilst now when we combine them they form a clear gel. Therefore with only 10% of Rika (DBS) being replaced with DBS-SCH_3 we have been able to significantly increase the solubility of each of the molecules in the different solvent systems and potentially extend the operating range of these additives.

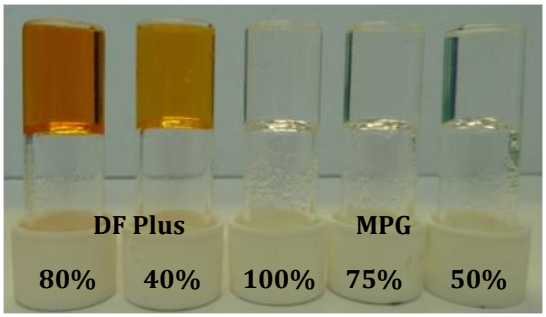

Figure 7.1 Gelation screening of hybrid gels at 0.5% w/v containing 90% Rika (DBS) with 10% DBS-SCH_3 in 80% DF Plus, 40% DF Plus (orange), 100% MPG, 75% MPG and 50% MPG (clear).

When we increase the amount of DBS-SCH_3 to 50% to create a hybrid gel with Rika (DBS) at 0.5 %w/v we find again the same results as seen with the addition of 10% DBS-SCH_3, see **Figure 7.2**. However what we also see is that opaque gels are now formed in 100% MPG, 50% MPG and 40% DF Plus. This must therefore be a result of the concentration of DBS-SCH_3. As we know DBS-SCH_3 has a lower solubility in glycol than Rika (DBS), therefore DBS-SCH_3 may be reaching its maximum at which it is soluble when combined with Rika (DBS) and what we are seeing is the beginning of the insolubility of either DBS-SCH_3 and/or Rika (DBS).

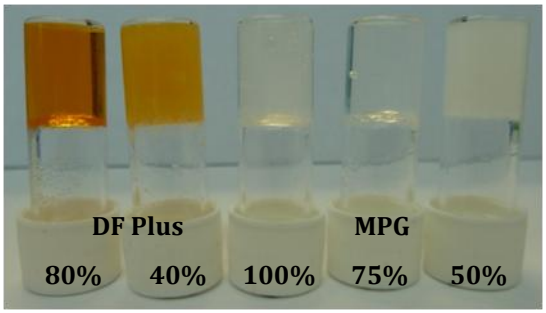

Figure 7.2 Gelation screening of hybrid gels at 0.5% w/v containing 50% Rika (DBS) and 50% DBS-SCH_3 in 80% DF Plus, 40% DF Plus (orange), 100% MPG, 75% MPG and 50% MPG (clear).

7.1.2 NMR Analysis

To try and determine if we were in fact making a hybrid gel between the two different LMWGs we performed NMR analysis on samples containing a final concentration of 0.5 %w/v with Rika (DBS) reduced by 10% with DBS-SCH_3 in 40% DF Plus as shown in **Figure 7.1**. Samples were prepared as described in Chapter 6 **Section 6.2.7** using a stock solution containing D_2O and DMSO as an internal standard. From **Figure 7.3** it is clear there are no peaks corresponding to either of the LMWG molecules and what can be seen is only the solvent (1,2-monopropylene glycol), therefore this would suggest that both molecules are immobilised, appearing invisible on the NMR time scale and potentially creating a hybrid gel network between themselves. Alternatively both of the molecules may be creating their own individual gel networks which then immobilise the solvent within their structures.

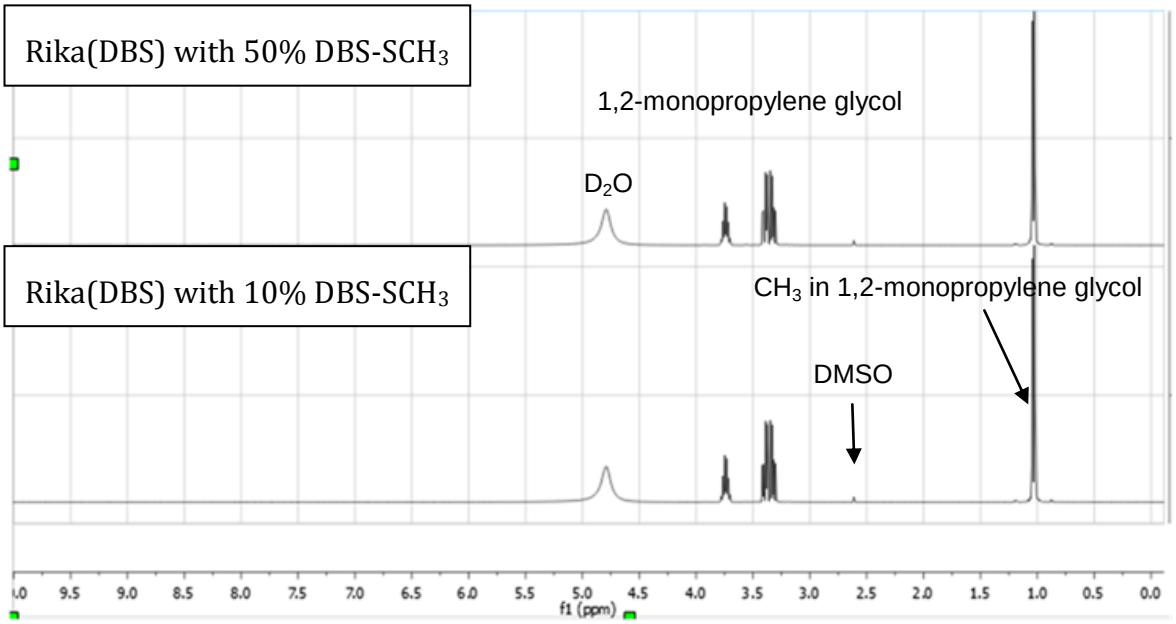

Figure 7.3 ^{1}H NMR analysis of 0.5% w/v samples containing 10% and 50% replacement of Rika (DBS) with DBS-SCH_3 in 80% DF Plus with D_2O and DMSO internal standard.

7.1.3 Reduced concentration gelation testing

The final desired concentration tested was 0.1 % w/v, which would be half the lowest concentration of polymer currently used within a Type II anti-icing fluid. Samples were made in the same way as described in **Section 7.1.1** with results recorded the next day. From **Figure 7.4** with 90% of Rika (DBS) and 10% DBS-SCH_3 in the various solvents we note that gels cannot be formed in 100% MPG, 75% MPG and 80% DF Plus. Previous gelation testing of each of the LMWG on their own in Chapter 3 showed that both molecules at 0.1% w/v and below exist in the soluble state so no change has been observed by combining the two LMWGs, and the same was observed when tested in 75% MPG and 80% DF Plus. Therefore, in this instance, both molecules being soluble in these solvents cannot aid the formation of a gel. However when each of the LMWGs was tested on their own in previous chapters in 50% MPG they both formed gels below 0.1% w/v and hence as a result when combined are also seen to form a gel. Samples were then tested at lower dilutions of DF Plus. As we can see from **Figure 7.4** that with each of the gelators combined in diluted DF Plus containing lowering amounts of MPG, gels are seen to form. However when tested individually Rika (DBS) below 0.1% w/v exists in the soluble state whilst DBS-SCH_3 exists in the insoluble state. Therefore by combining the two gelators the correct balance between hydrophilicity with hydrophobicity must be met in order for the gelators to interact

and form a gel network with the lowering glycol content and higher water content samples of DF Plus.

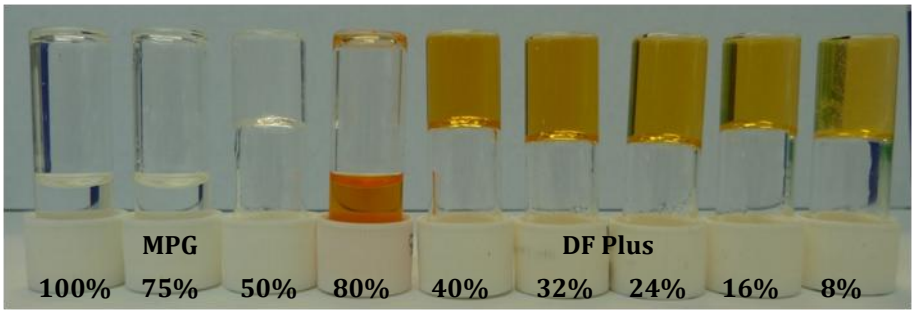

Figure 7.4 Gelation screening of 0.1% w/v samples with 90% Rika (DBS) and 10% DBS-SCH_3 in 100% MPG, 75% MPG, 50% MPG (clear), 80%, 40%, 32%, 24%, 16% and 8% MPG content (orange) in Type I de-icing fluid DF Plus.

When we increase the ratio of DBS-SCH_3 to 50%, equalling the concentration of Rika (DBS) in the same solvents, we can see from **Figure 7.5** that unlike the results shown in **Figure 7.4** we have increased the hydrophobic nature of the LWMG in 75% MPG which has allowed for the creation of a gel. In 50% MPG the gel now appears more opaque compared to **Figure 7.4** and this is most likely down to the fact that DBS-SCH_3 is imparting too much hydrophobicity that the gel network is starting to convert to the insoluble state. Likewise when we increased the concentration of DBS-SCH_3 to the more dilute solutions of DF Plus from 40% DF Plus and lower the gels appear more opaque, this may be a consequence of DBS-SCH_3 being insoluble in DF Plus on its own, however with the aid of Rika (DBS) it balances the solubility with the insolubility of the molecule in these solvents to form a gel.

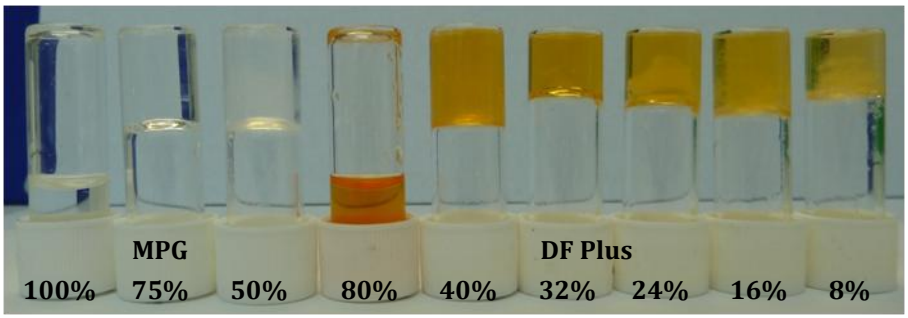

Figure 7.5 Gelation screening of 0.1% w/v samples containing 50% Rika (DBS) and 50% DBS-SCH_3 in 100% MPG, 75% MPG, 50% MPG (clear), 80%, 40%, 32%, 24%, 16%, 8% MPG content (orange) in Type I de-icing fluid DF Plus.

The research described here, testing the combination of two known LMWGs, where potentially one exists in the insoluble state with one that exists in the soluble state to balance one another out to form a gel, is still in its infancy and requires significant

further work. However, the early results would suggest that the problems we experience in very dilute glycol system could be reduced by using such combinations. We have shown with the reduction by 10% of the original gelator and the addition of a second gelator at 10% can increase the solubility in aqueous glycol mixtures at very low concentrations of 0.1% w/v. This therefore has huge potential when trying to devise a new de/anti-icing fluid as it allows for the cost of such a fluid to be greatly reduced as a consequence of lower glycol content and low concentration of LMWG compared to the concentrations currently used for polymers within anti-icing fluids. Not only this, but it may also provide yet further increased holdover times compared to those observed when LMWGs were tested individually in de-icing fluids. Increasing holdover times with increasing water content is completely counter intuitive to how the current polymeric anti-icing fluids work. Therefore this potentially opens up new avenues for the aviation industry to introduce a new fluid which is cheaper, protects for longer, is thermally reversible and more environmentally friendly, that can protect aircraft in winter conditions.

Should this type of hybrid gel system be successful it could be potentially used to create a gel network where each of the two LMWGs would use different triggers. This would allow one gel network to be switched on whilst the other remained dormant, then when the first gel network function had been depleted the other gel network could be switched on. These hybrid gels could also be used to indicate the end of the holdover performance of a fluid. A hybrid gel could contain a dye which is released upon dilution of the fluid with for example ice, and when it reaches 5 minutes before the end of its protection the dye could be released notifying pilots that the aircraft needs re-sprayed to be able to take-off safely. We therefore suggest that hybrid gels offer exciting potential for further development in this technology.

Chapter 8 Conclusions

Chapter 8 Conclusions

During this research a number of structurally different low molecular weight gelators based upon amino acids and sugars were synthesised. These LMWGs had previously been published in the literature as either having the ability to act as a hydrogelator or organogelator. Creating a library of pre-existing LMWGs allowed us to identify specific structural motifs which had the capability of forming a gel in industrially relevant solvents such as glycols commonly used within the aviation industry to protect aircraft during winter.

From a library of ten molecules, only three showed potential to be used with solvents such as glycols. These three molecules were *N*-dodecanoyl-L-alanine, ascorbic acid-6-palmitate and 1,3:2,4-Dibenzylidene-D-sorbitol (DBS). Although all three molecules showed the ability to form gels in one or more of the solvents tested, *N*-dodecanoyl-L-alanine and ascorbic acid-6-palmitate lacked the ability to form gels in aqueous mixtures of glycol. This inability to form gels in aqueous environments limited their use in this type of application. However, DBS was able to form gels at low concentrations and in dilute solvent systems which were thermally stable and were created from densely packed fibres forming 3D sample spanning networks. However, this molecule lacked the ability to form gels in pure water.

To induce enhanced gelation of DBS in water, we then created a library of DBS derivatives to include various different functional groups which would impart more hydrophobicity or hydrophilicity into the structure. From this, we found that not all DBS derivatives can be formed using the same one step condensation/dehydration synthesis and as a result trying to add branched substituents and/or more than one substituent to the DBS structure showed signs of polymerisation. A mixture of electron withdrawing and electron donating functional groups were added to the DBS structure and although the majority of the derivatives could gel one or more of the solvents it was apparent that derivatives with ether or thioether substituents performed better than the original DBS. DBS-OCH_3 and DBS-SCH_3 could gel the required solvents at low concentrations, with notably better thermal stability due to their increased hydrophilicity. The self-assembly of this family of gelators is primarily driven by hydrophobic effects, therefore as the water increases the thermal stability increases. Further derivatisation into longer and more complicated ethers was

conducted however this showed with the inclusion of alkyl chains, the molecules became too hydrophobic and could not form gels.

Analysis of the two major by-products produced through the synthesis of DBS was also performed but with their differing structures, monobenzylidene sorbitol (MBS) and tribenzylidene sorbitol (TBS) were too hydrophilic and too hydrophobic respectively, to form gels in the required solvents. Therefore obtaining the correct balance of hydrophobicity and hydrophilicity within a particular solvent is very important for a molecule to form a gel.

From this new library of DBS derivatives we therefore found two more potential candidates, DBS-OCH_3 and DBS-SCH_3 which could form gels at lower concentrations than DBS as well as having increased thermal stability. These attributes are very favourable in the de/anti-icing industry as low concentrations allow for low costs, more dilute systems allows for the reduction of glycol hence better environmental profiles and increased thermal stability ensures the fluids can be applied at high temperatures to remove frozen contamination from an aircraft.

Having highlighted three structurally similar LMWGs we then investigated how they self assembled through circular dichroism. Circular dichroism highlighted that the absorbance at specific wavelengths was a result of the functional groups attached to each molecule with more electron rich molecules absorbing at higher wavelengths. DBS was also potentially solvent dependent with the intensity of the peaks decreasing with increasing water content which agrees with the fact that the solubility of this molecule lowers with increasing amounts of water. Each LMWG self assembled and disassembled with varying temperature, although DBS-SCH_3 in 50% MPG showed different responses to temperature which we associated with the assembly of two different nanostructures.

Rheology demonstrated that gels formed with DBS and DBS-OCH_3 produced stiff gel networks which were solvent dependent but had similar stabilities regardless of solvent, however DBS-SCH_3 showed different results, where the stiffest gel was the most stable. DBS-SCH_3 was tested at much lower concentrations, hence less gel network, and this therefore explains the reduced stiffness values achieved for this LMWG. At lower concentrations, DBS-SCH_3 has greater capacity to assemble with better solubility which can form gels which are more resistant to strain. Each of the molecules compared to a standard fluid used in aviation has the ability to create gel structures which are 2-3 magnitudes stiffer but are very weak. Temperature analysis

confirmed the assembly and disassembly of these gel networks are temperature dependent with temperatures between 60-100°C. These gel networks therefore have the advantage of being used at low concentrations, in dilute systems where their assembly is greater but are weak with greater stiff networks. This potentially allows for these gels to protect an aircraft during winter whilst being removed easily from the surfaces avoiding any effects to the aerodynamics and the ability to be sprayed at temperatures that customers currently use.

SEM helped us to simulate what types of gel structures can be formed at differing temperatures, similar to what would be experienced in the de/anti-icing application. All of the LMWGs form very similar small twisted helical fibres which form entangled networks, with the exception of DBS-SCH_3 in 50% MPG. This forms flat tape-like fibres which are more crystalline. DBS-OCH_3 also shows signs of crystallisation but not as markedly as DBS-SCH_3. This fits with the view that the oxy-ether is more soluble than the thio-ether in the presence of water due to its ability to form better hydrogen bonds. Noticeably as more water is added to these gel networks the fibres are seen to be smaller and tightly packed together presumably because the water lowers the solubility which then causes more fibres to be nucleated. The size of the fibres produced is thought to be the reason behind the stiffness and thermal stability of the gel networks that are formed using these different DBS derivatives.

To demonstrate the potential industrial and commercial viability of using such gels within the de/anti-icing industry we investigated the use of the three LMWGs in a Type I de-icing fluid known as DF Plus. De-icing fluids are very complex mixtures of various different components including glycol, water, corrosion inhibitors, surfactants and defoamers etc, therefore being able to incorporate these LMWGs into such a fluid showed the potential these molecules can have in this type of application. The gelation ability of these LMWGs in DF Plus showed great promise with the molecules forming gels across a range of concentrations with increasing dilutions. DBS-SCH_3 struggled to form gels at high concentration but excelled at low concentrations. Therefore we have potentially found an alternative thickener technology for the use in bulk solvent systems such as de-icing fluids.

The incorporation into a de-icing fluid does not change the thermal behaviour as noted previously. We still observed that the self assembly was primarily driven by hydrophobic effects whereby the thermal stability increased as the water increased with the most dilute samples being the most thermally stable. Each of the gels formed

analogously to MPG described above, stiff gels where the stiffest gel was with the least dilution and vice versa for DBS and DBS-OCH_3, but again DBS-SCH_3 showed a different behaviour where the strength of the gel networks had doubled and the stiffness of the gels were solvent dependent with the most dilute being the stiffest. Each of the gels could be formed relatively quickly (4-14 minutes) and again were temperature dependent. This therefore allows these new fluids to be applied hot, which will then set quickly on a cold surface to protect an aircraft.

Including LMWG into a Type I de-icing fluid had no effect on the nanostructures that were formed. However, simulating high temperature application of gels showed that when the gels are applied at high temperature to cold surfaces the gel structure becomes more densely packed. There was also evidence of some crystalline structures being present however it was unclear if these were from one of the additional components of the Type I de-icing fluid, and again DBS-SCH_3 created flatter tape-like fibres when diluted compared to the other LMWGs.

Industrial testing with regards to how long these gel structures could protect an aircraft from frozen contamination and how the aerodynamics may be affected were conducted through WSET testing and time sweeps on the rheometer. WSET testing showed that these types of gel structures can in fact convert a Type I de-icing fluid into Type II or Type III anti-icing fluids depending on the concentration of gelator and dilution of solvent used. At all concentrations (high-low) the holdover was increased quite significantly however it was dependent on the solvent dilution. As the solvent was more dilute the holdover increased up to approximately 48-40% MPG then the behaviour was seen to reverse and act like a regular glycol water mixture. Therefore it is apparent that the solvent mixture has to be suited to these LMWG to provide the maximum holdover with holdover being created through the combination of gel strength and glycol content.

Aerodynamically, these LMWGs can be removed easily. Although they are very stiff and strong, the formation of the gel structure through non-covalent interactions allows these gels to be broken down easily and removed from a surface. However each of these LMWG shows thixotropic behaviour where they are seen to rebuild with time. This is not a problem as long as the fluid is removed fully from the aircraft before take-off.

These LMWGs have also shown the potential to be added to even more complex fluids, such as anti-icing fluids, which also contain polymeric thickeners. With the

incorporation of these LMWGs to anti-icing fluids it was evident that the presence of the polymer lowered the concentration of LMWG that was required to form a gel to four times less than what was required in a de-icing fluid. The thermal stability of the gels formed were shown to increase compared to gels formed with de-icing fluids due to the formation of a hybrid gel. The creation of hybrid gels in these fluids enhanced the strength and hence resistance to strain as well as the stiffness of the gel networks. However only marginal increases were observed in ABC 3 compared to the other products. This is presumably because of the nature of the polymer within each of the products having slightly different variations. The polymer within ABC 3 has the least amount of cross-linking with a high degree of hydrophobic modification with the opposite being true for ABC S Plus and ABC K Plus lying in the middle of the two. The hybrid gels have shown to be able to form relatively quickly in each of the different products with each of the gelators (10-44 minutes), with ABC S Plus forming the most quickly and ABC 3 the most slowly.

Through the use of SEM and NMR we were able to deduce that hybrid gels were being formed from the LMWG and polymer where each of their individual nanostructures was present. The long fibrous nature of the LMWG were observed to span throughout each of the samples with the globular structure of the polymer lying along the length of the fibres. This potentially suggests that in some anti-icing fluids interactions are occurring between the polymer and LMWG however they both form gels individually and are both seen to be present. Therefore the presence of both networks is giving rise to the enhanced properties and performances we detected.

In terms of the industrial application the formation of hybrid gels in anti-icing fluids significantly improves the holdover times that can be achieved by 10-66% when in undiluted products and 20-55% when diluted to 50%. These are significant increases with the best performance being observed when in ABC K Plus. Aerodynamically although the hybrid gels that are formed are very stiff and strong they have the potential to be broken down very easily, and in some cases are removed from a surface better than the original anti-icing products. Hybrid gels also have the ability to self heal and rebuild their structure to almost 90% of its original stiffness. Aerodynamically this potentially could be a problem if not removed from the surfaces effectively. However this property of these hybrid gels may be more suited for applications such as in biomedical science.

Throughout the industrial analysis it was evident that the current test methods of WSET and BLDT that are used to identify anti-icing fluid properties and performance could be improved to simulate real life application better. Therefore we suggest that these two methods could in fact be combined. This would allow for the holdover performance to be determined at set intervals where for instance an aircraft may take off before the holdover time has reached its maximum but at the same time identify how the formation of ice on top of an anti-icing fluid is removed effectively and how it affects the aerodynamics. At the moment each of these tests only tests the worst case scenario. By combining the techniques we could devise a fluid which is more efficient with better performance.

These conclusions therefore reinforce the idea that simple small molecules such as LMWGs can be tuned and optimised to incorporate different structural motifs in differing solvent systems to enhance the properties of gel systems. The use of LMWG in an application such as de/anti-icing aircrafts in winter shows that they have great compatibility in very aqueous systems, can be used across a large concentration range, with good thermal stability which ultimately creates stiff, strong gel networks which can provide extended holdovers with minimal effects to the aerodynamics of an aircraft.

Each of the properties with the addition of LMWG allows for fluids to be sprayed hot onto aircrafts, with the thermoreversibility associated with these molecules also preventing the degradation of the gel structure that is currently observed with anti-icing fluids, whilst still being able to be used with the current equipment found on airfields used to apply de/anti-icing fluids. The production of stiff strong gel structures allows for the conversion of a Type I de-icing fluid into a Type II and/or Type III anti-icing fluid that match current anti-icing fluids, whilst the formation of hybrid gels provide extended holdover times rivalling that of Type II and Type IV anti-icing fluids which do not affect the aerodynamics of an aircraft.

The use of LMWG therefore allows for a fluid to be created which would allow for the use of increased volumes of water, hence less glycol. This would decreases costs for the manufacturer and customers as well as lower the environmental impact, whilst introducing revolutionary technology that could transform the aviation industry.

Chapter 9 Experimental

9.1 Materials and Methods

9.1.1 Equipment

All chemicals and solvents used were commercially available from Sigma Aldrich and Alfa Aesar, and were used without further purification. Ascorbic acid–6–palmitate was purchased from Alfa Aesar and used as supplied. 1,3:2,4–Dibenzylidene–D–sorbitol was purchased from Rika International, commercial name "Geniset D" but in this study is referred to as "Rika" and was used without further purification. 1, 3:2, 4–Dibenzylidene–D–sorbitol was also synthesised in a number of ways previously published in the literature. 1, 2–monopropylene glycol (MPG), monoethylene glycol (MEG) and 1, 3–propanediol (PDO) were supplied by Kilfrost Limited. Commercial de-icing products known as Type I DF Plus, anti-icing products known as Type II (ABC 3 and ABC K plus) as well as Type IV anti-icing products known as ABC S Plus were all supplied by Kilfrost limited and were used as supplied. Thin layer chromatography was carried out on commercially available Merck aluminium backed TLC plates (60, F_{254}) and visualised using UV light or Ninhydrin stain. Each compound was characterised using a JEOL ECX400 spectrometer (^{1}H 400MHz, ^{13}C 100MHz). All chemical shifts (δ) are reported in ppm and referenced to a residual solvent peak. Coupling constants (J) values are reported in Hz. ^{1}H and ^{13}C were assigned with the help of COSY and HSQC spectra. The peaks are reported using the following notation: s – singlet, d – doublet, t – triplet, q – quartet, qn – quintet, m – multiplet. ATR-FTIR was carried out on a Perkin Elmer Spectrum 2 fitted with an ATR sampling accessory and Spectrum 10 software. Absorbance bands are reported as wavenumber of maximum absorbance (cm^{-1}). Electrospray ionization mass spectroscopy (ESI-MS) was carried out on a Bruker MicroTOF mass spectrometer. Melting points were measured on a Stuart SMP3 using glass capillary tubes. Melting points are recorded as ranges and are uncorrected. T_{gel} measurements were determined using a thermoregulated oil bath at 1°C increments. Circular dichroism (CD) was measured with a JASCO J810 circular polarimeter fitted with a peltier temperature control unit. A quartz cell with a path length of 1 mm was used with the following settings: Data Pitch – 0.5 nm, Scanning Mode – Continuous, Scanning Speed – 200 nm min^{-1}, Response – 1 s, Bandwidth – 2 nm, Accumulation – 5. All CD data are presented as

ellipticity and recorded in mdeg. Samples for scanning electron microscopy (SEM) were prepared by spreading a small amount of gel over an aluminium stub and dried in a dessicator. They were then sputtered coated with a 4 nm layer of Au/Pd using a Polaron Agar High Resolution Sputter Coater and imaged with a JEOL JSM-7600F FEGSEM. Transmission electron microscopy (TEM) was performed on copper backed TEM grids and left to air dry overnight and imaged using a FEI Tecnai G^2 fitted with a CCD camera. Images were collected by Meg Stark, Biology Technology Faculty at the University of York. Dynamic rheological measurements were performed on a Malvern Kinexus Pro^+ rheometer using 20 mm parallel plate geometry and a 1 mm gap. Samples were applied as hot solutions and left to cool to form the gel on the sample plate. Each sample was trimmed using a flat ended spoon to remove any excess fluid around the geometry before the test was started. Oscillatory amplitude, frequency and time sweeps were performed as well as temperature ramps. All measurements were performed within the linear viscoelastic region (LVR) and data interpreted using rSpace for Kinexus software. Water Spray Endurance Test (WSET) was carried out in a climatic (temperature and humidity) controlled tunnel at Kilfrost Limited. All tests were conducted at -5°C and samples tested at 100%, 75% and 50% dilutions.

9.2 Procedures

9.2.1 Preparation of gels

A known amount of gelator was accurately weighed out into a 2 ml glass vial. Solvent (1 ml) was then added to the vial using a Gilson pipette. The sample was sonicated for one hour before being heated in an oil bath to just below the boiling point of the solvent, until a homogeneous solution was formed. The sample was then left at room temperature overnight to cool, over which time the sample forms a gel.

9.2.2 Preparation of gel samples with a known de-icing fluid.

Samples were made at 1%, 0.5% and 0.1% w/v for screening purposes. To make the samples, the solid gelator was accurately weighed out into a 2 ml vial. Solvent (1 ml) was then added to the vial using a Gilson pipette in aliquots as shown in **Table 9.1**. Each sample was sonicated for 1 h before being heated in an oil bath to just below the boiling point of the solvent, until a clear homogeneous solution was formed. If, after one hour of heating, the sample did not form a clear homogeneous solution it was removed from the heat. The samples were left on the bench at room temperature overnight, during which time they formed gels.

Table 9.1 Aliquots of solvent required to make gels with DF Plus.

% of MPG in Sample	Volume of Type I DF Plus added (ml)	Volume of Water added (ml)
80%	1	0
72%	0.9	0.1
64%	0.8	0.2
56%	0.7	0.3
48%	0.6	0.4
40%	0.5	0.5
32%	0.4	0.6
24%	0.3	0.7
16%	0.2	0.8
8%	0.1	0.9

9.2.3 Preparation of Gel samples with known Anti-icing Fluids

Samples were prepared by accurately weighing the solid gelator into a 2 ml glass vial and adding 1 ml of solvent with a Gilson pipette. To prepare the hybrid gel samples Type II (ABC 3 and ABC K Plus) and Type IV (ABC S Plus) products were used as solvent without being diluted. Each sample was then sonicated for 1 h before being heated in an oil bath to below the boiling point of water, until clear homogeneous solutions were formed. If, after one hour of heating, the sample did not form a clear homogeneous solution it was removed from the heat. The samples were left on the bench at room temperature overnight, during which time they formed gels. Results were recorded the next day

9.2.4 Hybrid LMWG Gel Preparation

A known amount of one gelator was accurately weighed into a 2 ml glass vial. A known amount of a second gelator was then accurately weighed out into the same vial. 1 ml of solvent was added to the vial using a Gilson pipette. Each sample was sonicated for 1 h before being heated to below the boiling point of the solvent until a clear homogeneous solution was formed. The samples were then left to cool to room temperature on the bench overnight, with the results recorded the next day.

9.2.5 Hybrid Gel Systems with 10% and 50% Reduction

Gels of 0.5% w/v and 0.1% w/v were made as described below:

9.2.5.1 10% Hybrid-Gels

Samples were made by weighing out 90% of the final desired concentration of a gelator into a 2 ml glass vial. 10% of a second gelator was then weighed out accurately into the same vial to make the final concentration. 1 ml of solvent was added to the glass vial using a Gilson pipette and the samples sonicated for 1 h. They were then heated in an oil bath to below the boiling point of the solvent to form clear homogenous solutions and left to cool overnight at room temperature.

9.2.5.2 50% Hybrid-Gels

The same procedure was followed as in **Section 9.2.5.1** but 50% of each of the two different gelators was weighed out into the same vial to make the final concentration.

9.2.6 Minimum Gelation Concentration (MGC)

Gels of decreasing concentrations were formed as in **Section 9.2.1**. They were then inverted to identify if the gel could support itself under gravity. The lowest concentration at which a gel was stable when inverted was taken as the MGC.

9.2.7 Measuring T_{gel} Values

Gel samples were used to measure the T_{gel} value. The samples were placed in a thermostatic oil bath and the temperature increased at a rate of 1.0°C min^{-1}. As the temperature increased, the gel was removed from the oil bath at every 1°C increase and inverted (Tube inversion test). The temperature at which the gel can no longer support itself under gravity and collapses to the bottom of the vial was recorded as the T_{gel}, the temperature of the gel–sol transition. All T_{gel} values were repeated at least once and averaged.

9.2.8 Scale up of gel samples in a known de-icing fluid.

Samples were scaled up to 200 ml in glass Schott bottles. A known amount of gelator was weighed out into a Schott bottle, and solvent (Type I De-icing fluid and water) added as described in **Table 9.2**. The samples were sonicated for 1 hour then heated in an oil bath to just below the boiling point of water until a clear homogeneous solution was formed. Samples were left overnight for the gels to form and results recorded the next day.

Table 9.2 Aliquots of solvent used to prepare scale up samples.

% of MPG in Sample	Volume of Type I DF Plus added (ml)	Volume of Water added (ml)
80%	200	0
72%	180	20
64%	160	40
56%	140	60
48%	120	80
40%	100	100
32%	80	120
24%	60	140
16%	40	160
8%	20	180

9.2.9 Scale up of gel samples with Anti-icing Products.

All samples were scaled up to 200 ml. A known amount of gelator was weighed accurately into a glass Schott bottle and 200 ml solvent (Type II and Type IV anti-icing products) added. Samples were made for each of the different type of products. Samples were sonicated for 1 h before being heated in an oil bath to below the boiling point of the solvent until a clear homogenous solution was formed. Samples were then removed from the heat and left to cool at room temperature to allow for the gels to form.

Duplicate samples were made for all products.

9.2.10 Dilution of gels formed with Anti-icing products

Gels formed in **Section 9.2.9** were diluted to 50% for testing with WSET.

100 ml samples at 50% dilution for each of the anti-icing product gels were made by transferring 50 ml of the gel sample formed in **Section 9.2.9** to a measuring cylinder with 50 ml of hard water. Samples were mixed by inversion of the measuring cylinder.

These samples were left at room temperature for further testing with the WSET, detailed below.

9.2.11 Circular Dichroism (CD)

9.2.11.1 Sample Preparation

A known amount of gelator (0.2 mg, 0.02% w/v) (below the MGC) was weighed out into a 2 ml glass vial with 1 ml of solvent (MPG, 75:25 MPG:H_20 and 50:50 MPG:H_2O) added. Each sample was sonicated for 1 hour before being heated below the boiling point of the solvent until a clear homogenous solution was formed. Samples were then left to cool to room temperature and tested the following day.

Control samples of MPG, 75:25 MPG: H_2O and 50:50 MPG: H_2O were also prepared for subtraction and comparison purposes.

All samples are very dilute and are hence solutions and not gels.

9.2.11.2 Spectrum Measurement – Chiral Chromophore

The above control and test samples (400 µl) were transferred into a 1 mm pathlength quartz cell using a Gilson pipette. The cell was then placed into the instrument set to 20°C. Each sample was tested using the Spectrum Measurement analysis test method using the following settings: Sensitivity – Standard (100 mdeg), Start – 320 nm, End – 180 nm, Data Pitch – 0.5 nm, Scanning Mode – continuous, Scanning speed – 200 nm/min, Response – 2 sec, Band width – 2 nm, Accumulation – 5.

The result of each control sample (MPG, 75:25 MPG:H_2O and 50:50 MPG:H_2O) was then subtracted from each test sample containing the same solvent and the results recorded.

9.2.11.3 Spectrum Measurement – Self Assembly

As with the "Chiral Chromophore" description above the samples were transferred in the same way however, the instrument was set to 100°C. The cell was left in the instrument for 15 minutes before starting the spectrum measurement test method. The same parameters were then used as described above for Chiral Chromophore. This method was repeated for the same sample at 10°C reductions in temperature until 20°C was reached.

All control samples were run in this way and then subtracted from the relevant samples which contained the same solvent systems.

9.2.11.4 Interval Scan Measurement – Kinetics

The quartz cell was first of all placed into the instrument set to 100°C empty and with no lid on. Each sample in the vials was then heated using a heat gun and transferred as quickly as possible into the hot quartz cell using a Gilson pipette. The lid was placed on and the instrument set to 20°C and the test started immediately. The Interval Scan Measurement test method was then selected using the following parameters. Sensitivity – Standard (100 mdeg), Start – 320 nm, End – 180 nm, Data Pitch – 0.5 nm, Scanning mode – Continuous, Scanning speed – 200 nm/min, Response – 1 sec, Band width – 2 nm, Number of spectra – 20, Interval – 1 min, Accumulation – 3.

This test was then repeated as above with the interval changed to 30 sec and 15 sec respectively.

9.2.12 Preparation of rheology samples

For each sample a known amount of gelator was weighed out into a glass vial (10 ml) and solvent (8 ml of MPG, MEG, PDO, de-icing or anti-icing product) added. The samples were sonicated for 1 hour and then heated in an oil bath to just below the boiling point of the solvent until a clear homogeneous solution was formed. The samples were left overnight to form gels at room temperature for testing the next day.

9.2.12.1 Sample loading

As gels can be fragile if applied as a solid, the samples were applied as a solution and the gel allowed to set on the sample plate. The samples were temperature dependant therefore each vial was placed in a water bath and heated to just above the T_{gel} value until the solution formed. Using a spoon to reduce any shear or damage to the sample, ~2 ml of the solution was placed onto the sample stage on the rheometer set to 20°C and the geometry brought down to the gap of 1 mm. The sample was trimmed to remove any excess sample underneath the geometry and the hood placed on to the geometry to reduce evaporation before a test was started.

9.2.13 Rheology Testing

All rheological measurements were performed on a Malvern Kinexus Pro$^+$ rotational rheometer with a 20 mm diameter parallel plate. All experiments were carried out in oscillatory mode. A gap of 1 mm was used and all tests carried out at 20°C unless stated otherwise.

9.2.13.1 Amplitude Sweep

A sample was applied as above and left to equilibrate at 20°C for 15 minutes to allow the sample to reach temperature and the gel to form. The sample was then tested across a range of increasing strain (0.001 to 100%) at a set frequency of 1 Hz and set temperature of 20°C. This test determines the LVR (linear viscoelastic region) of each sample. A value from the LVR was then used for further tests.

9.2.13.2 Frequency sweep

The sample was applied as above and left to equilibrate for 10 minutes on the instrument. Using a known strain value from the LVR the sample was tested across a range of frequencies (0.01 to 100 Hz) at a set temperature of 20°C. Frequency sweeps allows the determination of what type of sample you are testing and provides a 'fingerprint' for each sample.

9.2.13.3 Temperature Ramp

The samples were applied as described above but this time to a hot sample stage set to 85°C. The test was carried out using a known strain value within the LVR at a set frequency of 1 Hz across a temperature range (85 to -5°C) at increments of 2°C/min. The test then equilibrated for 5 minutes at -5°C before completing a reverse temperature cycle at 2°C/min from -5 to 100°C. Temperature ramps provide information on the behaviour of a sample to increasing and decreasing temperature.

9.2.13.4 Time Sweep

Each sample was applied hot to a 20°C sample stage and the test started as quickly as possible. The test uses a known strain within the LVR at a set frequency of 1 Hz at a set temperature, 20°C, over 1 hour. Time sweeps identify how fast a gel can form under given fixed conditions.

9.2.14 Aerodynamic Testing using Rheology

Only samples described in **Sections 9.2.8** and **9.2.9** were tested for aerodynamic performance. To determine the effects of shear on gel samples and to identify if these gels would break down and be able to be removed from an aircraft after takeoff, time sweep rheological analysis was performed. A three step time sweep was performed as follows:

Step 1

Samples were applied hot as described in **Section 9.2.12.1** to the sample stage set at 20°C. Each sample was set to equilibrate for 15 minutes before the test was started to allow the gel to form. This test was then set to use a strain within the LVR with a frequency of 1 Hz at 20°C for 10 minutes.

Step 2

After Step 1, the second time sweep was changed to use a 10% strain (outside of the LVR) with the same parameters as in Step 1 for 10 minutes.

Step 3

The final step of the test involved the strain returning to within the LVR with the same parameters as in Step 1 but for 1 hour.

The 3 different steps described above constitute one test where the steps run consecutively one after the other with no breaks in between. This characterises the ability of the gel to set up on a surface, be broken down and then finally to recover or self heal.

To understand the effects of increasing strain, the test was repeated twice more for each sample with Step 2 changing to 50% and 100% strain values.

9.2.15 Field Emission Gun Scanning Electron Microscopy (FEG-SEM)

Samples for SEM imaging were prepared in two ways, see below. Once the samples were prepared and the xerogels formed, the samples were coated with a 4 nm layer of Au/Pd using a Polaron High Resolution Sputter coater and were imaged using a JEOL 7600F FEG-SEM.

9.2.15.1 Room Temperature Sample Preparation

Gels were formed as in **Section 9.2.1** and **9.2.2**. Once the gels had set, a small amount of gel was removed with a spatula and spread thinly onto an aluminium SEM stub. These were then placed on a polystyrene holder and placed in a dessicator to air dry for 2 days to 2 weeks depending on the solvent, to leave the xerogel.

9.2.15.2 Crash Cool Sample Preparation

Gels were formed as in **Section 9.2.1** and **9.2.2**. They were then placed into a hot oil bath at 98°C to fully dissolve. During this time the SEM stubs on a polystyrene holder was placed in the freezer at -21°C for 5 minutes for the stubs to reach low

temperature. One drop of the hot solution was then placed on to the cold SEM stub in the freezer, using a Pasteur pipette and spread over the surface. The stubs were placed back into the freezer for 2 hours to form gels at low temperatures. After two hours, the stubs were then placed in a dessicator at room temperatures for the samples to dry (3 days) and leave the xerogel.

9.2.16 Transmission Electron Microscopy (TEM).

TEM was only carried out on gel samples prepared in **Section 9.2.3**. A small amount of gel was removed from the vial with a spatula and brought very briefly into contact with a copper backed TEM grid. The small amount of material that had transferred to the grid was left to air dry overnight. The samples were then imaged using a FEI Tecnai G^2 fitted with a CCD camera.

9.2.17 Water Spray Endurance Test (WSET)

The water spray endurance test is a laboratory-based test developed to evaluate the holdover performance of de-icing and anti-icing fluids under freezing conditions. This test determines the length of time an aircraft has between application of a de/anti-icing fluid to taxiing and take-off before reapplication is required due to further ice contamination.

This test was carried out within a temperature-controlled climatic chamber, and conducted at -5°C. Within this chamber an aluminium frosticator plate, representative of an aircrafts' leading edge on a wing was setup. This was set at -5°C with a 10° angle. The frosticator consists of 6 test panels. Four panels were used for test samples with the remaining two acting as controls, with the use of aluminium square plates which are weighed before and after the test to identify the weight of ice formed throughout the test known as the "catch". The weight of the ice ("catch") formed during the test should be $\sim 5 \pm 0.2$ g/dm^2 h^{-1} as detailed in AS5901.

Each sample (75 ml) was applied to the top of the aluminium test panels by pouring the fluid from left to right ensuring the top lip (leading edge) was covered. The sample flowed down the test panel through gravitational forces and wet the panel. This was repeated for every sample tested. Once all samples were applied they were then left for 5 minutes on the frosticator plate to reach temperature. After 5 minutes the test was started by turning on the motor above the frosticator plate which holds a spray nozzle. This nozzle sprays water at a rate of 0.5 mm creating a fine mist which moves forward and backward over the frosticator plate covering the samples. As soon

as the spray was started the time was recorded. Gravity causes the fluid to run down the plate and coat it, however, this makes the fluid thinner at the top compared to the bottom. As the test progresses frost forms from the top edge of the panels and works its way down the panel. At 25 mm from the top edge is a line indicating the end of the test zone. As soon as the first shard of ice touched this line the time was recorded and used to calculate the holdover time for each sample. Each sample was treated in this way and when all samples were complete the test is stopped by stopping the spray and recording the end time. The control plates were weighed after the test and used to calculate the catch. Using the catch, end time of experiment and the completion time for each sample, holdover values were calculated.

All WSET tests were carried out twice and the results averaged.

9.2.17.1 De-icing products with gelators

Samples tested using the WSET were usually solutions at room temperature; however the gelator samples in Type I DF Plus were gels at room temperature and hence required a different approach. All de-icing samples prepared in **Section 9.2.8** with gelator incorporated into them were heated in an oil bath at 85°C until they formed solutions. A 75 ml aliquot was then transferred to a beaker and the sample applied straight away to the frosticator plate whilst hot and the test conducted as described above.

Control samples of the original Type I DF Plus were diluted in the same way as the gel samples described in **Section 9.2.8**. These were then tested on the WSET as described above and used for comparison with Type I DF Plus samples with added gelator.

9.2.17.2 Anti-icing Products with Gelators

Anti-icing samples made with gelators as described in **Section 9.2.9** and 50% diluted samples in **Section 9.2.10** were applied at room temperature. This is because anti-icing fluids are more commonly applied cold, unlike de-icing products which are applied hot. Control samples of the original anti-icing products undiluted and at 50:50 dilution were run alongside the gelator samples for comparison purposes for each test. The WSET was carried out for each of the different anti-icing products.

9.2.18 NMR Self Assembled Immobilisation Analysis

9.2.18.1 Sample Preparation

Samples prepared in **Section 9.2.9** were used to make the NMR samples. 1.0 g of the gel made in **Section 9.2.9** was weighed out into a 6 ml glass vial with 1 ml of stock solution added. The stock solution was made by adding 5 ml of D_2O into a 6 ml glass vial with 10 µl of acetone as internal standard. This was inverted to mix the contents before being used as the solvent. Each sample was then heated until a solution was formed; the hot solution was transferred to a hot NMR tube using a Gilson pipette, capped and labelled.

Control samples of the anti-icing products (ABC 3, ABC K Plus and ABC S Plus) were made by adding 1 ml of the anti-icing product to a 6 ml glass vial with 1 ml of the stock solution. The samples were transferred to an NMR tube by Gilson pipette capped and labelled.

All samples were tested for ^1H NMR using the JEOL ECX400 spectrometer and integration values compared.

Samples prepared in **Section 9.2.5** were tested in the same way described above but the solvent was made up of 2.5 ml of Type I DF Plus with 2.5 ml D_2O and 10 µl of DMSO as internal standard. The stock solution was also tested to act as a control sample.

9.3 Synthesis

9.3.1 Chapter 2

9.3.1.a *N*–Dodecanoyl-L-Alanine (2.10)[280]

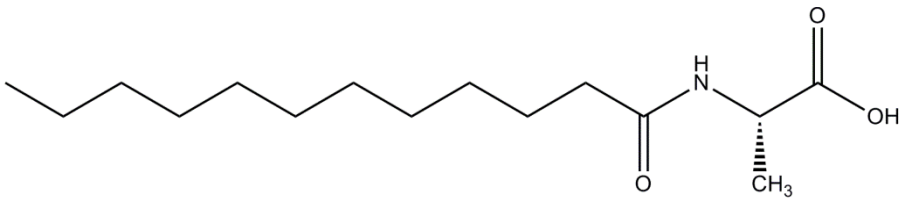

$C_{15}H_{29}NO_3$

271.21 gmol^{-1}

Compound **2.10** was synthesized by adding L–alanine (11.50 g, 0.13 mol) to a NaOH (5.29 g, 0.13 mol) aqueous solution. This was stirred in a round-bottom flask with a magnetic stirrer until a solution was formed. To this, dodecanoyl chloride (30.84 ml,

0.13 mol) was added and stirred at room temperature for 30 minutes. The mixture was adjusted to pH 3 using concentrated HCl. The resulting precipitate was filtered, washed with water (5 ml) and diethyl ether (5 ml), and then dried in the vacuum oven at 65°C overnight to give the desired product as a white powder (32.70 g, 120.57 mmol, 93% yield).

R_f: 0.26 (9:1, DCM: MeOH). ^{1}H NMR (400MHz, $MeOH_{d3}$) δ: 4.37 (d, J = 7.3 Hz, 1H, CON**H**), 4.03–3.97 (m, 1H, NHC**H**CH_3), 2.48 (t, J = 7.3 Hz, 2H, C**H**$_2$CONH), 1.70–1.54 (m, 2H, CH_3C**H**$_2$(CH_2)$_9$), 1.38 (d, J = 7.3 Hz, 3H, C**H**$_3$CHNHCO), 1.36–1.27 (m, 16H, (C**H**$_2$)$_8$), 0.92–0.88 (m, 3H, C**H**$_3$(CH_2)$_{10}$CO). ESI–MS: Calculated for ($C_{15}H_{29}NO_3$) $[M+Na]^+$ m/z = 294.2033, $[M+H]^+$ m/z = 272.2217. Found $[M+Na]^+$ m/z = 294.2040 (20%), $[M+H]^+$ m/z = 272.2220 (100%).

The above data are in agreement and referenced to previous published literature.[280]

9.3.1.b Bis (Leucine) Oxalyl Amide (2.11)[224]

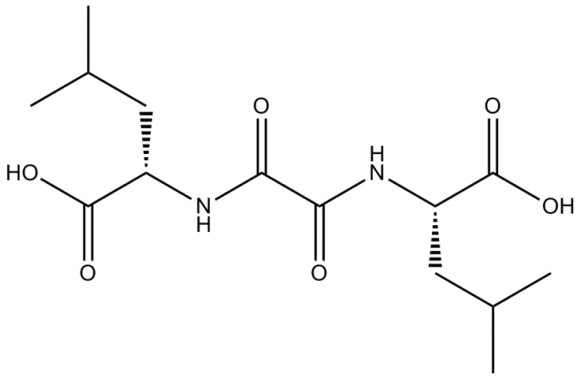

$C_{14}H_{24}N_2O_6$

316.16 gmol^{-1}

Compound **2.11** was synthesised by adding aqueous 2M KOH (5 ml) to a round-bottom flask with a magnetic mixer. To this L–leucine (0.87 g, 6.60 mmol) was added and stirred to form a solution. This solution was placed in a salt ice bath at -8°C and kept at this temperature for 40 minutes. A solution of oxalyl chloride (0.42 ml, 4.95 mmol) in dichloromethane (5 ml) and aqueous 4M KOH (2.10 ml) were added to the L–leucine solution simultaneously over 40 minutes using a syringe pump. Stirring was continued for 30 minutes at 0°C in an ice bath and for a further 30 minutes at room temperature. The mixture was acidified with 10% formic acid (3 ml).The precipitate was filtered, washed with water (5 ml) and dichloromethane (5 ml) and dried on the high vacuum line for 2 h to give a yellow powder (0.46 g, 1.45 mmol, 30% yield).

This product contained many impurities. It also did not yield enough solid to carry out gelation tests. As the reaction was very exothermic, it was not scaled up.

R_f: 0.34 (9:1, DCM: MeOH). ^{1}H NMR (400 MHz, D_2O_{d2}) δ: 4.21 (d, J = 7.1 Hz, 2H, N**H**), 3.28 (s, 1H, O**H**), 3.27 (s, 1H, O**H**), 2.17–2.12 (m, 2H, C**H**NH), 1.64–1.55 (m, 4H, NHCHC**H$_2$**), 1.35–1.25 (m, 12H, C**H$_3$**), 0.92–0.87 (m, 2H, CH_2C**H**$(CH_3)_2$). ESI–MS: Calculated for ($C_{14}H_{24}N_2O_6$) $[M+Na]^+$ m/z = 339.1524, $[M+H]^+$ m/z = 317.1707. Found $[M+Na]^+$ m/z = 339.1527 (100%), $[M+H]^+$ m/z = 317.1707 (25%).

The above data are in agreement and referenced to previous published literature.[224]

9.3.1.c Ascorbic acid–6–Palmitate (2.12)

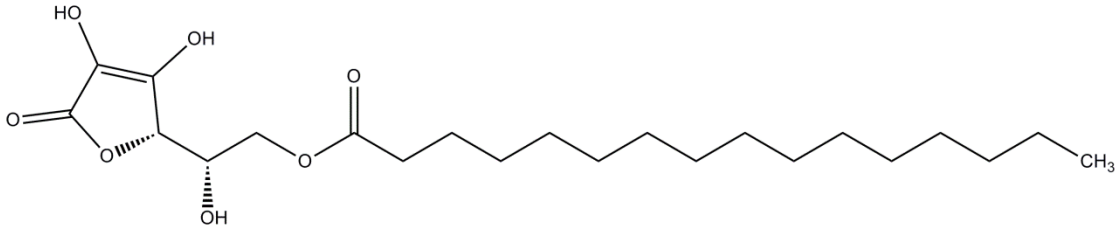

$C_{22}H_{38}O_7$

414.26 $gmol^{-1}$

Compound **2.12** was commercially available from Alfa Aesar, and was used without further purification.[173,419]

9.3.1.d 1, 3: 2, 4-Dibenzylidene-D-Sorbitol (2.17)[284,285,323,420]

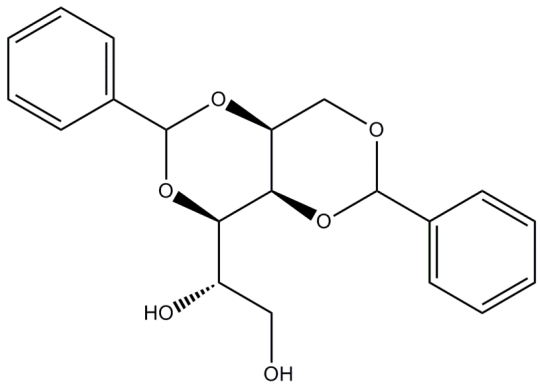

$C_{20}H_{22}O_6$

358.14$gmol^{-1}$

Compound 2.17 was synthesized by adding D–sorbitol (31.0 g, 0.17 mol) and methanol (100 ml) in a round-bottom flask with a magnetic mixer and stirred for 10 minutes, until a solution was formed. Benzaldehyde (31.5 g, 0.30 mol) and para-toluenesulfonic acid monohydrate (p-TSA) (40.5 g, 0.21 mol) were added to the

solution and mixed for 30 minutes at room temperature until the mixture formed a hard filter cake/thick paste. This was then broken up into pieces using a glass rod and fresh methanol (300 ml) added and stirred until absorbed into the filter cake/paste. This was transferred to a vacuum filter to remove as much liquid as possible. This was then transferred back into the round-bottom flask and fresh methanol (300 ml) added and stirred until absorbed and filtered as described above. A total of 3 washings were required. After the final wash, the filter cake was broken into pieces and air dried for 24 hours. The product was ground and dried to a constant weight giving a fine white powder (9.86 g, 27.53 mmol, 8% yield).

^{1}H NMR (400 MHz, $DMSO_{d6}$) δ: 7.50–7.44 (m, 4H, Ar-**H**), 7.39–7.35 (m, 4H, Ar-**H**), 5.67 (s, 2H, Ar-C**H**), 4.21 (d, J = 2 Hz, 1H, CHO**H**), 4.19–4.14 (m, 3H, C**H**$_2$-sugar, C**H**-sugar), 3.95 (d, J = 1.2 Hz, 1H, CH_2O**H**), 3.82 (dd, J = 9.3, 1.6 Hz, 1H C**H**-sugar), 3.79-3.74 (m, 1H, C**H**-sugar), 3.60-3.58 (m, 2H, C**H**$_2$-sugar), 3.45-3.41 (m, 1H, C**H**-sugar). ESI–MS: Calculated for ($C_{20}H_{22}O_6$) $[M+Na]^+$ m/z = 381.1304, $[M+H]^+$ m/z = 359.1481. Found $[M+Na]^+$ m/z = 381.1309 (100%), $[M+H]^+$ m/z = 359.1489 (20%).

The above data are in agreement and referenced to previous published literature.[284,285,323,420]

9.3.1.e *N*-dodecyl-D-gluconamide (2.13)[281]

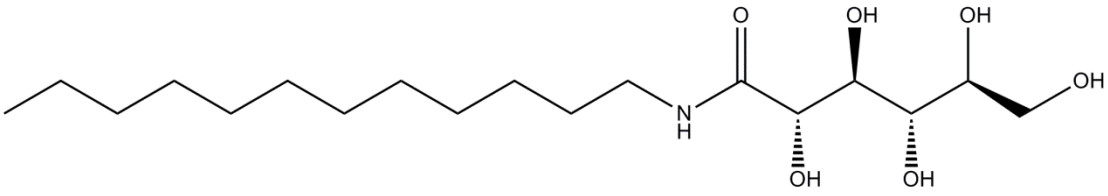

$C_{18}H_{37}NO_6$

363.26 gmol^{-1}

Gluconolactone (3.21 g, 0.02 mol) was added to a solution of dodecylamine (3.34 g, 0.02 mol) in methanol (25 mL). The mixture was refluxed for 30 minutes then left to cool to room temperature. This was then filtered and washed in ethanol, and dried overnight in the vacuum oven at 60°C. To give a white solid (5.77 g, 15.88 mmol, 88% yield).

The synthesis was scaled up by a factor of 10 with ease, which resulted in 57.7 g, 158.84 mmol (92% yield) of the product after drying.

R_f: 0.14 (9:1, DCM: MeOH). ^{1}H NMR (400 MHz, $DMSO_{d6}$) δ: 7.59 (t, J = 5.9 Hz, 1H, N**H**), 5.34 (d, J = 4.3 Hz, 1H, NCOC**H**), 4.53 (d, J = 3.8 Hz, 1H, CHO**H**), 4.46 (d, J = 3.6 Hz, 2H,

C**H**$_2$OH), 4.38 (d, J = 7.0 Hz, 1H, CHO**H**), 4.35–4.31 (m, 1H, C**H**CH$_2$OH), 3.89 (s, 1H, O**H**), 3.60–3.53 (m, 1H, O**H**), 3.50–3.43 (m, 2H, C**H**, CHO**H**), 3.38-3.33 (m, 1H, C**H**), 3.13–2.98 (m, 2H, C**H**$_2$NH), 1.43–1.38 (m, 2H, C**H**$_2$CH$_3$), 1.32–1.17 (m, 18H, (C**H**$_2$)$_9$), 0.89–0.81 (m, 3H, C**H**$_3$). ESI–MS: Calculated for ($C_{18}H_{37}NO_6$) $[M+Na]^+$ m/z = 386.2513, $[M+H]^+$ m/z = 364.2694. Found $[M+Na]^+$ m/z = 386.2490 (20%), $[M+H]^+$ m/z = 364.2680 (100%).

The above data are in agreement and referenced to previous published literature.[281]

9.3.1.f 1, 12-Digluconamidododecane (2.14)[225]

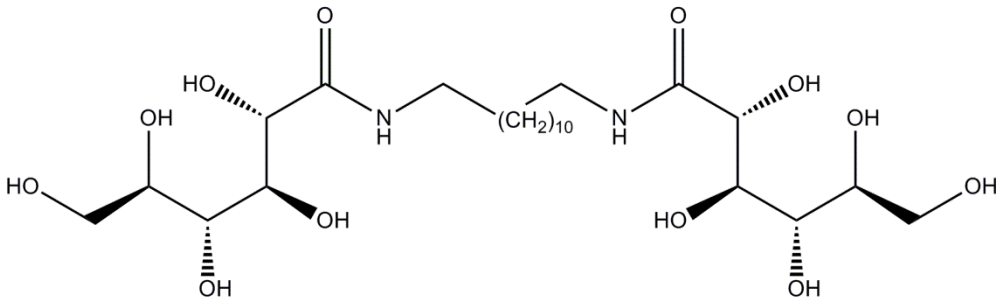

$C_{24}H_{48}N_2O_{12}$

556.32 gmol^{-1}

1,12-Diamidododecane (0.56 g, 2.80 mmol) was added to a solution of gluconolactone (1.00 g, 5.60 mmol) in methanol (50 mL) and stirred for 24 hours at room temperature. The mixture was filtered and dried overnight in vacuum oven at 60°C. This gave a white solid, (1.56 g, 2.8 mmol, 99% yield).

R_f: 0.12 (9:1, DCM: MeOH). ^{1}H NMR (400 MHz, $DMSO_{d6}$) δ: 7.59 (t, J = 5.9 Hz, 2H, N**H**), 5.38–5.31 (m, 2H, C**H**CONH), 4.54–4.53 (m, 2H, C**H**OH), 4.50–4.43 (m, 2H, C**H**OH), 4.40–4.38 (m, 2H, O**H**), 4.33 (t, J = 4.6 Hz, 2H, C**H**CH$_2$OH), 3.96 (s, 2H, O**H**), 3.88 (s, 2H, O**H**), 3.60–3.54 (m, 2H, O**H**), 3.46 (s, 2H, CH$_2$O**H**), 3.12–2.99 (m, 4H, NHC**H**$_2$), 1.45–1.35 (m, 4H, C**H**$_2$OH), 1.24 (app s, 20H, (C**H**$_2$)$_{10}$). ESI–MS: Calculated for ($C_{24}H_{48}N_2O_{12}$) $[M+Na]^+$ m/z = 579.3099, $[M+H]^+$ m/z = 557.3280. Found $[M+Na]^+$ m/z = 579.3098 (80%), $[M+H]^+$ m/z = 557.3273 (100%).

The above data are in agreement and referenced to previous published literature.[225]

9.3.1.g Diglucosaminododecane (2.15)[248]

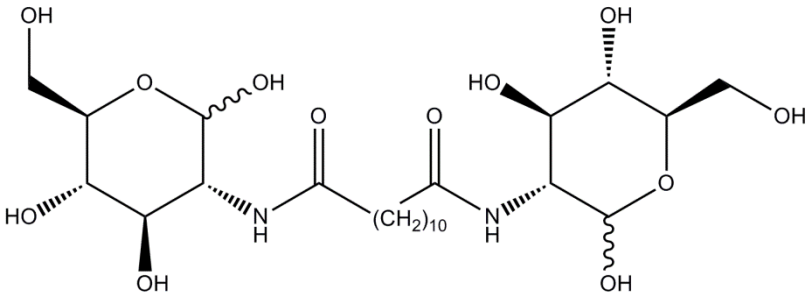

$C_{24}H_{44}N_2O_{12}$

552.29 gmol^{-1}

1,12-Dodecane dioyl dichloride (2.64 g, 9.87 mmol) was dissolved in DCM (7.5 mL) and added dropwise to a solution of mercaptothiozoline (2.13 g, 17.90 mmol) and triethylamine (1.97 g, 19.50 mmol) in DCM (40 mL) and stirred for 3 hours at room temperature.

The mixture was washed with 0.5M HCl, then 5% $NaHCO_3$. The organic phase was rotary evaporated and recrystallised from acetonitrile, to give a yellow powder (2.01 g, 52% yield).

Glucosamine (0.99 g, 4.62 mmol), triethylamine (0.53 g, 5.24 mmol) and the intermediate (0.94 g) described above were added to DMF (100 ml) and the mixture stirred at 70^{o}C for 6.5 hours, then at room temperature for 20.5 hours. The precipitate was filtered and dried overnight in a vacuum oven at 70°C, giving a white powder, (0.106 g, 0.19 mmol, 47% Yield).

R_f: 0.81 (9:1, DCM: MeOH), intermediate from step 1. R_f: 0.51 (7:3, Ethyl acetate:Cyclohexane), final product. ^{1}H NMR (400 MHz, $DMSO_{d6}$) δ: 7.95 (s, 2H, N**H**), 6.46 (d, J = 6.4 Hz, 2H, OC**H**OH), 4.92–4.88 (m, 4H, NHC**H**, NHCHC**H**), 4.57–4.51 (m, 1H, OC**H**CH_2), 4.44–4.40 (m, 2H, CHO**H**), 3.69–3.65 (m, 1H, CHO**H**), 3.63-3.61 (m,, 2H, C**H**OH), 3.51–3.50 (m, 1H, CH_2O**H**), 3.13–3.09 (m, 2H, C**H**OH), 3.07 (s, 1H, OC**H**CH_2), 3.05–3.03 (m, 2H C**H**OH), 2.10–2.03 (m, 4H, C**H$_2$**OH), 1.51-1.44 (m, 4H, C**H$_2$**CO), 1.23-1.20 (m, 16H, (C**H$_2$**)$_8$). ESI–MS: Calculated for ($C_{24}H_{44}N_2O_{12}$) $[M+Na]^+$ m/z = 575.2786, $[M+H]^+$ m/z = 553.2967. Found $[M+Na]^+$ m/z = 575.2802 (100%), $[M+H]^+$ m/z = 553.2981 (40%).

The above data are in agreement and referenced to previous published literature.[248]

9.3.1.h Pentadecylphenylglucopyranoside (2.16)[282,283]

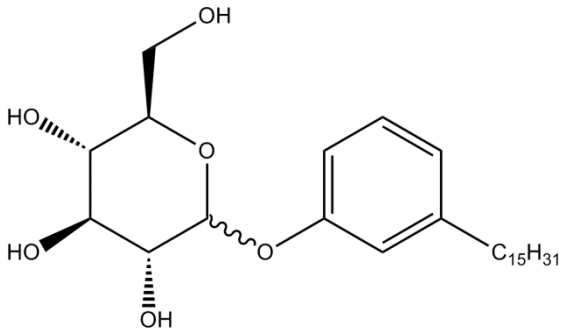

$C_{27}H_{46}O_6$

466.33 gmol^{-1}

This synthesis was put together from two papers as the first was incomplete and reported an end product which was still protected. A deprotection method was then discovered and adapted for this compound.

3-Pentadecylphenol (1.52 g, 4.99 mmol) in dry CH_2Cl_2 (10 mL) and 4Å molecular sieves (2.0 g) were added to glucose pentaacetate (3.90 g, 10 mmol) and $BF_3.OEt_2$ (0.75 g, 5.28 mmol). The mixture was stirred in an inert N_2 atmosphere at room temperature for 24 hours. It was then added to 5% $NaHCO_3$ (40 mL), washed with water (40 ml), and dried over anhydrous Na_2SO_4. This was filtered to remove Na_2SO_4 and rotary evaporated to remove DCM to give a cream coloured crude product. This was recrystallised from ethanol and dried on the high vacuum line for 2 h giving a white solid, (0.67 g, 21% yield).

The protected product (0.35 g, 0.55 mmol) was added to MeOH (100 mL) with K_2CO_3 (14 mg) and stirred at ~40°C. The reaction was monitored by TLC. The methanol was removed by rotary evaporation leaving a solid (2.2 g) which was recrystallised from DCM and filtered giving a white solid, (0.14 g, 0.30 mmol, 54% yield).

R_f: 0.98 (9:1, DCM: MeOH), acetyl protected product. R_f: 0.39 (9:1, DCM: MeOH) final product. ^{1}H NMR (400 MHz, $DMSO_{d6}$) δ: 8.17–8.08 (m, 1H, Ar-**H**), 7.82–7.73 (m, 3H, Ar-**H**), 6.24 (d, J = 4.9 Hz, 1H, OC**H**O), 6.05 (d, J = 4.6 Hz, 1H, CHO**H**), 5.98 (d, J = 5.2 Hz, 1H, CHO**H**), 5.79 (d, J = 7.4 Hz, 1H, CHO**H**), 5.52 (t, J = 5.8 Hz, 2H, Ar-C**H**$_2$), 4.66-4.62 (m, 2H, C**H**$_2$OH), 4.47–4.37 (m, 1H, CH_2O**H**), 4.31–4.06 (m, 4H, C**H**OH (X4)), 3.53–3.43 (m, 2H, C**H**$_2CH_3$), 2.17-2.14 (m, 24H, (C**H**$_2)_{12}$), 1.85–1.78 (m, 3H, C**H**$_3$). ESI–MS: Calculated for ($C_{27}H_{46}O_6$) $[M+Na]^+$ m/z = 489.3187. Found $[M+Na]^+$ m/z = 489.3193 (100%).

The above data is in agreement and referenced to previous published literature.[282,283]

9.3.1.i Ditoluidene-D-Sorbitol (2.18)[285,421]

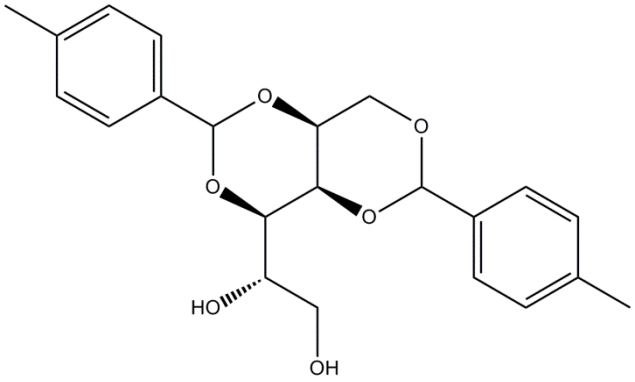

$C_{22}H_{26}O_6$

386.17 gmol^{-1}

A slurry of D-sorbitol (9.11 g, 50 mmol), p-tolualdehyde (11.80 mL, 100 mmol) in acetonitrile (100 mL) and p-toluenesulfonic acid monohydrate (1.90 g, 10 mmol) was added to a round-bottom flask and stirred. After just 1 hour a filter cake formed, which was broken down into smaller chunks and left to stir overnight. The mixture was washed with boiling H_2O (200 mL x2), cyclohexane (200 mL x2) and again with boiling H_2O (200 mL x4), filtered and dried in a vacuum oven at 110°C. The solid was ground giving a white solid, (14.7 g, 38.07 mmol, 75% yield).

^{1}H NMR (400 MHz, $DMSO_{d6}$) δ: 7.36-7.32 (m, 4H, Ar-**H**), 7.19-7.17 (m, 4H, Ar-**H**), 5.61 (s, 2H, Ar-C**H**), 4.83 (d, J = 5.8 Hz, 1H, CHO**H**), 4.18–4.11 (m, 3H, C**H$_2$**-sugar, C**H**-sugar), 3.92–3.90 (m, 1H, CHO**H**), 3.82 (dd, J = 9.3, 1.5 Hz, 1H, C**H**-sugar), 3.78–3.71 (m, 1H, C**H**-sugar), 3.61-3.56 (m, 2H, C**H$_2$**-sugar), 3.45–3.39 (m, 1H, C**H**-sugar), 2.30 (s, 6H, C**H$_3$**). ESI–MS: Calculated for ($C_{22}H_{26}O_6$) $[M+H]^+$ m/z = 387.1814. Found $[M+H]^+$ m/z = 387.1802 (100%).

The above data are in agreement and referenced to previous published literature.[285,421]

9.3.2 Chapter 3

9.3.2.a 1, 3:2, 4–Dibenzylidene–D–Sorbitol (3.10)

"Rika"

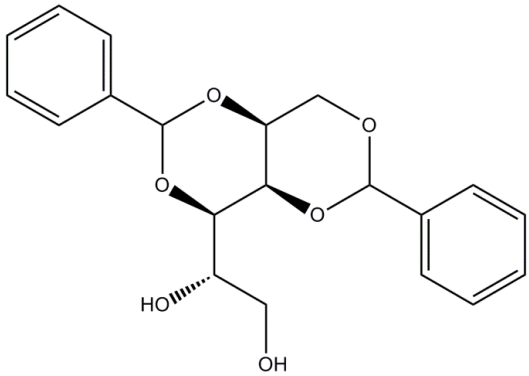

$C_{20}H_{22}O_6$

385.14 $gmol^{-1}$

This molecule was commercially available from New Japan Chemical Company, commercial name Geniset D and was used without further purification.

Generalised synthetic procedure for Dibenzylidene–D–sorbitol based gelators. Procedure A:

Gelators were synthesised by adding 4.90 g (0.03 mol) D-sorbitol to a three-necked round-bottom flask fitted with a Dean Stark trap. A mixture of cyclohexane (35 ml) and methanol (10 ml) was added to the flask. The mixture was stirred and heated to 50°C for 20 minutes under nitrogen.

In a round-bottom flask the appropriate para–benzaldehyde (0.05 mol) was added with p–toluene sulfonic acid monohydrate (p-TSA) (1.00 g 5.26 mmol) in methanol (20 ml) which was stirred at room temperature for 20 minutes. This was then added to the D–sorbitol solution dropwise and the temperature increased to 70°C for 2-4 h. The mixture was allowed to cool to room temperature where a paste was formed. This was then washed with cold ethanol (3 x 100 ml) to remove any starting materials. The crude product was dried on the high vacuum line for 2 hours and air dried overnight.

The impurities (mono and tri-substituted derivatives) were removed by washing with boiling water (4 x 100 ml) and boiling dichloromethane (4 x 100 ml).Finally dried in the vacuum oven at 70°C overnight.

This procedure is used throughout unless stated otherwise.

9.3.2.b 1, 3: 2, 4–Dibenzylidene–D–Sorbitol (3.11)

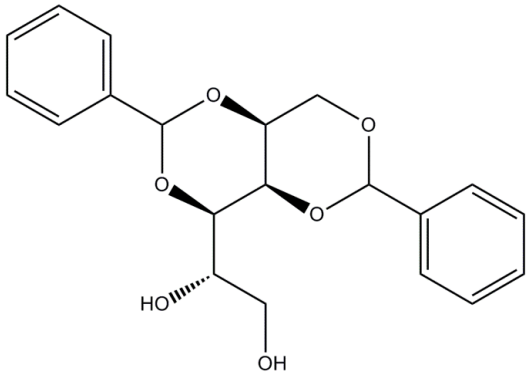

$C_{20}H_{22}O_6$

385.14 gmol^{-1}

General procedure A was followed using benzaldehyde. Compound **3.11** was a white solid (6.86 g, 17.81 mmol, 75% yield).

^{1}H NMR (400 MHz, $DMSO_{d6}$) δ: 7.50–7.44 (m, 4H, Ar-**H**), 7.41-7.35 (m, 6H, Ar-H), 5.67 (s, 2H, Ar-C**H**), 4.21 (d, J = 2 Hz, 1H, CHO**H**), 4.18-4.15 (m, 1H, CH_2O**H**), 4.14 (d, J = 4.0 Hz, 2H, C**H**$_2$-sugar), 3.95 (d, J = 3.2 Hz, 1H, C**H**-sugar), 3.85 (dd, J = 9.3, 1.7 Hz, 1H, C**H**-sugar), 3.79-3.74 (m, 1H, C**H**-sugar), 3.62-3.58 (m, 2H, C**H$_2$**-sugar), 3.47-3.42 (m, 1H, C**H**-sugar). ^{13}C NMR (100M Hz, $DMSO_{d6}$) δ: 139.28, 139.02, 129.17, 129.09, 128.53, 128.46, 126.71, 126.68 (Ar-**C**), 99.86, 99.80 (Ar-**C**H), 78.17 (**C**H-sugar), 70.63 (**C**H-sugar), 69.88 (**C**H$_2$-sugar), 69.71 (**C**H-sugar), 68.97 (**C**H-sugar), 68.27 (**C**H-sugar), 68.25 (**C**H-sugar), 63.19 (**C**H$_2$-sugar). ATR-FTIR ν_{max} (cm^{-1}): 3239 (OH, Alcohol), 2937 (CH, Aliphatic), 1453 (C=C, Aromatic), 1089 (C-O, Acetal). ESI–MS: Calculated for ($C_{20}H_{22}O_6$) $[M+Na]^+$ m/z = 381.1308. Found $[M+Na]^+$ m/z = 381.1309 (100%). Melting point: 177–181°C

9.3.2.c 1,3:2,4–Dimethylester Dibenzylidene–D–Sorbitol (3.12)

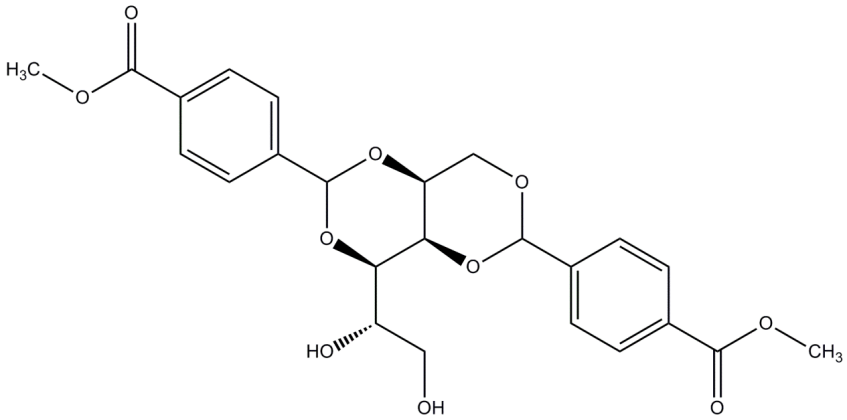

$C_{24}H_{26}O_{10}$

474.15 gmol^{-1}

General procedure A was used with 4–formylmethylbenzoate. Compound **3.12** was a white powder (7.67 g, 16.17 mmol, 64% yield).

^{1}H NMR (400 MHz, $DMSO_{d6}$) δ: 8.00-7.97 (m, 4H, Ar-**H**), 7.64-7.58 (m, 4H, Ar-**H**), 5.76 (s, 2H, Ar-C**H**), 4.94 (d, J = 5.9 Hz, 1H, CHO**H**), 4.50–4.43 (m, 2H, C**H$_2$**-sugar), 4.27–4.17 (m, 1H, C**H**-sugar), 4.01-3.98 (m, 1H, CH_2O**H**), 3.89 (dd, J = 9.3, 1.3 Hz, 1H, C**H**-sugar), 3.85 (s, 6H, C**H**$_3$COOC), 3.82–3.75 (m, 1H, C**H**-sugar), 3.64–3.55 (m, 2H, C**H$_2$**-sugar), 3.50–3.43 (m, 1H, C**H**-sugar). ^{13}C NMR (100 MHz, $DMSO_{d6}$) δ: 165.97, 165.93 (CH_3OO**C**), 143.26, 142.99, 129.70, 129.65, 128.97, 128.88, 126.74, 126.43 (Ar-**C**), 98.47, 98.39 (Ar-**C**H), 77.52 (**C**H-sugar), 70.11 (**C**H-sugar), 69.25 (**C**H_2-sugar), 68.46 (**C**H-sugar), 67.52 (**C**H-sugar), 62.49 (**C**H_2-sugar), 52.13 (**C**H_3-sugar). ATR-FTIR ν_{max} (cm^{-1}): 3246 (OH, Alcohol), 2954 (CH, Aliphatic), 1723 (C=O, ester), 1478 (C=C, Aromatic), 1092 (C-O, Acetal). ESI-MS: Calculated for ($C_{24}H_{26}O_{10}$) $[M+Na]^+$ m/z = 497.1433. Found $[M+Na]^+$ m/z = 497.1418 (100%). Melting Point: 172–177°C.

9.3.2.d 1, 3:2, 4–Dimethoxy Dibenzylidene–D–Sorbitol (3.13)

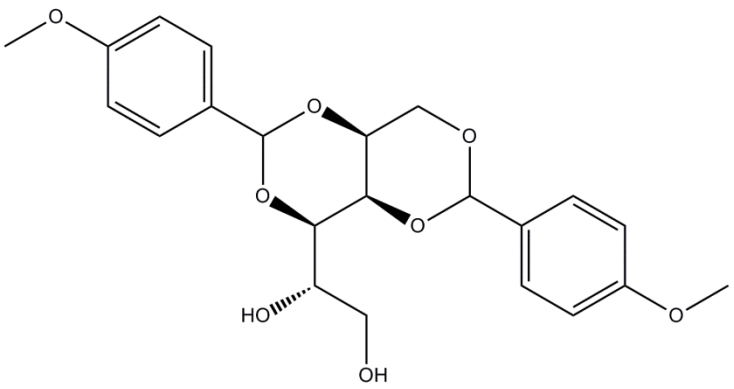

$C_{22}H_{26}O_8$

418.16 gmol^{-1}

General procedure A was used with 4-methoxybenzaldehyde. Compound **3.13** was a white powder (5.50 g, 13.15 mmol, 52% yield).

^{1}H NMR (400 MHz, $DMSO_{d6}$) δ: 7.40-7.36 (m, 4H, Ar-**H**), 6.94-6.90 (m, 4H, Ar-**H**), 5.59 (s, 2H, Ar-C**H**), 4.82 (d, J = 5.8 Hz, 1H, CHO**H**), 4.42-4.39 (m, 1H, C**H**-sugar), 4.17-4.10 (m, 3H, C**H$_2$**-sugar, C**H**-sugar), 3.89-3.86 (m, 1H, CH_2O**H**), 3.80 (dd, J = 9.2, 1.6 Hz, 1H, C**H**-sugar), 3.75 (s, 6H, OC**H$_3$**), 3.60–3.55 (m, 2H, C**H$_2$**-sugar), 3.44–3.38 (m, 1H, C**H**-sugar). ^{13}C NMR (100 MHz, $DMSO_{d6}$) δ: 159.93, 159.88, 131.72, 131.45, 128.02, 127.99, 113.80, 113.74 (Ar-**C**), 99.83, 99.76 (Ar-**C**H), 78.15, 70.51 (**C**H-sugar), 69.80 (**C**H_2-sugar), 68.84, 68.24 (**C**H-sugar), 63.14 (**C**H_2-sugar), 55.63 (O-**C**H_3). ATR-FTIR ν_{max} (cm^{-1}): 3210 (OH, Alcohol), 2928 (CH, Aliphatic), 1588 (C=C, Aromatic), 1094 (C-O, Acetal), 1005 (C-O, Ether). ESI-MS: Calculated for ($C_{22}H_{26}O_8$) $[M+Na]^+$ m/z = 441.1518. Found $[M+Na]^+$ m/z = 441.1520 (100%). Melting Point: 126–130°C

9.3.2.e 1, 3:2, 4–Diethoxy Dibenzylidene–D–Sorbitol (3.14)

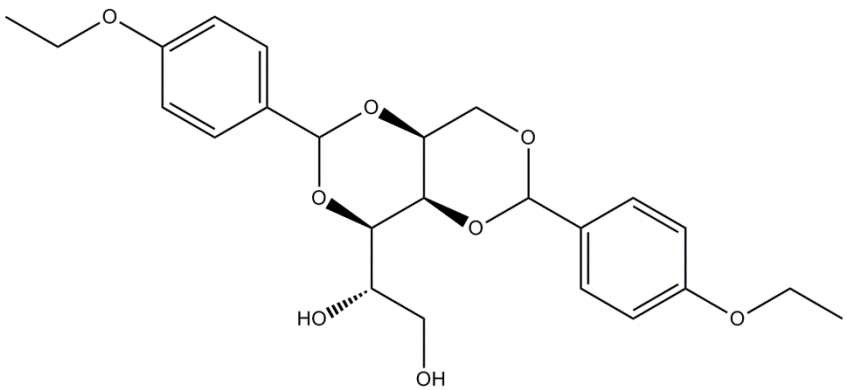

$C_{24}H_{30}O_8$

446.19 gmol^{-1}

General procedure A was used with 4-ethoxybenzaldehyde. Compound **3.14** was a white powder (6.54 g, 14.66 mmol, 58% yield).

^{1}H NMR (400 MHz, $DMSO_{d6}$) δ: 7.38-7.34 (m, 4H, Ar-**H**), 6.92-6.90 (m, 4H, Ar-**H**), 5.58 (s, 2H, Ar-C**H**), 4.13-4.09 (m, 1H, CHO**H**), 4.04-3.99 (m, 5H, OC**H**$_2$CH$_3$ and C**H**-sugar), 3.88 (s, 1H, CH_2O**H**), 3.81-3.79 (m, 2H, C**H$_2$**-sugar), 3.76–3.71 (m, 1H, C**H**-sugar), 3.60–3.55 (m, 2H, C**H**$_2$-sugar), 3.44–3.35 (m, 2H, C**H**-sugar), 1.32 (t, J = 7.0 Hz, 6H, OCH_2C**H**$_3$). ^{13}C NMR (100 MHz, $DMSO_{d6}$) δ: 159.21, 159.16, 131.58, 131.32, 128.02, 127.99, 114.25, 114.19, (Ar-**C**), 99.86, 99.80 (Ar-**C**H), 78.16, 70.54 (**C**H-sugar), 69.83 (**C**H$_2$-sugar), 68.86, 68.27 (**C**H-sugar), 63.54 (**C**H$_2$-sugar), 63.20 (CH_3**C**H_2O) 15.15 (**C**H_3CH_2O). ATR-FTIR ν_{max} (cm^{-1}): 3232 (OH, Alcohol), 2932 (CH, Aliphatic), 1585 (C=C, Aromatic), 1088 (C-O, Acetal), 1011 (C-O, Ether). ESI-MS: Calculated for ($C_{24}H_{30}O_8$) $[M+Na]^+$ m/z = 469.1820. Found $[M+Na]^+$ m/z = 469.1833 (100%). Melting Point: 123–126°C

9.3.2.f 1, 3:2, 4–Di^{n}propoxy Dibenzylidene–D–Sorbitol (3.15)

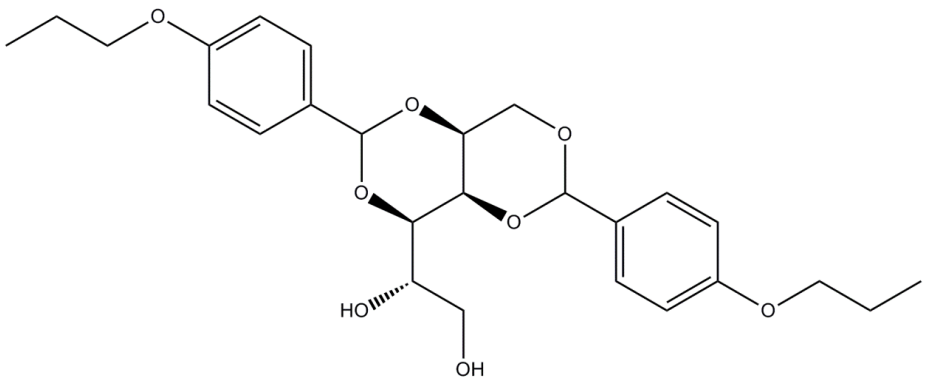

$C_{26}H_{34}O_8$

474.23 gmol^{-1}

General procedure A was used with 4-^{n}Propoxybenzaldehyde. Compound **3.15** was a white powder (1.39 g, 2.93 mmol, 29% yield).

^{1}H NMR (400 MHz, $DMSO_{d6}$) δ: 7.40-7.34 (m, 4H, Ar-**H**), 6.93-6.88 (m, 4H, Ar-**H**), 5.59 (s, 2H, Ar-C**H**), 4.82 (d, J = 5.7 Hz, 1H, CHO**H**), 4.42-4.34 (m, 1H, C**H**-sugar), 4.16–4.10 (m, 3H, C**H$_2$**-sugar, CH_2O**H**), 3.95–3.87 (m, 5H, OC**H**$_2CH_2CH_3$, C**H**-sugar), 3.82–3.71 (m, 1H, C**H**-sugar), 3.64-3.54 (m, 2H, C**H$_2$**-sugar), 3.45–3.38 (m, 1H, C**H**-sugar), 1.76-1.68 (m, 4H, CH_2C**H$_2$**CH_3), 0.99-0.95 (m, 6H, $(CH_2)_2$-C**H**$_3$). ^{13}C NMR (100 MHz, $DMSO_{d6}$) δ: 159.35, 159.29, 131.57, 131.31, 127.99, 127.96, 114.31, 114.24, (Ar-**C**), 99.82, 99.75 (Ar-**C**H), 78.15, 70.51 (**C**H-sugar), 69.45 (**C**H$_2$-sugar), 68.83, 68.23 (**C**H-sugar), 63.15 (**C**H$_2$-sugar), 22.54 (**C**H$_2$), 10.91 (**C**H$_3$). ATR-FTIR ν_{max} (cm^{-1}): 3218 (OH, Alcohol),

2957 (CH, Aliphatic), 1585 (C=C, Aromatic), 1094 (C-O, Acetal) 1011 (C-O, Ether). ESI-MS: Calculated for ($C_{26}H_{34}O_8$) $[M+Na]^+$ m/z = 497.2132. Found $[M+Na]^+$ m/z = 497.2146 (100%). Melting Point: 190–197°C

9.3.2.g 1, 3:2, 4–Dimethylthioether Dibenzylidene–D–Sorbitol (3.16)

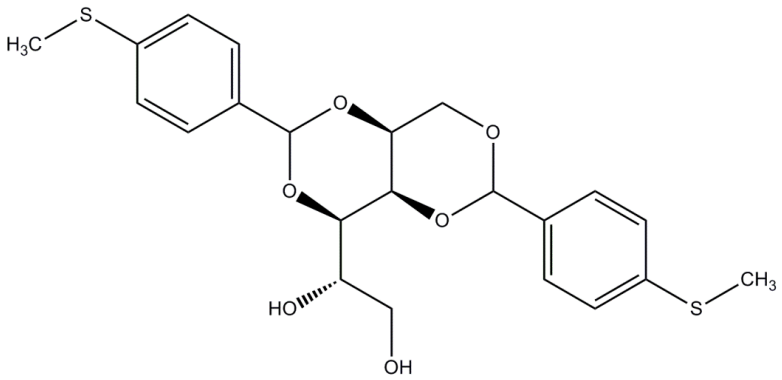

$C_{22}H_{26}O_6S_2$

450.12gmol^{-1}

General procedure A was used with 4-methylthiobenzaldehyde. Compound **3.16** was a white powder (9.95 g, 22.10 mmol, 88% yield).

^{1}H NMR (400 MHz, $DMSO_{d6}$) δ: 7.42-7.38 (m, 4H, Ar-**H**), 7.28-7.25 (m, 4H, Ar-**H**), 5.62 (s, 2H, Ar-C**H**), 4.20–4.11 (m, 3H, CHO**H** and C**H**$_2$-sugar), 3.94-3.91 (m, 1H, C**H**-sugar), 3.84-3.82 (m, 1H, CH_2O**H**-sugar), 3.77–3.74 (m, 2H, C**H**-sugar x2), 3.61-3.58 (m, 2H, C**H**$_2$-sugar), 3.46-3.41 (m, 1H, C**H**-sugar), 2.47 (s, 6H, SC**H**$_3$). ^{13}C NMR (100 MHz, $DMSO_{d6}$) δ: 138.57, 138.46, 135.35, 135.08, 126.69, 126.66, 125.32, 125.26 (Ar-**C**), 98.95, 98.90 (Ar-**C**H), 77.50, 69.95 (**C**H-sugar), 69.20 (**C**H$_2$-sugar), 68.27, 67.62 (**C**H-sugar), 62.52 (**C**H$_2$-sugar), 14.60 (S**C**H$_3$). ATR-FTIR ν_{max} (cm^{-1}): 3220 (OH, Alcohol), 2916 (CH, Aliphatic), 1497 (C=C, Aromatic), 1094 (C-O, Acetal), 733 (C-S, CSH$_3$). ESI-MS: Calculated for ($C_{22}H_{26}O_6S_2$) $[M+Na]^+$ m/z = 473.1069. Found $[M+Na]^+$ m/z = 473.1063 (100%). Melting point: 140 – 143°C

9.3.2.h 1, 3:2, 4–Dimethylsulfonyl Dibenzylidene–D–Sorbitol (3.17)

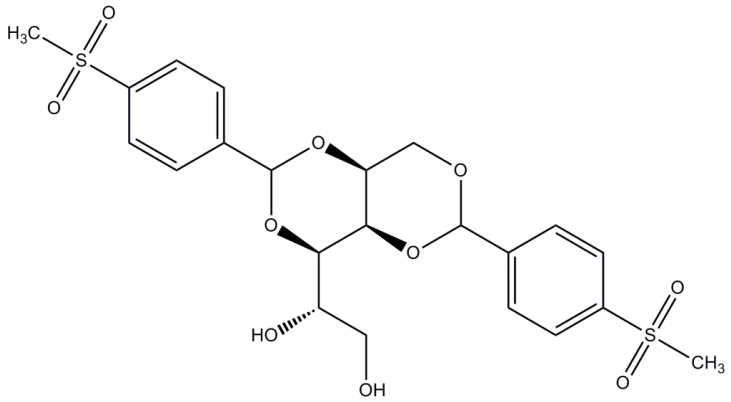

$C_{22}H_{26}O_{10}S_2$

514.10 gmol^{-1}

General procedure A was used with 4-methylsulfonylbenzaldehyde. Compound **3.17** was a yellow powder (5.03 g, 9.78 mmol, 65% yield).

^{1}H NMR (400 MHz, $DMSO_{d6}$) δ: 7.94-7.91 (m, 4H, Ar-**H**), 7.72-7.69 (m, 4H, Ar-**H**), 5.77 (s, 2H, Ar-C**H**), 4.24 (d, J = 2.0Hz, 1H, CHO**H**), 4.22–4.14 (m, 3H, C**H**$_2$-sugar and C**H**-sugar), 4.00 (d, J = 1.7 Hz, 1H, CH_2O**H**), 3.88 (dd, J = 9.4, 1.6 Hz, 1H, C**H**-sugar), 3.76-3.72 (m, 1H C**H**-sugar), 3.60–3.54 (m, 2H, C**H**$_2$-sugar), 3.46-3.41 (m, 1H, C**H**-sugar), 3.16-3.13 (m, 6H, SO_2C**H**$_3$). ^{13}C NMR (100 MHz, $DMSO_{d6}$) δ: 143.70, 143.45, 140.95, 140.89, 127.18, 127.16, 126.95, 126.86, (Ar-**C**), 98.18, 98.09 (Ar-**C**H), 77.47, 70.06 (**C**H-sugar), 69.27 (**C**H$_2$-sugar), 68.42, 67.61 (**C**H-sugar), 62.51 (**C**H$_2$-sugar), 43.57, 43.55 (SO_2**C**H$_3$). ATR-FTIR ν_{max}(cm^{-1}): 3269 (OH, Alcohol), 2929 (CH, Aliphatic), 1519 (C=C, Aromatic), 1093 (C-O, Acetal), 1293 (S=O, Sulfoxide). ESI-MS: Calculated for ($C_{22}H_{26}O_{10}S_2$) $[M+Na]^+$ m/z = 537.0863. Found $[M+Na]^+$ m/z = 537.0860 (100%). Melting Point: 149–152°C

9.3.2.i 1, 3:2, 4–Di(trifluorocarbon) Dibenzylidene–D–Sorbitol (3.18)

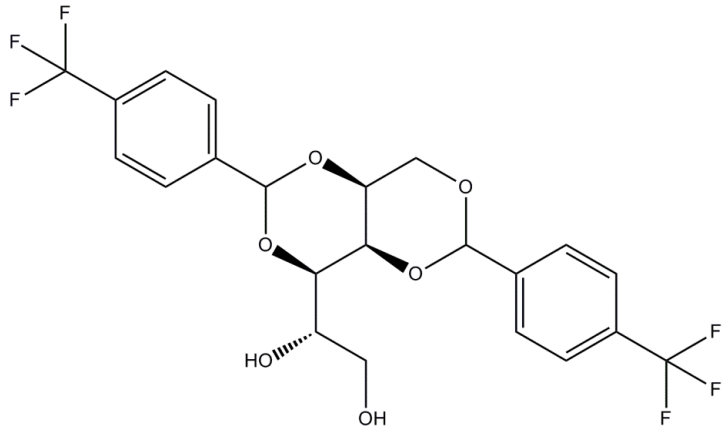

$C_{22}H_{20}F_6O_6$

494.12 gmol^{-1}

General procedure A was used with 4-trifluoromethylbenzaldehyde. Compound **3.18** was a white powder (3.69 g, 7.47 mmol, 50% yield).

^{1}H NMR (400 MHz, $DMSO_{d6}$) δ: 7.79–7.65 (m, 8H, Ar-**H**), 5.78 (s, 2H, Ar-C**H**), 4.40 (d, J = 5.9 Hz, 1H, CHO**H**), 4.30–4.16 (m, 2H, C**H**$_2$-sugar), 4.13-4.07 (m, 1H, C**H**-sugar), 4.02 (s, 1H, CH_2O**H**), 3.91 (dd, J = 9.4, 1.6 Hz, 1H, C**H**-sugar), 3.63-3.60 (m, 1H, C**H**-sugar), 3.58-3.54 (m, 2H, C**H**$_2$-sugar), 3.49-3.45 (m, 1H, C**H**-sugar). ^{13}C NMR (100 MHz, $DMSO_{d6}$) δ: 142.78, 142.53, 137.81, 128.10, 127.44, 127.31, 127.00, 126.98 (Ar-**C**), 125.02 (**C**F_3), 98.24, 98.16 (Ar-**C**H), 77.48, 70.07 (**C**H-sugar), 69.27 (**C**H_2-sugar), 68.43, 67.61 (**C**H-sugar), 62.50 (**C**H_2-sugar). ATR-FTIR ν_{max} (cm^{-1}): 3253 (OH, Alcohol), 2938 (CH, Aliphatic), 1522 (C=C, Aromatic), 1094 (C-O, Acetal), 1322 (C-F, Fluoro). ESI-MS: Calculated for ($C_{22}H_{20}F_6O_6$) $[M+Na]^+$ m/z = 517.070. Found $[M+Na]^+$ m/z = 517.1056 (100%). Melting point:156-160°C

9.3.2.j 1, 3:2, 4–Dinitro–Dibenzylidene–D–Sorbitol (3.19)

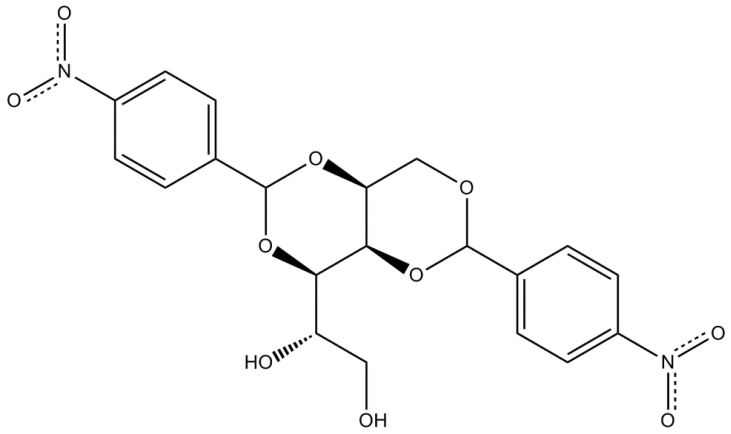

$C_{20}H_{20}N_2O_{10}$

448.11 gmol^{-1}

General procedure A was used with 4-nitrobenzaldehyde. Compound **3.19** was a yellow powder (1.05 g, 2.34 mmol, 18% yield).

^{1}H NMR (400 MHz, $DMSO_{d6}$) δ: 8.28-8.25 (m, 4H, Ar-**H**), 7.76-7.71 (m, 4H, Ar-**H**), 5.83 (s, 2H, Ar-C**H**), 4.98 (d, J = 5.9 Hz, 1H, CHO**H**), 4.51-4.49 (m, 1H, C**H**-sugar), 4.31–4.19 (m, 2H, C**H**$_2$-sugar), 4.06 (s, 1H, CH_2O**H**), 3.94-3.92 (m, 1H, C**H**-sugar), 3.78 (dd, J = 6.0, 2.6 Hz, 1H, C**H**-sugar), 3.64-3.59 (m, 2H, C**H**$_2$-sugar), 3.50-3.44 (m, 1H, C**H**-sugar). ^{13}C NMR (100 MHz, $DMSO_{d6}$) δ: 147.68, 147.65, 145.17, 144.91, 127.60, 127.59, 123.46, 123.37 (Ar-**C**), 97.97, 97.88 (Ar-**C**H), 77.51, 70.17 (**C**H-sugar), 69.34 (**C**H_2-sugar), 68.54, 67.59 (**C**H-sugar), 62.52 (**C**H_2-sugar). ATR-FTIR ν_{max} (cm^{-1}): 3367 (OH, Alcohol), 2876 (CH, Aliphatic), 1520 (N=O, Nitro), 1454 (C=C, Aromatic), 1339 (N=O, Nitro), 1093 (C-O, Acetal). ESI-MS: Calculated for ($C_{20}H_{20}N_2O_{10}$) $[M+Na]^+$ m/z 471.1012. Found $[M+Na]^+$ m/z = 471.1010 (100%). Melting point: 173–187°C

9.3.2.k 1, 3:2, 4–Dicarboxylic acid Dibenzylidene–D–Sorbitol (3.20)

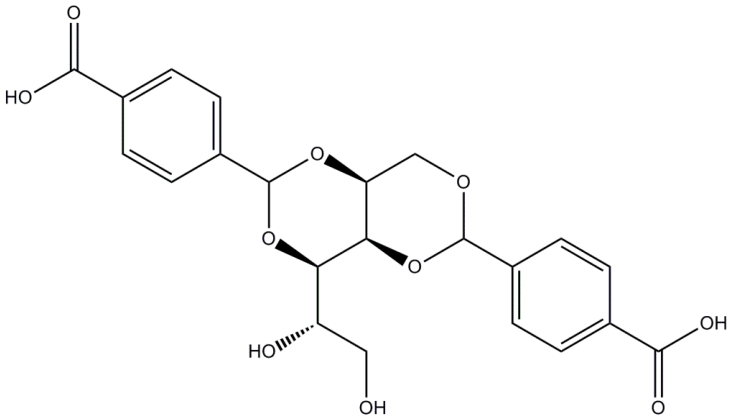

$C_{22}H_{22}O_{10}$

446.12 gmol^{-1}

Compound **3.12** (1.20 g 2.53 mmol) was added to a round-bottom flask with methanol (35 ml) and NaOH $_{(aq)}$ (1M, 35 ml). The mixture was refluxed overnight at 80°C. The solvent was removed by rotary evaporation. Deionised water (50 ml) was added to the flask and the mixture acidified to pH 3 using $NaHSO_4$. The product was washed with deionised water (4 x 100 ml) and dried on the high vacuum line for 2 h. The product was dried to a constant weight in the vacuum oven at 50°C for 2 days. The product was ground before being characterised, producing a white powder (0.89 g, 1.99 mmol, 78% yield).

^{1}H NMR (400 MHz, $DMSO_{d6}$) δ: 10.10 (s, 2H, COO**H**), 7.99-7.96 (m, 4H, Ar-**H**), 7.62-7.57 (m, 4H, Ar-**H**), 5.74 (s, 2H, Ar-C**H**), 4.25-4.23 (m, 1H CHO**H**) 4.21–4.13 (m, 3H, C**H**$_2$-sugar and C**H**-sugar), 3.99 (s, 1H, CH_2O**H**), 3.92-3.90 (m, 1H, C**H**-sugar), 3.83-3.80 (m, 1H, C**H**-sugar), 3.67-3.64 (dd, J = 11, 4.7 Hz, 2H, C**H$_2$**-sugar), 3.52-3.48 (m, 1H, C**H**-sugar). ^{13}C NMR (100 MHz, $DMSO_{d6}$) δ: 167.67, 167.65 (**C**OOH), 143.44, 143.16, 131.52, 131.46, 129.71, 129.62, 126.85, 126.84 (Ar-**C**), 99.20, 99.11 (Ar-**C**H), 78.12, 70.70, (**C**H-sugar) 69.85 (**C**H$_2$-sugar), 69.05, 68.17 (**C**H-sugar), 63.12 (**C**H$_2$-sugar). ATR-FTIR ν_{max} (cm^{-1}): 3433 (OH/COOH, Alcohol/Acid), 2871 (C-H, Aliphatic), 1686 (C=O, COOH), 1514 (C=C, Aromatic), 1090 (C-O, Acetal). ESI-MS: Calculated for ($C_{22}H_{22}O_{10}$ [M–H]$^-$ m/z = 445.1144. Found [M–H]$^-$ m/z = 445.1140 (100%). Melting point: Burns and turns brown > 297°C

9.3.2.l 1, 3:2, 4–Dihydrazide Dibenzylidene–D–Sorbitol (3.21)

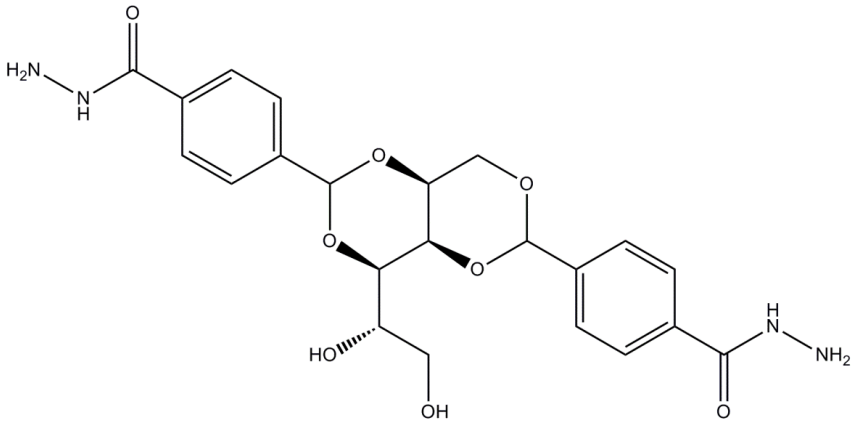

$C_{22}H_{26}N_4O_8$

474.18 gmol^{-1}

Compound **3.21** (1.10 g, 2.32 mmol), was weighed into a round-bottom flask with THF (40 ml) and hydrazine monohydrate (0.600 g, 0.012 mol). The reaction was refluxed at 65° for 24 hours. The reaction was left to cool to room temperature then washed with de-ionised water (3 x 100 ml). The product was dried on the high vacuum line before being dried in the vacuum oven at 65°C. Compound **3.21** was a white powder (2.83 g, 5.97 mmol, 83% yield).

^{1}H NMR (400 MHz, $DMSO_{d6}$) δ: 9.81 (s, 2H, NH_2N**H**CO), 7.84-7.82 (m, 4H, Ar-**H**), 7.56–7.49 (m, 4H, Ar-**H**), 5.71 (s, 2H, Ar-C**H**), 4.94 (d, J = 5.9 Hz, 1H, CHO**H**), 4.51-4.46 (m, 5H, N**H**$_2$NHCO and C**H**-sugar), 4.20-4.18 (m, 2H, C**H**$_2$-sugar), 3.98 (s, 1H, CH_2O**H**), 3.89-3.86 (dd, J = 10.4, 1.6 Hz, 1H, C**H**-sugar), 3.80-3.74 (m, 1H, C**H**-sugar), 3.63-3.59 (m, 2H, C**H**$_2$-sugar), 3.48-3.42 (m, 1H, C**H**-sugar). ^{13}C NMR (100 MHz, $DMSO_{d6}$) δ: 165.62 (**C**ONHNH$_2$), 141.23, 140.97, 133.49, 133.40, 126.74, 126.67, 126.06, 126.04 (Ar-**C**), 98.74, 98.67 (Ar-**C**H), 77.54, 70.10 (**C**H-sugar), 69.30 (**C**H$_2$-sugar), 68.45, 67.64 (**C**H-sugar), 62.58 (**C**H$_2$-sugar). ATR-FTIR ν_{max} (cm^{-1}): 3293 (N-H and OH, Alcohol), 2869 (C-H, Aliphatic), 1633 (C=O, Carbonyl), 1561 (C=C, Aromatic), 1090 (C-O, Acetal). ESI-MS: Calculated for ($C_{22}H_{26}N_4O_8$) $[M+Na]^+$ m/z = 497.1644, $[M+H]^+$ m/z = 475.1821. Found $[M+Na]^+$ m/z = 497.1643 (100%), $[M+H]^+$ m/z = 475.1823 (25%). Melting point: Burns and turns brown > 295°C.

9.3.2.m 1, 3–Benzylidene–D–Sorbitol (3.22)

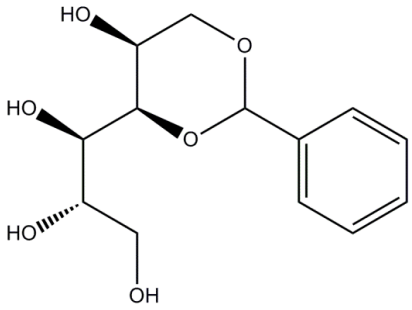

$C_{13}H_{18}O_6$

270.11 gmol^{-1}

General procedure A was followed using D–sorbitol 4.60 g (0.025 mol) with benzaldehyde (2.58 ml, 0.025 mol). This was treated in the same way as procedure A except for washing with water at the end. The product was only washed using dichloromethane. Compound **3.22** was a white powder (3.57 g, 13.22 mmol, 52% yield).

^{1}H NMR (400 MHz, $DMSO_{d6}$) δ: 7.50–7.46 (m, 2H, Ar-**H**), 7.38-7.31 (m, 3H, Ar-**H**), 5.54 (s, 1H, Ar-C**H**), 3.84–3.79 (m, 2H, CHO**H** and C**H**-sugar), 3.70–3.66 (m, 2H, C**H**$_2$-sugar), 3.65 (s, 1H, O**H**-sugar), 3.62 (s, 1H, O**H**-sugar), 3.60 (s, 1H, O**H**-sugar), 3.59–3.58 (m, 1H, C**H**-sugar), 3.57–3.54 (m, 2H, C**H**-sugar), 3.43-3.39 (m, 2H, C**H**$_2$-sugar). ^{13}C NMR (100 MHz, $DMSO_{d6}$) δ: 138.77, 128.65, 127.92, 126.55 (Ar-**C**), 100.15 (Ar-**C**H), 80.93, 79.40, 69.20 (**C**H-sugar), 62.76 (**C**H$_2$-sugar), 61.66 (**C**H-sugar), 61.05 (**C**H$_2$-sugar). ESI-MS: Calculated for ($C_{13}H_{18}O_6$) $[M+Na]^+$ m/z = 293.1003, $[M+H]^+$ m/z = 271.1181. Found $[M+Na]^+$ m/z = 293.0996 (100%), $[M+H]^+$ m/z = 271.1176 (25%).

9.3.2.n 1, 3:2, 4, 5, 6–Tribenzylidene–D–Sorbitol (3.23)

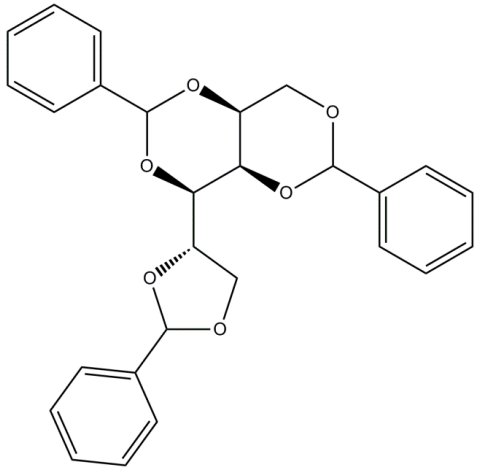

$C_{27}H_{26}O_6$

446.17 gmol^{-1}

General procedure A was followed using D–sorbitol (3.65 g, 0.02 mol) and benzaldehyde (6.12 ml, 0.06 mol). The filtrate was collected and rotary evaporated then dried on the high vacuum line before finally being dried in the vacuum oven at 65°C. Compound **3.33** was an off-white powder (2.64 g, 5.92 mmol, 30% yield).

^{1}H NMR (400 MHz, $DMSO_{d6}$) δ: 7.52–7.35 (m, 15H, Ar-**H**), 5.87 (app s, 2H, Ar-C**H**), 5.73 (s, 1H, Ar-C**H**), 4.91-4.88 (m, 1H, C**H**-sugar), 4.52-4.41 (m, 2H, C**H**$_2$-sugar), 4.33-4.31 (m, 1H, C**H**-sugar), 3.94-3.93 (m, 1H, C**H**-sugar), 3.87-3.84 (m, 2H C**H$_2$**-sugar), 3.80-3.75 (m, 1H, C**H**-sugar), ^{13}C NMR (100 MHz, $DMSO_{d6}$) δ: 138.46, 138.22, 137.82, 129.32, 128.76, 128.31, 128.17, 128.12, 127.10, 126.70, 126.29, 126.05 (Ar-**C**), 102.90, 99.40, 99.36 (Ar-**C**H), 77.60, 69.53 (**C**H-sugar), 69.20 (**C**H$_2$-sugar), 69.10, 68.88 (**C**H-sugar), 67.09 (**C**H$_2$-sugar). ESI-MS: Calculated for ($C_{27}H_{26}O_6$) $[M+Na]^+$ m/z = 469.1607, $[M+H]^+$ m/z = 447.1822. Found $[M+Na]^+$ m/z = 469.1622 (100%), $[M+H]^+$ m/z = 447.1802 (25%)

Abbreviations

A	Area
ADF/s	Aviation De-icing Fluid/s
AEA	Association of European Airlines
Ala	Alanine
AMIL	Anti-icing Materials International Laboratory
AMS	Aerospace Materials Specification
APS	APS Inc
APU	Auxiliary Power Unit
Ar	Aromatic
Arg	Arginine
AS	Aerospace Standard
Asp	Aspartate/Aspartic Acid
ASTM	American Society for Testing and Materials
ATR-FTIR	Attenuated Total Reflectance-Fourier Transform Infrared
BLDT	Boundary Layer Displacement Thickness Test
BOD	Biochemical oxygen demand
C18	Alkyl chain with 18 carbons
ca.	Circa
CAAC	Civil Aviation Administration of China
CCD	Charge coupled device (camera)

CD	Circular Dichroism
CFR	Code of Federal Regulations
COSY	Correlation Spectroscopy
CSF	Cerebral spinal fluid
d	Doublet
D_2O	Deuterium oxide
Da	Daltons
DAQCP	De-icing/Anti-icing Quality Control Pool
DBS	1,3:2,4-Dibenzylidene-D-sorbitol
DBS-CF_3	1,3:2,4-Ditrifluoro dibenzylidene-D-sorbitol
DBS-CH_3	1,3:2,4-Methyldibenzylidene-D-sorbitol
DBS-CO_2CH_3	1,3:2,4-Dimethylester dibenzylidene-D-sorbitol
DBS-$CONHNH_2$	1,3:2,4-Dihydrazide dibenzylidene-D-sorbitol
DBS-COOH	1,3:2,4-Dicarboxylic acid dibenzylidene-D-sorbitol
DBS-NO_2	1,3:2,4-Dinitro dibenzylidene-D-sorbitol
DBS-$O(CH_2)_2CH_3$	1,3:2,4-Di^{n}propoxy dibenzylidene-D-sorbitol
DBS-OCH_2CH_3	1,3:2,4-Diethoxy dibenzylidene-D-sorbitol
DBS-OCH_3	1,3:2,4-Dimethoxy dibenzylidene-D-sorbitol
DBS-SCH_3	1,3:2,4-Dimethylthioether dibenzylidene-D-sorbitol
DBS-SO_2CH_3	1,3:2,4-Dimethylsulfonyl dibenzylidene-D-sorbitol
DCDBS	1,3:2,4-Di(3,4-dichlorobenzylidene)-D-sorbitol
DCM	Dichloromethane

DF	De-icing Fluid
DMF	Dimethylformamide
DMSO	Dimethylsulfoxide
EASA	European Aviation Safety Agency
EPA	Environmental Protection Agency
EPU/s	Energy processing unit/s
ESI-MS	Electrospray Ionisation-Mass Spectroscopy
$E_T(30)$	Reichardt's
F	Force
FAA	Federal Aviation Administration
FEGSEM	Field Emission Gun Scanning Electron Microscopy
Fmoc	Fluorenylmethoxycarbonyl group
FTIR	Fourier Transform Infrared
g	Grams
G'	Storage/Elastic Modulus
G''	Viscous/Loss Modulus
G*	Complex Modulus
GdL	Glucono-δ-Lactone
$gdm^{-2}h$	grams per decimeter per hour
h	hours
H	Height
HA	Acid

HOT	Holdover Time
HSA	*R*-12-hydroxystearic acid
HSQC	Heteronuclear single-quantum correlation spectroscopy
Hz	Hertz
IR	Infrared
I	Insoluble
J	Coupling Constant
JFK	John Fitzgerald Kennedy
kPa	Kilo Pascals
LMWG/s	Low Molecular Weight Gelator/s
LOUT	Lowest operational use temperature
L-Phe-AQ	L-phenlalanyl-amidoquinoline
LVR/LVER	Linear Visco-elastic Region
M	Molar
m	Multiplet
MBS	2,4-Monobenzylidene-D-sorbitol / 1,3-Monobenzylidene-D-sorbitol
mdeg	Millidegrees
MEG	Monoethylene glycol
MeOH	Methanol
mg	Milligram
mg/ml	Milligram per millilitre

MGC	Minimum Gelation Concentration
MHz	Mega Hertz
MicroToF	Micro time of flight
min^{-1}	Per minute
mins	Minutes
ml	Millilitre
mm	Millimeter
mmol	Millimole
mol	Mole
MPG	1,2-Monopropylene glycol
MS	Mass Spectroscopy
NJC	New Japan Chemical Company
nm	Nanometers
NMR	Nuclear Magnetic Resonance
OAT	Outside air temperature
Pa	Pascals
PAA	Polyacrylic Acid
PDMS	Polydimethylsiloxane
PDO	1,3-Propanediol
PEGDM	Polyethyleneglycol dimethacrylate
PG	Partial Gel
PIC	Pilot in command

ppm	Parts per million
PPy	Polypyrrole
PTFE	Polytetrafluoroethylene
p-TSA	para-Toluenesulfonic acid monohydrate
q	Quartet
qn	Quintet
R_f	Retention Factor
RI	Refractive Index
S	Soluble
s	Singlet
SAE	Society of Automotive Engineers
SAFIN	Self-Assembled Fibrillar Network
sec	Seconds
SEM	Scanning Electron Microscopy
SLIPS	Slippery Liquid-Infused Porous Surfaces
SLUGS	Self Lubricating Organogels
SMI	Scientific Materials International
t	Triplet
TBS	1,3:2,4:5,6-Tribenzylidene-D-sorbitol
TCCA	Transport Canada Civil Aviation
T_d	Temperature of dissassembly
TEM	Trasmission Electron Microscopy

T_f	Temperature of formation
T_{gel}	Transition temperature from gel to solution
THF	Tetrahydrafuran
TLC	Thin Layer Chromatography
u/D	Displacement
UK	United Kingdom
US	United States
UV-Vis	Ultra violet - visible
V	Velocity
VT-CD	Variable temperature circular dichroism
WSET	Water Spray Endurance Test
% w/v	Percent weight by volume
µl	Microlitre
µm	Micrometer
^{13}C NMR	Carbon Nuclear Magnetic Resonance
^{1}H NMR	Proton Nuclear Magnetic Resonance
2,4,5-TMDBS	1,3:2,4-Di(2,4,5-trimethylbenzylidene)-D-sorbitol
2,4,6-TMDBS	1,3:2,4-Di(2,4,6-trimethylbenzylidene)-D-sorbitol
3D	Three dimensional
ɣ	Gamma
δ	Phase Angle / Chemical Shift
ε_r	Dielectric constant

θ	Ellipticity
λ	Wavelength

References

1. Transport Canada, *When in Doubt... Small and Large Aircraft, Aircraft Critical Surface Contamination Training For Aircrew and Groundcrew*, Ontario, Canada., 2004.
2. Federal Aviation Administration, *Revised FAA-Approved Deicing Program Updates, Winter 2014-2015*, FAA, 2015.
3. Federal Aviation Administration, *Hazards Following Ground Deicing and Ground Operations in Conditions Conducive to Aircraft Icing.*, Indiana University., 2013.
4. Kilfrost Ltd, *Training Manual Qualification For De/Anti-icing of Aeroplanes*, Haltwhistle, Northumberland, 2011.
5. Federal Aviation Administration, *FAA International De/Anti-icing approved Program*, U. S., 2008.
6. T. H. G. Megson, *Aircraft Structures for Engineering Students*, 4th edn., Butterworth-Heinemann, 2007.
7. G. Gribble, *Aircraft Ground De-icing / Anti-icing*, http://www.internationalflightresources.com/aircraft-ground-deicinganti-icing-0, Accessed 14.4.16.
8. G. D. McBain, *Theory of Lift: Introductory Computational Aerodynamics in MATLAB/Octave*, Wiley, 2012.
9. Association of European Airlines, *Background Information for De-Icing / Anti-Icing of Aeroplane on the Ground*, 2015.
10. D. McLean, *Understanding Aerodynamics: Arguing from the Real Physics.*, Wiley, 2012.
11. S. Gudmundsson, *General Aviation Aircraft Design Applied Methods and Procedures*, 1st edn., Butterworth-Heinemann, Oxford, 2014.
12. F. A. Administration., *Aviation Maintenance Technician Handbook-Airframe.*, AMT Exams, , 2012.
13. J. Lewis, *Airplane Aerodynamics and the Effects of Icing, Deicing and Coatings*, Kilfrost Ltd, Haltwhistle, 2014.
14. G. S. Sawhney, *Fundamentals of Fluid Mechanics*, 2nd edn., I. K. International Pvt Ltd, 2011.
15. J. B. Seaborn, *Understanding the Universe An Introduction to Physics and Astrophysics*, Springer, New York, 1998.
16. Federal Aviation Administration, *Aircraft Icing Handbook.* , Atlantic City International Airport, 1991.
17. M. H. Sadraey, *Aircraft Design A Systems Engineering Approach*, Wiley, 2013.
18. G. L. Dillingham, *Aviation Safety: Preliminary Information on Aircraft Icing and Winter Operations: Congressional Testimony*, Diane Publishing, 2010.
19. G. Cramoisi, *Air Crash Investigations Death in the Potomac The Crash of Air Florida Flight 90*, lulu.com, 2013.

20. National Transportation Safety Board, *Aircraft Accident Report NTSB-AAR-82-8 Air Florida, Inc, Boeing 737-222, N62AF, Collision with 14th Street Bridge, Near Washington National Airport, Washington D C January 13 1982*, Springfield, Virginia, 1982.

21. V. P. Moshansky, *Commission of Inquiry into the Air Ontario Crash at Dryden, Ontario.*, Canada, 1992.

22. LLC Books, *Transportation Disasters In 1989: 1989 Road Accidents, Aviation Accidents and Incidents in 1989, Maritime Incidents In 1989*, General Books, 2010.

23. Federal Aviation Administration, *Title 14 Code of Federal Regulations (CFR) Part 121*, FAA, 2015.

24. Transport Canada Civil Aviation, *Guidelines for Aircraft Ground Icing Operations TP14052E*, Canada, 2005.

25. European Aviation Safety Agency, *Regulation of Ground de-Icing and Anti-icing Services in the EASA Member States*, 2009.

26. Federal Aviation Administration, *SUBJ: Revised FAA-Approved Deicing Program Updates, Winter 2015-2016*, 2015.

27. Federal Aviation Administration, *Title 14 Code of Federal Regulations (CFR) Part 135*, 2015.

28. Transportation Research Board of the National Academies, *Airport Cooperative Research Program (ACRP) Fact Sheets Deicing Prractices*, 2009.

29. Federal Aviation Administration, *Design of Aircraft Deicing Facilities*, 2013.

30. Federal Aviation Administration, *Title 14 Code of Federal Regulations (CFR) Part 39 and 91*, 2016.

31. Association of European Airlines, *Recommendations for De-icing / Anti-icing Aeroplanes on the Ground*, 2015.

32. SAE International, *Aerospace Material Specification - AMS 1424 Deicing/Anti-icing Fluid, Aircraft SAE Type I*, SAE Aerospace, 2012.

33. SAE International, *Aerospace Materials Specification - AMS 1428 Fluid, Aircraft Deicing/Anti-icing, Non-Newtonian (Pseudoplastic), SAE Types II, III, and IV*, SAE Aerospace, 2010-12.

34. J. Leroux, *Guide to Aircraft Ground Deicing*, 2016.

35. Federal Aviation Administration, *FAA Holdover Time Guidelines*, 2015-2016.

36. International Air Transport Association (IATA), *IATA De-Icing / Anti-Icing Quality Control Pool (DAQCP)*, http://www.iata.org/whatwedo/safety/audit/Pages/daqcp.aspx, Accessed 17.2.16.

37. Kilfrost Ltd, *Kilfrost Winter Division Best Practice Guide*, Kilfrost Ltd, Haltwhistle, 2014.

38. Transport Canada, *When in Doubt.. Small and Large Aircraft*, Transport Canada, Canada, 2004.

39. D. Kotker, *New Deicing / Anti-Icing Fluids For Commercial Airplanes*, 2013.

40. A. Beisswenger, C. Laforte and J. Perron, *Issues and Testing of Non-Glycol Aircraft Ground Deicing Fluids 2011-38-0058*, 2011.

41. Civil Aviation Authority, *Aircraft De-Icing Holdover Time Guidance on the De-Icing and Anti-Icing of Aircraft on the Ground*, https://www.caa.co.uk/default.aspx/default.aspx?catid=2520&pagetype=90&pageid=, Accessed 8.9.15, 2015.

42. J. Fraga, *Aero QTR_04.10 Safe Winter Operations*, 2010.

43. Civil Aviation Authority, *Aircraft De-Icing and Anti-Icing Fluids Guidance for Aircraft and Aerodrome Operators around Winter Operations*, https://www.caa.co.uk/default.aspx/default.aspx?catid=2520&pagetype=90&pageid=, Accessed 8.9.15, 2015.

44. J. Hille, *Aero QTR_1.07 Deicing and Anti-Icing Fluid Residues*, 2007.

45. M. Chaput, *Heathrow's Vader Deicing Facility Forges Ahead*, http://deicinginnovations.com/?p=7628, Accessed 9.12.15, 2015.

46. B. Vogel, *Force is with Heathrow as Vader project nears Completion*, http://www.ihsairport360.com/article/7159/force-is-with-heathrow-as-vader-project-nears-completion, Accessed 15.12.15, 2015.

47. Federal Aviation Administration, *Design of aircraft Deicing Facilities Part I*, U S Department of Transportation, Indiana University, 1993.

48. P. Thompson, *How and Why We 'De-Ice' Aircraft Before Takeoff*, http://flightclub.jalopnik.com/how-and-why-we-de-ice-aircraft-before-takeoff-165791, Accessed 11.4.16, 2016.

49. Hatch Mott MacDonald, *Aircraft Deicing Technology Update-*, 2010.

50. DFS Deutsche Flugsicherung, *Aircraft De-icing Plan Stuttgart Airport*, Stuttgart Airport, 2014-2015.

51. G. M. Zlotky, *Aircraft Ground Deicing: An Automated Approach*, SAE International, 2003.

52. E. Salenieks, J. Dejak and M. M. Monaghan, *Central de-icing facility at Toronto's airport Largest facility of its kind in the world*, 2000.

53. J. S. Yong, *Evaluation of the Environmental Impacts and alternative Technologies of Deicing / Anti-icing Operations at Airports*, 2000.

54. The Dow Chemical Company, *UCAR ADF/AAF ULTRA+ Aircraft Deicing / Anti-Icing Fluid for Safe Winter Operations*, Michigan, 2007.

55. Environmental Protection Agency, *Preliminary Data Summary Airport Deicing Operations (Revised) EPA-821-R-00-016*, Washington D C, 2000.

56. Environmental Protection Agency, *Source Water Protection Practices Bulletin Managing Aircraft and Airfield Deiciing Operations to Prevent Contamination of Drinking Water*, 2002.

57. London Luton Airport, *Surface Water Discharge at Luton Airport*, Luton, 2015.

58. H. N. Conkle, S. F. Kuczek, S. P. Chauhan, K. L. Simmons, W. D. Samuels and M. Wyderski, *Enviornmentally Friendly, Non-Glycol Type I Aircraft Deicing Fluid*, SAE International,, 2003.

59. R. Sapienza, W. F. Ricks and A. R. Johnson, *US Patent* 6506318 B1, 2003.

60. The Dow Chemical Company, *UCAR PG Aircraft Deicing Fluids Concentrate "55/45"*, The Dow Chemical Company, Michigan, 2004.

61. A. Beisswenger and J. L. Laforte, *SAE International*, 2003, 1-7.

62. A. Vasilyeva, *Aircraft Deicing Operations*, Airport Systems Planning & Design, 2009.

63. Z. Goraj, *Int. Congress Aeronautical Sci.*, 2004, 1-10.

64. M. J. Kreder, J. Alvarenga, P. Kim and J. Aizenberg, *Nature Reviews.*, 2016, **1**, 1-15.

65. C. Laforte, C. Blackburn and J. Perron, *A Review of Icephobic Coating Performances over the Last Decade*, SAE International, 2015.

66. L. Cao, A. K. Jones, V. K. Sikka, J. Wu and D. Gao, *Langmuir.*, 2009, **25**, 12444-12448.

67. S. Farhadi, M. Farzaneh and S. A. Kulinich, *Appl. Surface. Sci.*, 2011, 6264-6269.

68. C. Blue, *Creating a Coating of Water-repellant Microscopic Particles to Keep Ice off Airplanes*, American Physical Society (APS), 2012.

69. L. Zhu, J. Xue, Y. Wang, Q. Chen, J. Ding and Q. Wang, *ACS Appl. Mater. Interfaces.*, 2013, **5**, 4053-4062.

70. D. Vollmer and H.-J. Butt, *Nature.*, 2015, **527**, 41-42.

71. B. Dixon, A. Walsh, B. Gall and M. Goodwin, *Novel Phase change Materials Icephobic coating for Ice Mitigation in Marine Environments*, The 12th Annual General Assembly of IAMU AGA12, 2012.

72. S. Wang, Z. Yang, G. Gong, J. Wang, J. Wu, S. Yang and L. Jiang, *J. Phys. Chem. C.*, 2016.

73. K. Golovin, S. P. R. Kobaku, D. H. Lee, E. T. DiLoreto, J. M. Mabry and A. Tuteja, *Sci. Adv.*, 2016, **2**, 1-12.

74. N. Withers, *Icephobic coating gives ice the slip*, Chemistry world, 2016.

75. Wyss Institute, *SLIPS: Slippery Liquid-Infused Porous Surfaces*, Harvard University, 2013.

76. P. W. Wilson, W. W. Lu, H. Xu, P. Kim, M. J. Kreder, J. Alvarenga and J. Aizenberg, *Phys. Chem. Chem. Phys.*, 2013, **15**, 581-585.

77. P. Kim, T.-S. Wong, J. Alvarenga, M. J. Kreder, W. E. Adorno-Martinez and J. Aizenberg, *J. Am. Chem. Soc.*, 2012, **6**, 6569-6577.

78. R. Dou, J. Chen, Y. Zhang, X. Wang, D. Cui, Y. Song, L. Jiang and J. Wang, *ACS Appl. Mater. Interfaces.*, 2014, **6**, 6998-7003.

79. C. Urata, G. J. Dunderdale, M. W. England and A. Hozumi, *J. Mater. Chem.*, 2015, **3**, 12626-12630.

80. G. C. Maity, *J. Phys. Sci.*, 2007, **11**, 156-171.

81. J. H. van Esch and B. L. Feringa, *Angew. Chem. Int. Ed.* , 2000, **39**, 2263-2265.

82. J. L. Atwood and J. W. Steed, *Organic Nanostructures*, Wiley VCH, 2008.

83. D. K. Smith, *Supramolecular Chemistry: From Molecules to Nanomaterials*, Wiley, Gale, P. A, Steed, J. W., 2012.

84. G. M. Whitesides, *Small*, 2005, **1**, 172-179.

85. T. Graham, *Phil. Trans. Roy. Soc.*, 1861, **151**, 183.

86. D. J. Lloyd, *The Problem of Gel Structure*, The Chemical Catalog, New York, 1926.

87. R. G. Weiss, *J. Am. Chem. Soc.*, 2014, **136**, 7519-7530.

88. P. H. Hermans, *Colloid Science.*, Elsevier, Amsterdam, 1949.

89. P. J. Flory, *Faraday Discuss. Chem. Soc.*, 1974, **57**, 7-18.

90. M. George and R. G. Weiss, *Acc. Chem. Res.*, 2006, **39**, 489-497.

91. J. W. Steed, *Chem. Comm.*, 2011, **47**, 1379-1383.

92. M.-O. M. Piepenbrock, G. O. Lloyd, N. Clarke and J. W. Steed, *Chem. Rev.*, 2010, **110**, 1960-2004.

93. P. Terech and R. G. Weiss, *Chem. Rev.*, 1997, **97**, 3133-3159.

94. R. G. Weiss and P. Terech, *Molecular Gels: Materials with Self-Assembled Fibrillar Networks*, Springer, Dordrecht, Netherlands, 2006.

95. L. A. Estroff and A. D. Hamilton, *Chem. Rev.*, 2004, **104**, 1201-1218.

96. B. Escuder and J. F. Miravet, *Functional Molecular Gels*, Royal Society of Chemistry, Cambridge, 2013.

97. M. de Loos, B. L. Feringa and J. van Esch, *Eur. J. Org. Chem.*, 2005, 3615-3631.

98. G. C. Maity, *J. Phys. Sci.*, 2013, **17**, 169-178.

99. H. B. Bohidar, P. Dubin and Y. Osada, *Polymer Gels Fundamentals and Applications*, American Chemical Society, Washington D. C., 2002.

100. P. J. Flory, *J. Phys. Chem.*, 1942, **46**, 132-140.

101. N. M. Sangeetha and U. Maitra, *Chem. Soc. Rev.*, 2005, **34**, 821-836.

102. A. R. Hirst, B. Escuder, J. F. Miravet and D. K. Smith, *Angew. Chem. Int. Ed.*, 2008, **47**, 8002-8018.

103. G. Yu, X. Yan, C. Han and F. Huang, *Chem. Soc. Rev.*, 2013, **42**, 6697-6722.

104. S. Banerjee, R. K. Das and U. Maitra, *J. Mater. Chem.*, 2009, **19**, 6649-6687.

105. J. Cui, J. Zheng, W. Qiao and X. Wan, *J. Colloid Interface. Sci.*, 2008, **326**, 267-274.

106. L. Chen, J. Raeburn, S. Sutton, D. G. Spiller, J. Williams, J. S. Sharp, P. C. Griffiths, R. K. Heenan, S. M. King, A. Paul, S. Furzeland, D. Atkins and D. J. Adams, *Soft Matter*, 2011, **7**, 9721-9727.

107. J. P. Desvergne, *Beilstein J. Org. Chem.*, 2010, **6**, 846-847.

108. J. Raeburn, A. Z. Cardoso and D. J. Adams, *Chem. Soc. Rev.*, 2013, **42**, 5143-5156.

109. K. J. Skilling, F. Citossi, T. D. Bradshaw, M. Ashford, B. Kellam and M. Marlow, *Soft Matter*, 2014, **10**, 237-256.

110. D. J. Abdallah and R. G. Weiss, *Adv. Mater.* , 2000, **12**, 1237-1247.

111. D. K. Kumar and J. W. Steed, *Chem. Soc. Rev.*, 2014, **43**, 2080-2088.

112. F. M. Menger and K. L. Caran, *J. Am. Chem. Soc.*, 2000, **122**, 11679-11691.

113. K. A. Houton, K. L. Morris, L. Chen, M. Schmidtmann, J. T. A. Jones, L. C. Serpell, G. O. Lloyd and D. J. Adams, *Langmuir.*, 2012, **28**, 9797-9806.

114. D. J. Adams, K. Morris, L. Chen, L. C. Serpell, J. Bacsa and G. M. Day, *Soft Matter.*, 2010, **6**, 4144-4156.

115. K. Hanabusa and M. Suzuki, *Polym. J.*, 2014, **46**, 776-782.

116. Y. Wang, L. Tang and J. Yu, *Cryst. Growth. Des.*, 2008, **8**, 884-889.

117. M. de Loos, J. van Esch, I. Stokroos, R. M. Kellogg and B. L. Feringa, *J. Am. Chem. Soc.*, 1997, **119**, 12675-12676.

118. L. Chen, K. Morris, A. Laybourn, D. Elias, M. R. Hicks, A. Rodger, L. C. Serpell and D. J. Adams, *Langmuir*, 2010, **26**, 5232-5242.

119. V. A. Mallia, P. D. Butler, B. Sarkar, K. T. Holman and R. G. Weiss, *J. Am. Chem. Soc.*, 2011, **133**, 15045-15054.

120. J. Cui, Z. Shen and X. Wan, *Langmuir.*, 2010, **26**, 97-103.

121. P. Terech, N. M. Sangeetha and U. Maitra, *J. Phys. Chem. B*, 2006, **110**, 15224-15233.

122. J. R. Moffat and D. K. Smith, *Chem. Commun.*, 2008, 2248-2250.

123. N. Zweep and J. H. van Esch, in *Functional Molecular Gels*, The Royal Society of Chemistry, 2014, pp. 1-29.

124. J. H. Van Esch, *Langmuir*, 2009, **25**, 8392-8394.

125. D. K. Smith, *Tetrahedron*, 2007, **63**, 7283-7284.

126. P. Dastidar, *Chem. Soc. Rev.*, 2008, **37**, 2699-2715.

127. P. D. Beer, P. A. Gale and D. K. Smith, *Supramolecular Chemistry*, Oxford University Press, 1999.

128. X. Yang, G. Zhang and D. Zhang, *J. Mater. Chem.*, 2012, **22**, 38-50.

129. F. Fages, *Low Molecular Mass Gelators: Design, Self-Assembly, Function*, Springer, 2005.

130. S. S. Rohner, J. Ruiz-Olles and D. K. Smith, *RSC. Adv.*, 2015, **5**, 27190-27196.

131. G. Cravotto and P. Cintas, *Chem. Soc. Rev.*, 2009, **38**, 2684-2697.

132. D. Bardelang, F. Camerel, J. C. Margeson, D. M. Leek, M. Schmutz, Z. Badruz, Md., K. Yu, D. V. Soldatov, R. Ziessel, C. I. Ratcliffe and J. A. Ripmeester, *J. Am. Chem. Soc.*, 2008, **130**, 3313-3315.

133. K. Isozaki, H. Takaya and T. Naota, *Angew. Chem. Int. Ed.*, 2007, **46**, 2855-2857.

134. F. Ye, S. Chen, G. Tang and X. Wang, *Colloids Surf. A.*, 2014, **452**, 165-172.

135. T. Naota and H. Koori, *J. Am. Chem. Soc.*, 2005, **127**, 9324-9325.

136. M. J. Clemente, R. M. Tejedor, P. Romero, J. Fitremann and L. Oriol, *New. J. Chem.*, 2015, **39**, 4009-4019.

137. P. Fatas, J. Bachl, S. Oehm, A. I. Jimenez, C. Cativiela and D. Diaz Diaz, *Chem. Eur. J.*, 2013, **19**, 8861-8874.

138. N. Koumura, M. Kudo and N. Tamaoki, *Langmuir*, 2004, **20**, 9897-9900.

139. K. J. H., M. Seo, Y. J. Kim and S. Y. Kim, *Langmuir*, 2009, **25**, 1761-1766.

140. K. Murata, M. Aoki, T. Suzuki, T. Harada, H. Kawabata, T. Komori, F. Ohseto, K. Ueda and S. Shinkai, *J. Am. Chem. Soc.*, 1993, **116**, 6664-6676.

141. D. J. Adams, M. F. Butler, W. J. Frith, M. Kirkland, L. Mullen and P. Sanderson, *Soft Matter*, 2009, **5**, 1856-1862.

142. D. J. Adams and P. D. Topham, *Soft Matter*, 2010, **6**, 3707-3721.

143. D. J. Cornwell, B. O. Okesola and D. K. Smith, *Soft Matter*, 2013, **9**, 8730-8736.

144. D. J. Cornwell, B. O. Okesola and D. K. Smith, *Angew. Chem. Int. Ed.*, 2014, **53**, 12461-12465.

145. D. J. Cornwell and D. K. Smith, *Mater. Horiz.*, 2015, **2**, 279-293.

146. D. J. Adballah and R. G. Weiss, *Chem. Mater.*, 2000, **12**, 406-413.

147. R. Stan, N. Chira, C. Ott and C. Todasca, *Rev. Chim.*, 2008, **59**, 273-276.

148. C. Bize, J. C. Garrigues, M. Blanzat, I. Rico-Lattes, O. Bistri, B. Colasson and O. Reinaud, *Chem. Commun.*, 2010, **46**, 586-588.

149. J. A. Foster, M. O. M. Peipenbrock, G. O. Lloyd, N. Clarke, J. A. K. Howard and J. W. Steed, *Nature Chem.*, 2010, **2**, 1037-1043.

150. M. M. Piepenbrock, N. Clarke, J. A. Foster and J. W. Steed, *Chem. Commun.*, 2011, **47**, 2095-2097.

151. Z. Yang, H. Gu, D. Fu, P. Gao, J. K. Lam and B. X, *Adv. Mater.*, 2004, **16**, 1440-1444.

152. S. Toledano, R. J. Williams, V. Jayawarna and R. V. Ulijn, *J. Am. Chem. Soc.*, 2006, **128**, 1070-1071.

153. K. J. C. van Bommel, M. C. A. Stuart, B. L. Feringa and J. Van Esch, *Org. Biomol. Chem.*, 2005, **3**, 2917-2920.

154. D. M. Wood, B. W. Greenland, A. L. Acton, F. Rodriguez-Llansola, C. A. Murray, C. J. Cardin, J. F. Miravet, B. Escuder, I. W. Hamley and W. Hayes, *Chem. Eur. J.*, 2012, **18**, 2692-2699.

155. B. O. Okesola and D. K. Smith, *Chem. Commun.*, 2013, **49**, 11164-11166.

156. S. Bhattacharya and Y. Krishnan-Ghosh, *Chem. Commun.*, 2001, 185-186.

157. S. R. Jadhav, P. K. Vermula, R. Kumar, S. R. Raghavan and G. John, *Angew. Chem. Int. Ed.*, 2010, **49**, 7695-7698.

158. H. Oh, N. Yaraghi and S. R. Raghavan, *Langmuir*, 2015, **31**, 5259-5264.

159. L. Milanesi, C. A. Hunter, N. Tzokova, J. P. Waltho and S. Tomas, *Chem. Eur. J.*, 2011, **17**, 9753-9761.

160. W. Zhao, D. Wang, H. Lu, Y. Wang, X. Sun, S. Dong and J. Hao, *Langmuir*, 2015, **31**, 2288-2296.

161. S. Wu, J. Gao, T. J. Emge and M. A. Rogers, *Soft Matter*, 2013, **9**, 5942-5950.

162. L. E. Buerkle and S. J. Rowan, *Chem. Soc. Rev.* , 2012, **41**, 6089-6102.

163. W. Edwards, C. A. Lagadec and D. K. Smith, *Soft Matter*, 2011, **7**, 110-117.

164. G. Palui, A. Garai, J. Nanda, A. K. Nandi and A. Banerjee, *J. Phys. Chem. B*, 2010, **114**, 1249-1256.

165. M. A. Rogers, A. J. Wright and A. G. Marangoni, *Soft Matter*, 2008, **5**, 1594-1596.

166. D. J. Abdallah and R. G. Weiss, *J. Braz. Chem. Soc.*, 2000, **11**, 209-218.

167. T. Kato, N. Mizoshita, M. Moriyama and T. Kitamura, *Low Molecular Mass Gelators - Design, Self-Assembly, Function*, Springer, 2005.

168. N. Minakuchi, K. Hoe, D. Yamaki, S. Ten-no, K. Nakashima, M. Goto, M. Mizuhata and T. Maruyama, *Langmuir*, 2012, **28**, 9259-9266.

169. J. Le Bideau, L. Viau and A. Vioux, *Chem. Soc. Rev.*, 2011, **40**, 907-925.

170. K. Hanabusa, H. Fukui, M. Suzuki and H. Shirai, *Langmuir*, 2005, **21**, 10383-10390.

171. T. Kato, Y. Hirai, S. Nakaso and M. Moriyama, *Chem. Soc. Rev.*, 2007, **36**, 1857-1867.

172. H. Eimura, M. Yoshio, Y. Shoji, K. Hanabusa and T. Kato, *Polym. J.*, 2012, **44**, 594-599.

173. P. K. Vemula, U. Aslam, V. A. Mallia and G. John, *Chem. Mater.*, 2007, **19**, 138-140.

174. M. L. Muro-Small, J. Chen and A. J. McNeil, *Langmuir*, 2011, **27**, 13248-13253.

175. J. Puigmarti-Luis and D. B. Amabilino, eds. B. Escuder and J. F. Miravet, Royal Society of Chemistry, Cambridge, 2014.

176. S. Bhattacharya and A. Pal, *J. Phys. Chem. B*, 2008, **112**, 4918-4927.

177. D. K. Kumar, D. A. Jose, A. Das and P. Dastidar, *Chem. Commun.*, 2005, 4059-4061.

178. P. C. Xue, Y. Zhang, J. H. Jia, D. F. Xu, X. F. Zhang, X. L. Liu, H. P. Zhou, P. Zhang, R. Lu, M. Takafuji and H. Ihara, *Soft Matter*, 2011, **7**, 8296-8304.

179. D. Dasgupta, A. Thierry, C. Rochas, A. Ajayaghosh and J. M. Guenet, *Soft Matter*, 2012, **8**, 8714-8721.

180. P. Xue, L. R., X. Yang, L. Zhao, D. Xu, Y. Liu, H. Zhang, H. Nomoto, M. Takafuji and H. Ihara, *Chem. Eur. J.*, 2009, **15**, 9824-9835.

181. A. R. Hirst, I. A. Coates, T. R. Boucheteau, J. F. Miravet, B. Escuder, V. Castelletto, I. W. Hamley and D. K. Smith, *J. Am. Chem. Soc.*, 2008, **130**, 9113-9121.

182. S. Liu, W. Yu and C. Zhou, *Soft Matter*, 2013, **9**, 864-874.

183. N. Yan, Z. Xu, K. K. Diehn, S. R. Raghavan, Y. Fang and R. G. Weiss, *J. Am. Chem. Soc.*, 2013, **135**, 8989-8999.

184. Y. Q. Lan, M. G. Corradini, X. Liu, T. E. May, F. Borondics, R. G. Weiss and M. A. Rogers, *Langmuir*, 2014, **30**, 14128-14142.

185. Y. Lan, M. G. Corradini, R. G. Weiss, S. R. Raghavan and M. A. Rogers, *Chem. Soc. Rev.*, 2015, **44**, 6035-6058.

186. M. Bielejewski, A. Lapinski, R. Luboradzki and J. Tritt-Goc, *Langmuir*, 2009, **25**, 8274-8279.

187. J. Gao, S. Wu and M. A. Rogers, *J. Mater. Chem.*, 2012, **22**, 12651-12658.

188. A. R. Hirst and D. K. Smith, *Langmuir*, 2004, **20**, 10851-10857.

189. G. Zhu and J. S. Dordick, *Chem. Mater.*, 2006, **18**, 5988-5995.

190. L. G. S. Brooker, G. H. Keyes and D. W. Heseltine, *J. Am. Chem. Soc.*, 1951, **73**, 5350-5356.

191. J. H. Hildebrand and R. L. Scott, *The Solubility of Non-Electrolytes*, 3rd edn., Dover Publications, Reinhold, 1959.

192. M. J. Kamlet, J. L. M. Abboud, M. H. Abraham and R. W. Taft, *J. Org. Chem.*, 1983, **48**, 2877-2887.

193. C. Laurence, P. Nicolet, M. T. Dalati, J. L. M. Abboud and R. Notario, *J. Phys. Chem.*, 1994, **98**, 5807-5816.

194. J. Catalan, V. Lopez, P. Perez, R. Martin-Willamil and J. G. Rodriguez, *Liebigs. Ann. Chem.*, 1995, **1995**, 241-252.

195. J. Catalan, C. Diaz, C. Lopez, P. Perez, J. L. G. de Paz and J. G. Rodriguez, *Liebigs. Ann. Chem.*, 1996, **1996**, 1785-1794.

196. J. Catalan and C. Diaz, *Liebigs. Ann. Chem.*, 1997, **1997**, 1941-1949.

197. J. Catalan, *Chem. Phys. Lett.*, 1994, **223**, 159-161.

198. C. G. Swain, M. S. Swain, A. L. Powell and S. Alunni, *J. Am. Chem. Soc.*, 1983, **105**, 502-513.

199. P. J. Flory, *J. Chem. Phys.*, 1949, **17**, 223-240.

200. P. J. Flory, *J. Chem. Phys.*, 1941, **9**, 660-661.

201. M. Raynal and L. Bouteiller, *Chem. Commun.*, 2011, **47**, 8271-8273.

202. K. K. Diehn, H. Oh, R. Hashemipour, R. G. Weiss and S. R. Raghavan, *Soft Matter*, 2014, **10**, 2632-2640.

203. C. M. Hansen, *Prog. Org. Coat.*, 2004, **51**, 77-84.

204. D. J. Mercurio and R. J. Spontak, *J. Phys. Chem. B.* , 2001, **105**, 2091-2098.

205. J. R. Ilzhoefer, B. C. Broom, S. M. Nepa, E. A. Vogler, S. A. Khan and R. J. Spontak, *J. Phys. Chem. B*, 1995, **99**, 12069-12071.

206. M. Tenma, N. Mieda, S. Takamatsu and M. Yamaguchi, *J. Polym. Sci. B.*, 2008, **46**, 41-47.

207. W. C. Lai and S. C. Tseng, *Nanotechnology*, 2009, **20**, 1-6.

208. J. M. Guenet, *Macromol. Symp.*, 2006, **241**, 45-50.

209. A. Dawn, T. Shiraki, S. Haraguchi, S. Tamaru and S. Shinkai, *Chem. Asian J.*, 2011, **6**, 266-282.

210. J. Raeburn and D. J. Adams, *Chem. Commun.*, 2015, **51**, 5170-5180.

211. G. John, B. V. Shankar, S. R. Jadhav and P. K. Vemula, *Langmuir*, 2010, **26**, 17843-17851.

212. D. J. Abdallah, L. Lu and R. G. Weiss, *Chem. Mater.*, 1999, **11**, 2907-2911.

213. M. A. Rogers and A. G. Marangoni, *Cryst. Growth. Des.*, 2008, **8**, 4596-4601.

214. J. F. Toro-Vazquez, J. Morales-Rueda, A. Torres-Martinez, M. A. Charo-Alonso, V. A. Mallia and R. G. Weiss, *Langmuir*, 2013, **29**, 7642-7654.

215. P. Terech, V. Rodriguez, J. Barnes and G. McKenne, *Langmuir*, 1994, **10**, 3406-3418.

216. T. Tamura, T. Suetake, T. Ohkubo and K. Ohbu, *J. Am. Oil Chem. Soc.*, 1994, **71**, 857-861.

217. X. Huang and R. G. Weiss, *Tetrahedron*, 2007, **63**, 7375-7385.

218. M. Suzuki, M. Yumoto, M. Kimura, H. Shirai and K. Hanabusa, *Chem. Eur. J*, 2003, **9**, 348-354.

219. M. Suzuki, M. Yumoto, M. Kimura, H. Shirai and K. Hanabusa, *Helv. Chim. Acta*, 2003, **86**, 2228-2238.

220. M. Suzuki, S. Owa, M. Yumoto, M. Kimura, H. Shirai and K. Hanabusa, *Tetrahedron. Lett.*, 2004, **45**, 5399-5402.

221. K. Hanabusa, A. Itoh, M. Kimura and H. Shirai, *Chem. Lett.*, 1999, 767-768.

222. A. Heeres, C. Van der Pol, M. Stuart, A. Friggeri, B. L. Feringa and J. van Esch, *J. Am. Chem. Soc.*, 2003, **125**, 14252-14253.

223. J. Brinksma, B. L. Feringa, R. M. Kellogg, R. Vreeker and J. van Esch, *Langmuir*, 2000, **16**, 9249-9255.

224. J. Makarevic, M. Jokic, B. Peric, V. Tomisic, B. Kojic-Prodic and M. Zinic, *Chem. Eur. J.*, 2001, **15**.

225. R. Garelli-Calvet, F. Brisset, I. Rico and A. Lattes, *Synth. Commun.*, 1993, **23**, 35-44.

226. K. Hanabusa, Y. Matsumoto, T. Miki, T. Koyama and H. Shirai, *J. Chem. Soc., Chem. Commun.*, 1994, 1401-1402.

227. E. J. de Vries and R. M. Kellogg, *J. Chem. Soc., Chem. Commun.*, 1993, 238-240.

228. S. Fleming and R. V. Ulijn, *Chem. Soc. Rev.*, 2014, **43**, 8150-8177.

229. W.-K. Jung, N. Rajapakse and S.-K. Kim, *Eur. Food. Res. Technol.*, 2005, **220**, 535-539.

230. N. S. de Groot, T. Parella, F. X. Aviles, J. Vendrell and S. Ventura, *Biophys. J.*, 2007, **92**, 1732-1741.

231. J. J. Panda, A. Mishra, A. Basu and V. S. Chauhan, *Biomacromolecules*, 2008, **9**, 2244-2250.

232. J. Ryu and C. B. Park, *Angew. Chem. Int. Ed.*, 2009, **48**, 4820-4823.

233. M. Reches and E. Gazit, *Nat. Nanotechnol.*, 2006, **1**, 195-200.

234. J. Kim, T. H. Han, Y. I. Kim, J. S. Park, J. Choi, D. G. Churchill, S. O. Kim and H. Ihee, *Adv. Mater.*, 2010, **22**, 583-587.

235. A. Comotti, S. Bracco, G. Distefano and P. Sozzani, *Chem. Commun.*, 2009, 284-286.

236. Y. Zhang, H. W. Gu, Z. M. Yang and B. Xu, *J. Am. Chem. Soc.*, 2003, **125**, 13680-13681.

237. R. Vegners, I. Shestakova, I. Kalvinsh, R. M. Ezzell and P. A. Janmey, *J. Pept. Sci.*, 1995, **1**, 371-378.

238. A. Mahler, M. Reches, M. Rechter, S. Cohen and E. Gazit, *Adv. Mater.*, 2006, **18**, 1365-1370.

239. V. Jayawarna, M. Ali, A. Jowitt, A. E. Miller, A. Saiani, J. E. Gough and R. V. Ulijn, *Adv. Mater.*, 2006, **18**, 611-614.

240. R. Orbach, L. Adler-Abramovich, S. Zigerson, I. Mironi-Harpaz, D. Seliktar and E. Gazit, *Biomacromolecules.*, 2009, **10**, 2646-2651.

241. V. Jayawarna, S. M. Richardson, A. R. Hirst, N. W. Hodson, A. Saiani, J. E. Gough and R. V. Ulijn, *Acta. Biomater.*, 2009, **5**, 934-943.

242. A. M. Smith, R. J. Williams, C. Tang, P. Coppo, R. F. Collins, M. L. Turner, A. Saiani and R. V. Ulijn, *Adv. Mater.*, 2008, **20**, 37-41.

243. M. Zhou, A. M. Smith, A. K. Das, N. W. Hodson, R. F. Collins, R. V. Ulijn and J. E. Gough, *Biomaterials*, 2009, **30**, 2523-2530.

244. Y. Zhang, Z. M. Yang, F. Yuan, H. W. Gu, P. Gao and B. Xu, *J. Am. Chem. Soc*, 2004, **126**, 15028-15029.

245. Z. M. Yang, G. L. Liang, M. L. Ma, Y. Gao and B. Xu, *J. Mater. Chem*, 2007, **17**, 850-854.

246. Z. M. Yang, G. L. Liang and B. Xu, *Chem. Commun.*, 2006, 738-740.

247. G. L. Liang, Z. M. Yang, R. J. Zhang, L. H. Li, Y. J. Fan, Y. Kuang, Y. Gao, T. Wang, W. W. Lu and B. Xu, *Langmuir*, 2009, **25**, 8419-8422.

248. F. Brisset, R. Garelli-Calvet, J. Azema, C. Chebli, I. Rico-lattes and A. Lattes, *New. J. Chem.*, 1996, **20**, 595-605.

249. G. John, G. Zhu, J. Li and J. S. Dordick, *Angew. Chem. Int. Ed.*, 2006, **45**, 4772-4775.

250. T. Shimizu, R. Iwaura, M. Masuda, T. Hanada and K. Yase, *J. Am. Chem. Soc.*, 2001, **123**, 5947-5955.

251. D. K. Smith, *Chem. Comm*, 2006, 34-44.

252. D. K. Smith, *Adv. Mater.*, 2006, **18**, 2773-2778.

253. J. van Esch, R. M. Kellogg and B. L. Feringa, *Tetrahedron Lett.*, 1997, **38**, 281-284.

254. J. Van Esch, S. De Feyter, R. M. Kellogg, F. De Schryver and B. L. Feringa, *Chem. Eur. J.*, 1997, **3**, 1238-1243.

255. J. Van Esch, F. Schoonbeek, M. De Loos, H. Kooijman, A. L. Spek, R. M. Kellogg and B. L. Feringa, *Chem. Eur. J.*, 1999, **5**, 937-950.

256. F. S. Schoonbeek, J. H. Van Esch, R. Hulst, R. M. Kellogg and B. L. Feringa, *Chem. Eur. J.*, 2000, **6**, 2633-2643.

257. M. De Loos, A. G. J. Ligtenbarg, J. Van Esch, H. Kooijman, A. L. Spek, R. Hage, R. M. Kellogg and B. L. Feringa, *Eur. J. Org. Chem.*, 2000, 3675-3678.

258. K. Y. Lee and D. J. Mooney, *Chem. Rev.*, 2001, **101**, 1869-1880.

259. F. R. Lupi, D. Gabriele, N. Baldino, P. Mijovic, O. I. Parisi and F. Puoci, *Food. Funct.*, 2013, **4**, 1512-1520.

260. E. J. Howe, B. O. Okesola and D. K. Smith, *Chem. Commun.*, 2015, **51**, 7451-7454.

261. M. A. Augustin and Y. Hemar, *Chem. Soc. Rev.*, 2009, **38**, 902-912.

262. M. A. Rogers, T. Strober, A. Bot, J. F. Toro-Vazquez, T. Stortz and A. G. Marangoni, *Int. J. Gastronomy Food Sci.*, 2014, **2**, 22-31.

263. G. Malle and T. Luukas, *US Patent* 2013/0039862 A1, 2013.

264. T. Saito, T. Teshigawara, M. Reger, H. Hoffman, Y. Sugiyama and M. Kitajima, US Patent 2014/0134255 A1, 2014.

265. T. Schamper, M. Jablon, M. H. Randhawa, A. Senatore and J. D. Warren, *J. Soc. Cosmet. Chem.*, 1986, **37**, 225-231.

266. B. O. Okesola, V. M. P. Vieira, D. J. Cornwell, N. K. Whitelaw and D. K. Smith, *Soft Matter*, 2015, **11**, 4768-4787.

267. B. O. Okesola and D. K. Smith, *Chem. Soc. Rev.*, 2016.

268. B. O. Okesola, S. K. Suravaram, A. Parkin and D. K. Smith, *Angew. Chem. Int. Ed.*, 2016, **55**, 183-187.

269. P. K. Vemula, N. Wiradharma, J. A. Ankrum, O. R. Miranda, G. John and J. M. Karp, *Curr. Opin. Biotech.*, 2013, **24**, 1174-1182.

270. R. G. Ellis-Behnke, Y. X. Liang, S. W. You, D. K. C. Tau, S. Zhang and K. F. So, *Proc. Natl. Acad. Sci. USA*, 2006, **103**, 5054-5059.

271. K. J. C. Van Bommel, C. van der Pol, I. Muizebelt, A. Friggeri, A. Heeres, A. Meetsma, B. L. Feringa and J. van Esch, *Angew. Chem. Int. Ed.*, 2004, **43**, 1663-1667.

272. A. Friggeri, B. L. Feringa and J. Van Esch, *J. Control. Release.*, 2004, **97**, 241-248.

273. P. J. Brynes, P. Bevilacqua and A. Green, *Anal. Biochem.*, 1981, **116**, 408-413.

274. T.-M. Wang and M. A. Rogers, *Lipid Technology.*, 2015, **27**, 175-178.

275. L. F. Kretschmer, *US Patent* 2003/0109495, 2003.

276. D. R. Trivedi and P. Dastidar, *Chem. Mater.*, 2006, **18**, 1470-1478.

277. D. R. Trivedi, A. Ballabh and P. Dastidar, *Chem. Mater.*, 2003, **15**, 3971-3973.

278. D. R. Trivedi, A. Ballabh, P. Dastidar and B. Ganguly, *Chem. Eur. J.*, 2004, **10**, 5311-5322.

279. S. Mukherjee, C. Shang, X. Chen, X. Chang, K. Liu, C. Yu and Y. Fang, *Chem. Commun.*, 2014, **50**, 13940-13943.

280. T. Sakai, H. Kawai, M. Kamishohara, A. Odagawa, A. Suzuki, T. Uchida, T. Kawasaki, T. Tsuruo and N. Otake, *J. Antibiot.*, 1995, **48**, 504-508.

281. C. L. Mehltretter, M. S. Furry, R. L. Mellies and J. C. Rankin, *J. Am. Oil. Chem. Soc.*, 1952, **29**, 202-207.

282. G. John, M. Masuda, Y. Okada, K. Yase and T. Shimizu, *Adv. Mater.*, 2001, **13**, 715-718.

283. X. Huang, M. Dong, J. Liu, K. Zhang, Z. Yang, L. Zhang and L. Zhang, *Molecules.*, 2010, **15**, 8689-8701.

284. J. M. Gardlik and R. V. Burkes, *US Patent* 5106999, 1992.

285. C. Xie, J. Li and J. Xia, *US Patent* 20060079720 A1, 2006.

286. V. J. Nebot and D. K. Smith, in *Functional Molecular Gels*, eds. B. Escuder and J. F. Miravet, Royal Society of Chemistry, Cambridge, 2014, pp. 30-66.

287. T. Imae, Y. Takahashi and H. Muramatsu, *J. Am. Chem. Soc.*, 1992, **114**, 3414-3419.

288. T. Imae, N. Hayashi, T. Matsumoto, T. Tada and M. Furusaka, *J. Colloid Interface. Sci*, 2000, **225**, 285-290.

289. X. Luo, B. Liu and Y. Liang, *Chem. Commun.*, 2001, 1556-1557.

290. S. Nandi, H. J. Altenbach, B. Jakob, K. Lange, R. Ihizane and M. P. Schneider, *Org. Lett.*, 2011, **13**, 1980-1983.

291. T. J. Schamper, M. M. Perl and J. D. Warren, *US Patent* 4720381, 1988.

292. J. Mattai, C. Ortiz, E. Guenin and J. Afflitto, *US Patent* 6338841 B1, 2002.

293. E. A. Vogler, T. A. Shepard and J. C. Graper, *US Patent* 5547577, 1996.

294. R. Stan, C. Ott, N. Sulca, A. Lungu and H. Iovu, *Materiale Plastice*, 2009, **46**, 230-235.

295. A. Esposito, T. Schamper and E. C. Henry, *US Patent* 7799318 B2, 2010.

296. G. A. Brennan, *US Patent* 3267052, 1966.

297. T. Ando and H. Yamazaki, *US Patent* 3846363, 1974.

298. J. A. Muszik and W. Dierichs, *US Patent* 3576776, 1971.

299. H. Fukuo and S. Tsujio, *US Patent* 6203910 B1, 2001.

300. N. Mohmeyer, P. Wang, H. W. Schmidt, S. M. Zakeeruddin and M. Gratzel, *J. Mater. Chem.*, 2004, **14**, 1905-1909.

301. V. R. Basrur, J. Guo, C. Wang and S. R. Raghavan, *ACS Appl. Mater. Interfaces.*, 2013, **5**, 262-267.

302. W.-C. Lai and C.-C. Chen, *Soft Matter*, 2014, **10**, 312-319.

303. E. A. Wilder, K. S. Wilson, J. B. Quinn, D. Skrtic and J. M. Antonucci, *Chem. Mater.*, 2005, **17**, 2946-2952.

304. R. B. Kasat, W. Lee, D. R. McCarthy and N. G. Telyan, *US Patent* 5490979, 1996.

305. E. L. Roehl, *US Patent* 4346079, 1982.

306. E. L. Roehl and H. B. Tan, *US Patent* 4154816, 1979.

307. S. Yamasaki and H. Tsutsumi, *Bull. Chem. Soc. Jpn.*, 1995, **68**, 123-127.

308. S. Yamasaki, Y. Ohashi, H. Tsutsumi and K. Tsujii, *Bull. Chem. Soc. Jpn.*, 1995, **68**, 146-151.

309. M. Watase, Y. Nakatani and H. Itagaki, *J. Phys. Chem. B.*, 1999, **103**, 2366-2373.

310. E. A. Wilder, R. J. Spontak and C. K. Hall, *Mol. Phys.*, 2003, **101**, 3017-3027.

311. D. Alperstein and D. Knani, *Polym. Adv. Technol.*, 2013, **24**, 391-397.

312. M. J. Meunier, *Ann. Chim. Phys*, 1891, **22**, 412-432.

313. P. Thomas and M. Sibi, *Compt. Rend.*, 1926, **182**, 314-316.

314. P. Thomas and M. Sibi, *Compt. Rend.*, 1926, **183**, 282-284.

315. C. J. Donahue, *J. Chem. Educ.*, 2006, **83**, 862-869.

316. L. F. Fieser, G. C. Harris, E. B. Hershberg, M. Morgana, F. C. Novello and S. T. Putnam, *Ind. Eng. Chem.*, 1946, **38**, 768-773.

317. K. J. Mysels, *Ind. Eng. Chem.*, 1949, **41**, 1435-1438.

318. J. K. Wolfe, R. M. Hann and C. S. Hudson, *J. Am. Chem. Soc.*, 1942, **64**, 1493-1497.

319. S. J. Angyal and J. V. Lawler, *J. Am. Chem. Soc.*, 1944, **66**, 837-838.

320. L. V. Vargha, *Ber. Dtsch. Chem. Ges.*, 1935, **68**, 1377-1384.

321. T. G. Bonner, E. J. Bourne, P. J. V. Cleare and D. Lewis, *J. Chem. Soc. B.*, 1968, 827-830.

322. D. J. Brecknell, R. M. Carman, J. J. Kibby and L. T. Nicholas, *Aust. J. Chem.*, 1976, **29**, 1859-1863.

323. K. Murai, G. Akazome, Y. Choshi, T. Kobayashi and A. Tsuji, *US Patent* 3721682, 1973.

324. H. Uchiyama, *US Patent* 4131612 A, 1978.

325. H. Uchiyama, *US Patent* 4267110 A, 1981.

326. H. Uchiyama, *US Patent* 4483952 A, 1984.

327. G. Machell, *US Patent* 4562265, 1985.

328. K. Murai, T. Kobayashi and K. Fujitani, *US Patent* 4429140 A, 1984.

329. T. Kobayashi, *US Patent* 5120863, 1992.

330. T. Kobayashi and K. Kujitani, *US Patent* 4902807, 1990.

331. J. P. Salome and G. Fleche, *US Patent* 5023354, 1991.

332. W. A. Scrivens and J. M. Salley, *US Patent* 5731474, 1998.

333. J. G. Lever, D. L. Dotson, J. D. Anderson, J. R. Jones and S. R. Sheppard, *US Patent* 6500964 B2, 2002.

334. P. V. Uppara, P. Aduri, M. Sakhalkar and U. Ratnnaparkhi, *US Patent* 2013/0281716 A1, 2013.

335. A. Pavankumar and P. V. Uppara, *US Patent* 8871954, 2014.

336. R. Feng, L. Chen, Z. Hou and J. Song, *Trans. Tianjin Univ.*, 2007, **13**, 35-41

337. R. Stan, S. Rosca, C. Ott, S. Rosca, E. Perez, I. Rico-lattes and A. Lattes, *Rev. Roum. Chim.*, 2006, **51**, 609-613.

338. J. Li, K. Fan, X. Guan, Y. Yu and J. Song, *Langmuir.*, 2014, **30**, 13422-13429.

339. P. F. Deng, Y. Q. Feng, F. H. Xu and J. Song, *Fine. Chem.*, 2007, **24**, 1056-1060.

340. M. H. Randhawa and T. J. Schamper, *US Patent* 4719102, 1988.

341. H. Burkett, F. Schultz and J. Cassady, *J. Org. Chem.*, 1961, **26**, 2072-2075.

342. T. N. Sorrell, *Organic Chemistry*, University Science Books., 2006.

343. J. Clayden, N. Geeves and S. Warren, *Organic Chemistry*, 2nd edn., Oxford University Press, Oxford, 2012.

344. D. L. Dotson and W. A. Scrivens, *US Patent* 6121332, 2000.

345. S. Grassi, E. Carretti, L. Dei, C. W. Branham, B. Kahr and R. G. Weiss, *New. J. Chem.*, 2011, **35**, 445-452.

346. A. Pal and J. Dey, *Langmuir.*, 2011, **27**, 3401-3408.

347. J. Raeburn, C. Mendoza-Cuenca, B. N. Cattoz, M. A. Little, A. E. Terry, A. Z. Cardoso, P. C. Griffiths and D. J. Adams, *Soft Matter.*, 2015, **11**, 927-935.

348. D. K. Smith, *Chem. Soc. Rev.*, 2009, **38**, 684-694.

349. G. Gottarelli, S. Lena, S. Masiero, S. Pieraccini and G. P. Spada, *Chirality.*, 2008, **20**, 471-485.

350. Y. S. Dagdas, A. Tombuloglu, A. B. Tekinay, A. Dana and M. O. Guler, *Soft Matter.*, 2011, **7**, 3524-3532.

351. W. C. Johnson Jr, *Proteins: Struct. Funct. Genet.*, 1990, **7**, 205-214.

352. A. Micsonai, F. Wien, L. Kernya, Y.-H. Lee, M. Refregiers and J. Kardos, *Proc. Natl. Acad. Sci. USA.*, 2015, **112**, 3095-3103.

353. K. Hanabusa, Y. Maesaka, M. Kimura and H. Shirai, *Tetrahedron. Lett.*, 1999, **40**, 2385-2388.

354. O. Lebel, M.-E. Perron, T. Maris, S. F. SZalzal, A. Nanci and J. D. Wuest, *Chem. Mater.*, 2006, **18**, 3616-3626.

355. H. G., R. B. H. Tan, P. J. A. Kenis and C. F. Zukoski, *J. Phys. Chem. B.*, 2007, **111**, 14121-14129.

356. J. W. Goodwin, *Rheology for chemists : An Introduction*, 2nd. edn., Royal Society of Chemistry, Cambridge, 2008.

357. H. A. Barnes, *An Introduction to Rheology*, Elsevier, Amsterdam., 1989.

358. N. Phan-Thien, *Understanding Viscoelasticity: An Introduction to Rheology*, Springer., New York, 2012.

359. R. J. Hunter, *Foundations of Colloid Science*, Oxford University Press, Oxford : New York, 1987.

360. A. Rao, *Rheology of Fluid, Semisolid, and Solid Foods: Principles and Applications*, 3rd. edn., Springer, New York, 2013.

361. T. A. Instruments., *Understanding Rheology of Structured Fluids AAN016*, T A Instruments., 2013.

362. A. Y. Malkin and A. I. Isayev, *Rheology: Concepts, Methods, and Applications.*, ChemTec., Toronto., 2006.

363. R. Clark, *Understanding Rheology*, CP Kelco, 2009.

364. A. Franck, *Measuring and Evaluating Oscillation Data*, T A Instruments. Germany.

365. F. Mazzeo, *Testing and Unknown Materials Using a Rheometer*, T A Instruments.

366. T. A. Instruments., *Rheological Characterisation of "Stiff" Samples (Part 1)*, T A Instruments., 2014.

367. A. Hill, *Rheology Basics: Introducing the Malvern Kinexus A Practical Measurement Perspective*, Malvern, 2014.

368. M. Zhang, D. Xu, X. Yan, J. Chen, S. Dong, B. Zheng and F. Huang, *Angew. Chem. Int. Ed.*, 2012, **51**, 7011-7015.

369. R. M. GmbH., *Introduction to Rheology Basics V2.1 E*, RheoTec, 2010.

370. P. S. Santos, M. G. Abiad, M. A. Carignano and O. H. Campanella, *Rheol. Acta.*, 2011, **51**, 3-11.

371. R. Boistelle and J. P. Astier, *J. Crsyt. Growth.*, 1988, **90**, 14-30.

372. S. Z. D. Cheng and B. Lotz, *Polymer.*, 2005, **46**, 8662-8681.

373. G. Tan, V. T. John and G. L. McPherson, *Langmuir.*, 2006, **22**, 7416-7420.

374. R. Yu, N. Lin, W. Yu and X. Y. Liu, *Cryst. Eng. Comm.*, 2015, **17**, 7967-8164.

375. F. Rodriguez-Llansola, J. F. Miravet and B. Escuder, *Chem. Commun.*, 2009, 209-211.

376. M. Lescanne, A. Colin, O. Mondain-Monval, F. Fages and J.-L. Pozzo, *Langmuir.*, 2003, **19**, 2013-2020.

377. Z. Wu, S. Yang and W. Wu, *Cryst. Eng. Comm.*, 2016, **18**, 2222-2238.

378. P. Terech, *Specialist Surfactants*, Chapman & Hall, London, 1997.

379. X. Huang, P. Terech, S. R. Raghavan and R. G. Weiss, *J. Am. Chem. Soc.*, 2005, **127**, 4336-4344.

380. J.-L. Li, B. Yuan, X.-Y. Liu, R.-Y. Wang and X.-G. Wag, *Soft Matter.*, 2013, **9**, 435-442.

381. Hatch Mott MacDonald, *Aircraft Deicing Technology Update-*, 2013.

382. SAE International, *SAE Aerospace Standard AS5901 Water Spray and High Humidity Endurance Test Methods for SAE AMS1424 and AMS1428 Aircraft De/Anti-icing Fluids*, SAE, 2003.

383. Flybe, *Flybe Ground De-icing Training* Flybe Aviation Services, 2011-2012.

384. ICAO, *Manual of Aircraft Ground De-Icing / Anti-Icing Operations (Doc 9640-AN/940)*, International Civil Aviation Organization, 2000.

385. SAE International, *AS5900 Standard Test Method for Aerodynamic Acceptance of SAE AMS1424 and AMS1428 Aircraft De/Anti-icing Fluids*, SAE, 2003.

386. J. Wang, Z. Wang, J. Gao, L. Wang, Z. Yang, D. Kong and Z. Yang, *J. Mater. Chem.*, 2009, **19**, 7892-7896.

387. J. Wang, H. Wang, Z. Song, D. Kong, X. Chen and Z. Yang, *Colloids Surf.*, 2010, **80**, 155-160.

388. M. George and R. G. Weiss, *Chem. Mater.*, 2003, **15**, 2879-2888.

389. C. S. Love, V. Chechik, D. K. Smith, I. Ashworth and C. Brennan, *Chem Commun.*, 2005, **45**, 5647-5649.

390. D. D. Diaz, K. Rajagopal, E. Strable, J. Schneider and M. G. Finn, *J. Am. Chem. Soc.*, 2006, **128**, 6056-6057.

391. N. Karim, T. D. Jones, K. M. Lewandowski, B. D. Craig, S. B. Mitra and J. Yang, *US Patent* 0305196, 2009.

392. N. Karim, T. D. Jones, K. M. Lewandowski, B. D. Craig, S. B. Mitra and J. Yang, *US Patent* 8552086, 2013.

393. R. Huang, W. Qi, L. Feng, R. Su and Z. He, *Soft Matter.*, 2011, **7**, 6222-6230.

394. P. Zorlutuna, N. Annabi, G. Camci-Unal, M. Nikkhah, J. M. Cha, J. W. Nichol, A. Manbachi, H. Bae, S. Chen and A. Khademhosseini, *Adv. Mater.*, 2012, **24**, 1782-1804.

395. K. Hamada and H. Uchiyama, *US Patent* 4016118, 1977.

396. G. R. Titus and J. L. Williams, *US Patent* 4808650, 1989.

397. J. W. Rekers, *US Patent* 5049605, 1991.

398. T. D. Danielson, J. Rockwood and N. A. Mehl, *US Patent* 8653165, 2014.

399. Y. Kawai, K. Sasagawa, M. Maki, H. Ueda and M. Miyamoto, *US Patent* 4314039, 1982.

400. J. Xu, J. Li, B. W. Bolt, K. D. Lake Jr, J. D. Sprinkle, B. M. Burkhart and K. A. Keller, *US Patent* 8022133, 2011.

401. W. C. Lai and C. H. Wu, *J. Appl. Polym. Sci.*, 2010, **115**, 1113-1119.

402. E. A. Wilder, C. K. Hall, S. A. Khan and R. J. Spontak, *Langmuir.*, 2003, **19**, 6004-6013.

403. J. M. Smith and D. E. Katsoulis, *J. Mater. Chem.*, 1995, **5**, 1899-1903.

404. T. A. Shepard, C. R. Delsorbo, R. M. Louth, J. L. Walborn, D. A. Norman, N. G. Harvey and R. J. Spontak, *J. Polym Sci. B.*, 1997, **35**, 2617-2628.

405. H. Uchiyama, *US Patent* 4483956, 1984.

406. W. C. Lai, S. J. Tseng, S. H. Tung, Y. E. Huang and S. R. Raghavan, *J. Phys. Chem. B.*, 2009, **113**, 8026-8030.

407. E. A. Wilder, C. K. Hall and R. J. Spontak, *J. Colloid Interface. Sci.*, 2003, **267**, 509-518.

408. M. Kristiansen, M. Werner, T. Tervoort and P. Smith, *Macromolecules.*, 2003, **36**, 5150-5156.

409. B. Fillon, A. Thierry, B. Lotz and J. C. Wittmann, *J. Therm. Anal.*, 1994, **42**, 721-731.

410. J. You, W. Yu and C. Zhou, *Ind. Eng. Chem. Res.*, 2014, **53**, 1097-1107.

411. T. Sutthatang, U. Wichai and S. Wangsoub, *JOM-J. Min. Met. Mats.*, 2013, **23**, 1-8.

412. L. Balzano, G. Portale, G. W. M. Peters and S. Rastogi, *Macromolecules*, 2008, **41**, 5350-5355.

413. W. Frassdorf, M. Fahrlander, K. Fuchs and C. Friedrich, *J. Rheol.*, 2003, **47**, 1445-1454.

414. D. J. Mercurio, S. A. Khan and R. J. Spontak, *Rheol. Acta.*, 2001, **40**, 30-38.

415. J. Cao, K. Wang, W. Cao, Q. Zhang, R. Du and Q. Fu, *J. Appl. Polym. Sci.*, 2009, **112**, 1104-1113.

416. M. Dumitras and C. Friedrich, *J. Rheol*, 2004, **48**, 1135-1146.

417. M. Fahrlander, K. Fuchs and C. Friedrich, *J. Rheol*, 2000, **44**, 1103-1119.

418. W.-C. Lai, *J. Phys. Chem. B.*, 2011, **115**, 11029-11037.

419. S. Palma, R. H. Manzo, D. Allemandi, L. Fratoni and P. L. Nostro, *J. Pharm. Sci.*, 2002, **91**, 1810-1816.

420. C. Xie, L. R. Rieth and T. D. Danielson, *US Patent* 7662978 B2, 2010.

421. C. Xie, J. Li and J. Xia, *WO Patent* 2006044187, 2006.